COMPUTER SIMULATION OF FORM-ROLL DESIGN.

RICHARD JOHN DOWNES.

Doctor of Philosophy.

THE UNIVERSITY OF ASTON IN BIRMINGHAM.

JANUARY 1991.

THE UNIVERSITY OF ASTON IN BIRMINGHAM.

COMPUTER SIMULATION OF FORM-ROLL DESIGN.

Richard John Downes.

Doctor of Philosophy 1991.

SUMMARY.

Modern structural design creates a demand for products which are light but possess high strength. The objective is a reduction in fuel consumption and weight of materials to satisfy both economic and environmental criteria. Cold roll forming has the potential to fulfil this requirement.

The bending process is controlled by the shape of the profile machined on the periphery of the rolls. A CNC lathe can machine complicated profiles to a high standard of precision, but the expertise of a numerical control programmer is required. A computer program was developed during this project, using the expert system concept, to calculate tool paths and consequently to expedite the procurement of the machine control tapes whilst removing the need for a skilled programmer. Codifying the expertise of a human and the encapsulation of knowledge within a computer memory, destroys the dependency on highly trained people whose services can be costly, inconsistent and unreliable.

A successful cold roll forming operation, where the product is geometrically correct and free from visual defects, is not easy to attain. The geometry of the sheet after travelling through the rolling mill depends on the residual strains generated by the elastic-plastic deformation. Accurate evaluation of the residual strains can provide the basis for predicting the geometry of the section. A study of geometric and material non-linearity, yield criteria, material hardening and stress-strain relationships was undertaken in this research project. The finite element method was chosen to provide a mathematical model of the bending process and, to ensure an efficient manipulation of the large stiffness matrices, the frontal solution was applied. A series of experimental investigations provided data to compare with corresponding values obtained from the theoretical modelling.

A computer simulation, capable of predicting that a design will be satisfactory prior to the manufacture of the rolls, would allow effort to be concentrated into devising an optimum design where costs are minimised.

KEYWORDS:

Cold Roll Forming.

Expert System

Finite Element Method.

Mathematical Model.

Elastic-Plastic Analysis.

Acknowledgements.

I would like to take this opportunity to express my gratitude to everyone who has assisted over the course of this research. In particular, I am deeply indebted to my tutor Dr. I. M. Cole for his supervision. My thanks also to Hadley Industries Ltd., for their help in obtaining the experimental data. Finally, I would like to recognise the efforts of the staff at the Computing Services faculty at Southampton University for their help, advice and encouragement whilst preparing this thesis.

Contents.

List of Figures.

CHAPTER ONE.

THE COLD ROLL FORMING PROCESS.

1.1 Introduction.

The evolution of engineering design has progressively changed from the physically robust and massive structures of the past to the slender and streamlined characteristics of modern designs. This is not solely due to current vogues and the fickle nature of public opinions for shapes which are pleasing to the eye. The main reason is based on simple economics, as the structure with superfluous strength is usually heavier and requires more material. It is, therefore, more costly to produce and will consume extra fuel if motion has to be imparted. The high strength but low weight characteristic has the potential to reduce fuel and material requirements, which benefits both economic and environmental criteria.

Sheet metal products are capable of providing many of the requirements of modern designs having a large strength to weight ratio and being relatively cheap to produce. A sheet metal manufacturing process called Cold Roll Forming, which has the acronym C.R.F., is an outstanding example of the type of product that attains contemporary design requirements. The basic principles of the process are illustrated diagrammatically in Fig 1.1. The sheet is passed through a series of rolls which progressively bend it to the required section geometry. The rolls, commonly called form-rolls, are located on horizontal spindles on the rolling mill. The section view shown in Fig 1.1(a) indicates that at each stage of the mill there is a top form-roll and a bottom form-roll.

The shape of the profiles machined on the periphery of the form-rolls will determine the amount of bending that is applied to the sheet at each stage. Sheets with a thickness of less than 3 mm is normally used, although it is possible to form sheet which is more than twice this size. Generally, however, the process is most suited to thin sheet, and the thickness remains unaltered by the cold roll forming operation.

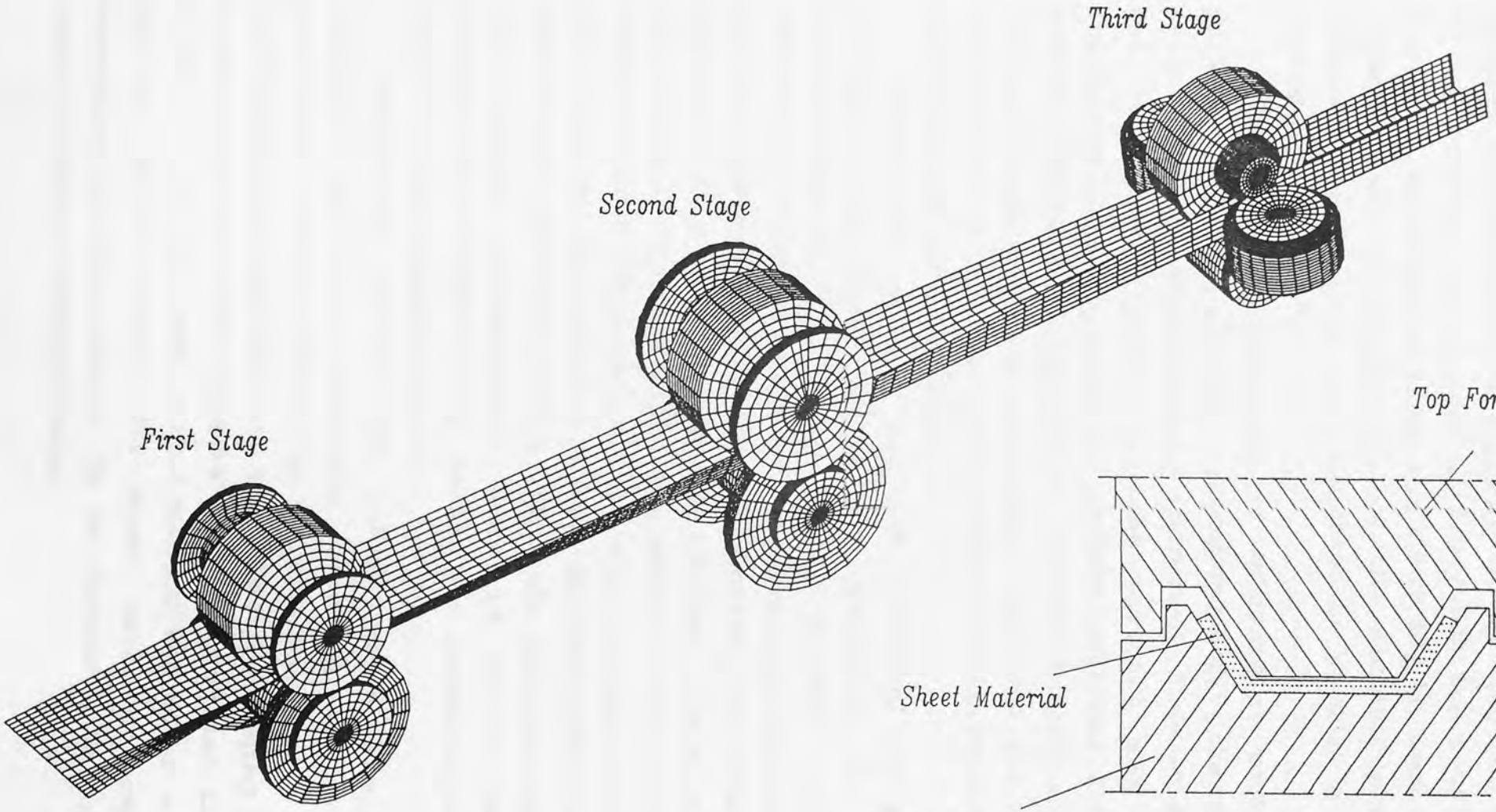

Figure 1.1

Schematic View of the Cold Roll Forming Process.

Figure 1.1(a)

Cross-Section of a Form-Roll Stage.

Only the first three stages of the forming process are shown in Fig 1.1, and the amount of bending applied at each stage is perhaps considerably larger than normal to allow the diagram to highlight the progressive bending characteristics of the process. It is most unlikely for the total number of stages to be as few as three and there may be more than twenty depending on the complexity of the section geometry. The complete set of form rolls required to produce a section is called a "schedule".

The sheet is subjected to substantial work hardening during the C.R.F. process and consequently its strength to weight ratio is significantly increased. This stimulates the use of C.R.F. products in the aircraft and automobile industries. Its capacity to produce sections with a large overall length make the C.R.F. product highly suitable for railway locomotives and carriages. They also are widely used in the building industry, particularly for corrugated roofing, guttering and wall cladding.

The C.R.F. process has the potential to produce an extremely wide range of section geometry. It is almost unrestricted in the shapes it can produce. An important restriction, however, is the stipulated sheet thickness, which must be constant over the entire section. The overall length of the C.R.F. product is normally limited only by handling and transportation requirements. The sheet is usually cut to the required width and wound into coils by the material supplier. It is then fed into the C.R.F. mill directly from the coil and cut to the specified length after the section geometry has been formed. Consequently, there is not a considerable increase in manufacturing costs for products with large overall length specifications.

Production rates from C.R.F. mills are extremely impressive and it is relatively common to combine auxiliary operations such as piercing or spot welding, which are performed simultaneously with the cold roll forming operation. A wide range of sheet material can be used and the surface texture of the finished rolled section can be of a very high quality. It is common for sheet metal covered with a decorative plastic coating to be formed in a C.R.F. mill without visible surface damage.

The major disadvantage of cold roll forming compared with rival sheet metal bending processes is the likelihood of geometric and visual defects. Curvature of the section in the width or overall length direction is a very common production problem. The product straightness tolerances can also be violated by a regular wave deformation, or it may twist about its central axis. Although an excellent surface finish can be obtained, however, if the design of the form-roll schedule is erroneous, the rolling operation can create small surface cracks or wrinkles which are extremely difficult to eradicate.

There are two fundamental causes of production defects.

1) The design of the form-roll schedules may be faulty which is frequently the result of an excessive amount of bending applied at one or more stages of the mill.
2) The problem may be due to a change in rolling conditions which is often caused by a material properties variation, resulting in product defects from a schedule which previously had been producing satisfactory products.

The quality of the schedule is dependent on the individual skills of the C.R.F. designer. Important decisions such as the total number of stages in the schedule and the amount of bending applied by each stage are normally based on the knowledge gained from previous schedule designs. There is no universally recognised scientific design theory which provides guiding principles. The schedule design is normally a trial and error procedure. The form-rolls are tested on the mill and the required modifications are carried out until a satisfactory section is produced. When a schedule has been verified and is capable of producing the required section, it is not necessarily the optimum design. Since form-rolls are very expensive to manufacture, each schedule should involve as few stages as possible. The paramount objective is to design a schedule which produces the section to the specified standards whilst keeping costs as low as possible.

Stringent quality control of the sheet metal properties would be extremely costly. In reality the material properties of the sheet supplied to the C.R.F. company usually vary considerably and this can result in production problems. These

variations in sheet material properties can be overcome by making adjustments to the mill or its auxiliary equipment. Assuming an experienced mill setter is available, this normally is an adequate solution, and production problems of this nature are rarely substantially troublesome.

The many advantages of using CAD/CAM systems in the manufacturing industry are prolifically documented. A CAD/CAM software package specifically designed for the cold-roll forming industry has been developed over a number of years at Aston University[1],[2]. The CAM side of the system improved the speed and efficiency of NC control tape production, for machining the profiles on the form-rolls. The CAD side is largely an automatic draughting facility for the rapid procurement of high quality engineering drawings. It does the trivial or repetitious tasks in schedule design, allowing the designer to concentrate more time on the important decision-making features. The system at Aston University is typical of the CAD/CAM packages used in the C.R.F. industry. They provide excellent support for traditional schedule design methods, but do not provide assistance in aspects of the design which have paramount importance. The number of stages in the schedule and the degree of bending applied by each stage are decisions which the designer must currently make without guidance from computer programs.

The need for a design theory for form-roll schedules is indubitable. The introduction of scientific principles will help to reduce the necessity for the trial and error procedures which have to be applied currently. If the geometry of the section is very similar to a section which has been successfully produced in the past, it is likely that the prototype design will not require extensive modifications. Otherwise, the testing of a new schedule on the C.R.F. mill frequently results in substantial alterations, including changes to the total number of stages used.

The shape of the sheet after it has passed through the C.R.F. mill is entirely dependent on the residual strains created by the elasto-plastic deformation. If the residual strains were accurately evaluated, the shape of the sheet could be predicted and it would be possible to verify a schedule design before the form-rolls were manufactured and

trial and error procedures would then be avoided. Unfortunately, a mathematical analysis that accurately predicts the magnitude and distribution of the strains is inordinately complicated to formulate. A good approximation of the residual strains, however, could provide the basis for the development of a scientific method for form-roll design.

The CAM part of the software package developed at Aston University improved the efficiency of control tape procurement for machining the form-roll profiles. It is essential, however, that the user is an experienced NC part programmer. An understanding of the machining cycles of an NC lathe is required, including knowledge of the cutting tools and their capabilities. The software package would be improved substantially if an automatic profile machining program was available that did not require expertise from the user.

1.2 Research Objectives.

The main objectives of the research project were :-

(1) To carry out a study of the common methods and practices used in the cold roll forming industry.

(2) To undertake a survey of the modern techniques applied to roll schedule design, with emphasis on CAD/CAM software packages and techniques that introduce a scientific approach to the design work.

(3) To apply an expert system concept to the procurement of NC control tapes for machining the profile on form-rolls.

(4) To investigate the different theories associated with an elasto-plastic stress/strain evaluation of sheet metal, due to deformations similar to those produced by the C.R.F. mill.

(5) To produce a software package which provides a good approximation of the strains created in the sheet material due to its passage though the C.R.F. mill.

(6) To carry out laboratory studies to investigate the correlation between strain values obtained experimentally and theoretical values provided by computer simulation.

CHAPTER TWO.

THE ROLLING MILL AND AUXILIARY EQUIPMENT.

2.1 Introduction.

A description of the main design features of a cold roll forming mill is given in this section. The auxiliary equipment which is frequently used is also discussed. It would be impossible to design the form-roll schedules if the basic characteristics of the rolling mill and its auxiliary equipment were not fully understood. Although a detailed description is not necessary, it is essential that the existence of the equipment is acknowledged, together with its capabilities and limitations.

There are a number of fitments, usually involving idler rollers, which can be seen working successfully on rolling mills throughout the country. They can be classified, however, as special equipment used to overcome production problems on specific section geometry. Only the equipment found in most C.R.F. companies, which can be described as standard C.R.F. equipment, is considered.

2.2 The C.R.F. Rolling Mill.

The structural design of a C.R.F. rolling mill is relatively simple and all mills will be basically the same in principle. Each stage will have two horizontal spindles for locating and driving the top and bottom form-rolls. Usually the lower spindle will be fixed and the upper spindle has an adjustment mechanism to allow vertical movement. This is to enable the clearance between the upper and lower form-rolls to be varied and thus the force which they grip the sheet can be changed. A variable speed electric motor is used to rotate the spindles, with a transmission system that usually involves an endless chain. If the speed of rotation of the spindles at one particular stage is to be different from the other stages, (or if the rotational speed of the upper form-roll needs to be different from the lower form-roll) then a gearing system is employed.

The main structure of the mill must house the spindles, locate the auxiliary equipment, and provide the mountings for the electric motor and its transmission system. It is often designed in modular form, with each stage sometimes being a separate structure. The mill, then, consists of a number of modules bolted together. This gives greater flexibility regarding the number of stages used to produce the desired section geometry. The total number of stages will rarely be less than five and can be over thirty if the section geometry is very intricate.

The above description of the C.R.F. mill is a generalisation of the requirements. There are many features which have not been mentioned. Some stages may not be connected to the transmission system, allowing both form-rolls to be free of any rotational drive from the motor (i.e. they are allowed to "idle"). Furthermore, a common arrangement is for the bottom form-roll spindle to be connected to the drive system but not the top form-roll. There are examples where the same rotational speed is applied to all the spindles in the mill which are connected to the drive system. Conversely, a gearing system may be used to vary the rotational speed, so that all the spindles in the mill may have a different rotational speed. These features are discussed in section 3.4 when mill setting techniques are described.

Some rolling mills are designed with the objective of producing a specific section, so the form-rolls are intended to be permanently located on their spindles. In most cases, however, different sets of form-rolls can be mounted so that the mill can produce a very wide range of different section geometry. In this case the mills are designed so that it is relatively rapid and simple to change the form-rolls. One type of design has the characteristics of a very rapid change-over time by having a short spindle length and no support arrangement at one end. The form-rolls are changed by removing a single nut and washer. It is often referred to as the "overhung" or "outboard" design, but it is only suitable for rolling sections of a narrow width. If the spindle is supported at both ends, its length can be increased to allow a wider sheet to be rolled. This extra support also provides greater rigidity so that thicker sections can be formed. It is

usually described as the "inboard" mill design. Of course the time it takes to change the form-rolls will be increased considerably.

The capacity of the mill is dependent on the total number of stages available (which controls the geometric complexity of the section), the length of the form-roll spindles (which controls the maximum sheet width that can be rolled), and both the spindle diameter and electric motor power rating (which control the maximum sheet thickness that can be rolled). Notably, the length of spindle is an important feature. A mill which can produce 2 m wide corrugated sheets for the building industry will obviously require a spindle of over 2 m in length, but it would be unsuitable for rolling roof guttering from a sheet of 200 mm width.

Rolling mill design is a straightforward task compared with form-roll design. Basically it is a simple construction, which makes it a relatively small capital investment when initially purchased (it is the design and manufacture of the form-rolls that substantially increases the cost). Installation costs will be very small since a solid foundation will not be necessary. The bending forces created in the process are relatively small, which means the electric motor is often of low power. The power rating is usually between 7.5 and 80 kW. It usually is a variable speed motor to avoid the cost of gearing to enable the speed of rolling to be adjusted.

2.2.1 The Flying Shear.

There are two methods for feeding the sheet metal into the rolling mill. With the "cut length" method the sheet is already cut to its overall length specification before it is fed into the mill. Instead of the sheet being in short lengths, if the "continuous feed" method is adopted it is guided into the mill from a large coil and cut to the desired overall length after it has passed through the C.R.F. rolling mill. This feed method has many advantages and it is usually preferred for large batch quantities. The flying shear cuts the sheet to its overall length after it has passed through the rolling mill and is used when a "continuous feed" mode is employed. To avoid stopping the sheet, which could significantly slow down the production rate, the flying shear

is designed to cut whilst the sheet is still moving. The formed sheet is guided through a die and blade assembly, which is rapidly accelerated from an initial stationary position to the speed of the sheet. The blade then cuts the sheet, and the assembly travels back to its previously stationary position. There are reports of a flying shear device in publications dated 1947, so it is not a new concept. Modern flying shears can achieve an accuracy of 0.3 mm from the specified nominal overall length, with a cutting stroke of approximately 60 cuts/min. In order to achieve high production rates, particularly if the overall length of the product is relatively short, say about 50 mm, a flying shear mechanism is essential. The only alternative is to stop the rolling mill and cut the sheet using a standard press fitted with a shear blade. This method is still adopted by some C.R.F. companies although most have at least one flying shear because the market for C.R.F. products has a large percentage with an overall length less than 240 mm.

2.2.2 Decoil Drum and Strip Accumulators.

The decoil drum controls the unwinding of the coil when the continuous feed method is adopted. Its main purpose is to locate the coil and allow it to unwind gradually as the sheet strip is pulled into the mill by the rotating form-rolls. A brake device is sometimes included to oppose the forces applied by the form-rolls. Generally it is a simple design, with the main requirement being a quick and efficient coil changing procedure. Decoil drums do not require a large capital investment even for the smallest of C.R.F. companies, so it is a fairly common equipment item.

When a coil is first loaded into the mill it is gradually fed through the form-rolls and the finish section is guided through the die on to the flying shear. This is done very carefully at a speed far below the normal rolling speed because of the likelihood of sheet alignment problems and the instant forming which must take place immediately the sheet enters the form-rolls, (refer to section 3.2.2, where the forming length is described). This procedure is often termed "threading" or "inching through the leading edge" and it slows down the overall production rates considerably. In order avoid

a loss of production due to threading the sheet from the new coil is welded to the end of the exhausted coil, with the result that there will be no "leading edge" to feed through. The mill is stopped whilst the welding operation is performed, but in spite of this a significant amount of time is saved. Oxyacetylene welding or spot welding is sometimes carried out, but the preferred method is a TIG butt weld because it does not significantly increase the thickness of the sheet. Most materials which are commonly cold rolled can be TIG welded easily, with aluminum alloy being the only notable exception.

A further delay in production is caused by the loading of the coils into the decoil drums. A device called a strip accumulator can reduce this time. It is placed between the decoil drum and the mill and acts as a storage device. It can store enough sheet to keep the mill running for about two minutes, depending on the capacity of the accumulator. Its design is relatively simple, consisting of a number of rollers on which the sheet is wound. When the coil currently mounted on the decoil drum is exhausted, a new coil is loaded and welded to the end of the old coil. The mill continues to work at the normal speed during this operation because the sheet is being supplied by the accumulator. The coil changing and welding must be completed in about two minutes to avoid the accumulator being completely emptied. Strip accumulators are rarely found in the cold roll forming industry, possibly due to their large physical size which makes them costly. They are much more common in strip rolling and the British Steel Corporation uses them to achieve continuous high speed rolling operations.

2.2.3 Guides and Rollers.

It is common practice to have a pair of plain cylindrical rollers at the front of the rolling mill. They are called straightening rollers and the gap between them is set to equal the nominal thickness of the sheet. As the sheet is pulled into the mill from the decoil drum it passes though the straightening rollers. The thickness of the sheet remains unaltered by its passage through the straightening rollers, which sometimes may involve two or even three pairs of rollers, all set with a gap equal to the sheet thickness. They

are not driven from the electric motor so the rotation is solely due to the sheet travelling between them.

The sheet must be accurately aligned along the horizontal plane as it travels through the form-rolls. This is often achieved by profiles on the periphery of the form-rolls, as explained in section 3.2.5, but there are circumstances where sheet guides must be used. They are either short lengths of 90 deg. angle section, or a small device incorporating one or more rollers. Guides are bolted directly onto the mill frame. Their only purpose is to guide the sheet along the desired path, so the rollers are not powered by the electric motor. The frame of the mill is designed to allow easy and simple mounting of the guides, which have to be positioned to the overall width of the sheet. Sheet alignment is very important if the overall width is narrow, for example, less than 200 mm, otherwise production problems such as curvature may develop. This is also true if the sheet is fed into the rolling mill already cut to its overall length, where accurate alignment of the strip becomes essential.

2.2.4 Bending Fixtures.

Bending fixtures of various designs are often used by cold roll forming companies, particularly if narrow section of less than 250 mm is being rolled. They are used to straighten out curvatures or to correct section geometry after the sheet has been formed in the C.R.F. mill. They are only used because the C.R.F. mill has failed to produce the section to the desired tolerances. It is indicative of the current standards of form-roll schedule design that so many bending fixtures are used on a regular basis throughout the industry.

2.3 Types of C.R.F. Rolls.

Most of the sheet bending operations carried out on the cold roll forming mill are either by form-rolls or side-rolls. This tooling is explained in detail in this section. There are cases, however, where the sheet bending operations cannot be done by either form-rolls or side-rolls and also there are occasions when the designer decides that it would be better if another bending method is used. This is when

auxiliary rolls are employed and these attachments will also be described.

2.3.1 Form-Rolls.

Form-rolls are the main bending device in the cold roll forming process. They consist of a top form-roll and a bottom form-roll which are mounted on separate spindles and together constitute one stage of the mill. Rotational drive is applied by the mill electric motor, although it is unlikely that all the form-rolls will be driven. The most common arrangement is for the bottom form-roll to be driven but not the top form-roll.

If this is the case, the rotation of the top form-roll will be entirely due to the movement of the sheet as it passes through the stage. The general layout of the rolling mill and form-rolls was shown schematically in Fig. 1.1. A more detailed description of the form-rolls is now given and Fig 2.1(a) illustrates the usual configuration. Attention is drawn to the terminology used in Fig 2.1(b) and details of the main features are listed below.

(1) Centre-to-Centre Distance.

The centre-to-centre distance is the vertical distance between the axes of the form-roll spindles. Usually the bottom spindle is fixed and the top spindle is adjustable so that the centre-to-centre distance can be altered.

2) Drive Surfaces.

The "drive surface" is the portion of the form-roll profile which grips the sheet and because of its rotation, will pull the sheet into the form-rolls. For the top form-roll it is between points A and B in Fig 2.1(b) and for the bottom form-roll its between points C and D. The drive surface is always the same length for the top and bottom form-rolls. This is the only force present that pulls the sheet into the rolling mill.

(3) Pinch Diameters.

The pinch diameter is the diameter of the form-rolls at the drive surface portion of the profile.

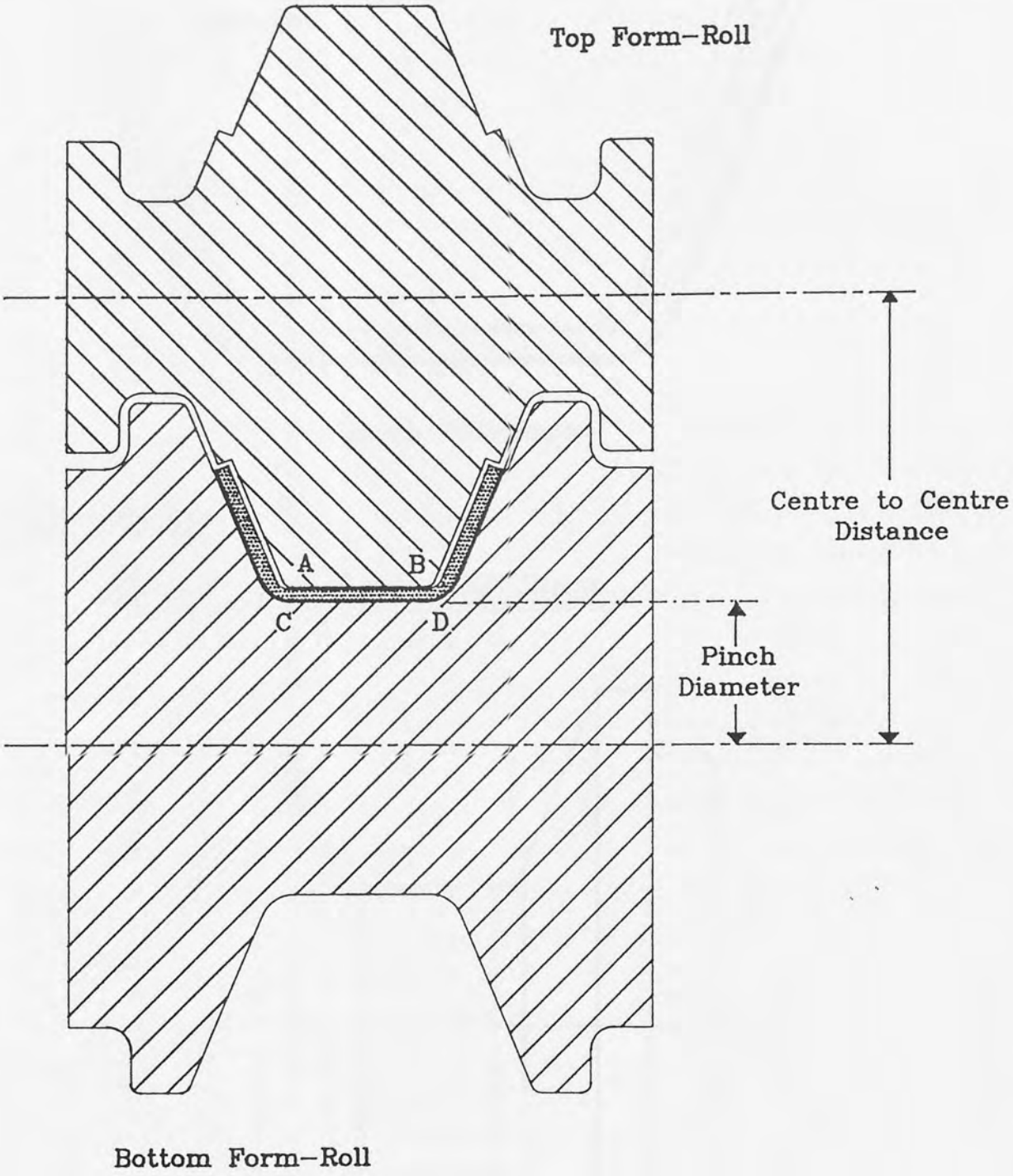

Figure 2.1(a)

A Typical Form–Roll Stage

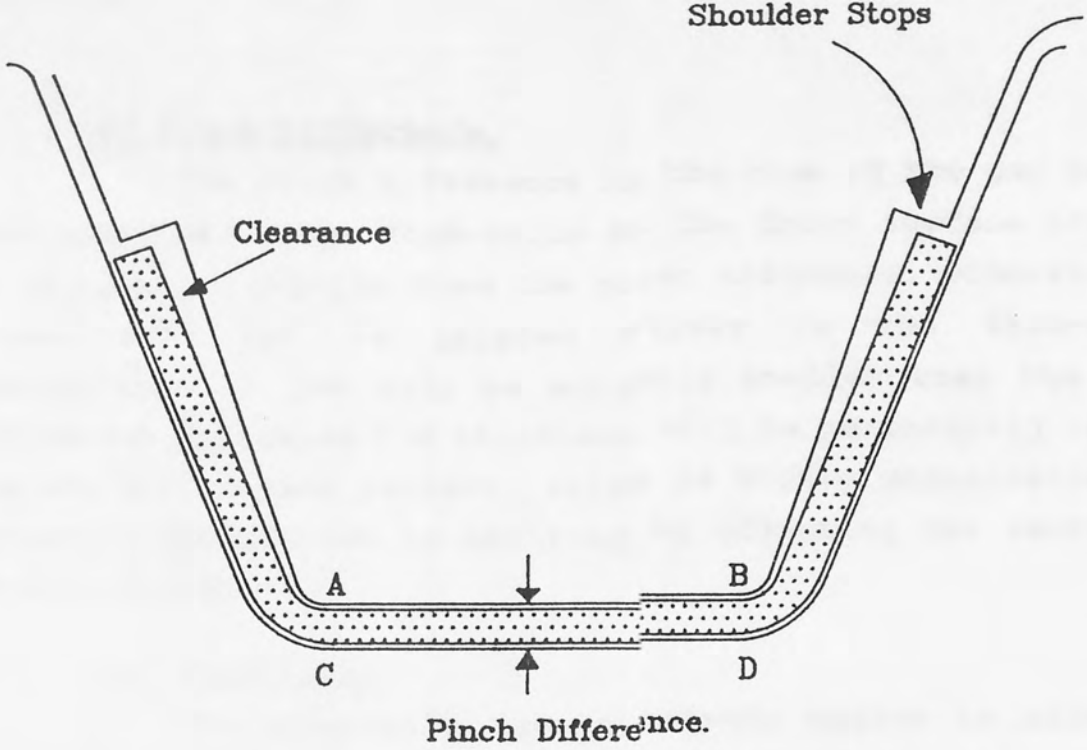

Figure 2.1(b)

Details of a Form–Roll Stage

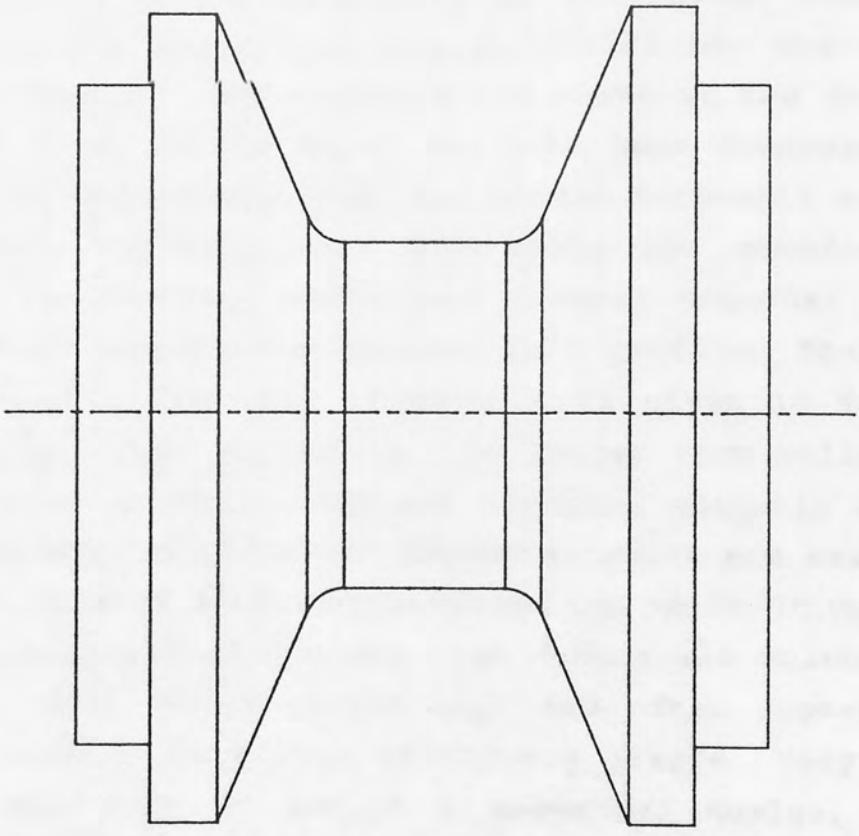

Figure 2.2

A Typical Segmented Roll.

(4) *Pinch Difference.*

The pinch difference is the size of the gap between the upper and lower form-rolls at the drive surface portion. It will be no greater than the sheet thickness, otherwise the sheet will not be gripped firmly in the form-rolls. Conversely, it can only be slightly smaller than the sheet thickness otherwise the thickness will be permanently reduced during the rolling process, which is highly undesirable. The pinch difference can be modified by adjusting the centre-to-centre distance.

(5) *Clearance.*

The form-rolls have clearance angles to allow the sheet to travel through the mill so that all the unwanted resistance forces are reduced to a minimum. The only position where both top and bottom form-rolls contact the sheet is at the drive surface and this generally applies to all designs. In Fig 2.1(b), the edges of the sheet are being bent upwards, so that the bottom form-roll is in contact over the entire width of the sheet. The top form-roll has the clearance to ensure that it only contacts the sheet at the drive surface. If the edges of the sheet had been bent downwards, then the opposite would apply (i.e. the bottom form-roll would have the clearance angles). Some form-rolls are manufactured in a number of separate parts and clamped together on the mill spindle to create the desired roll profile. They are called "segmental rolls" and an example is given in Fig 2.2. This design is often chosen for the larger form-rolls because it makes both manufacturing and handling slightly easier. If a large number of different segmental rolls are available, then a wide range of different profiles can be built up, which will reduce manufacturing costs. The form-rolls which are mounted on the first stage of the mill are often segmented because their profile is always relatively simple. Very large form-rolls may have to be of a segmented design, due to the capacity of the lathes available, but generally it depends on company policy whether to use them or not. Some companies prefer to use a segmental design whenever possible, while others only do this if the form-rolls are very large.

2.3.2 Side-Rolls.

If the sheet is bent through an angle of 90 deg or greater, the top and bottom form-rolls cannot do the task and side-rolls must be used. An example of this is shown in Fig 2.3. Generally, side-rolls will have a plain cylindrical geometry and are not powered by the mill motor. Their rotation is purely due to the motion of the sheet. Side-rolls can be used together with a set of form-rolls on the same stage, or they can be the only rolls at the stage as shown in Fig 2.4.

2.3.3 Auxiliary Rolls.

There are some bending operations which cannot be performed by the form-rolls and side-rolls alone. If this is the case then auxiliary rolls may be the solution and Fig 2.5 shows a typical example. They are usually plain cylindrical rolls that are not driven by the mill motor, so they are similar to side-rolls in this respect. They are only used when an alternative solution cannot be found. Determined attempts are usually made to avoid having to use them because the bending they impart is not controlled.

2.3.4 Roll Material.

A low carbon steel roll is inexpensive and will be capable of doing the required forming even on relatively thick sheet. Unfortunately, it will wear rather quickly and this will result in a deterioration of the surface texture of the formed sheet. For small batch quantities, however, it can be the best choice. For a longer roll life, hardened alloy tool steel or a high carbon chromium steel is chosen. These are far more costly but will last longer so are essential for very large batch quantities.

The rolls are sometimes ground and polished to reduce the possibility of marking the sheet. This is particularly important if the sheet material is relatively soft, or if a high quality surface finish is stipulated.

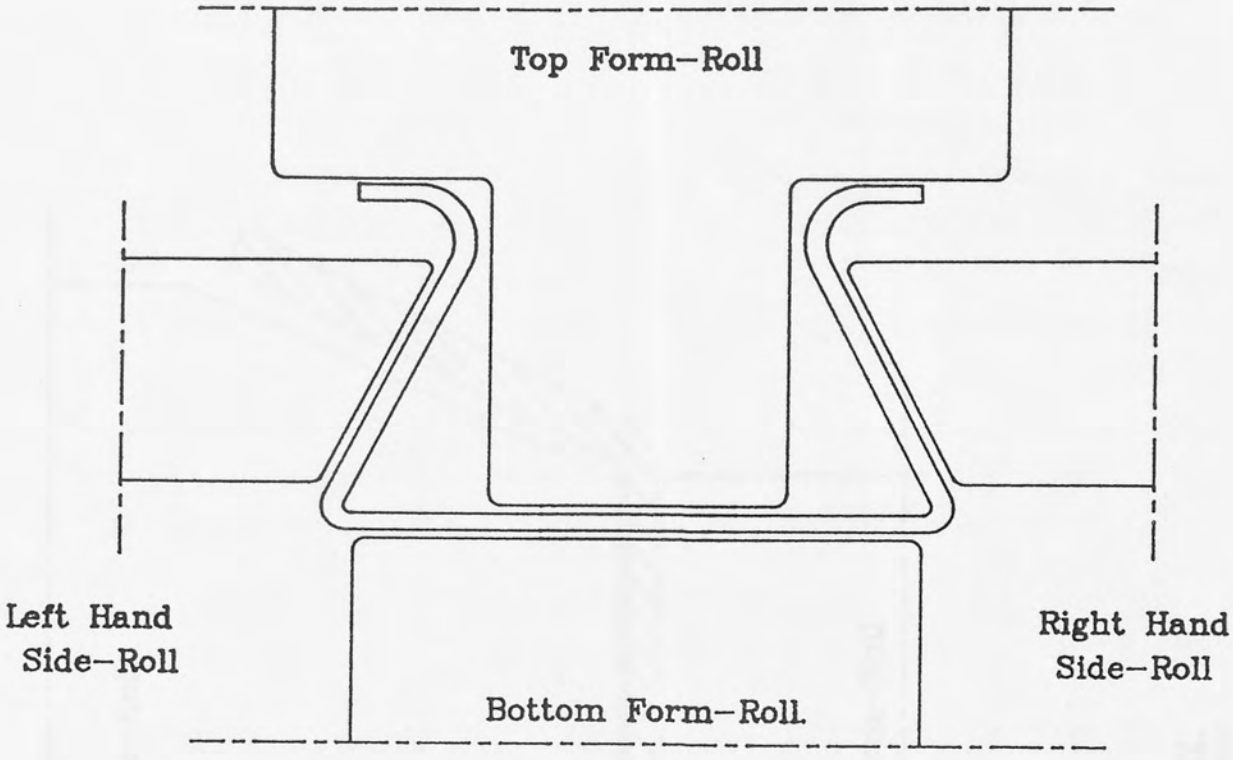

Figure 2.3

An example of Side–Rolls.

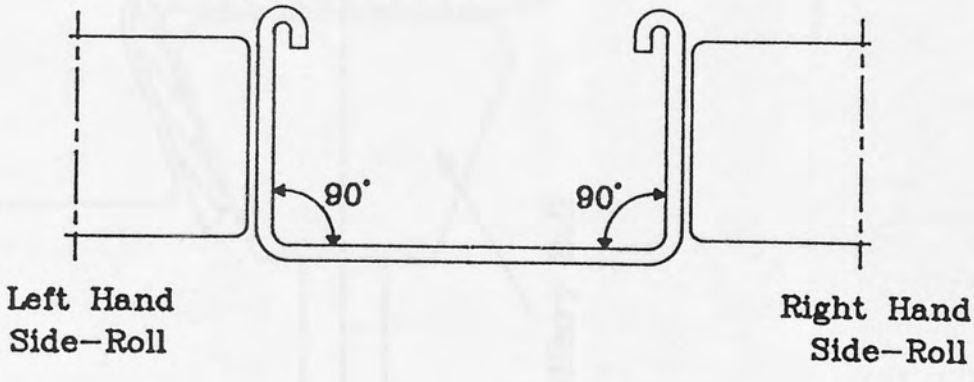

Figure 2.4

Using Side–Rolls to form 90° bends.

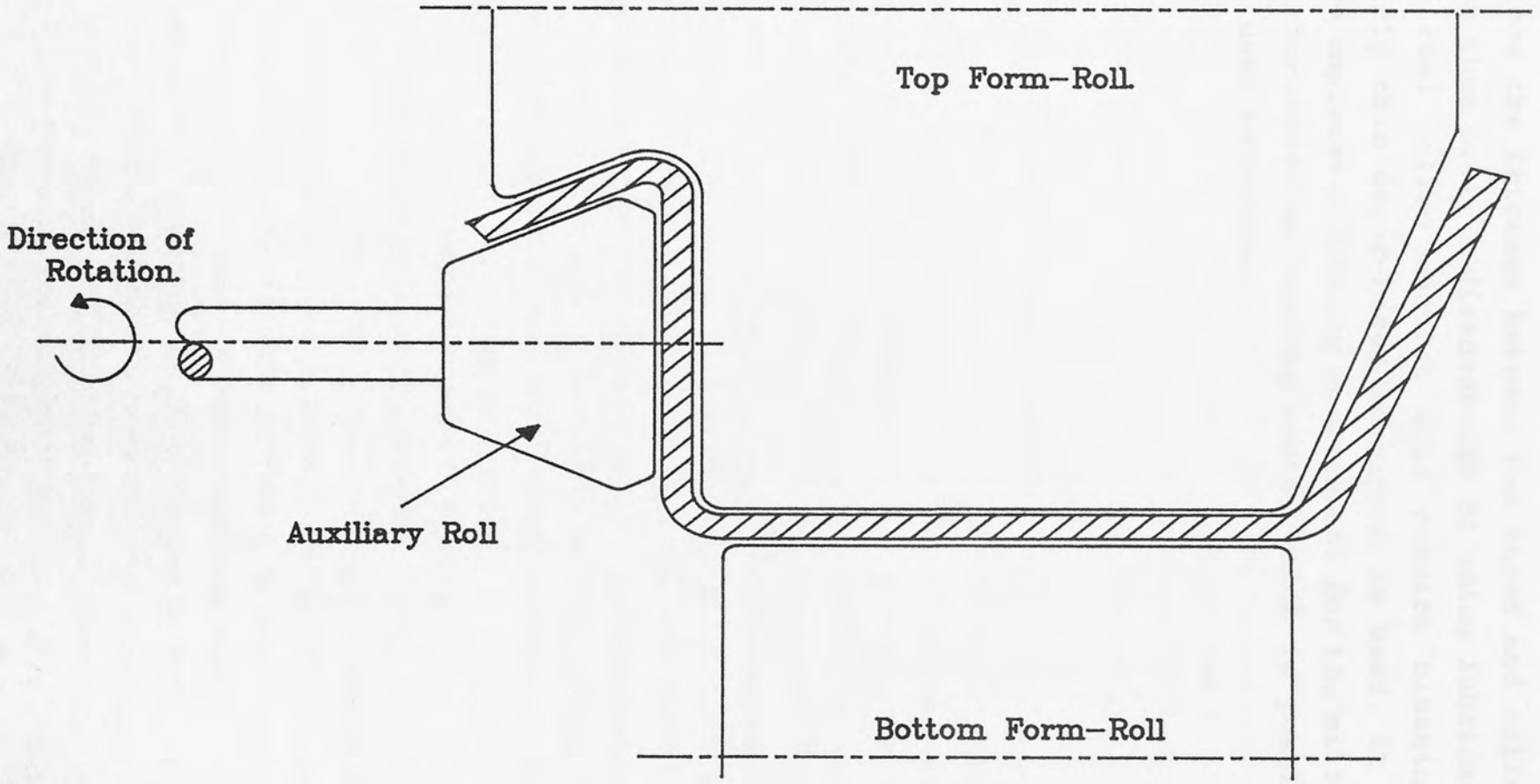

Figure 2.5

Use of an Auxiliary Roll.

2.3.5 Roll Lubrication.

Lubrication of the rolls will help to avoid scratches and marks on the finished rolled product. It will help to keep the rolling surfaces clean and free from small particles that may otherwise score the sheet or the roll profile. Wear will also be reduced since the lubrication will reduce the friction between the sheet and rolls, and help to keep them cool. A disadvantage of using lubricant is that the finished rolled section will require cleaning, even if a fairly thin water-based lubricant is used. It does create a more unpleasant working environment for the mill operators and it increases the running costs, which is possibly why it is not used extensively.

CHAPTER THREE.

ROLL DESIGN.

3.1 Introduction.

The decisions which the designer has to make when designing a form-roll schedule are discussed in this section. The absence of scientifically derived rules that can be applied during the design procedure will be emphasised. So many of the design decisions are based purely on past experience that it takes many years before a designer becomes proficient in the craft. It has often been stated that roll design is an art rather than a science and the description of the design procedure given in this section will undoubtedly confirm this opinion.

3.2 Preliminary Decisions.

The first decision which the designer has to make is to select the rolling mill to be used. It is usual for a form-roll schedule to be designed for a specific rolling mill, so features such as the size of the form-roll spindles, the total number of stages available, and the availability of side-rolls and auxiliary rolls, are known from the outset.

The decision on the method used to feed the sheet into the mill has a powerful influence on the roll design. If the sheet is cut to its overall length before being fed into the mill, severe bending operations at the first 3 or 4 stages should be avoided and also more sheet guides are needed compared with continuous sheet feed.

An upward bending mode is chosen in the majority of cases. There are occasions, however, when downward bending has been the solution when attempts to use upward bending have failed. Generally, the approach is to choose upward bending first and, if considerable problems ensue, consider trying the downward bending mode. Sometimes there must be both upward and downward bending due to the geometry of the section. The decision discussed here, however, is whether the majority of the bending is either an upward or downward mode. There is one important feature which should also be considered, the use of

upward or downward bending controls the general orientation of the section as it travels through the mill. If side-rolls or auxiliary rolls are used on the later stages, difficulties may occur because they cannot be positioned without causing an obstruction to the sheet movement. The section sometimes has to be rotated around to enable the rolls to carry out their task.

3.2.1 Selection of the Active Bends for each Stage.

Most section geometry will involve more than one bend region. If a stage imparts a bending moment to a particular bend region, then the bend is said to be "active" at that stage. Which bends are active at each stage in the mill is one of the major decisions which the designer makes. Attempts have been made to devise a general rule to help designers, but without success. One suggestion was to select the bend closest to the sections vertical centre line, and to form this in the first few stages of the mill. The concept was to avoid the selection of another bend until the present one had been completely formed. Hence the next active bend would be the one closest to the vertical centre line of the section, which had not yet been formed. General rules have always been inoperative, because designers not only have to produce a form-roll schedule which produces a satisfactory finished product, but also the total number of stages involved must be considered. Form-rolls are very expensive and so the number required must be kept as small as possible to minimise costs.

A designer will recall how a similar section had been successfully rolled in the past and base the selection of active bends for each stage on that information. This may result in four or more active bends at one stage. A general rule does not exist, so the choice of one designer can differ greater from that of another, particularly if they have received their training in different companies.

3.2.2 Magnitude of Bending at each Stage.

When a bend region is selected to be active at a stage, a further major decision must be made. The designer must specify the angle to be moved through, therefore defining

how severe the bending will be at the stage. The quality of the finished product will depend on this more than on any other design decision. It is generally agreed throughout the C.R.F. industry that if the forming is too severe then the geometry of the finish section will be unacceptably distorted. To reduce costs, however, it is important that each stage bends the sheet as much as possible so that the number of stages in the schedule is reduced. The objective is to make the bending at each stage as severe as possible, but not to the extent that the finish product violates its geometrical tolerances.

A number of empirically derived theories have been formulated to recommend how severe the bending should be. The most common type is to suggest a sequence of bending angles to form a particular bend. For example, Kalvzhskii[3] recommended that for a 90 deg bend, the sequence should be as follows :-

8, 18, 30, 44, 58, 70, 80, 88, 90

This approach is possibly very similar to the way a designer will always recall how it was successfully done in previous form-roll schedules. Unfortunately, a number of most important features will have been neglected if this kind approach is used. The characteristics of the rolling mill, the method of feeding the sheet into the mill and the sheets thickness, width and material properties will all influence the bending process. Also it is unlikely that the geometry of the section can be ignored, because the forming of a 90 deg bend on a simple U-channel must be different from forming a 90 deg bend on a sheet with a highly complicated section geometry.

A paper by Angel[4] published in 1949 introduced the idea of using a "Forming Angle". Because of its historical significance, the theories proposed by Angel are frequently referred to in publications involving cold roll forming, although the practical value of his idea are extremely questionable. Angel's forming angle method is illustrated in Fig 3.1 which shows a 90 deg bend being formed.

The forming angle of 1 deg 25 min was derived from extensive empirical studies involving the forming of simple sections. From the application of simple trigonometry a "Forming Length" is obtained from which the total number of stages to be used is determined. Since the pitch of the mill

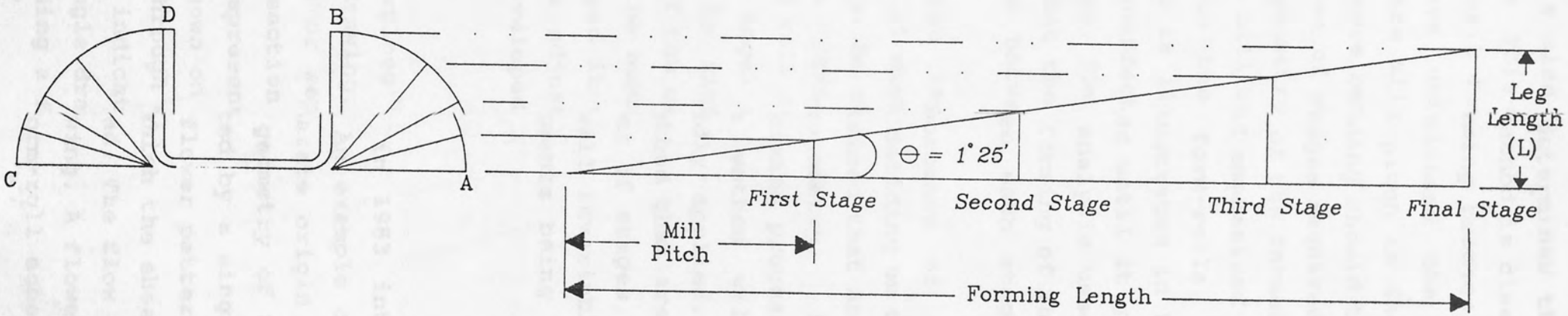

Figure 3.1

Definition of Angel's Forming Length.

will be known, this analysis also determines the amount of bending at each of the stages. This method is clearly an over-simplification of the cold roll forming process. There have been many authors who have criticized the method and emphasized its naivety. If the mill pitch is increased then Angel's method will suggest more bending should take place at each stage and the total number of stages required is reduced.

Sarantis[5] studied the geometry of the formed sheet as it approached each stage of the mill and emphasised that most of the forming occurs close to the form-rolls. This is an important characteristic and is illustrated in Fig 3.2. The shape of the sheet remains unaffected until it gets within a certain distance of the stage. The analysis used in Angel's method appears to consider that the forming of the sheet is a gradual and uniform process between each stage, which is indubitably incorrect.

Cadney[6] highlighted the importance of longitudinal stretching, (see section 3.3.2) when deciding on the degree of bending applied at each stage. He claimed that Angel's method being based on simple trigonometry, is totally unrepresentative of the cold roll forming process.

It is unlikely that Angel's method will design a successful schedule if it is rigidly applied. There are, however, modified versions of the method that are used, often as a guide for determining the number of stages. If a design method of any type is employed it will invariably be a very flexible one with intuitive adjustments being made by the designer as the design is developed.

3.2.3 Flower Patterns.

A paper by Vanderploeg[7] in 1953 introduced the concept of flower pattern drawing. An example of a top hat channel section on a common or separate origin is shown in Fig 3.3(a) and 3.3(b). The section geometry of the sheet at each stage of the mill is represented by a single line, the sheet thickness not being shown on flower patterns. Both the active bends and the angle through which the sheet is bent at each of the mill stages are indicated. The flow of the metal is vividly depicted in a single drawing. A flower pattern is not simply a method of defining a form-roll schedule, it can

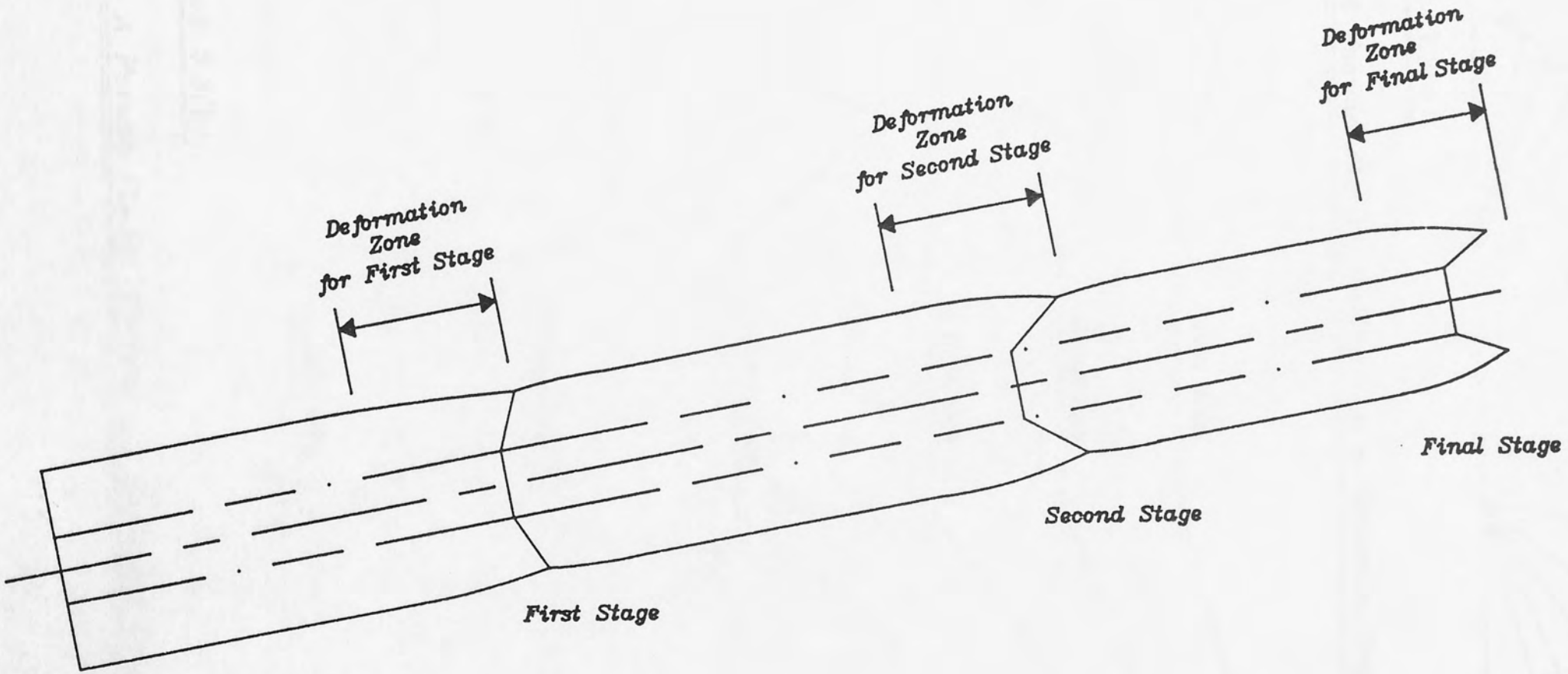

Figure 3.2

Progression of the sheet through the mill showing the deformation regions.

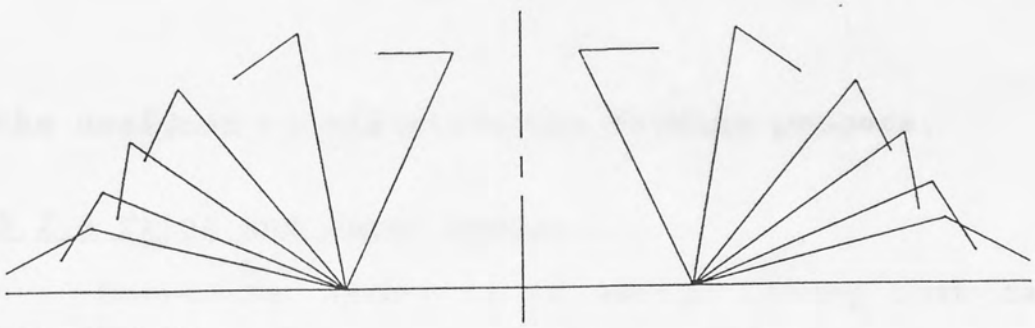

Figure 3.3(a)

A Pseudo Flower Pattern on a Common Origin.

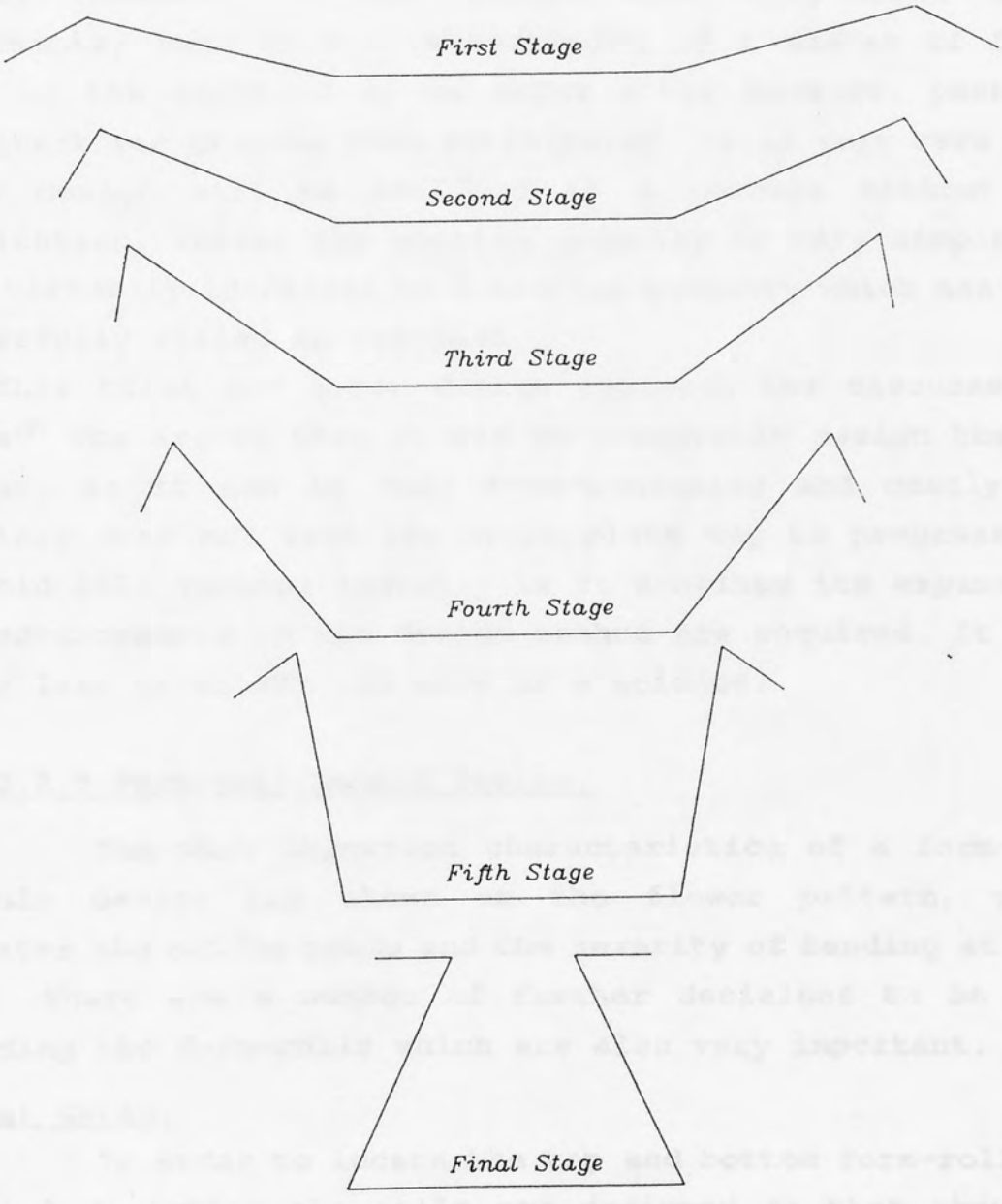

Figure 3.3(b)

A Pseudo Flower Pattern on Separate Origins.

help the designer to visualise the forming process.

3.2.4 Trial and Error Design.

Currently, there is no design theory that can be applied to form-roll schedule design. The designer is totally dependent on the recollection of successful designs used in the past on similar section geometry. In practice, even the most experienced designers submit a schedule design which produces disastrous results when it is tested on the mill. Usually, however, a new design will only need minor adjustments, such as the re-machining of a number of form-rolls or the addition of an extra stage because, perhaps, springback was greater than anticipated. It is very rare that a new design will be verified as a success without any modification, unless the section geometry is very simple, or it is virtually identical to a section geometry which has been successfully rolled in the past.

This trial and error design approach was discussed by Rhodes[8] who argued that it was an acceptable design theory. However, as it can be very time-consuming and costly, it certainly does not seem the appropriate way to progress. If the cold roll forming industry is to continue its expansion, then advancements in the design method are required. It must become less of an art and more of a science.

3.2.5 Form-Roll Detail Design.

The most important characteristics of a form-roll schedule design are shown on the flower pattern, which indicates the active bends and the severity of bending at each stage. There are a number of further decisions to be made regarding the form-rolls which are also very important.

a) Gates.

In order to locate the top and bottom form-rolls in an axial direction the rolls are designed so that they fit closely together. This is achieved by machining profiles on each end of the roll, as Fig 3.4 shows. Usually referred to as "Gates" or "Extended Contours" they are particularly relevant when rolling thick sheet or for a section geometry that is both complicated and unsymmetrical. It is not necessary to

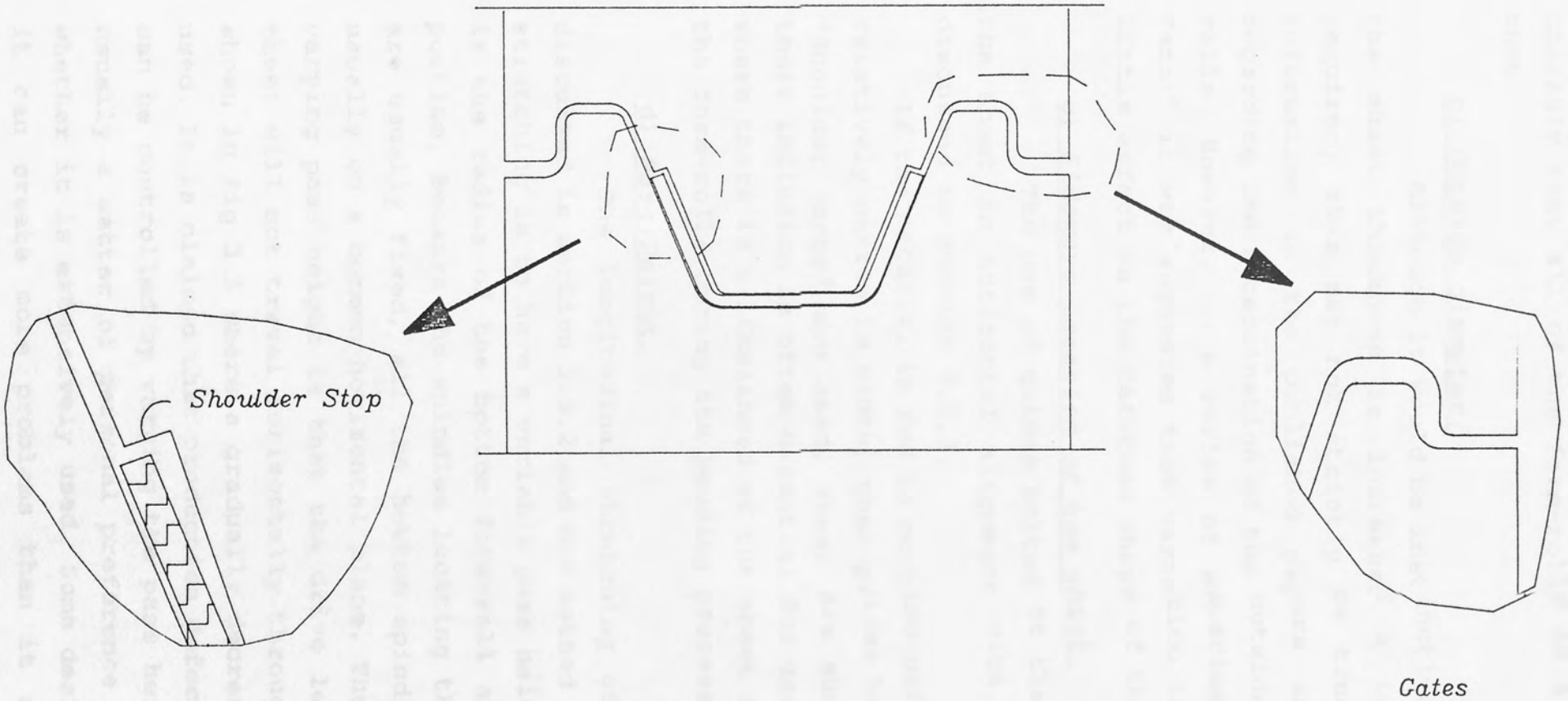

Figure 3.4

An Illustration of Gates and Shoulder Stops.

have gates if bending forces are relatively small, so it is unlikely that all of the form-rolls in a schedule will have them.

b) *Outside diameter.*

Although it would be instinctive to assume that, as the sheet thickness is increased a larger form-roll is required, this may not strictly be true. There is little information in the published papers and research theses regarding the determination of the outside diameters of form-rolls. However, in a series of experiments carried out by Kato[9] it was suggested that variation of roll diameter had little effect on the deformed shape of the sheet.

c) *Sideways location of the sheet.*

The use of guides bolted to the mill frame to keep the sheet in horizontal alignment with the form-rolls was discussed in section 2.2.3.

If the material is fed in continuously from a coil and is relatively narrow in width, then guides become unnecessary if "Shoulder Stops" are used. These are shown in Fig 3.4, and their inclusion is often essential for unsymmetrical sections where there is a likelihood of the sheet slipping sideways in the form-rolls during the bending process.

d) *Pass Height.*

The longitudinal stretching of the sheet will be discussed in section 3.3.2 and one method of balancing out the stretching is to have a variable pass height. The pass height is the radius of the bottom form-roll at its drive surface portion. Because the spindles locating the bottom form-rolls are usually fixed, all the bottom spindles on the mill are usually on a common horizontal plane. The effect of having a varying pass height is that the drive length portion of the sheet will not travel horizontally through the mill. This is shown in Fig 3.5 where a gradually decreasing pass height is used. It is claimed that production defects such as curvature can be controlled by varying the pass height, although it is usually a matter of personal preference (or company policy) whether it is extensively used. Some designers consider that it can create more problems than it actually solves and therefore do not advocate its use.

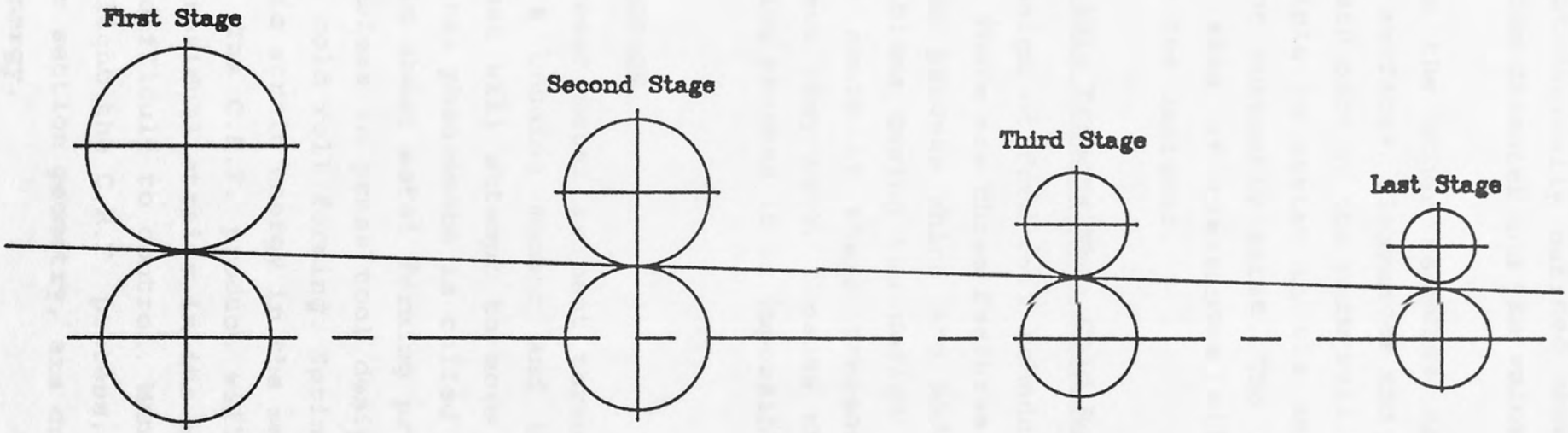

Figure 3.5

Variation of Pass Height by reducing the diameter of the Bottom Form–Roll

e) *Drive Surface, Clearance and Pinch Difference.*

The centre-to-centre distance and the pinch diameters are automatically defined once a decision on the size of the outside diameter and the value of the pass heights has been made.

This leaves the other features discussed in section 2.3.1; the drive surfaces, clearances and pinch differences to be defined for each part of the form-roll. It is apparent that a guiding principle to assist in the design of these three features does not currently exist. The length of the drive surface or the size of clearances will be a subjective decision made by the designer.

3.3 Undesirable Effects When Cold Roll Forming.

The design of form-roll schedules is an extremely formidable task. There are three features associated with the cold roll forming process which are undesirable and create considerable problems during the design operation. Although the designer is aware of their presence and attempts to control the effect they have, because they are an inherent part of the forming process it is impossible to eradicate them completely.

3.3.1 Springback.

When sheet metal is bent through an angle by the application of a bending moment and the moment is then removed, the sheet will attempt to move back to its former shape. This natural phenomenon is called springback and will occur in all cold sheet metal forming processes. It creates considerable problems in press tool design and is even more troublesome when cold roll forming. Springback is due to the release of elastic strain energy in the section following the forming process. The C.R.F. product will have an irregular distribution of residual strains in its section, which makes springback very difficult to control. Many of the production problems which blight the C.R.F. process, such as curvature, wave or erroneous section geometry, are due to the release of elastic strain energy.

The C.R.F. designer will attempt to avoid incorrect

section geometry by bending the metal through a slightly greater angle than is desired. The springback effect will then create the desired geometry. This is called "overbending" and many schedules will have one or more "overbend stages" making up the last few stages of the mill. They usually consist of side-rolls or auxiliary rolls only and if the degree of springback changes (due to a change in material properties for example) a complete stage may be taken out of the forming process.

Prediction of the degree of springback is a most difficult task. Research has shown that it will depend mainly on the material being formed, its thickness and the bend radius. An approximation of springback proposed by Gardiner[10] is one of the most popular ways of attempting to quantify it. Panton[11] used the Gardiner formula in an investigation involving the prediction of the amount of overbend required. Unfortunately, the current research carried out involving springback may not be exactly applicable to cold roll forming. The analysis used by Gardiner was for a bending mechanism similar to a press tool.

Attempts to predict the degree of springback have achieved only limited improvements and it causes considerable problems in all cold sheet metal forming operations.

3.3.2 Longitudinal Straining.

One of the main causes of production defects in C.R.F. products is the longitudinal straining of the section. The effect is illustrated in Fig 3.6 which analyses the travel of the sheet between two stages. Assuming the pass height of both the stages are identical, the idealized movement of point P_1 would be along an orthogonal line in the XY plane, between the stages. The point P_2 will move out of the XY plane during its movement between the stages. Its path will not be linear, although it is shown as a straight line in Fig 3.6 for simplicity. The distance travelled by P_1 is significantly less than P_2, resulting in tensile strains being generated in the region of P_2. Excessive longitudinal strain of the section is both undesirable and unavoidable. The designer can specify a variable pass height, so that the point P_1 will also move along the Z axis as it travels between the stages, which

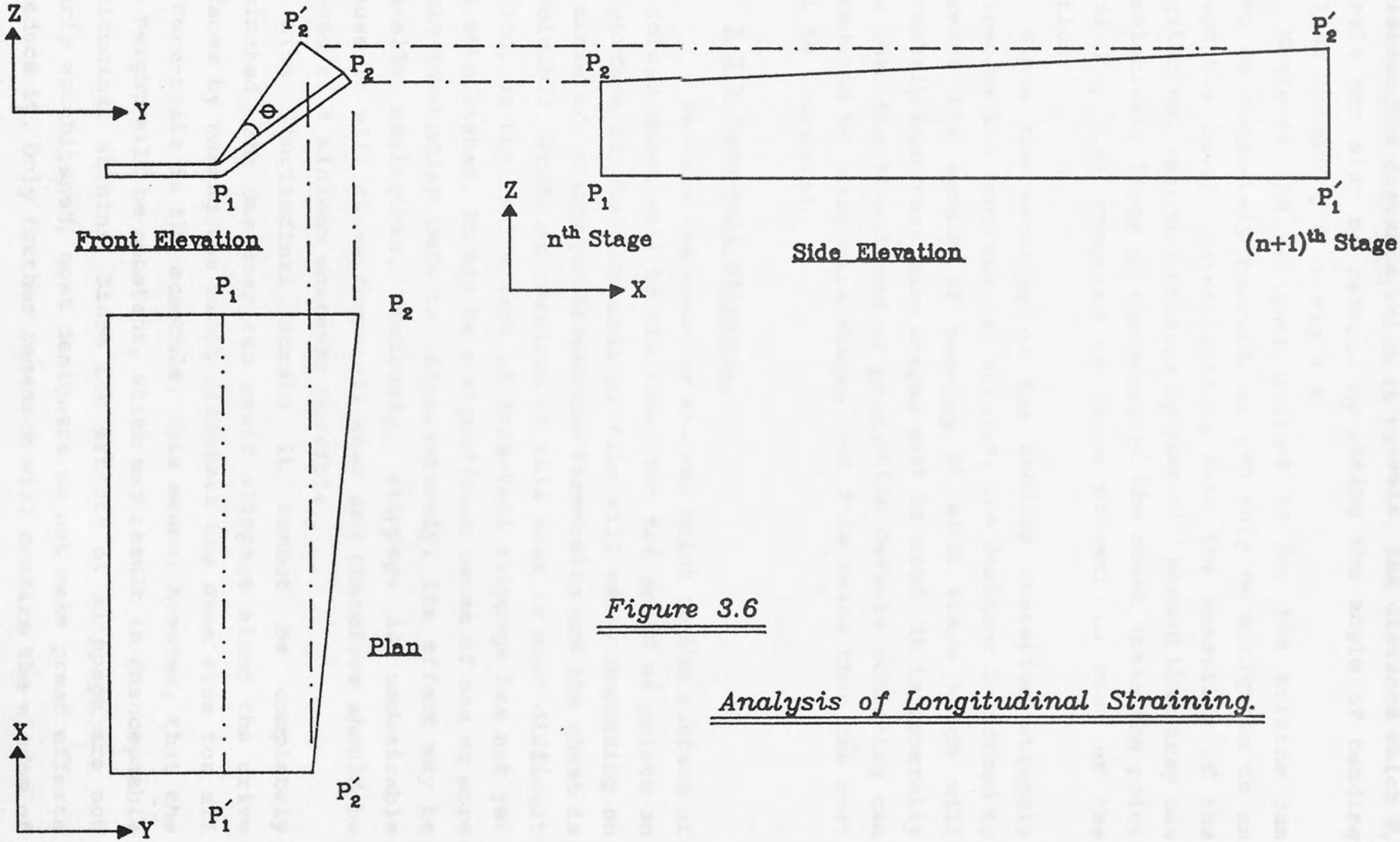

Figure 3.6

Analysis of Longitudinal Straining.

increases the distance which it travels. The distance which P_2 travels can also be reduced by making the angle of bending smaller (reducing θ in Fig 3.6).

Whatever the designer decides to do, the strains can never be completely removed, it can only be mitigated to an acceptable level. Investigations into the measuring of the longitudinal residual strains by Panton[11] showed that they can be relatively large at the edges of the sheet (near the point P_2 of Fig 3.6) compared to those present in rest of the section.

Since the severity of the bending operation strongly influences the longitudinal strains, the designer is forced to decrease the amount of bending at each stage which will ultimately mean that more stages must be used. It is generally true that the likelihood of production defects occurring can be reduced by using more stages, but this means that the cost will be increased.

3.3.3 Form-Roll Slippage.

Because the speed of the any point on the surface of the formed sheet will be the same, but the speed of points on the surface of the form-roll profile will vary, depending on the diameter, slippage between the form-rolls and the sheet is unavoidable. Profound research in this area is most difficult to find, so the real effect of form-roll slippage has not yet been established. It may be a significant cause of one or more of the production defects. Alternatively, its effect may be generally negligible. Obviously, slippage is undesirable because it will cause form-roll wear and therefore should be reduced to a minimum wherever possible.

Like longitudinal strain it cannot be completely eliminated. The designer can avoid slippage along the drive surfaces by making the pinch diameters the same size for all the form-rolls in the schedule. This means, however, that the pass height will be constant, which may result in unacceptable longitudinal strains. Since the effects of slippage are not clearly established, most designers do not make great efforts to reduce it. Only further research will confirm the wisdom of this attitude.

3.4 Mill Setting.

The mill setter can control the quality of the finished section by making adjustments to the mill. Minor anomalies in the design of the form-roll schedule, or changes caused by variation of material properties, can be overcome by the adjustment of a number of settings. Which mill adjustments are chosen will be dependent on the mill setter because they are generally based on past experience. All the setting techniques have the common objective of changing the pattern of straining in the sheet. It is usually a trial and error procedure to obtain the required setting conditions so the value of having an experienced mill setter available is considerable.

A form-roll schedule which involves major design faults cannot be salvaged by the mill setter, but a poor design can be made to produce an acceptable product. The faults created by material property changes can usually be overcome.

a) Adjustment of Vertical Pressure.

The form-roll spindle is moved upwards or downwards to change the force being applied at the drive surfaces.

b) Adjustment of Mill Pitch.

The distance between the stages is either increased or decreased.

c) Adjustment to the Form-Roll Alignment.

Both the top and bottom form-rolls are moved from their previous alignment position (the pinch difference is not changed by this adjustment).

d) Adjustment of Sheet Alignment.

The sheet is moved away from its previous path using guides or idler rolls.

e) Adjustment of Rotational Speed.

CHAPTER FOUR.

CAD/CAM Systems Used In The C.R.F. Industry.

4.1 Introduction.

The computerisation of the design and production facets of an engineering manufacturing company has many advantages and most are applicable to the C.R.F. industry.

When a CAD/CAM system was installed at a local C.R.F. company, Hadley Industries Ltd, Smethwick, a number of substantial benefits followed and the company enjoyed a period of expansion. The most notable improvement occurred in the lead times for the manufacture of new form-roll schedules. The time taken at the design stage was significantly reduced with many time-consuming tasks being carried out by the computer and far less numerical errors were made. An improvement in the standard of design become evident, probably because the designers had more time to spend on the most essential phase of the design, the formulation of the flower pattern. Investment in a CNC lathe, and the CAM software to assist the procurement of the machine control tapes, improved efficiency of the manufacturing phase. Machining times were reduced since the previous method involved a manually operated centre lathe which required a highly skilled operator. The capability of the computer to carry out numerical analysis quickly and without error, allowed the CNC machine control tape to be produced in a much shorter time than was previously possible using manual programming techniques.

4.2 Turnkey and Tailored Systems.

Having made the decision to install a CAD/CAM system, a choice between two fundamentally different types of software package must be made. A "turnkey" system involves a number of smaller commercial packages that have been configured to work together, a task usually done by the vendor. The advantages of this option include the speed of installation since there is no time lag for software development. Most vendors provide an after-sale service which can be invaluable and they may customise one or more of the

packages to suit the company's requirements. The biggest disadvantage is that the packages will be of a general purpose nature unless extensive customisation is implemented. Many of the facilities available in the turnkey system will never be used by the purchaser and some undesirable effects may occur due to the linking together of software packages which are not fully compatible. The general characteristics of the final assembly of packages is often not impressive. A tailored system is the alternative to the turnkey system, where the software has been specially designed for the companies requirements. Included in this group are packages which consists of smaller general purpose packages which have been used as building blocks in an extensive customisation project. The disadvantages of the turnkey system are avoided and the tailor-made package will often provide facilities which could not be obtained without writing the software especially for the task. It is also a system which will be easier to use and understand, which is an important quality for a CAD/CAM package in the engineering industry. The cost will depend on the individual circumstances, but the turnkey system is certainly not always the cheapest.

4.3 Tailor-made Packages used in the C.R.F.Industry.

There are a number of examples of CAD/CAM software packages which have been developed for the C.R.F industry, such as the package developed by Rhodes[12] for "M.T.I.R.A". There have also been publications describing the systems in use in other countries. For example the "ROLLDATA"[14] program used in the United States, and the packages developed for Industrie Secco[13] in Italy , Delta Ltd.[15] in Canada, John Lysaght[16] in Australia and the Kawasaki Tubular Steel Corporation[17] in Japan. All are tailor-made packages for the C.R.F. industry but it is highly unlikely that they are very similar because the nature of the package will always be largely dependent on the individual requirements of the company involved. One major limitation that all the CAD/CAM systems will have is that the generation of the flower pattern will be dependent on the skills of the designer. Some packages do provide facilities which are intended to assist in some of the decisions which have to be made, but none will

automatically generate a flower pattern which is guaranteed to be successful. If the section geometry is very similar to a section which has been rolled in the past, then it is feasible that a CAD/CAM package could recommend a flower pattern based on the knowledge obtained from previously successful flower pattern. Generally, however, all the major decisions involved in flower pattern design will be made by the designer without substantial assistance from the computer.

4.4 The "ROLFOM" Package.

Aston University has developed a CAD/CAM system for the C.R.F. industry called "ROLFOM"; in association with Hadley Industries. ROLFOM is written in FORTRAN 77[18], which is a very common computer language that is particularly efficient when processing mathematical data. Different versions of the FORTRAN language do exist, but the differences are so minor that there is almost one universal FORTRAN language. Because its so popular, compilers or interpreters are available for all of the common processor chips.

For the graphics requirements, the ROLFOM package uses the GINO-F[19] suite of programs. The development work was carried out on a VAX 11/750 at Aston University and was initially installed at Hadley Industries on a ICL PERQ computer. Later it was updated to run on a micro VAX II with a network configuration involving two terminal workstations. The ROLFOM system provides both computer aided draughting computer aided manufacturing facilities. The following two sections give a more detailed description.

4.5 ROLFOM - the CAD Programs.

The CAD software packages used in the engineering industry are often divided into three broad categories. A geometrical modelling package involves the representation and display of solid geometry, usually in three dimensions. Wire-frame models are used extensively due to their simplicity, but there are many other methods which achieve a more realistic situation. Numerical modelling involves a mathematical analysis to obtain a numerical solution which is used to improve the quality of the design. A typical example is a

material stress analysis to assess the load carrying capabilities of a structure, or a control simulation to investigate the stability of a system. Automated draughting allows the rapid and efficient production of engineering drawings. Modifications to the drawings are simple to achieve and the hard copy is usually of a high quality.

The larger CAD packages are a combination of these three categories. The CAD section of the ROLFOM programs is mainly an automated draughting package. Due to the trial and error procedure generally applied in form-roll schedule design, it is essential that modifications to the design drawings are easily carried out. The ROLFOM package does involve a geometrical modelling capability, because a wire-frame model can be generated which provides a visualisation of the bending process. A numerical option is also available since there is a stress analysis program which assesses the strains and predicts the geometry of the sheet between each stage. Both facilities are intended to improve flower pattern design, but their success has been limited. The major success of the CAD section of ROLFOM, when in an industrial environment, was its automated draughting capabilities.

Each of the main programs which constitute ROLFOM's automated draughting software will now be discussed. Because data are taken from the ROLFOM package for the expert system development work and the numerical modelling carried out in this research project, it is important that the purpose of ROLFOM's main CAD programs are described.

4.5.1 Finish Section Program.

This program defines the finish section geometry and calculates the sheet width. The finish section geometry is taken from the production drawing and defines the shape that the cross-section of the sheet should be after travelling through the rolling mill. The ROLFOM user inputs data under a number of headings that are displayed on the screen and the finish section drawing is generated from this information. A limitation of the ROLFOM package is that the finish section drawing, and therefore the profiles of the form-rolls, must have a geometry which is entirely composed of either straight lines or circular arcs. Curves which are not circular cannot

be drawn, although this limitation will rarely be restrictive. The drawings units can either be imperial or metric.

The finish section drawing is produced as a standard draft. The user is requested to input information such as the paper size and details of the title box, when it is required. The general layout of the finish section drawing is not very versatile. For example, it is not a simple task to make major modifications and this can be a considerable disadvantage. An example of a finish section drawing is shown in Fig 4.1 and the data input required to generate Fig 4.1 is given in Appendix 1.

The sheet width is calculated automatically by taking data from the files created by the finish section program, and applying a bending allowance theory to the bend regions. The length of the straight portions of the finish section are simply added together, because it is assumed that their length is not altered by the bending process. Because of the severe plastic deformation that occurs, the length of the flat sheet which makes up the bend region is very difficult to calculate accurately. The strain changes through the thickness of the sheet, from compression at the inside face to tension on the outside face. There will be a layer somewhere within the metal thickness which does not experience a significant change in length. The problem is find the radius of this layer as shown in Fig 4.2. The value of this radius, R_m, has been expressed as being equal to R_i+kt, where k is unknown and R_i is the bend radius. The length of the sheet required to form the bend radius is then found from the simple equation.

$$\text{Arc Length} = R_m\theta$$

The sheet width is estimated by a summation of the lengths of all the linear portions and bend region portions which make up the finish section. The result is placed in the title box on the finish section drawing under the heading "STRIP SIZE".

The American Society of Mechanical Engineers Handbook[20] recommend that k is given a value of 0.4475 and this was used by Angel[4]. There are a number of formulae that have been used in the past, so it is generally a most uncertain area. It is agreed, however, that the value of k will depend on the inside radius of the bend R_i and the material thickness t. This is

Figure 4.1

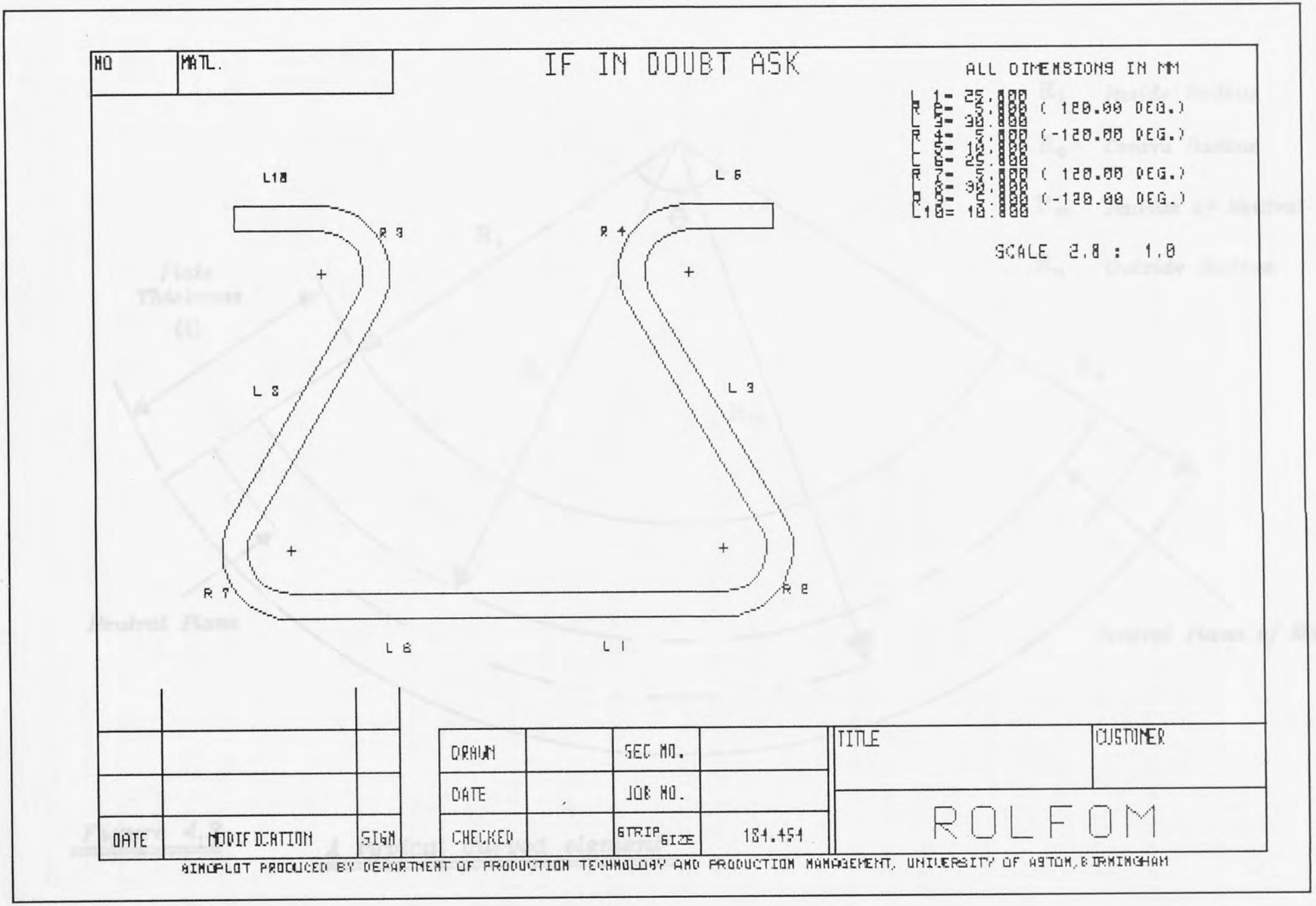
NO
MATL.
IF IN DOUBT ASK
ALL DIMENSIONS IN MM
L 1= 25.000
R 2= 50.0000 (180.00 DEG.)
L 2= 90.0000
R 3= 50.0000 (-120.00 DEG.)
L 3= 150.0000
R 4= 50.0000 (120.00 DEG.)
L 4= 90.0000
R 5= 50.0000 (-120.00 DEG.)
L 5= 10.0000
SCALE 2.8 : 1.0
L10
R 3
L 6
R 4
L 7
L 9
R 7
R 8
L 8
L 1
DATE
MODIFICATION
SIGN
DRAWN
DATE
CHECKED
SEC NO.
JOB NO.
STRIP SIZE
184.454
TITLE
CUSTOMER
ROLFOM
AIMCPLOT PRODUCED BY DEPARTMENT OF PRODUCTION TECHNOLOGY AND PRODUCTION MANAGEMENT, UNIVERSITY OF ASTON, BIRMINGHAM

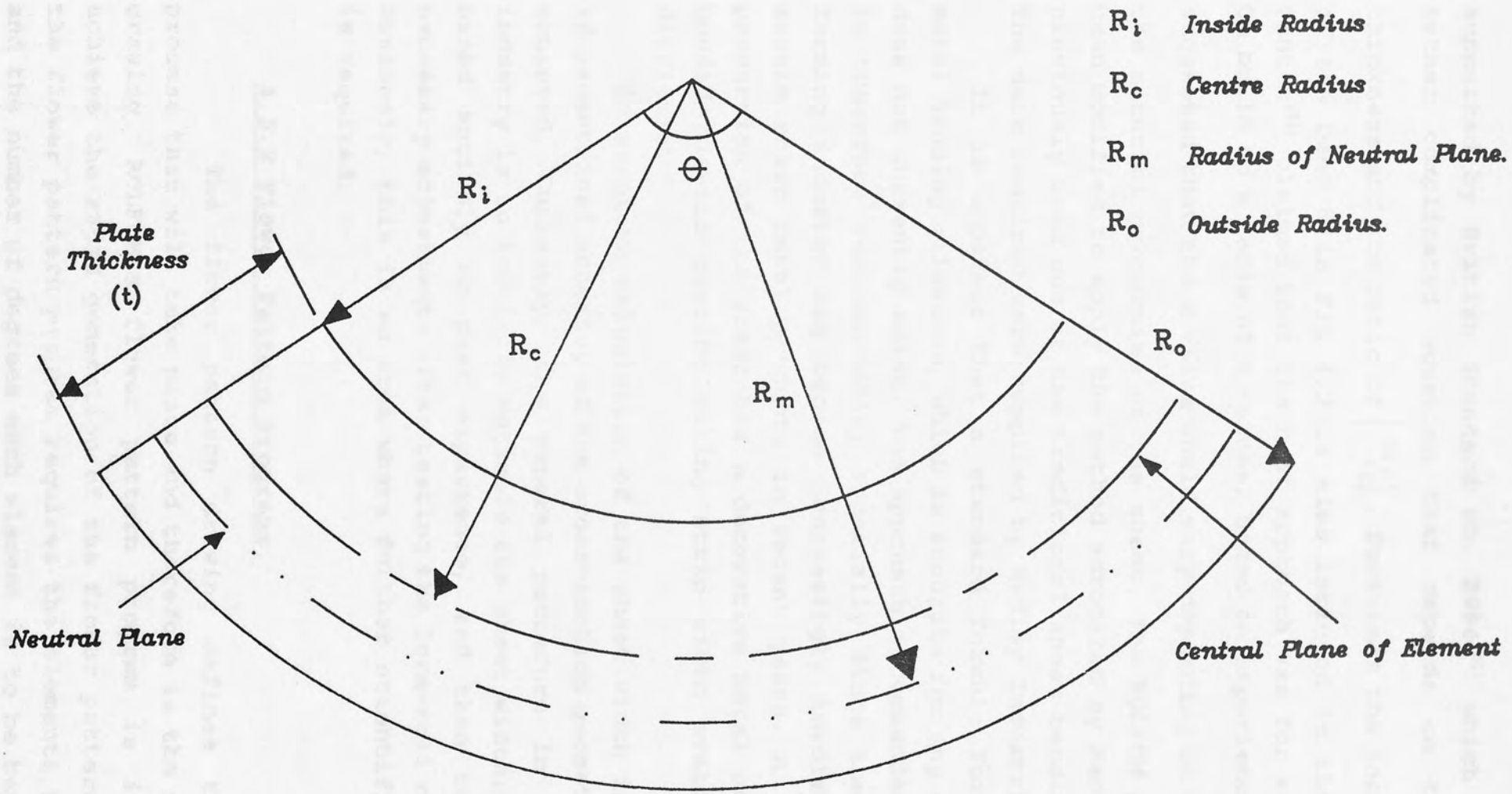

Figure 4.2 *A typical curved element*

supported by British Standard No. 2994[21] which proposes a rather complicated equation that depends on the radius, thickness and the ratio of $\left({}^{Ri}/_{t} \right)$. Sometimes the included angle of the bend θ in Fig 4.2 is also included in the analysis. Panton[11] claimed that the best approach was for each company to build up a table of k values, based on experience alone and suggested that the k value would vary depending on θ, $\left({}^{Ri}/_{t} \right)$ and the material properties of the sheet. The ROLFOM package has been modified to apply the method advocated by Panton, having previously used one of the traditional sheet bending formula. The data required were supplied by Hadley Industries Ltd.

It is apparent that a standard formula for the sheet metal bending allowance, which is accurate for any conditions, does not currently exist. The approach recommended by Panton is therefore recommendable, especially since the cold roll forming industry has become increasingly involved in more exotic sheet metal products in recent years. A significant proportion of the sheet has a decorative metal coating or a bonded plastic coating making strip width evaluation very difficult.

An accurate calculation of the sheet width is essential if geometrical accuracy of the cross-section geometry is to be achieved. Currently, the general procedure in the C.R.F. industry is to initially estimate the sheet width, conjecture based entirely on past experience, and then to make any necessary adjustments after testing the form-roll on the mill. Obviously, this is an area where further scientific research is required.

4.5.2 Flower Pattern Programs.

The flower pattern drawing defines the bending process that will take place and therefore is the main design drawing. ROLFOM's flower pattern program is intended to achieve the rapid generation of the flower pattern drawings. The flower pattern program requires the elements to be bent, and the number of degrees each element is to be bent through, for each stage of the C.R.F. schedule. Data is entered under a number of headings that are displayed on the screen and an

example is shown in Appendix 1. The program acts as an automatic draughting facility and does not assist the user regarding the design of the flower pattern.

There is a choice of output format. The flower pattern can be drawn using either a common or a separate origin. This is illustrated in Fig 4.3(a) and Fig 4.3(b) which shows the forming of a fluted channel section and is solely intended to identify the concept of common and separate origins (it is not necessarily how this section would be formed). The flower pattern program has an edit facility to allow the radii of bend regions to be modified. This is particularly useful if the degree of springback causes problems. The size of the radius at the bend region will strongly influence the amount of springback that occurs.

4.5.3 Template Program.

The importance of the template program has been substantially reduced by the introduction of NC and CNC machinery to manufacture the form-rolls. Originally, it was used to provide information for the production drawings for the manufacture of a template gauge. At Hadley Industries Ltd, the form-rolls were previously manufactured on a manually-operated lathe, with a copy attachment being used to machine the profile. The profile is a metal plate with a thickness of about 3.2 mm, which has the desired profile on a reduced scale machined along one of its edges. When mounted in the copy attachment, it enables the cutting tool to be guided along the required path. If an NC machine tool is available it is not necessary to manufacture template gauges.

The use of NC machining has not made the template program totally redundant. It can be used to provide the geometrical data for the manufacture of the die block used in the flying shear. The geometry of the finish section is produced in the die block by electro-chemical discharge machining. The finish section is accurately located by the die block during the cutting operation. Since the template program stores the geometrical data defining each form-roll profile, it is used to generate the wire-frame model of the bending process which is described in section 4.5.6.

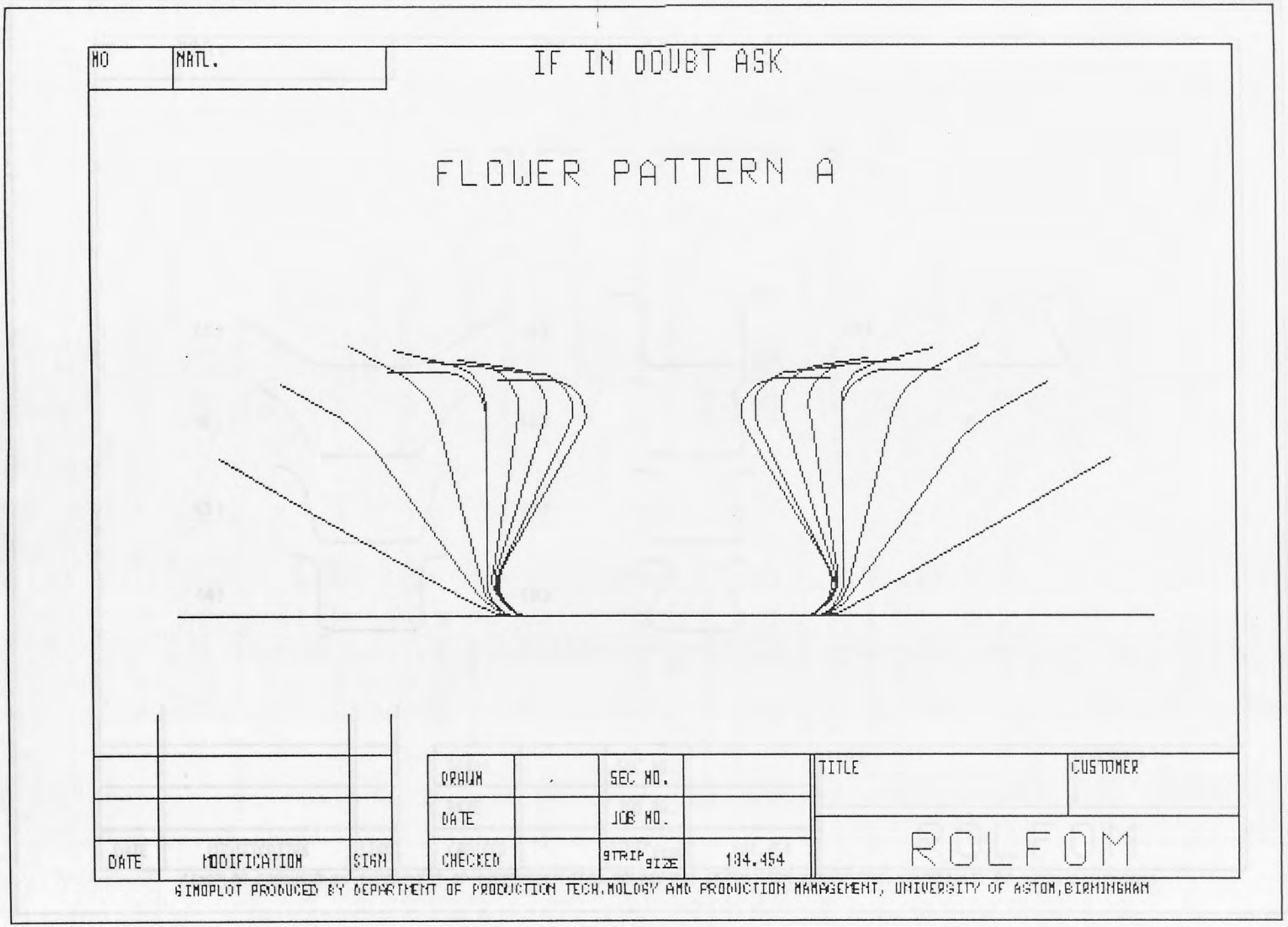
NO
MATL.
IF IN DOUBT ASK
FLOWER PATTERN A
DATE
MODIFICATION
SIGN
DRAWN
DATE
CHECKED
SEC NO.
JOB NO.
STRIP SIZE
184.454
TITLE
CUSTOMER
ROLFOM
SINOPLOT PRODUCED BY DEPARTMENT OF PRODUCTION TECHNOLOGY AND PRODUCTION MANAGEMENT, UNIVERSITY OF ASTON, BIRMINGHAM

Figure 4.3(a)

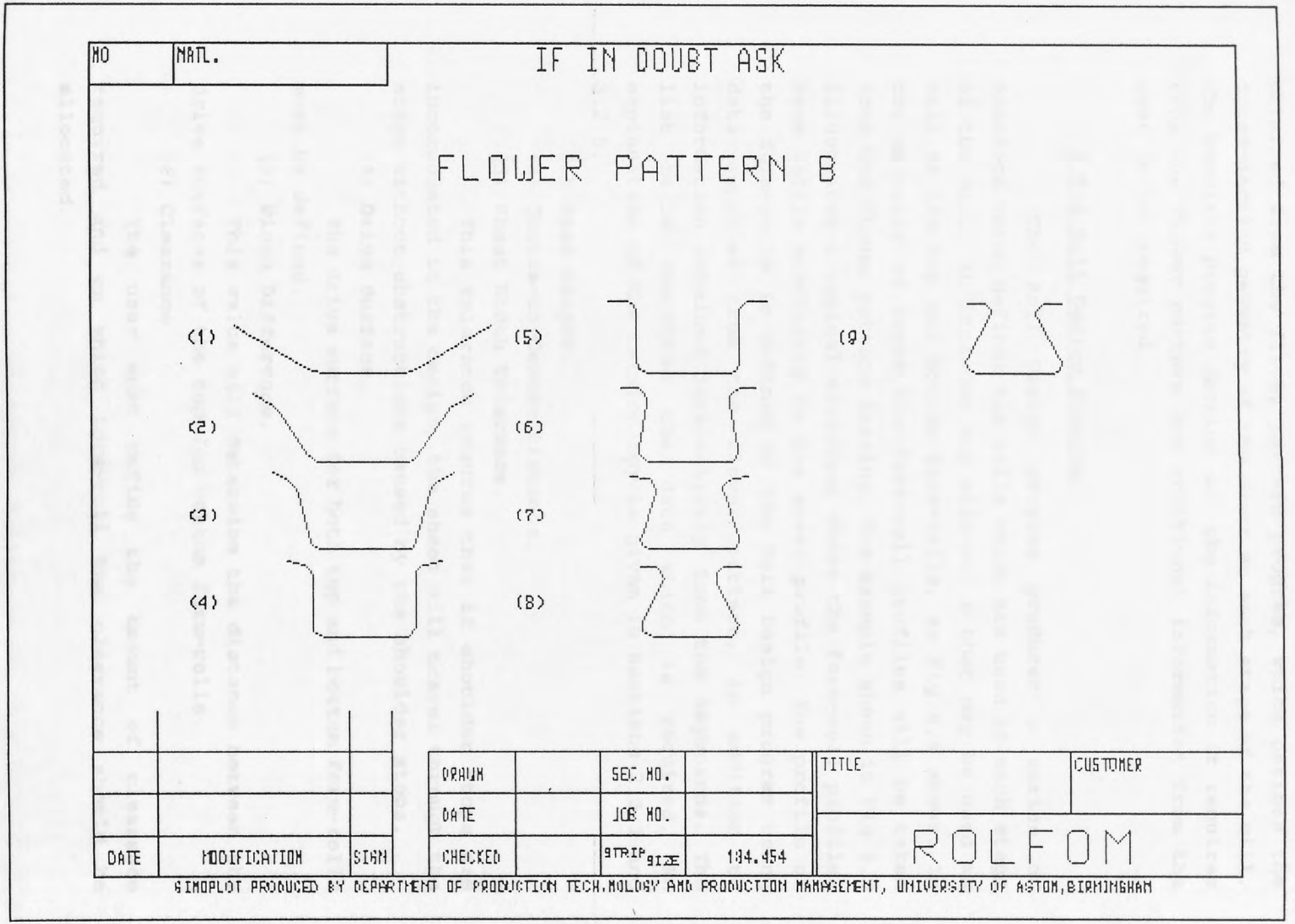
NO
MATL.
IF IN DOUBT ASK
FLOWER PATTERN B
(1)
(2)
(3)
(4)
(5)
(6)
(7)
(8)
(9)
DRAWN
DATE
CHECKED
SEC NO.
JOB NO.
STRIP SIZE
184.454
TITLE
CUSTOMER
ROLFOM
DATE
MODIFICATION
SIGN
SIMOPLOT PRODUCED BY DEPARTMENT OF PRODUCTION TECHNOLOGY AND PRODUCTION MANAGEMENT, UNIVERSITY OF ASTON, BIRMINGHAM

Figure 4.3(b)

The geometrical data of each form-roll profile is obtained from the flower pattern program, which defines the cross-section geometry of the sheet at each stage of the mill. The template program obtains all the information it requires from the flower pattern and additional information from the user is not required.

4.5.4 Roll Design Program.

The Roll Design program produces a series of drawings which defines the rolls which are used at each stage of the mill. It includes any side-rolls that may be used as well as the top and bottom form-rolls, as Fig 4.4 shows. In the majority of cases the form-roll profiles will be taken from the flower pattern drawing. The example shown in Fig 4.5 illustrates a typical situation where the form-roll profiles have little similarity to the sheet profile. The profile of the form-rolls is defined by the Roll Design program using data supplied from the flower pattern, in addition to information obtained interactively from the keyboards. The list below describes the data which is required. An explanation of the terminology is given in sections 2.3.1 and 3.2.5.

(1) **Pass Height.**

(2) **Centre-to-Centre Distance.**

(3) **Sheet Width Tolerance.**

This tolerance ensures that if shoulder stops are incorporated in the design, the sheet will travel through the stage without obstructions caused by the shoulder stops.

(4) **Drive Surface.**

The drive surface for both top and bottom form-rolls must be defined.

(5) **Pinch Difference.**

This value will determine the distance between the drive surfaces of the top and bottom form-rolls.

(6) **Clearance.**

The user must define the amount of clearance required and on which form-roll the clearance should be allocated.

Figure 4.4

PROGRAMMED SCALE = 1.000
PERMISSIBLE XSCALE = 0.625
PERMISSIBLE YSCALE = 0.984
PLOTTED SCALE = 0.625

PASS HEIGHT = 53.340
C-C DISTANCE = 152.600

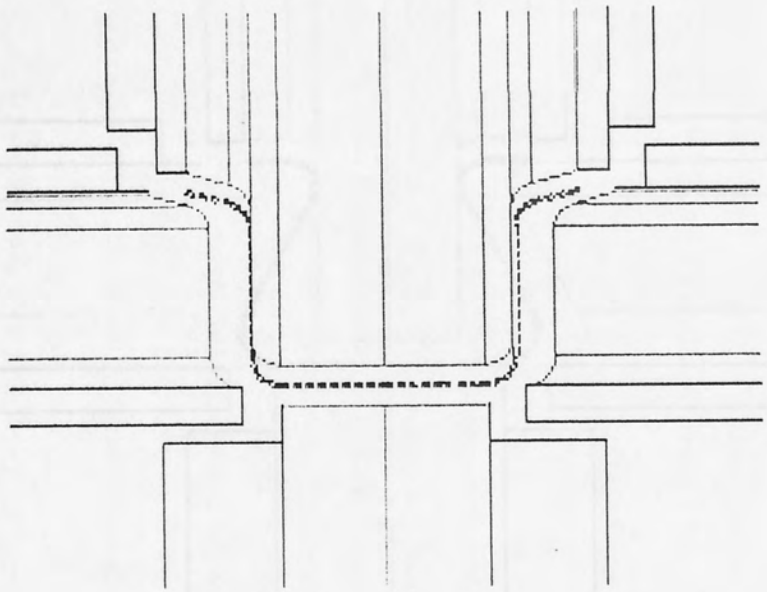

STAGE 4

PROGRAMMED SCALE = 1.000
PERMISSIBLE XSCALE = 0.749
PERMISSIBLE YSCALE = 1.014
PLOTTED SCALE = 0.749
PASS HEIGHT = 53.340
C-C DISTANCE = 147.840
STAGE 9

Figure 4.5

(7) **Gates.**

There are three types of gate available each requiring four dimensions to define.

Information is supplied by the user for each of the stages in the schedule, or, in the case of features such as pass height and pinch differences, it can be defined as a common value for all of the stages.

Some of the stages may incorporate side-rolls. To draw them using the Roll Design Program the user must enter two values from the keyboard. The surface of the sheet which is in contact with the side-roll must be defined together with either the side roll diameter or the distance from the section centre line to the side-roll spindle centre-line. An example of the input required for the Roll Design Program is given in Appendix 1.

Modifications to the form-rolls generated by the Roll Design Program can be carried out using the Roll Editor Program which is discussed in the following section.

4.5.5 Roll Editor Program.

It was explained in section 4.4.1 that the geometry of the sheet section, and hence the form-roll profiles, consist of either straight lines or circular arcs. The ROLFOM package divides up each form-roll profile into either linear or circular arc portions and calls each one an "element". An example of this is shown Fig 4.6. This approach used by the Roll Editor Program allows the user to identify an element and make modifications to it, or to insert an entirely new element into the profile. The following list explains the different options which are available.

(1) Replacing an existing element with a different one.
(2) Inserting a new element at any position on the drawing.
(3) Deleting an element.
(4) Replacing a sharp corner with a circular bend region.
(5) Enlarging a specified area of the drawing to assist the editing procedures.

L1
L2
L3
L4
L5
L6
L7
L8
L9
L10
L11
L12
L14
L15
L16
L17
ROLFOM
E18612T
SC: 1.00

Figure 4.6

4.5.6 Wire-Frame Program.

A wire-frame model of the sheet, as it passes through the form-roll schedule, is generated by the Wire-Frame program. This visualisation of how the metal is formed to the desired shape will identify regions of severe forming and also regions where the severity of forming could possibly be increased. This facility is essentially for the experienced designer, who can make a judgement on whether the forming process is likely to be successful by observing how the sheet is progressively bent to the required geometry. The Wire-Frame model is of less value to an inexperienced eye. An example is shown in Fig 4.7(a) where a roll schedule to form a fluted channel is being analysed. In this particular case the flower pattern was designed for demonstration purposes and, therefore, not intended to show how the sheet should be bent in order to obtain this particular section geometry.

A plan view of the model can also be generated, as Fig 4.7(b) also demonstrates. The Wire-Frame program uses data from the flower pattern and no additional information is required by the wire-frame model.

4.6 ROLFOM-The CAM Programs.

A fully computerised manufacturing system will have computer facilities to plan, control and manage all the routine tasks of a manufacturing plant. The initial introduction of computer aided techniques into industry resulted in the installation of mini and mainframe computers. In recent years, however, there has been a rapid growth in the use of microcomputers linked to a network system. This is largely due to financial reasons, with both the hardware and software being marginally cheaper. The considerable advancement in computer technology, and in network systems in particular, has also made the large mainframe computers less competitive regarding capability and storage capacity.

One of the most important advantages of a CAM system is that it can provide a common link between all the different main departments of a company. Computer aided facilities for inventory planning, forecasting, costing, scheduling, part programming and process planning can provide a communication

Figure 4.7(a)

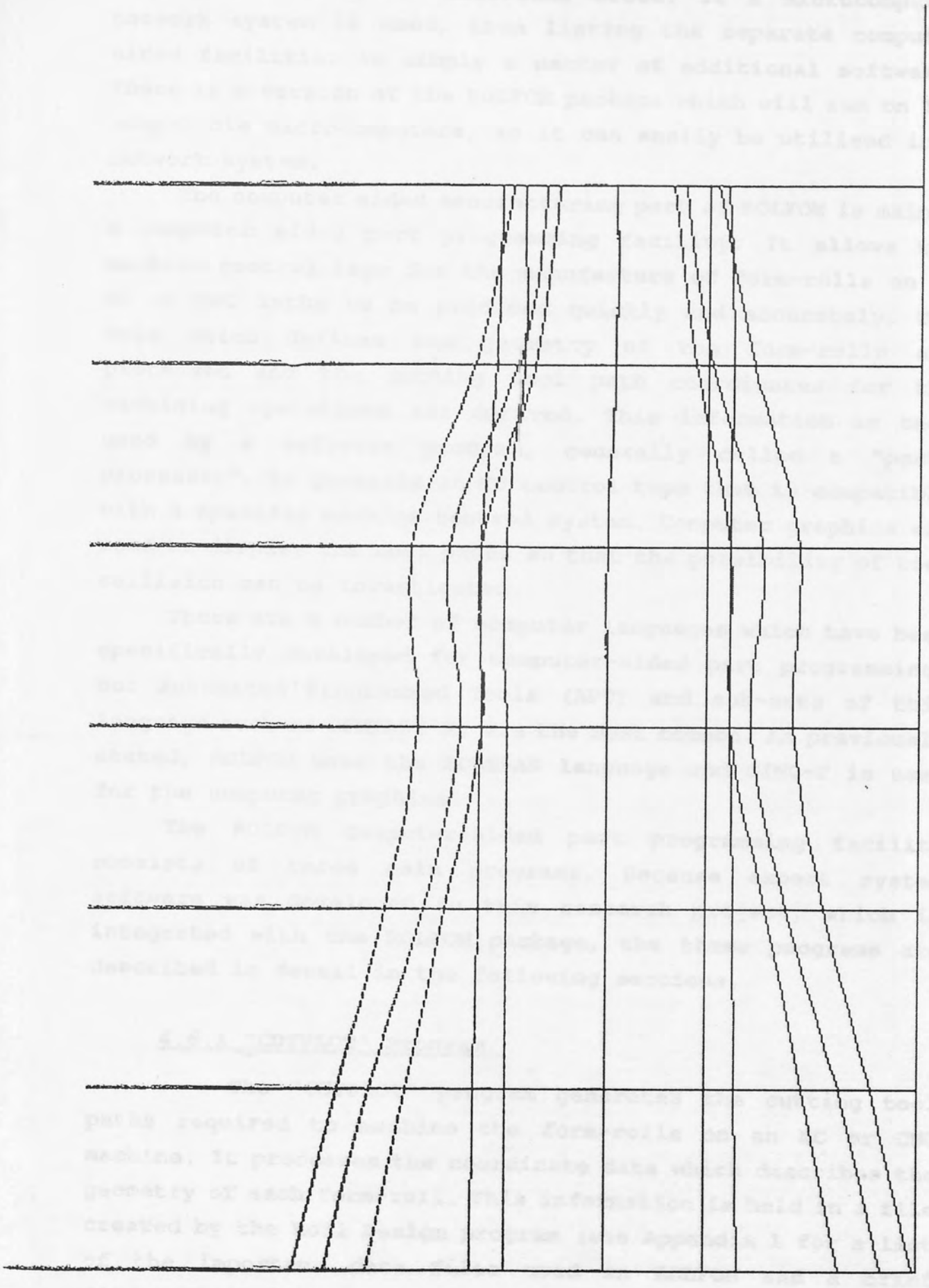

Figure 4.7(b)

framework between the different areas. If a microcomputer network system is used, then linking the separate computer aided facilities is simply a matter of additional software. There is a version of the ROLFOM package which will run on IBM compatible microcomputers, so it can easily be utilised in a network system.

The computer aided manufacturing part of ROLFOM is mainly a computer aided part programming facility. It allows the machine control tape for the manufacture of form-rolls on an NC or CNC lathe to be produced quickly and accurately. The data which defines the geometry of the form-rolls are processed and the cutting tool path coordinates for the machining operations are derived. This information is then used by a software program, generally called a "post-processor", to generate an NC control tape that is compatible with a specific machine control system. Computer graphics are used to display the tool paths so that the possibility of tool collision can be investigated.

There are a number of computer languages which have been specifically developed for computer-aided part programming, but Automated Programmed Tools (APT) and sub-sets of this language such as COMPACT II, are the most common. As previously stated, ROLFOM uses the FORTRAN language and GINO-F is used for the computer graphics.

The ROLFOM computer-aided part programming facility consists of three main programs. Because expert system software was developed in this research project, which is integrated with the ROLFOM package, the three programs are described in detail in the following sections.

4.6.1 "CUTPLOT" Program.

The "CUTPLOT" program generates the cutting tool paths required to machine the form-rolls on an NC or CNC machine. It processes the coordinate data which describes the geometry of each form-roll. This information is held in a file created by the Roll Design program (see Appendix 1 for a list of the important data files used in ROLFOM and a brief description of their contents).

The diameter of the blank required to manufacture each form-roll is calculated by establishing the form-rolls largest diameter and adding 10 mm. From a list of available raw material blank diameters, the diameter which is closest to the value calculated, but larger than that value, is the one that is selected.

To use the CUTPLOT program the user must input the following information.

(1) *The cutting tool to be used.*

A tool must be selected from a tool library. All the tools in the library have had their geometry defined and this data is stored in a file which the CUTPLOT program can access. The radius at the cutting point of the tool is an important dimension is because it is required in the "tool offset" calculations which are discussed in section 5.5.2.

For the tool selected in (1) the following information must be entered.

(2) *Depth of cut.*

(3) *Cutting speed.*

This is entered in revs/min of the spindle speed.

(4) *Cutting feed.*

This is entered in mm/rev of the machine spindle.

(5) *Depth of finish cut.*

If the tool being used is a roughing tool, then this value defines the amount of material left on for the finish tool to remove.

(6) *Elements to be machined by this tool.*

As the profile of the form-roll is divided into linear and circular elements, the elements which this tool will machine must be defined.

One limitation of the ROLFOM part programming facility is that the speed, feed and depth of cut for a particular tool must be defined every time the tool is used. This task, carried out by the part programmer, can be very time consuming.

Hadley Industries Ltd mount the blank on a mandrel which is held in the three-jaw chunk of the CNC lathe and supported by a revolving centre. The blank is first drilled and bored, in order to allow it to be located on the mandrel. CUTPLOT was designed to generate the tool path coordinates for the machining operations to produce the profile on the periphery of the blank. The CNC machine control unit uses a datum of X=0, Z=0 at the centre of the back face of the blank as Fig 4.8 indicates.

The hand of the tools may appear to be incorrect. Both the Mori-Seki CNC lathe at Hadley Industries and the Torshalla (S160) CNC lathe at Aston University locate the tools in the manner indicated in Fig 4.8. This results in the direction of rotation of the workpiece being opposite to a standard manual centre lathe. The right-hand (or R.H.) tool will travel left to right during its cutting traverse and the left-hand (or L.H.) tool will travel right to left.

The rough and finish tool cycles are shown in Fig 4.9 and Fig 4.10 respectively. The L.H. finish tool makes a single cutting traverse from right to left, which produces the specified form-roll geometry. This machining process is similar to that when the cutting tool is guided by a profile copy attachment on a manually-operated centre lathe so, consequently, the operation is often described as "profile machining". The R.H. finish tool has a similar cutting action but the traverse is from left or right.

There are two special machining cycles available, called "POCKET" and "GROOVE" and both are for producing recesses.

(a) **Pocket Cycle.**

The pocket cycle is for machining a relatively large recess and Fig 4.11(a) illustrates the sequence of cutting traverse which are involved.

The cycle uses two tools and the first selection is usually the left hand pocket tool. It cuts into the workpiece and moves down a line, called a "dig_in" line, then traverses from right to left in the normal way as Fig 4.11(a) shows. Following this, the right hand pocket tool is selected to remove the remaining material as shown in Fig 4.11(b). To obtain the specified tolerances for the recess, the right hand and left hand finish tools are used

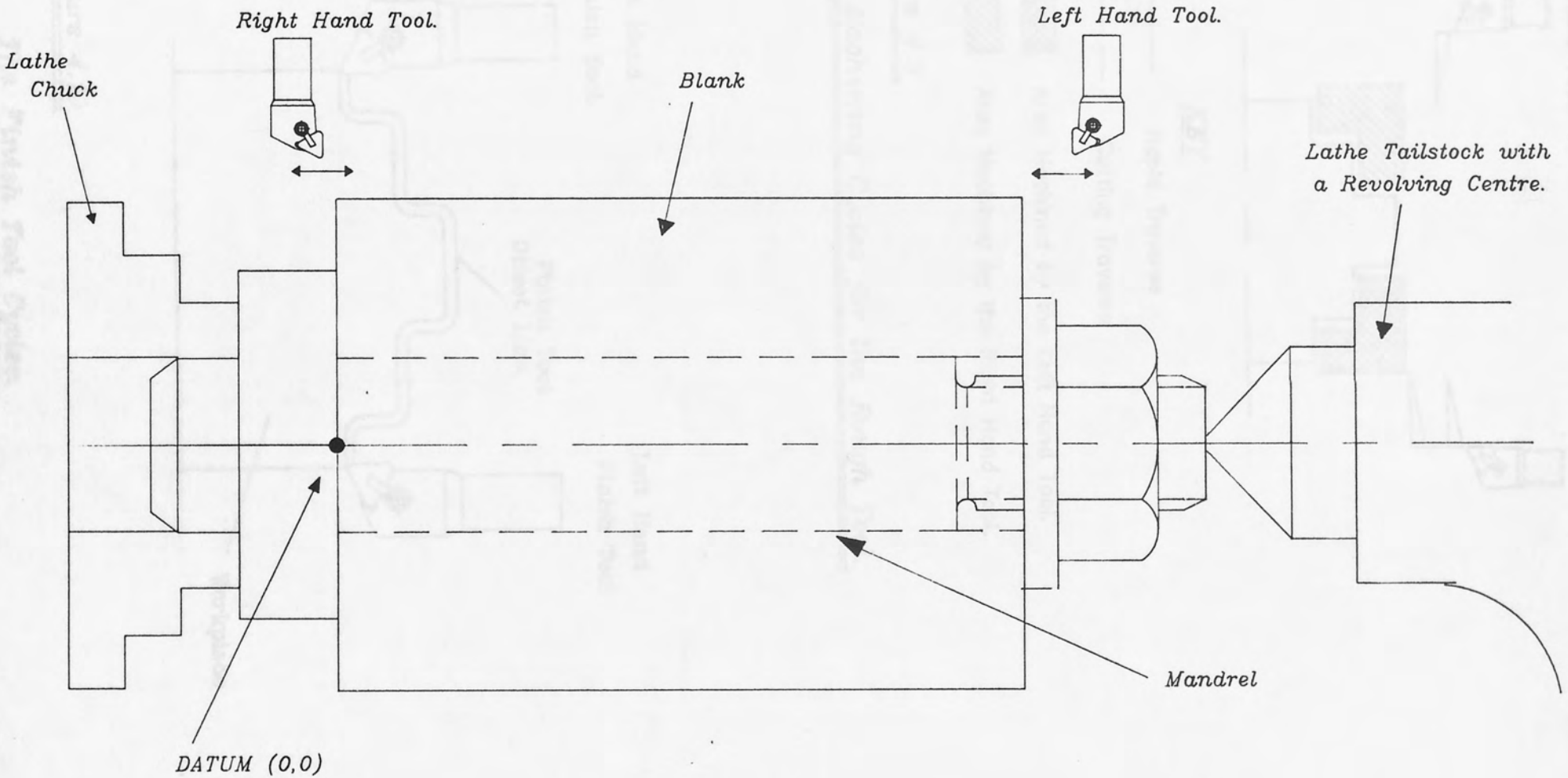

Figure 4.8 The Lathe Mandrel.

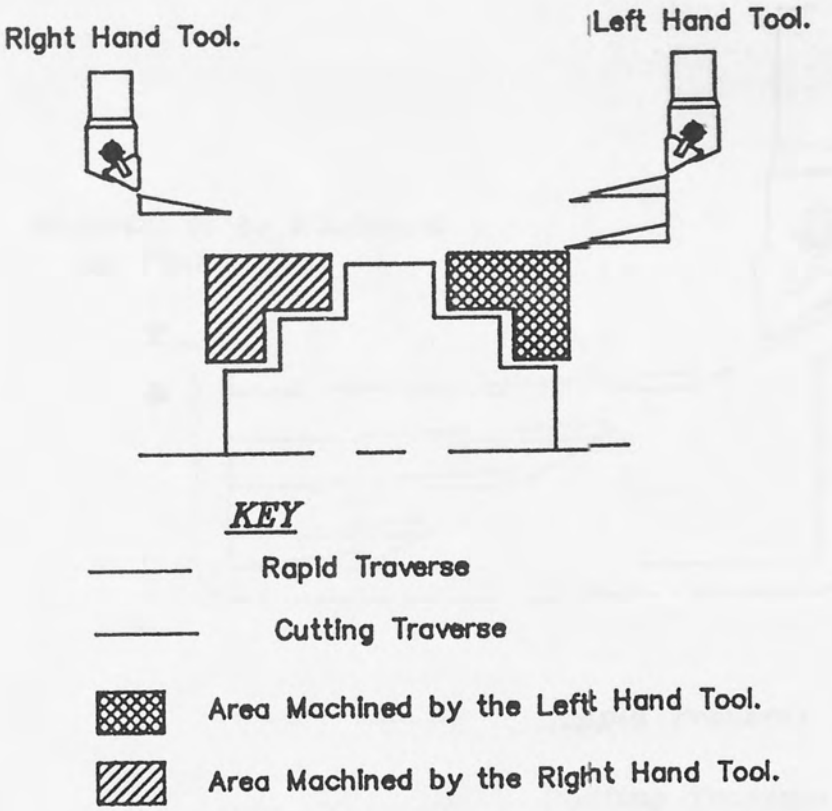

Figure 4.9

Machining Cycles for the Rough Tool.

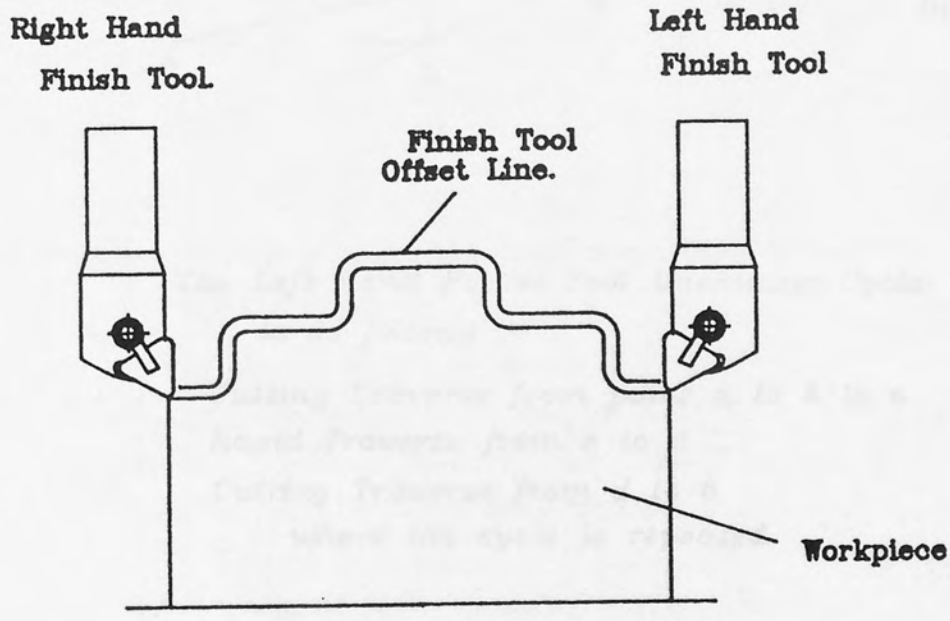

Figure 4.10

The Finish Tool Cycles.

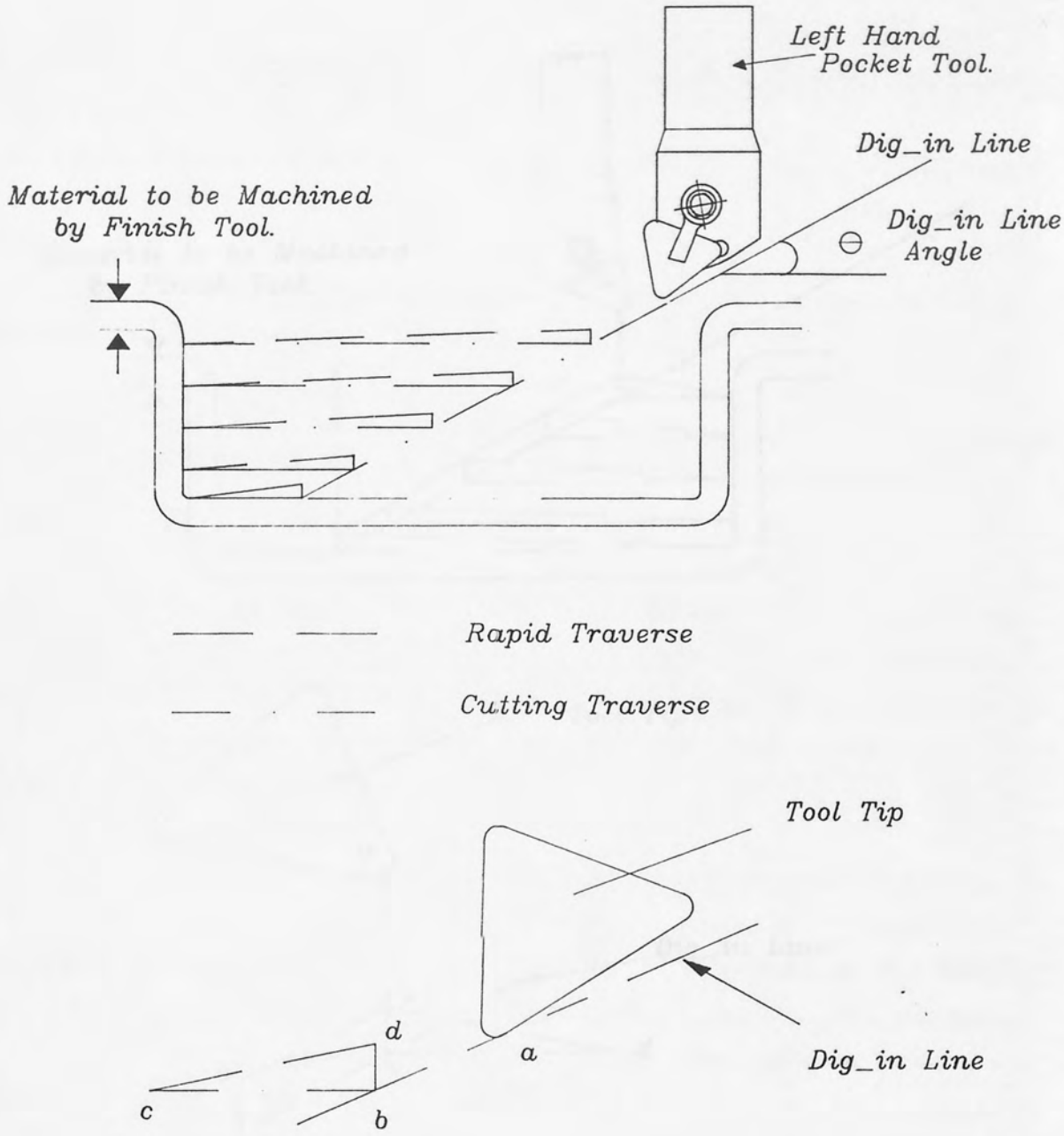

The Left Hand Pocket Tool Machining Cycle is as follows :-

Cutting Traverse from point a to b to c
Rapid Traverse from c to d
Cutting Traverse from d to b
where the cycle is repeated.

Figure 4.11(a)

Machining Cycles for the Left Hand Pocket Tool.

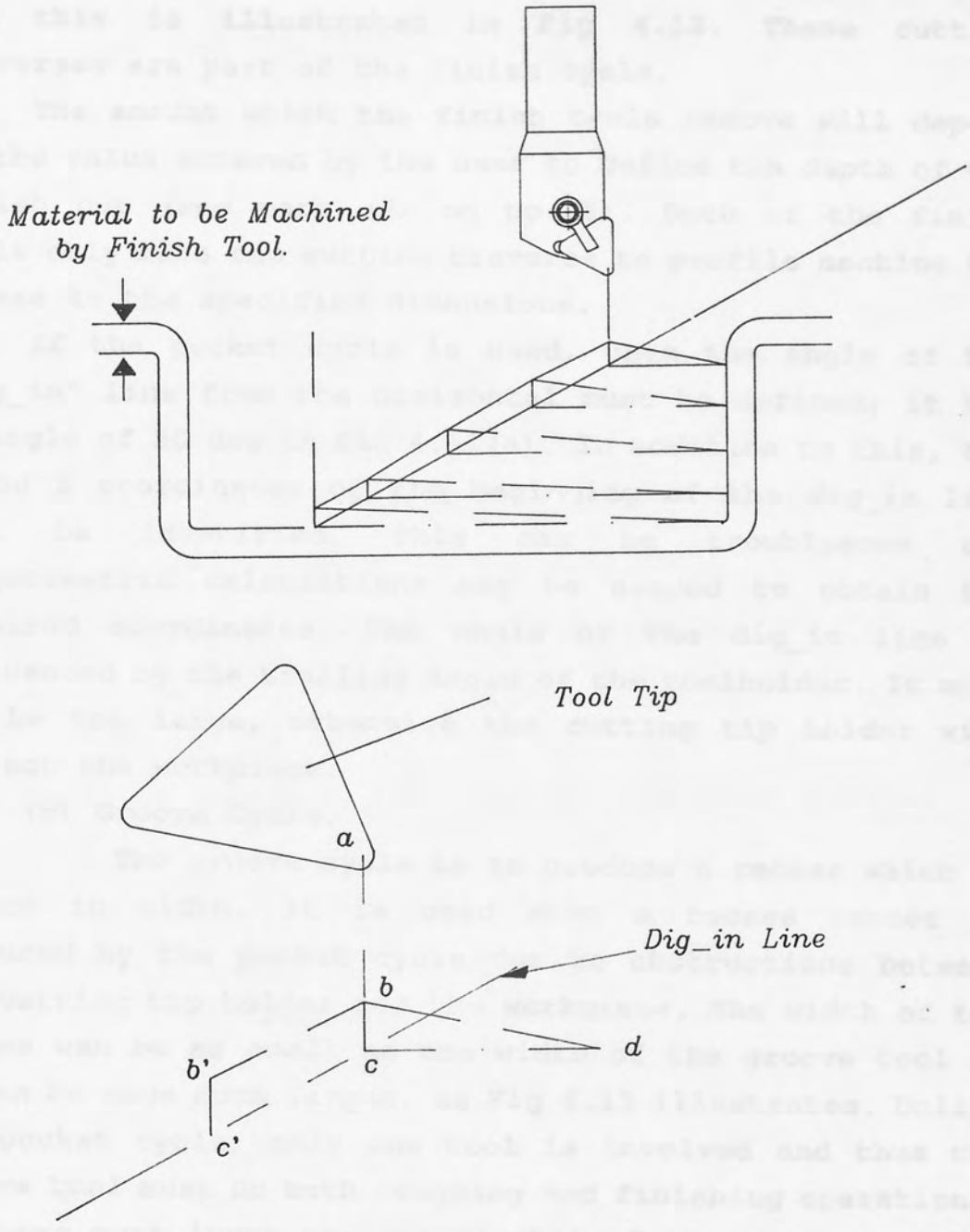

The Right Hand Pocket Tool Machining Cycle is as follows :-

Rapid Traverse from point a to b
Cutting Traverse from points b to c to d
Rapid Traverse from points d to b to b'
where the cycle is repeated.

Figure 4.11(b)

Machining Cycles for the Right Hand Pocket Tool.

and this is illustrated in Fig 4.12. These cutting traverses are part of the finish cycle.

The amount which the finish tools remove will depend on the value entered by the user to define the depth of the finish cut (see part (5) on pp.58). Both of the finish tools only make one cutting traverse to profile machine the recess to the specified dimensions.

If the pocket cycle is used, then the angle of the "dig_in" line from the horizontal must be defined; it has an angle of 30 deg in Fig 4.11(a). In addition to this, the X and Z coordinates of the beginning of the dig_in line must be identified. This can be troublesome and trigonometric calculations may be needed to obtain the required coordinates. The angle of the dig_in line is influenced by the trailing angle of the toolholder. It must not be too large, otherwise the cutting tip holder will contact the workpiece.

(b) **Groove Cycle.**

The groove cycle is to produce a recess which is narrow in width. It is used when a recess cannot be produced by the pocket cycle due to obstructions between the cutting tip holder and the workpiece. The width of the recess can be as small as the width of the groove tool or it can be made much larger, as Fig 4.13 illustrates. Unlike the pocket cycle, only one tool is involved and thus the groove tool must do both roughing and finishing operations. The user must input the coordinates of the start position of the tool and the profile elements which are to be machined. Currently, there is no finish operation using the groove tool in the CUTPLOT program. Hence the surface texture of the machined surfaces is unlikely to be very smooth.

A typical graphical output from the CUTPLOT program is shown in Fig 4.14. The program relies on the skill and diligence of the part programmer. There is no guidance regarding which tools to use and the best speeds and feeds for a particular machining operation. The selection of tools for the pocket cycle can be most important since the angle of the dig_in line must relate to the trailing angle of the tool holder. Unfortunately, the CUTPLOT program does

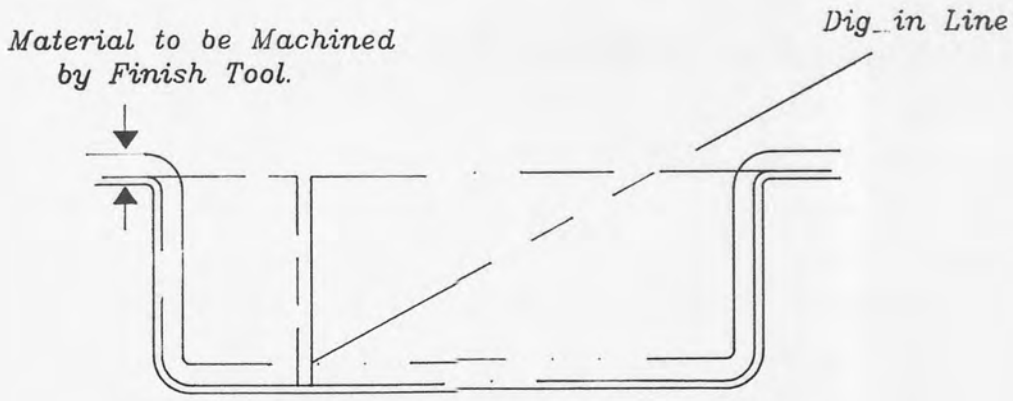

——————— Rapid Traverse for the Left Hand Finish Tool.

— — — — Cutting Traverse for the Left Hand Finish Tool.

— — — — Rapid Traverse for the Right Hand Finish Tool.

——————— Cutting Traverse for the Right Hand Finish Tool.

Figure 4.12

Finish Tool Cycles for Machining a Recess.

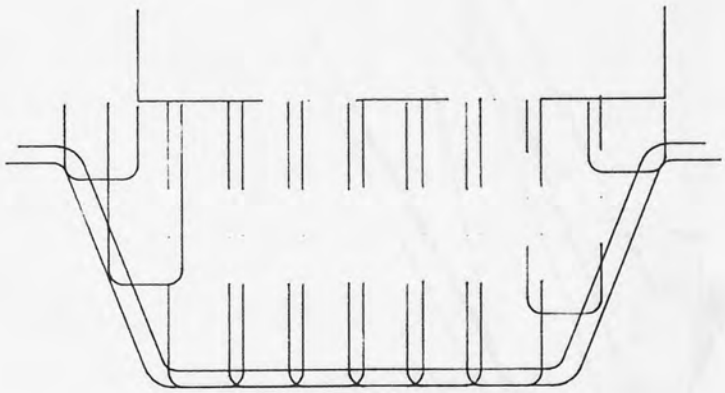

The machining cycle of the Groove Tool is as follows:-

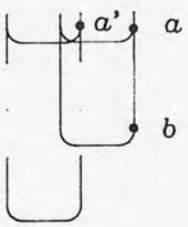

The Groove Tool is positioned at point a

A Cutting Traverse to point b is performed

Rapid Traverse back to point a and continued to a' where the machining cycle is repeated.

The Width of the Groove Tool is indicated by the different line types.

Figure 4.13

Machining Cycle for the Groove Tool.

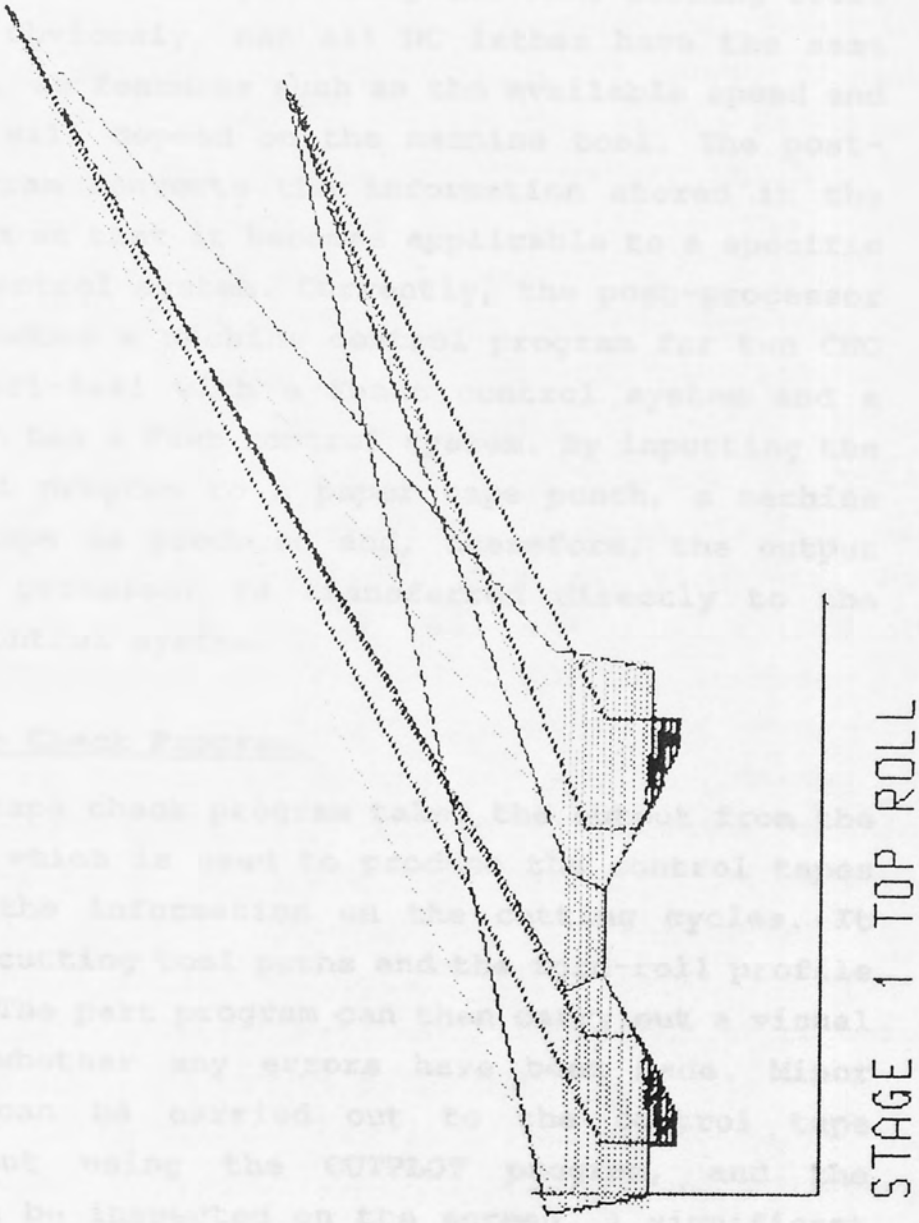

Figure 4.14

not check for possible tool collisions, so mistakes are easily made. A further disadvantage is the requirement of defining the coordinates for the beginning of the dig_in line and the start position of the groove tool for the pocket and groove cycles. This has created difficulties when ROLFOM has been used in an industrial environment.

4.6.2 Post-Processor Programs.

The CUTPLOT program generates the tool path coordinates required to machine the form-roll profiles. Any NC lathe can use the data providing the same cutting tools are employed. Obviously, not all NC lathes have the same control system, so features such as the available speed and feed settings will depend on the machine tool. The post-processor program converts the information stored in the CUTPLOT program so that it becomes applicable to a specific machine tool control system. Currently, the post-processor program can produce a machine control program for two CNC lathes, the Mori-Seki with a Fanuc control system and a Torshalla which has a Saab control system. By inputting the machine control program to a paper tape punch, a machine tool control tape is produced and, therefore, the output from the post processor is transferred directly to the machine tool control system.

4.6.3 Tape Check Program.

The tape check program takes the output from the post-processor which is used to produce the control tapes and processes the information on the cutting cycles. It then draws the cutting tool paths and the form-roll profile on the screen. The part program can then carry out a visual check to see whether any errors have been made. Minor modifications can be carried out to the control tape program, without using the CUTPLOT program, and the alterations can be inspected on the screen. A significant amount of time can be saved by making modifications in this way because the repeated use of the CUTPLOT program can be time-consuming.

4.6 General Review of ROLFOM.

The ROLFOM package has been working successfully in an industrial environment for a number of years. Hadley Industries has been involved in the research based at Aston University from the outset. They have claimed that lead times have been reduced substantially and a general advancement in design standards has been evident. The investment in a CNC lathe and the application of numerical control techniques have resulted in a more efficient form-roll manufacturing operation.

Some progress has been obtained in creating a database of information derived from previously successful designs, particularly regarding the calculation of sheet widths (i.e. the assessment of bending allowance values based on empirical studies). This is an area, however, which will require considerable expansion in future if the full benefits of this approach are to be exploited.

The improvements that the ROLFOM package provided at Hadley Industries is typical of any CAD/CAM software installation at a design and manufacturing company. The trivial and repetitive tasks are computerised and this enables the highly skilled personnel to concentrate their time on more important matters. This explains why the general standard of the design work exhibited a notable improvement. The major limitation of ROLFOM, however, is that it only supports the traditional methods of form-roll design. It does not assist in any way with the design of the flower pattern, it only allows the flower pattern drawings to be drawn rapidly and efficiently. The general quality of the design depends on the skills of the designer, who relies on past experience and the recollection of previous flower pattern designs which were successful on similar section geometry.

Panton[11] attempted to introduce a scientific approach to flower pattern design by applying a numerical modelling technique to the cold roll forming process. The software was considered as unsuitable for its addition to the version of ROLFOM installed in an industrial environment at Hadley Industries. His research, however, did emphasize the considerable complexity of deriving a mathematical model of

the C.R.F. bending process. The development of a design method with a scientific basis for the production of flower patterns is clearly the area to which future research efforts should be directed. The present trial and error approach is evidently not satisfactory.

The reports from Hadley Industries have suggested that the CAM side of ROLFOM would benefit from further research. A significant period of time is usually taken in the procurement of the machine control tapes. An experienced part-programmer with knowledge of CNC machining is an essential requirement. The research carried out by Vasiliou[22], which involved the development of expert system software to replace the expertise of the part-programmer, was aimed at overcoming these limitations. Vasiliou succeeded in building a firm basis for future research and the approach he advocated will provide a major advancement in the overall performance of the ROLFOM package. The software that he developed, however, was limited regarding the form-roll geometry which it could process. Further research was a necessity and the improvements which were carried out in this research project are discussed in the next chapter.

CHAPTER FIVE.

THE EXPERT SYSTEM PART-PROGRAMMING AID.

5.1 Introduction.

The concept of building a machine which has the capability of exhibiting human intelligence has fascinated many great scientists and inventors. With the steady advancement of computer technology, it is no longer a concept that is confined in the realms of science fiction. The representation of factual knowledge in the form of computer software and the manipulation of the software by a process which is analogous to human reasoning, can be achieved by contemporary scientists using powerful computers which are now widely available.

In 1957 a machine called "Perceptron" was built which was an extremely crude model of the retina of the eye, but could recognize certain patterns. It was this type of research project which began to give the concept of artificial intelligence a semblance of realism. Undoubtedly, it was the introduction of extremely powerful computer systems used as research tools that created the opportunity for significant advancement. The research projects based at Carnegie Mellon University in the United States are particularly notable. A major project resulted in the emergence of a software system which could solve puzzles and was given the name "General Problem Solver" or "GPS". Progress in this area was extremely slow and the problem of designing software which could accurately mimic the characteristics of human intelligence remained intractable even with the commissioning of powerful computers. It was largely due to Feigenbaum[23], together with a number of other American researchers like Lederberg[24] and Shortcliffe[25], that a different approach was developed. Software which was capable of solving general problems had to store knowledge from an extremely large area. The knowledge domain was extremely wide and this was the main source of difficulty. In order to continue the progress and subsequently design successful artificial intelligence systems, a means of reducing the size of the knowledge domain became essential.

The result of this predicament was the birth of the expert system concept.

The development of machines that are capable of truly creative thinking would be a monumental step in scientific achievement. The need for such a machine, however, is debatable if the cost and effort involved is assessed alongside the practical value. A machine which can carry out undemanding and mundane tasks, although human intelligence of some degree is still required would, however, be a most valuable asset in an industrial environment. It would free the human, who previously was engaged in doing this work, to concentrate on work that demands a higher level of creativity. Consequently, it is most likely that the majority of expert systems which will be used in industry will be engaged in doing routine tasks rather than being involved in problem solving activities at the highest level.

5.2 The Expert System Concept.

A human of average intelligence will have a knowledge domain which is extremely wide, although there will be no great depth. The human who is an expert on a particular subject will also have a wide knowledge domain, but there will be a great depth of knowledge in the area in which the person is considered to be an expert. In order to solve problems which require a high level of expertise, the human expert will use this knowledge which is a domain that has great depth but is not very wide. The wide but shallow knowledge domain that constitutes general knowledge will not be used.

The problem of a wide knowledge domain resulted in extremely slow progress in projects that attempted to devise a general problem-solving system. It was soon realised that, if the knowledge domain was narrow but deep, instead of very wide and shallow, the prospects of developing a successful software system was considerably enhanced. Consequently, research became concentrated on software that could mimic the problem-solving capability of a human expert, where the problems were not of a general nature but required knowledge from a narrow but deep domain.

Artificial intelligence can be described as the science of making a machine achieve objectives which, if done by a human, would require intelligence. The definition of expert system software is not clearly defined, but it is indubitably a subset of the artificial intelligence concept. Generally, it can be described as computer software which can solve problems by extracting knowledge from a narrow but deep knowledge domain and arriving at solutions using techniques which are similar to those applied by a human expert. If the knowledge domain is wide, then the complexity of the software is greatly increased. Not only will it become much more difficult to rapidly converge on a proposed solution to the problem, but the representation of knowledge, in the form of computer coding, becomes extremely complicated.

5.3 Rudiments of an Expert System.

There has been an abundance of literature and research papers in recent years on the subject of expert systems, particularly from Japan and the U.S.A. Unfortunately, this has resulted in many different terms and definitions being used and conflicting opinions on how the concept of an expert system should be explained. It is generally agreed, however, that all expert systems will have three main constituent parts. These are given the names "Knowledge Base", "Database" and "Inference Engine" in this research thesis, although universally accepted names do not exist. The constituent parts of an expert system are shown schematically in Fig 5.1.

5.3.1 Knowledge Base.

The software routines in the Knowledge Base store the facts and rules associated with the knowledge domain. A totally complete Knowledge Base, containing all the knowledge that exists in the domain, will be impossible to achieve in most cases. It is obviously important, however, that sufficient knowledge is available to solve the problem.

The objective is to capture the expertise of the most experienced and talented human experts in the field and translate it to computer data. How difficult this is depends

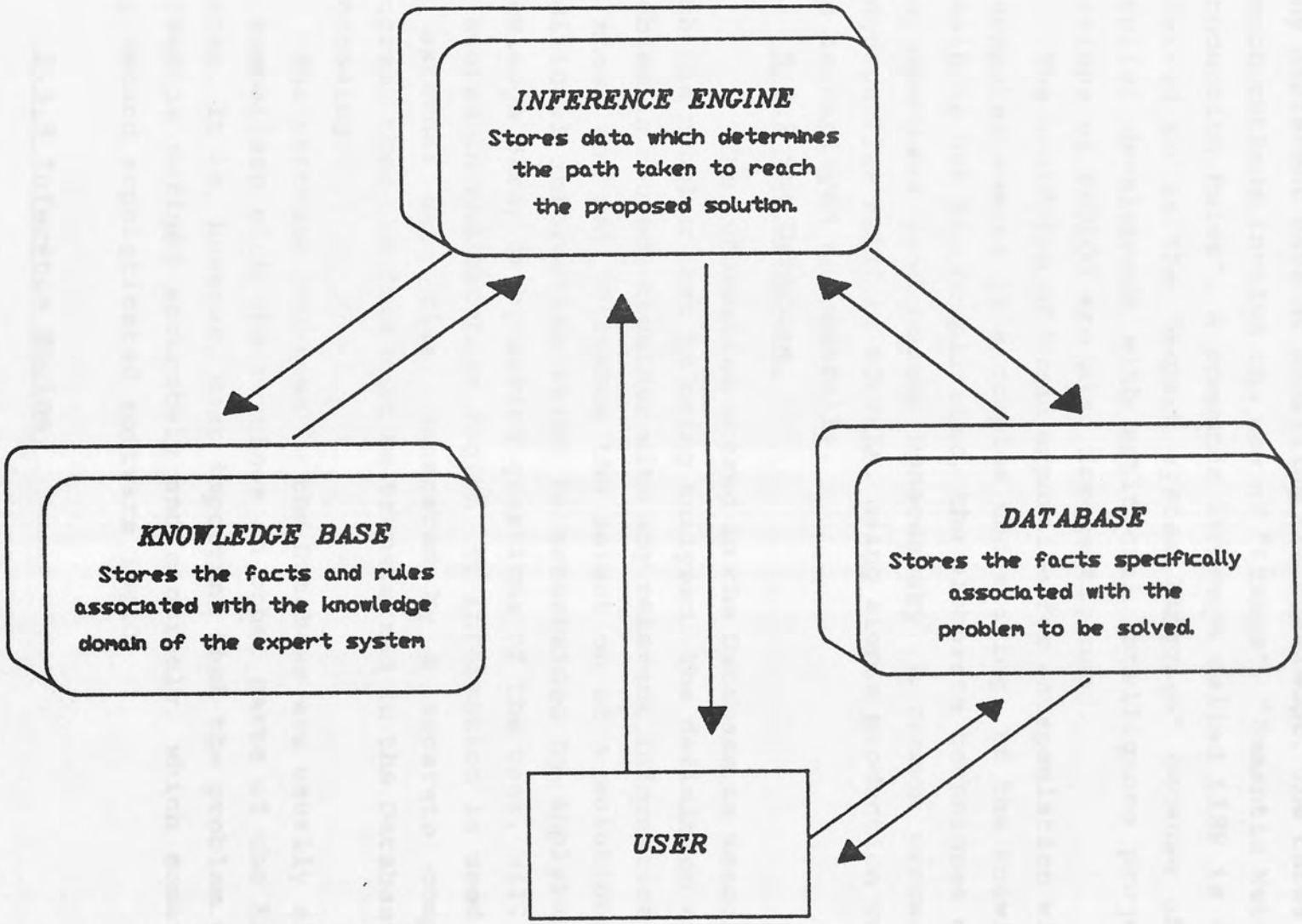

Figure 5.1

Major constituents of an Expert System.

on the complexity of the knowledge in the domain. There are many different ways of modelling the knowledge. The three most common methods involve the use of "Frames", "Semantic Nets" or "Production Rules". A computer language called LISP is often referred to as the "expert system language" because of its parallel development with artificial intelligence projects. Versions of PROLOG are also frequently used.

The codifying of human expertise for encapsulation within a computer memory is a complex undertaking. If the knowledge domain is not too complicated, the elaborate techniques which are sometimes used become unnecessary. A common procedural language like BASIC or FORTRAN, using simple production rules, can be employed successfully.

5.3.2 The Database.

The information stored in the Database is associated with the problem that is being analysed. The definition of the problem is stored, together with any relevant information that is known and may influence the selection of a solution. Any additional information which is ascertained by applying the Knowledge Base, or by asking questions of the user, will also be stored in the Database region. If information is used from an external data file, generated by a separate computer program, then the file must be transferred to the Database for processing.

The software routines in the Database are usually simple in comparison with the routines in other parts of the Expert System. It is, however, most important that the problem to be solved is defined accurately and concisely, which sometimes may demand sophisticated software logic.

5.3.3 Inference Engine.

The Inference Engine part of the expert system is a problem-solving algorithm. It uses the data stored in the Knowledge Base in a sequential manner, depending on a predetermined pattern, and refers to the information held in the Database, with the objective of inferring new facts about the problem. The new information is stored in the Database and this process will continue until the circumstances are reached which allow a solution to be proposed. If the problem is

complicated the large number of different paths to a solution can result in a state of total confusion. The software of the Inference Engine must be skillfully designed to avoid this possibility, but it was this which proved an insuperable obstacle in the development of a general problem-solving software system. An elaborate Inference Engine will adopt sophisticated logic analysis and search techniques to study all the possibilities and select the best one to use under the circumstances which prevail. The quality of an Expert System will largely depend on how rapidly it can converge to a solution. This will be entirely dependent on the efficiency of the Inference Engine. It is often the most complicated software in an Expert System and the most difficult to design. Conversely, in certain cases, the decisions that the Inference Engine makes are extremely trivial. This happens when the rules stored in the Knowledge Base are applied in the same sequence for every problem that is studied. The Expert System is then described as being "data driven" and is likely to converge to a solution in an extremely short time.

5.4 Expert System for Part-Programming.

The CUTPLOT program stored in the CAM part of ROLFOM which was discussed in section 4.6.1, must be used by an experienced part-programmer. There are a number of important decisions which have to be made which require a knowledge of the machining practices on a lathe. The user of the CUTPLOT program has to choose the tool to machine each area of the form-roll profile and decide when the pocket or groove cycles should be employed. The amount of material left on for the finish tools to remove and the selection of speeds and feeds must also be defined. In addition, a number of calculations are usually required to find an appropriate dig_in line angle when pocketing and the starting point coordinates for both the pocket and groove tools. Perhaps more important is the investigation to detect the likelihood of tool collision, which is particularly applicable to the pocket tools. Such tooling must protrude from the toolholder by a certain distance if deep recesses are being machined.

There is profile geometry that the ROLFOM package cannot produce and this must be recognised by the part-programmer. If a recess is too small for a pocket cycle, a groove cycle is the only alternative. Unfortunately, the groove tool can only be programmed to traverse in and out, as Fig 5.2 shows, because there are no facilities in the CUTPLOT program to allow it to "profile machine" like a finish tool. The result is that a small recess can only be machined accurately if its geometry is very simple.

Vasiliou[22] applied the expert system approach to the part-programming facility of ROLFOM in a research project submitted in 1985. He had identified the limitations of the CUTPLOT program and attempted to introduce a more elaborate part-programming facility. The fundamental rules and the basic facts that Vasiliou stored in the Knowledge Base of his expert system were both resourceful and innovative but, unfortunately, there were important limitations. The majority of the software routines were designed to integrate with existing routines in the CUTPLOT program. The overall effect was to make the expert system behave in a rather cumbersome manner. The inspection for a possible tool collision only involved the pocket tools, which were checked to ensure that a suitable dig_in line angle was selected. This important facility was incomplete, since many other possible tool collisions should be checked. However, its main limitation was that neither the groove nor pocket cycles were improved, since the same cycles as in the CUTPLOT program where employed. Only simple recess geometry could be processed.

Vasiliou had shown that the concept of using an expert system as a part-programming aid was both practical and potentially very useful. The expert system which he designed, however, required further development before it could be feasibly installed in an industrial environment.

5.5 "ROLCUT" The Expert System Option.

The CAM part of ROLFOM required further improvement. The major disadvantage of the CUTPLOT program was that it was time-consuming and the user should ideally be an experienced part-programmer. The expert system approach used by Vasiliou overcame these limitations, but it could only process simple

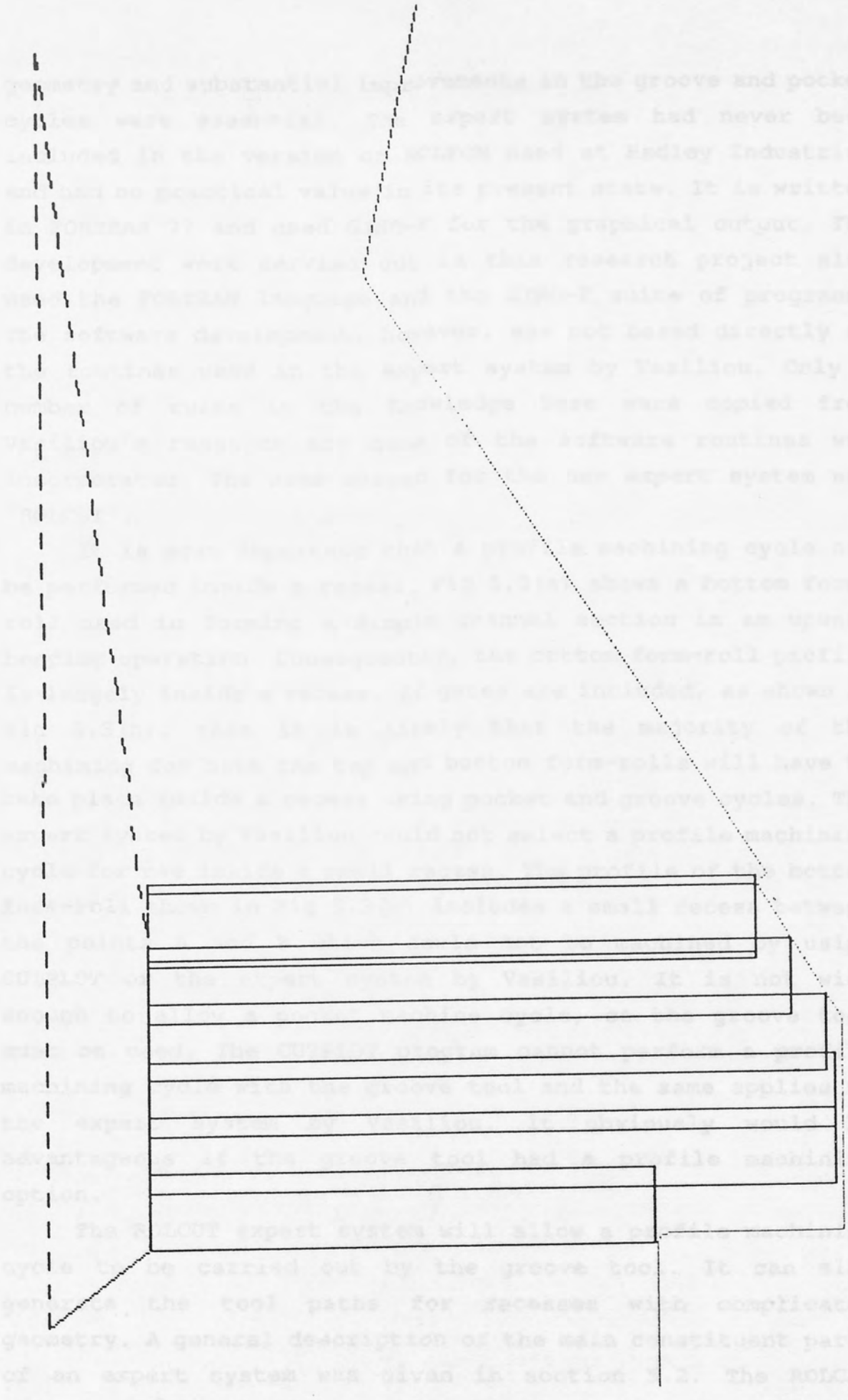

Figure 5.2 Groove cycles created by ROLFOM.

geometry and substantial improvements in the groove and pocket cycles were essential. The expert system had never been included in the version of ROLFOM used at Hadley Industries and had no practical value in its present state. It is written in FORTRAN 77 and used GINO-F for the graphical output. The development work carried out in this research project also used the FORTRAN language and the GINO-F suite of programs. The software development, however, was not based directly on the routines used in the expert system by Vasiliou. Only a number of rules in the Knowledge Base were copied from Vasiliou's research and none of the software routines was incorporated. The name chosen for the new expert system was "ROLCUT".

It is most important that a profile machining cycle can be performed inside a recess. Fig 5.3(a) shows a bottom form-roll used in forming a simple channel section in an upward bending operation. Consequently, the bottom form-roll profile is largely inside a recess. If gates are included, as shown in Fig 5.3(b), then it is likely that the majority of the machining for both the top and bottom form-rolls will have to take place inside a recess using pocket and groove cycles. The expert system by Vasiliou could not select a profile machining cycle for use inside a small recess. The profile of the bottom form-roll shown in Fig 5.3(c) includes a small recess between the points A and B which could not be machined by using CUTPLOT or the expert system by Vasiliou. It is not wide enough to allow a pocket machine cycle, so the groove tool must be used. The CUTPLOT program cannot perform a profile machining cycle with the groove tool and the same applies to the expert system by Vasiliou. It obviously would be advantageous if the groove tool had a profile machining option.

The ROLCUT expert system will allow a profile machining cycle to be carried out by the groove tool. It can also generate the tool paths for recesses with complicated geometry. A general description of the main constituent parts of an expert system was given in section 5.2. The ROLCUT program will now be discussed in detail in the following three sections. The method used to describe the problem in the form of computer code stored in the Database, and the basic

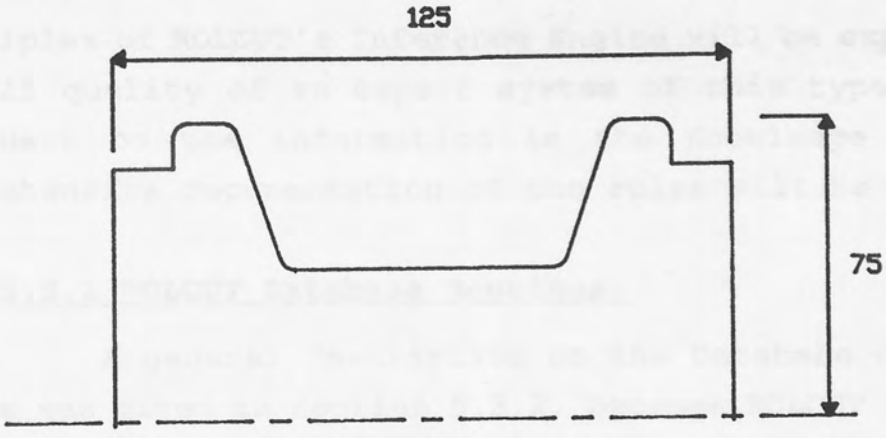

Figure 5.3(a)

A typical Bottom Form–Roll.

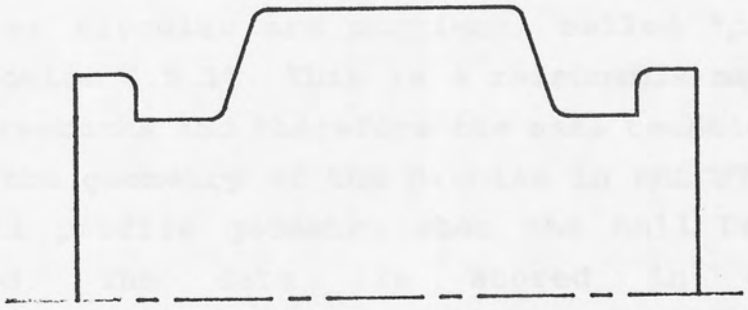

Figure 5.3(b)

A typical Top Form–Roll.

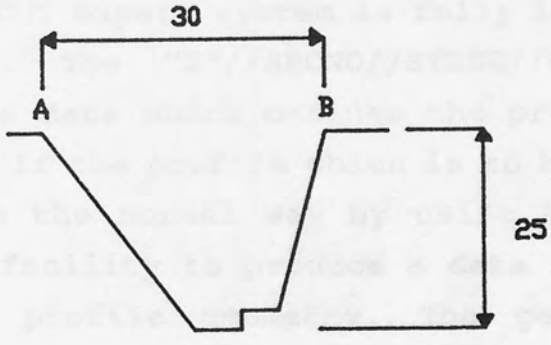

All dimensions are in mm.

Figure 5.3(c)

A small recess requiring contour grooving.

principles of ROLCUT's Inference Engine will be explained. The overall quality of an expert system of this type is largely dependent on the information in the Knowledge Base, so a comprehensive documentation of the rules will be given.

5.5.1 ROLCUT Database Routines.

A general description on the Database of an expert system was given in section 5.3.2. Because ROLCUT is an expert system for the automatic generation of cutting tool paths to produce a workpiece profile on a NC lathe, the problems submitted for analysis will vary depending on the geometry of the profile. The definition of each problem, therefore, requires a description of the profile geometry using a method which is compatible for storage in the Database routines. When ROLFOM is used, each form-roll profile is divided into either linear or circular arc portions, called "profile elements" (see section 4.5.1). This is a reasonable method that has no major drawbacks and therefore the same technique is applied to define the geometry of the problem in ROLCUT. ROLFOM defines the roll profile geometry when the Roll Design program is executed. The data are stored in a file called "**E**"//SECNO//STAGE//POS, where SECNO and STAGE are the section number and the stage number of the profile. POS indicates the position of the roll, (i.e the Top, Bottom roll or the Left or Right hand side rolls). When this file is processed by the Roll Editor program the profile is drawn on the computer screen. The ROLCUT expert system is fully integrated with the ROLFOM package. The "**E**"//SECNO//STAGE//POS file can be accessed and the data which defines the profile is extracted for processing. If the profile which is to be machined has not been defined in the normal way by using ROLFOM, the ROLCUT Database has a facility to produce a data file which is used to define the profile geometry. The geometry definition facility is accessed automatically if the appropriate file generated by ROLFOM cannot be found. An example of using ROLCUT to define the geometry of the profile is shown in Appendix 2.

The "**E**"//SECNO//STAGE//POS file must be processed before it can be used by the Inference Engine software in the ROLCUT program. The Inference Engine routines require the format as

described in Fig 5.4. For each element, nine values are required including the element identification number which must always begin with the element 1 on the left hand side of the profile, as Fig 5.5 illustrates. The numbering of the elements is very important because it influences the simple sort routine which is applied by the Inference Engine software. The final modified data are stored in a file named **"PROFILE"**//SECNO. When ROLCUT is used to generate the profile geometry the data are automatically stored in this format.

The Database stores the coordinates of the cutting tool paths which are generated by the expert system. The coordinate data are modified slightly so that they are compatible with the GRAPHICS program which uses the GINO-F library. This enables the form-roll geometry and tool paths to be displayed on the screen using a similar format (see Fig 5.6). The tool path coordinates are categorized into files and this allows the tool paths for the individual cycles to be displayed. The pocket tool paths, for example, can be displayed separately from the other cutting cycles. This is particularly useful when profile machining cycles are applied following a pocket cycle. A careful inspection of the tool paths can then be made to ensure there are no tool collisions, which is always a likely possibility with this type of machining operation. The tool paths of all the machining cycles can be displayed together, but often this is quite confusing and a careful check for tool collision becomes a difficult task. The advantage of having a sophisticated colour monitor is emphasized when data of this nature are displayed. Each tool can have its path identified by a different colour and some monitors allow a specified area of the display to be enlarged. The main reason for having the option of displaying the tool paths separately for each machining cycle was for the situation where colour monitors and plotters were not available.

A description of the geometry of the cutting tool is stored in a file in the Database. Each tool is given a number which corresponds to the tool station it will occupy in the turret of the machine. Reference should be made to Fig 5.7 which shows the tool library TOOLIB1 which is applicable to the Torshalla CNC lathe at Aston University. The radius of the

Contour Number	Contour Type (1-Linear 2-Circular)	Length or Radius	Angle of Circular Contour	Arc Centre Coordinates		Finish Coordinates		Contour Code
				X	Z	X	Z	

The contours which make up a Form-Roll profile are classified by the "Contour Code". Details of the Code are given below :-

For Linear Contours the Codes are :-

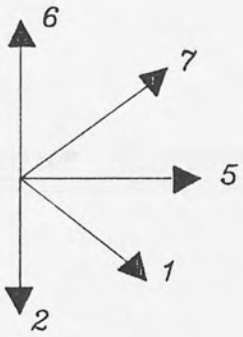

For Circular Contours the Codes are :-

The Contour Codes are organised so that contours with a code of 5 or less will be machined by the Left Hand Tools. Similarly, contours with a code greater or equal to 5 are machined by the Right Hand Tools. Examples of the contours and the corresponding tooling are shown below :-

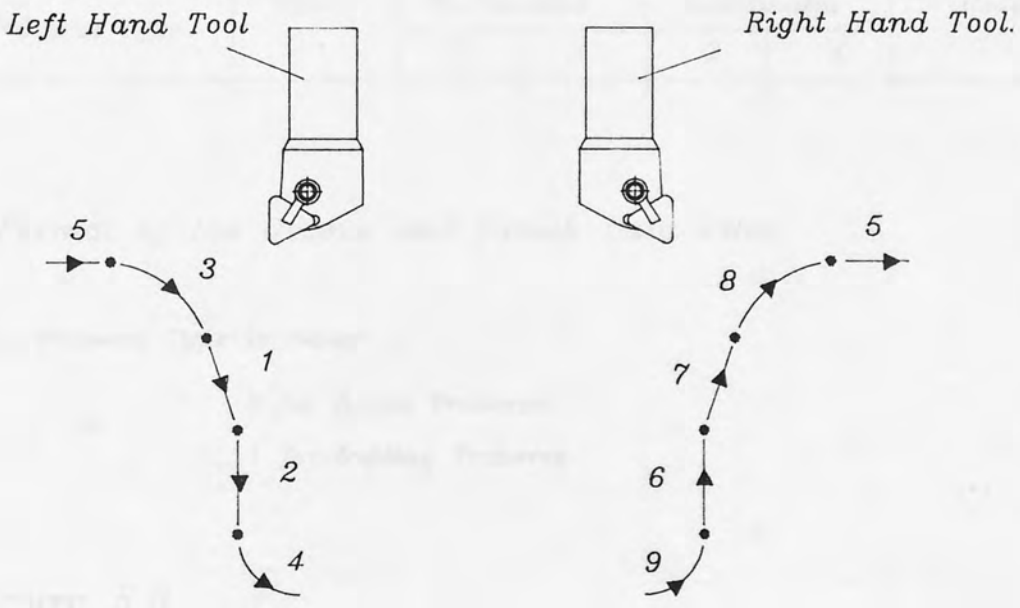

Figure 5.4

Details of Contour Codes.

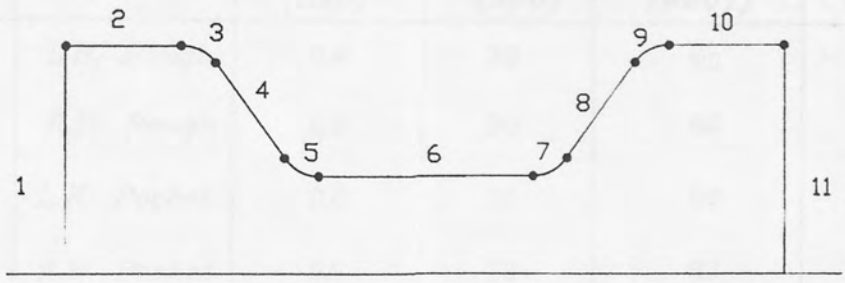

Figure 5.5

Contour Numbering System.

Tool Number or Traverse Type	*Z – Coordinate*	*X – Coordinate*

Format of the Rough and Pocket Data Files.

Tool Number or Traverse Type	*Contour Type*	*Arc Centre Coordinates*		*Finish Coordinates*		*Contour Code*
		Z	*X*	*Z*	*X*	

Format of the Groove and Finish Data Files.

The Traverse Type is either :–

0 for Rapid Traverse

or

1 for Cutting Traverse.

Figure 5.6

Format of the Tool Data Files.

Tool Number	Tool Type	Radius of Tool Tip (RAD)	Tool Trailing Angle (ANG)	Tool Protrusion (PROT)	Tool Width (WID)
1	L.H. Rough	0.8	30	80	30
2	R.H. Rough	0.8	30	80	30
3	L.H. Pocket	0.8	30	80	30
4	R.H. Pocket	0.8	30	80	30
5	L.H. Finish	0.4	30	80	30
6	R.H. Finish	0.4	30	80	30
8	Groove	0.2	-	80	5

Tool Library – TOOLIB1

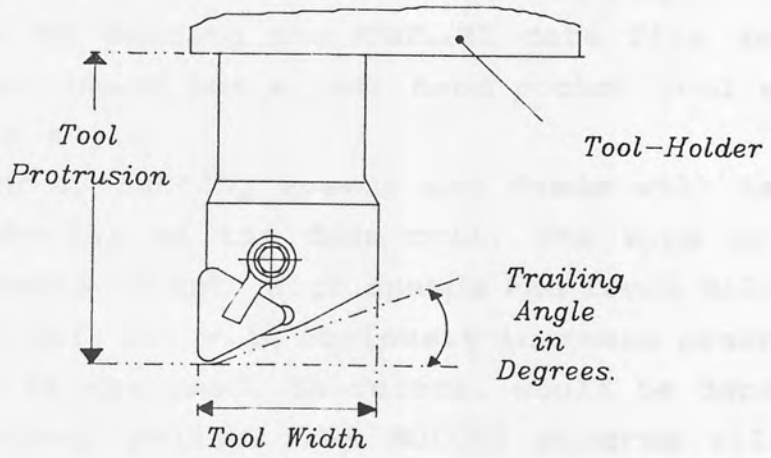

Tool Number	Tool Type	Radius of Tool Tip	Tool Trailing Angle	Tool Protrusion	Tool Width
1	L.H. Rough	0.8	30	80	30
2	R.H. Rough	0.8	30	80	30
3	L.H. Pocket	0.8	45	80	30
4	R.H. Pocket	0.8	30	80	30
5	L.H. Finish	0.4	30	80	30
6	R.H. Finish	0.4	30	80	30
8	Groove	0.2	-	80	5

Modified Tool Library – TOOLIB1

Figure 5.7

Definition of the Tool Libraries

point of the cutting tool tip is particularly important and a value must be entered for all the tools in the library. The reason for this is explained in section 5.5.2 where the tool offset calculations are discussed. The contents of the tool library will depend on the tools available, but the numbering system will be fixed so that tool number 1, in tool station 1, will always be the left hand rough tool. Each tool library only has tool numbers 1 to 8, because the Torshalla lathe has an eight-tool station turret, with tool station 7 not being used. There are five different tool libraries available, each library contains a set of standard tools. The user can create a customised tool library by editing one of the TOOLIB data files and entering information about the tool to be used under the appropriate column, this is also shown in Fig 5.7. This has been produced by editing the TOOLIB1 data file and the result is a library which has a left hand pocket tool with a increased trailing angle.

The selection of cutting speeds and feeds will largely depend on the material of the form-roll, the type of tool involved and the depth of cut. High speeds and feeds will tend to reduce the tool life but will obviously increase production rates. The actual values used, therefore, would be dependent on individual company policy. The ROLCUT program allots a speed and feed to each tool in the tool library, and each type of tool generally has the same value, as Fig 5.8 indicates. The list shown is suitable for the Torshalla lathe tool and this data is stored in a file called "SandF". Clearly, if different form-roll materials are to be machined, the speeds and feeds would have to be altered accordingly. Because the machine setter usually selects the speeds and feeds based purely on past experience, the ROLCUT program has been designed to use customised values. The "SandF" file can be altered easily by editing the appropriate "Speed" and "Feed" columns in the SandF file. The speeds are in m/min and the feed is in mm/rev of the workpiece. This means that the speeds and feeds of the tool are easily changed if any problems arises.

The output from ROLCUT must be compatible with the Post-processor program in ROLFOM, because this program is used to produce the machine control tapes. ROLCUT only replaces the

Machine Cycle	Tool Type	Speed (m/min)	Feed (mm/rev)
Rough	Left Hand Tool	95.755	0.05
	Right Hand Tool	89.771	0.05
Pocket	Left Hand Tool	71.816	0.05
	Right Hand Tool	65.832	0.05
Groove	Groove Tool	47.877	0.08
Finish	Left Hand Tool	1436.3	0.13
	Right Hand Tool	1412.4	0.13

Figure 5.8

Typical speeds and feeds for machining Mild Steel.

CUTPLOT program; the Post-processor and Tape Checking programs are still required. This is achieved using the CONVERT program which transforms the data created by ROLCUT into the appropriate format.

The profile to be machined can be described as the "problem" and the generated cutting tool paths as the "solution". Both the problem definition and the proposed solution are stored in the Database region, which generally follows the standard practices in expert system design. Any additional information which is related to the problem and will influence the selection of the solution is also stored in the Database. This is why the modified profile geometry data used by the Inference Engine, the geometry of tooling and the speeds and feeds to be used are all stored in the ROLCUT Database.

5.5.2 ROLCUT Inference Engine.

A general description of the Inference Engine of an expert system was given in section 5.3.3. The type of expert system required to machine profiles on a lathe does not require complicated Inference Engine software. The selection of the rules from the Knowledge Base is relatively straightforward. The main reason for this is that all the problems presented to the expert system are similar, so they are solved by applying the same procedures every time. If the expert system is written in a procedural language such as BASIC or FORTRAN the rules can be applied in a fixed order automatically, due to the structure of the coding. Software routines to select rules from the Knowledge Base will be unnecessary. This is why a "data driven" expert system, where every rule is applied in an identical order for every problem, can have an extremely trivial Inference Engine, with no software routines specifically dedicated to rule selection.

ROLCUT does not have a "data driven" Inference Engine. The rules are grouped together in the Knowledge Base, however, and the groups are applied in the same order regardless of the profile geometry. It is not a "data driven" system but it is only marginally more sophisticated.

Before the tool paths are calculated, the Inference Engine applies a software routine stored in the Knowledge Base to convert the geometrical data into the format which the ROLCUT program requires. This is applicable only if the profile has been defined using ROLFOM's CUTPLOT program. The software routine which converts the data is called the "PROFDAT" routine.

The raw material blank diameter is determined using a software routine called "BLANK" which refers to a file in the Database that defines the available standard blank diameters.

During the calculation of the tool paths for the machining cycles, the Inference Engine software must apply a group of rules in the Knowledge Base called the "OFFSET" rules. The machine control unit of the CNC lathe will locate the position of the coordinates of the centre point of the radius of the cutting tip, as Fig 5.9(a) indicates. It is, therefore, necessary to calculate the locus of this datum point when generating the cutting tool paths. It is the path of this point which is displayed by the GINO-F software routine. The definition of a profile element offset path is given in Fig 5.9(b) and, for every element which is machined the corresponding offset path must be calculated. These calculations are based on simple trigonometry. A detailed account of the mathematical analysis involved in establishing the tool offset path is given in Appendix 2. The Inference Engine software will select the PROFDAT, BLANK, and OFFSET groups of rules stored in the Knowledge Base whenever they are required in the analysis.

The major part of the ROLCUT Inference Engine, however, is the "SORT" routines, which directly control the order in which the groups of rules, stored in the Knowledge Base, are applied. The rule selection procedures and the importance of the SORT routine will be explained using the example shown in Fig 5.10 which shows a profile which requires both the pocket and groove cycles to be applied. All the figures involving cutting tool paths shown in the remaining part of this chapter are examples of the graphics output from the ROLCUT program.

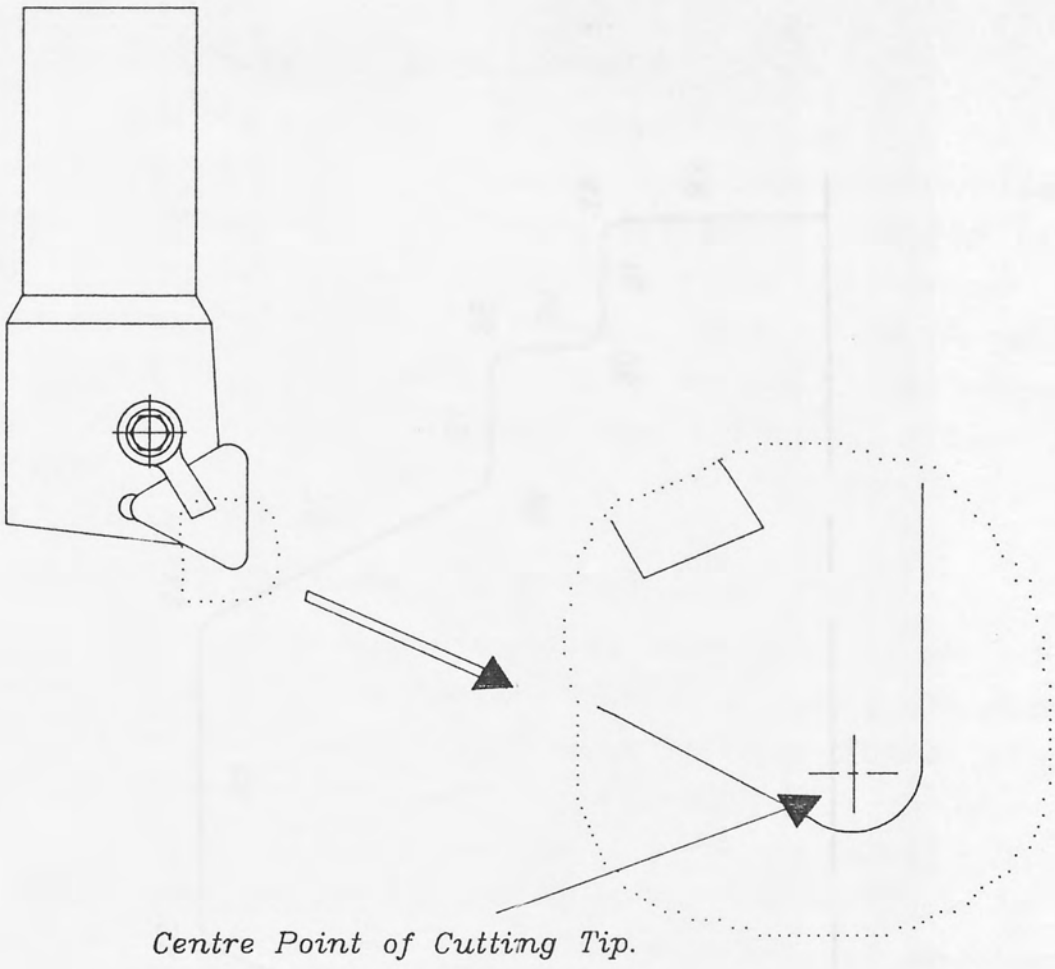

Figure 5.9(a)

Location of Centre Point of Tool Tip.

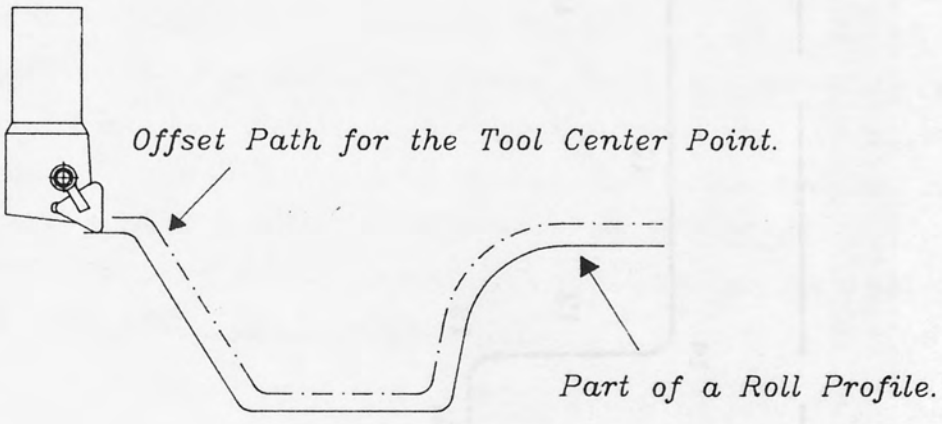

Figure 5.9(b)

Offset Path of Tool Tip.

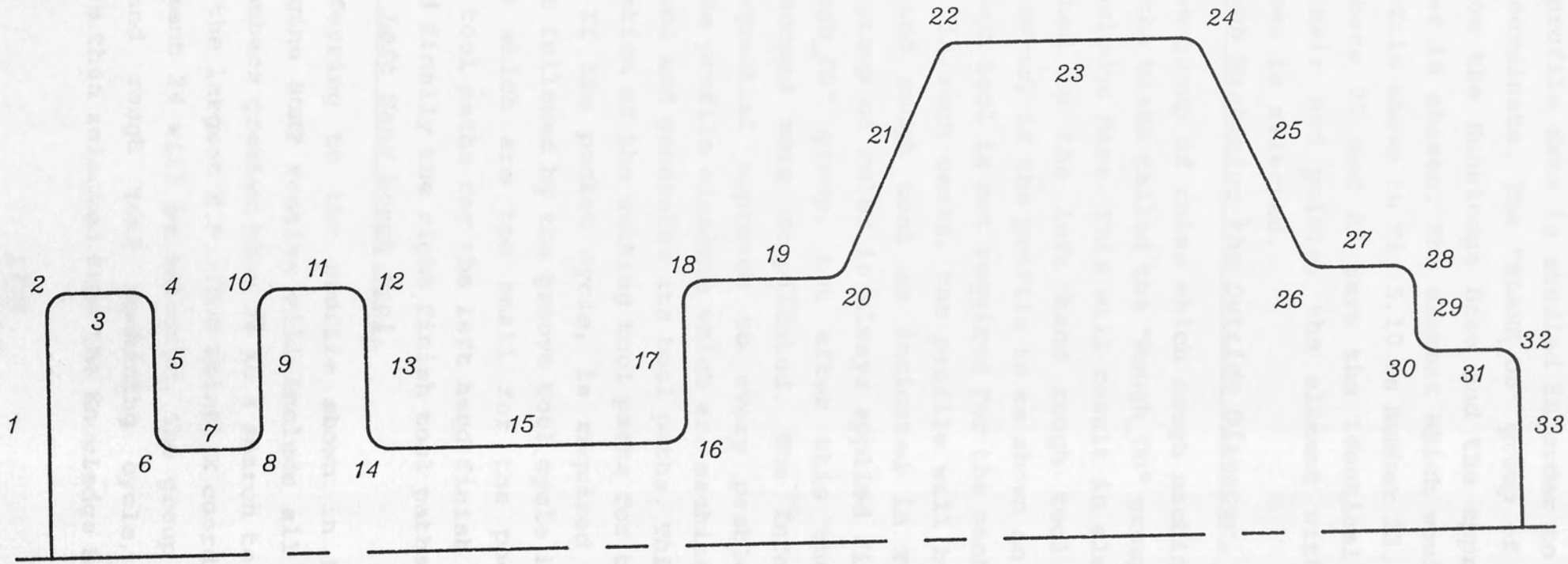

Figure 5.10

The specimen profile to be machined.

(a) Selection of Blank Diameter.

At the beginning of every analysis, the file which stores the profile data is studied in order to establish the largest X coordinate. The "BLANK_OD" group of rules is then selected from the Knowledge Base and the appropriate blank size diameter is chosen. The element which would be selected from the profile shown in Fig 5.10 is number 23. Although both element numbers 22 and 23 have the identical X coordinate values of their end points, the element with the greater element number is selected.

(b) Rough Machining the Outside Diameter.

The group of rules which rough machine the outside diameter of the blank called the "Rough_OD" group are selected from the Knowledge Base. This will result in element 23 being rough machined by the left hand rough tool as shown in Fig 5.11. However, if the profile is as shown in Fig 5.12, the left hand rough tool is not required for the machining of this section and, in such cases, the profile will be machined by the right hand rough tool as indicated in Fig 5.12. The "Blank_Dia" group of rules is always applied first, followed by the "Rough_OD" group, but after this the rule group selection becomes more complicated. The Inference Engine adopts a sequential approach to every problem. It first identifies the profile elements which are machined by the left hand rough tool and generates its tool paths. This is followed by the generation of the cutting tool paths for the right hand rough tool. If the pocket cycle, is required this will be analysed next followed by the groove tool cycle if the profile has recesses which are too small for the pocket tool to machine. The tool paths for the left hand finish tool are then generated and finally the right finish tool paths are defined.

(c) The Left Hand Rough Tool.

Referring to the profile shown in Fig 5.10 the Inference Engine SORT routine will include all the elements which have numbers greater than 23 in a search to identify the element with the largest E.P. (End Point) X coordinate. In the example, element 24 will be selected. The group of rules for the Left Hand rough tool machining cycle, called the "LH_Rough" are then selected from the Knowledge Base. The only

Figure 5.11

Figure 5.12

exception to this procedure is if an element selected in the first sort is numbered (N-1), where N is the total number of elements is the profile. This would mean that the profile would have its largest diameter at the extreme right hand side as shown in Fig 5.12. The Inference Engine software will then go directly to the routine which analyses the elements to be machined by the Right Hand rough tool. After element 24 has been rough machined, the sort routine is employed again to identify the greatest EP X coordinate from the elements numbered 25 or greater (i.e from elements 25 to 32 in the example). This time element 25 is selected and the rules in the "Left Hand Rough" group are applied again.

The procedure is repeated, the sort routine will analyse element numbers 26 to 32 inclusively and element number 26 is selected for rough machining. Having machined element 26, it is apparent the element 27 will also have been rough machined during the same cutting operation. The next sort, therefore, which involves elements 27 to 32, will select element 27 for rough machining. When the "LH-Rough" group of rules is applied it will conclude that there is no machining to be done and so element 27 will then be recorded as being rough machined. The sort routine is so efficient that it takes a negligible time to complete and, therefore, the application of special software routines to identify the situation where a sort will return an element that does not need machining was considered as being unnecessary. When the (N-1) element has been rough machined (in the example it will be element number 32) the Inference Engine terminates the selection of elements to be machined by the left hand rough tool. The cutting paths for the left hand rough tool to machine the profile are shown in Fig 5.13(a).

(d) *The Right-Hand Rough Tool.*

The sort routine then processes element numbers which are less than 23. This routine, which is similar to the sort routine for the left hand rough tool, will select elements with the highest end point X coordinate values, but if two elements have the same diameter then the one with the lowest element number is chosen. The element selected will be 22 and the group of rules for the right-hand rough tool, called "RH_Rough", is applied. When this element has been

Figure 5.13

machined the next sort is commissioned between the element numbers 21 to 1. From this operation, the element 21 will be selected for machining in the usual way. The sort of element 1 to 20 will create the same situation that was discussed in the left hand rough tool cycles, where elements 19, 11 and 3 will all be rough machined as a result of the rough machining of element 20. The Inference Engine software will apply the rules in the "RH-Rough" group in the normal way, but because all the elements involved have been machined in the previous machining of element 20, nothing will be done and control is returned to the Inference Engine software. Finally a sort between elements 1 to 3 is done which results in element 2 being selected and machined. Fig 5.13(b) shows the tool paths for the right and left hand roughing cycles.

(e) *The Pocket Cycles.*

Referring to the profile shown in Fig 5.10 the profile element numbers 4, 5, 6, 7, 8, 9 and 10 as well as numbers 12, 13, 14, 15, 16, 17 and 18 have not yet been rough machined. The Inference Engine software will assess the possibility of implementing the pocket cycles by applying the rules stored in the Knowledge Base in the group called "POCKET". If all the elements in the profile had been rough machined the "POCKET" group would not be applied. The elements that have not been machined will always be grouped together, because they will be part of a recess in the profile geometry. In Fig 5.10 the elements 4 to 10 and 12 to 18 have not been machined. The group of elements involving the highest element numbers are studied first. The principle of the pocket cycles was explained in section 4.6.1. The left hand pocket tool is selected and the dig_in line, which determines the cutting path into the recess region, is defined. The dig_in line angle is 2 deg less than the toolholder trailing angle. The positioning of the dig_in line is explained in Fig 5.14(a). The rules in the group called "Pocket_Crash" stored in the Knowledge Base, are applied. This will ensure that both the left hand and right hand pocket tools can perform the required cutting cycles without being obstructed by the workpiece. Details are illustrated in Fig 5.14(b). If the problem of tool obstruction occurs, then the groove cycle will be implemented

Figure 5.13(b)

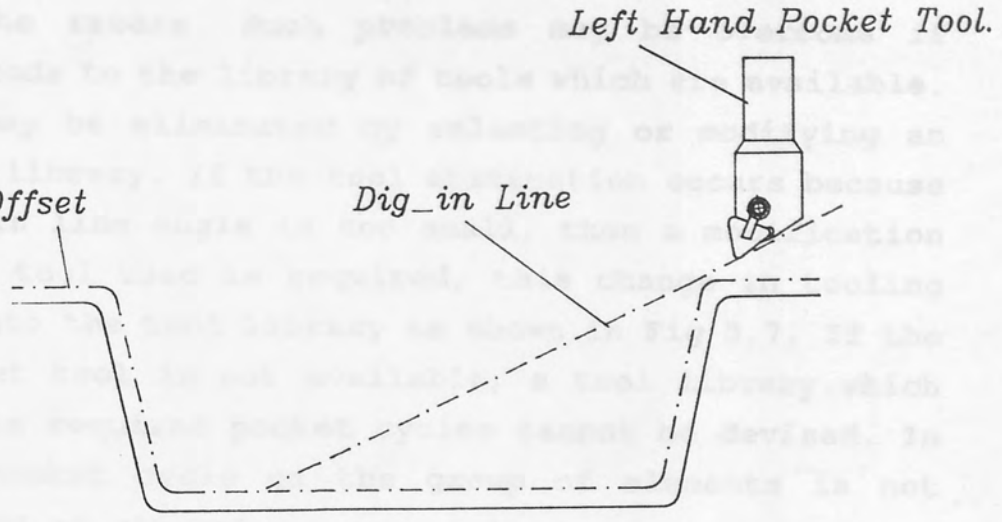

Figure 5.14(a)

Position of Dig_in Line.

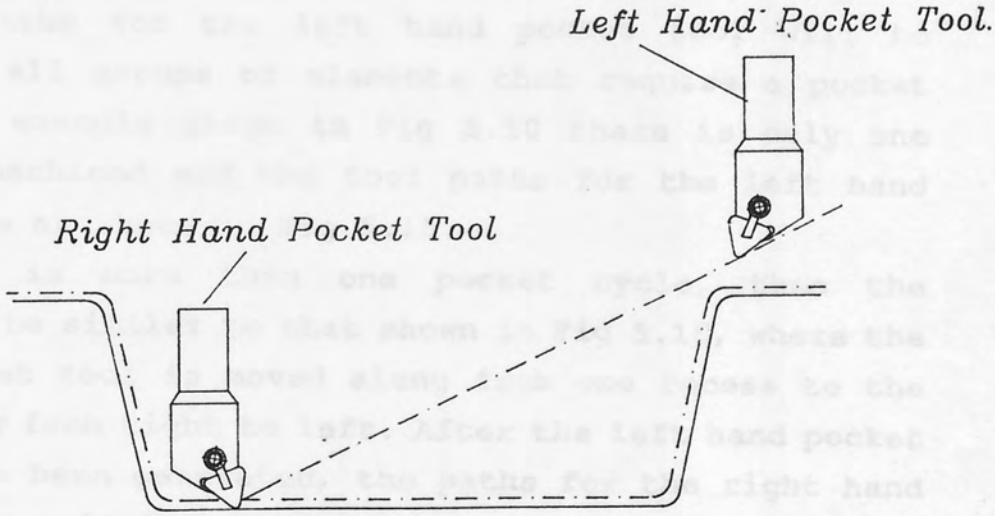

Figure 5.14(b)

Check for clearence on right hand tool.

to machine the recess. Such problems may be overcome if reference is made to the library of tools which are available. The problem may be eliminated by selecting or modifying an existing tool library. If the tool obstruction occurs because the tool dig_in line angle is too small, then a modification to the pocket tool used is required, this change in tooling must be put into the tool library as shown in Fig 5.7. If the required pocket tool is not available, a tool library which can perform the required pocket cycles cannot be devised. In this case a pocket cycle on the group of elements is not carried out and an attempt to groove these elements must be made.

For the profile shown in Fig 5.10 the group of elements numbered 12 to 18 does not create any problem regarding tool obstructions, if the tool library shown in Fig 5.7 is used. The element group 4 to 10, however, cannot be rough machined using a pocket cycle, because the dig_in line for the pocket tools does not reach the bottom of the recess. The Inference Engine software will check on every group of elements in the profile which has not been machined and carry out an investigation to establish if a pocket cycle can be performed. The cutting paths for the left hand pocket tool will be generated for all groups of elements that require a pocket cycle. In the example shown in Fig 5.10 there is only one pocket to be machined and the tool paths for the left hand pocket tool are as shown in Fig 5.15.

If there is more than one pocket cycle, then the procedure will be similar to that shown in Fig 5.16, where the left hand pocket tool is moved along from one recess to the next travelling from right to left. After the left hand pocket tool paths have been generated, the paths for the right hand pocket tool are calculated. The principles are identical to those used by the "CUTPLOT" program in ROLFOM (see section 4.6.1). The pocket tool paths for the profile shown in Fig 5.10 are displayed in Fig 5.17 and the example where a number of recesses are machined by the pocket cycle is shown in Fig 5.18.

The profiles which have been studied so far have involved recesses with very simple geometry. ROLCUT can successfully process a recess which involves complicated geometry by

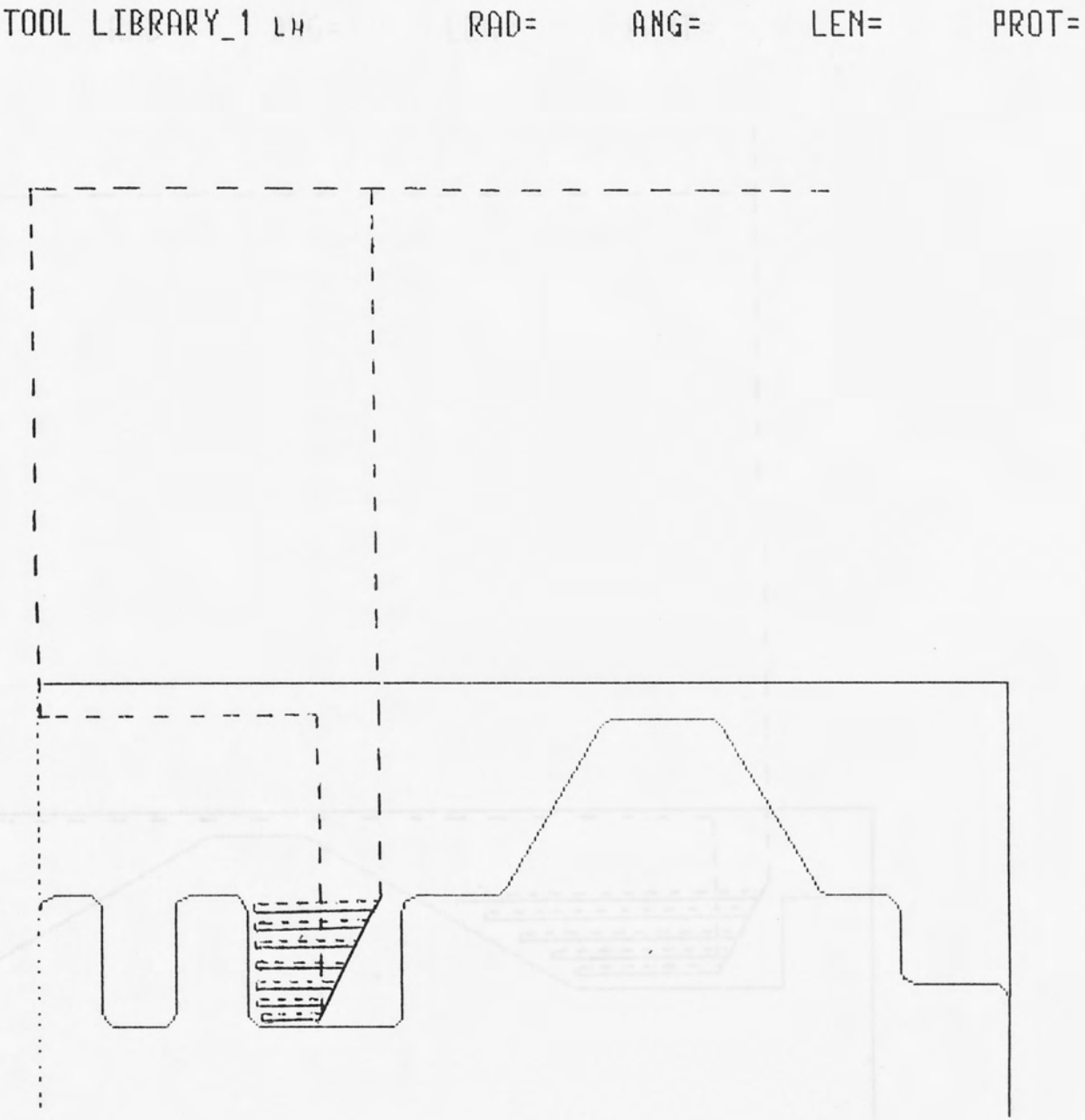

Figure 5.15

Figure 5.16

Figure 5.17

Figure 5.18

generating a combination of complex pocket and groove cycles. This will be discussed later in this section.

(f) *Groove Cycles.*

If there are elements in the profile which have not been rough machined, after the rules in the "POCKET" group have been applied, then the possibility of carrying out a groove cycle is investigated. The major difference with the groove tool, compared with the other cutting tools is that the same tool carries out both the rough and finish cycles. The principles of the groove cycles are explained in section 4.6.1. The considerable enhancement which ROLCUT possesses, however, allows a finish cut to be taken by the groove tool using a profile machining cycle. This will improve the surface texture of the profile which has been cut using a groove tool. It also results in the capability of machining complex geometrical shapes in a recess region of a profile.

Positioning the groove tool ready to begin a cutting traverse is shown in Fig 5.19(a). How far the tool must traverse into the workpiece is ascertained by studying the locus of the two corners of the blade, as Fig 5.19(b) shows. A special case is also illustrated in Fig 5.19(c) where an intersection of two profile elements occurs between the two corner point loci of the tool. An investigation is carried out to ensure that the groove cycle can be performed without tool obstruction. A group of rules in the Knowledge Base called the "GROOVE_CRASH" are applied and the dimensions which are checked are shown in Appendix 2. If there are no suitable groove tools available, the profile cannot be machined and modifications to it must be made.

A finish cut is applied to produce the specified dimensions of the recess region using a profile machining cycle. If the total width of the recess is less than twice the width of the blade of the groove tool, a finish cut is not employed. The groove tool path for the profile shown in Fig 5.10 is displayed in Fig 5.20, and an example of a profile which involves more than one groove cycle is shown in Fig 5.21.

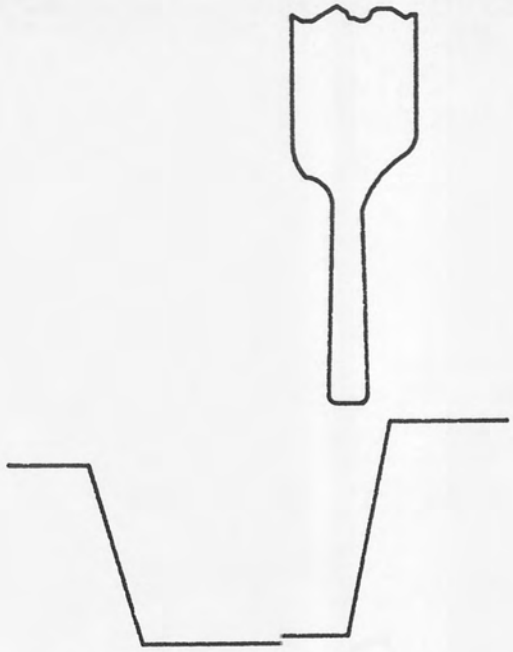

Figure 5.19(a)

Location of Groove Tool prior to machining.

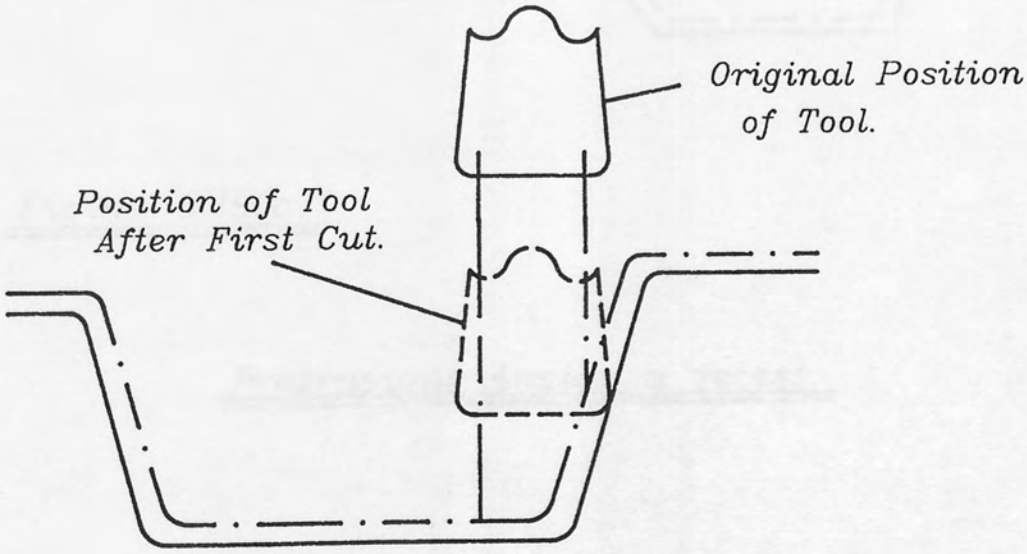

Figure 5.19(b)

Control of depth of cut.

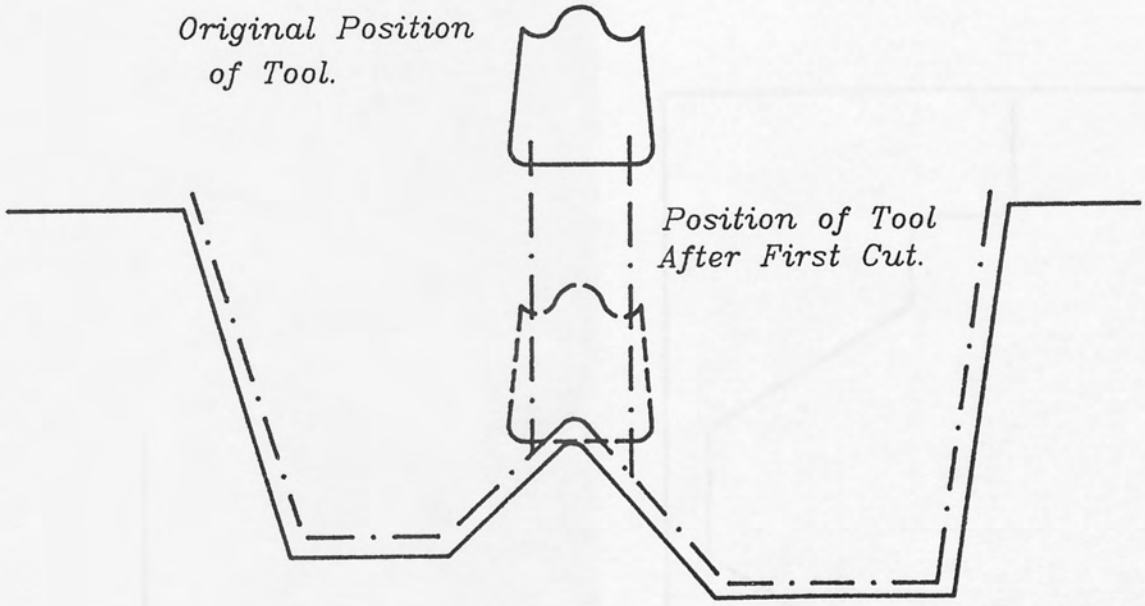

Figure 5.19(c)

Protrusions inside a recess.

Figure 5.20

Figure 5.21

(g) *Finish Tool Cycles.*

At the beginning of the ROLCUT program, the user is requested to define the depth of cut for the finish machine cycles. A default value of 0.5 mm is proposed. It is important that the geometry of the finish tools corresponds to the geometry of the pocket tools. The protrusion of the finish tools from the turret, for example, must be equal to or greater than that of the pocket tools. This is necessary because the finish tools have to finish machine the recess regions which have been rough machined by the pocket cycles. Such checks are not carried out when the finish tool is used.

The finish cycles in ROLCUT are virtually identical to that used by ROLFOM. The rules in the Knowledge Base which control the finish cycle are in a group named "Finish". The left hand finish tool is selected first, followed by the right hand finish tool.

A useful feature of ROLCUT finish cycle is that it can machine the edge steps in the form-roll (see section 3.2.5). If the steps are not too large or their angle is not too great, they are produced in a single cutting traverse. This is discussed in detail later in this section.

The elements which have been machined by the groove cycle are always ignored by the finish cycle. The tool paths for the left hand and right hand finish tool cycle, for the profile in Fig 5.10, are shown in Fig 5.22(a) and Fig 5.22(b).

The combined tool paths for all the machining cycles are shown in Fig 5.23. It can be very difficult to identify the different machining cycles with the combined tool path display unless the profile is very simple. However, the colours used to identify the different tools help to clarify the display greatly. ROLCUT's Inference Engine software can make resourceful decisions that allow a relatively complicated profile geometry to be machined. The following examples explain the methods used to overcome some of the problems which may be confronted.

The previous descriptions of the pocket cycle involved an area of the profile with a relatively simple geometry as Fig 5.14(a) shows. This is the most common recess geometry that is likely to occur in form-roll profiles, but occasionally a more complicated recess may be encountered. A

Figure 5.22

TOOL LIBRARY_1 RH.FINISH RAD=0.40 ANG= 70.0 LEN= 18.0 PROT= 50.0

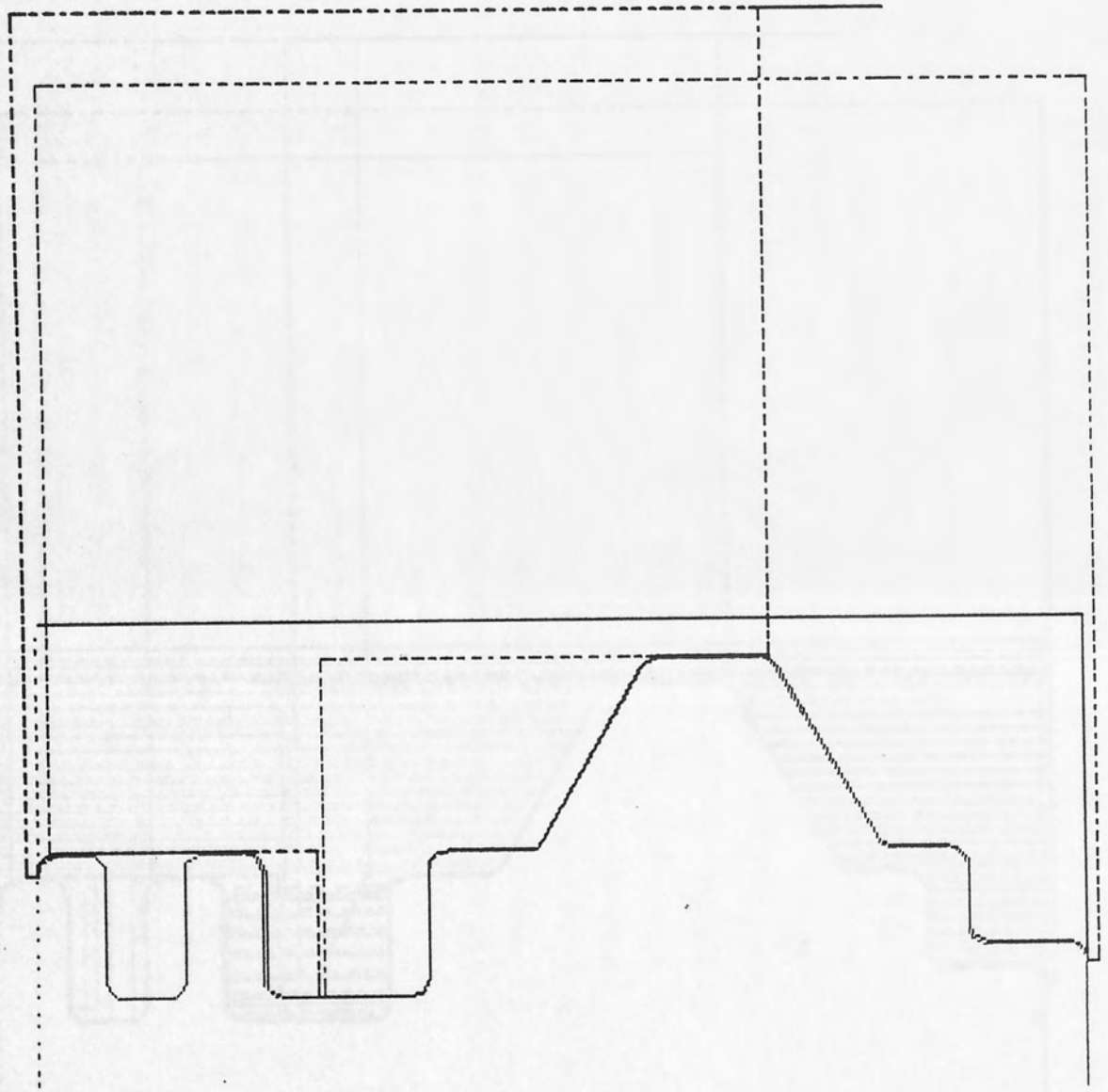

Figure 5.22(b)

Figure 5.23

problem arises if the dig_in line does not intersect with the element which has the smallest diameter among the elements which make up the recess. An example is shown in Fig 5.24 which involves a recess with relatively simple geometry. The rules in the "Pocket" group will initially consider a dig_in line which passes through the point A. When this situation occurs the dig_in line is moved so that it passes through point B, as shown in Fig 5.24, whereupon it will intersect with the element with the smallest diameter. If both the left hand and right hand pocket tools can carry out their machining operation without obstructions, the pocket cycle will be applied using this new dig_in line.

A more complicated recess geometry is shown in Fig 5.25(a). If this occurs, the pocket cycle will be applied using the dig_in line that passes through the point A, assuming that no tool obstructions are detected by the "Pocket_Crash" group of rules. The elements which are not rough machined by the pocket tools will be machined by the groove tool. The combined tool paths generated by ROLCUT, for the profile in Fig 5.25(a), is shown in Fig 5.25(b). This is an example where a recess region is machined using a combination of pocket and groove cycles. A far more intelligent analysis is demanded in the case of the geometry shown in Fig 5.26(a). When a recess region includes a projection inside the recess, (i.e. in Fig 5.26(a) elements 6 to 12 form the projection) a special situation occurs. The Inference Engine software inspects every recess region and, if this situation is detected, then a group of rules named "Xpocket" is applied. Separate areas are identified for the pocket cycle to machine and Fig 5.26(a) shows the way in which the profile is divided up. The region labelled 1 would be rough machined by the pocket cycle, followed by the region labelled 2, which will use the same dig_in line . The region labelled 3 is then machined after moving the dig_in line from point A to B as shown in Fig 5.26(b). If any of the pocket cycles cannot be carried out due to obstructions, then the elements involved are machined using the groove tool. In Fig 5.26(c), the combined tool paths are shown that were generated by ROLCUT for the profile in Fig 5.26(a). The case were the region labelled 2 is too small to allow a pocket

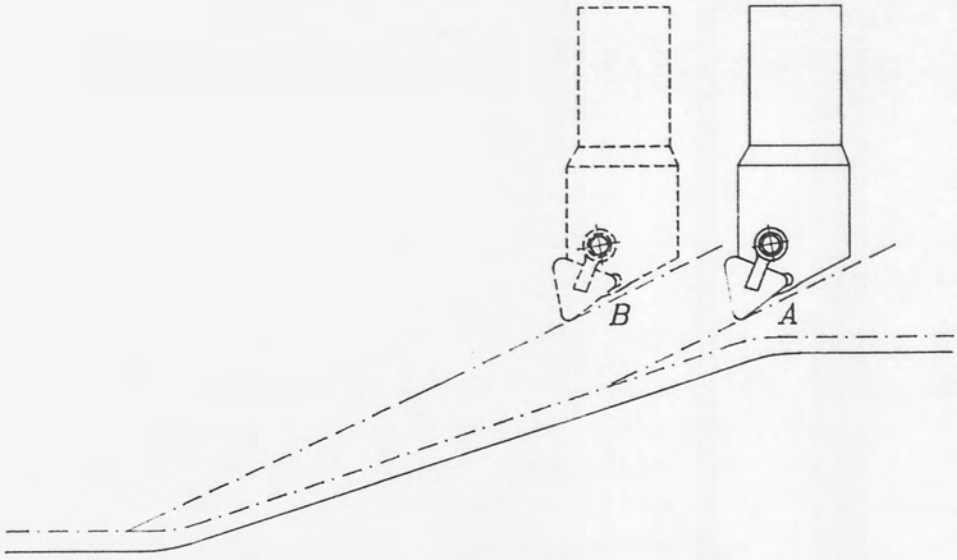

Figure 5.24

Repositioning of the Dig_in Line.

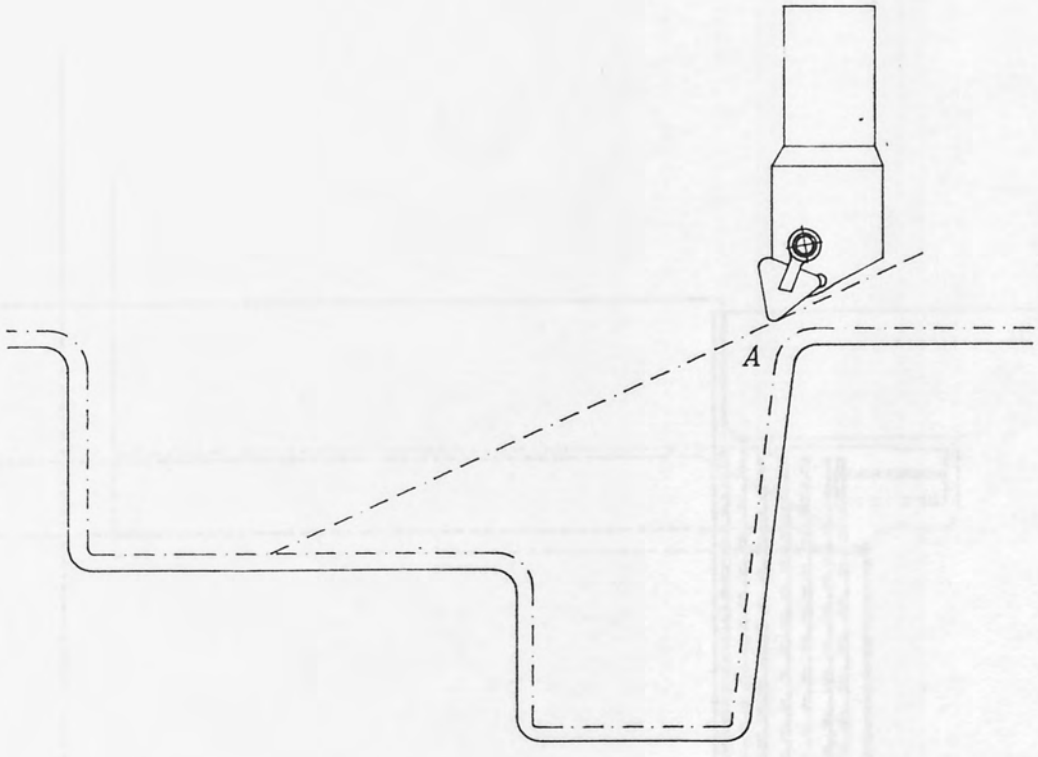

Figure 5.25(a)

Machining Of A More Complex Recess Geometry.

Figure 5.25(b)

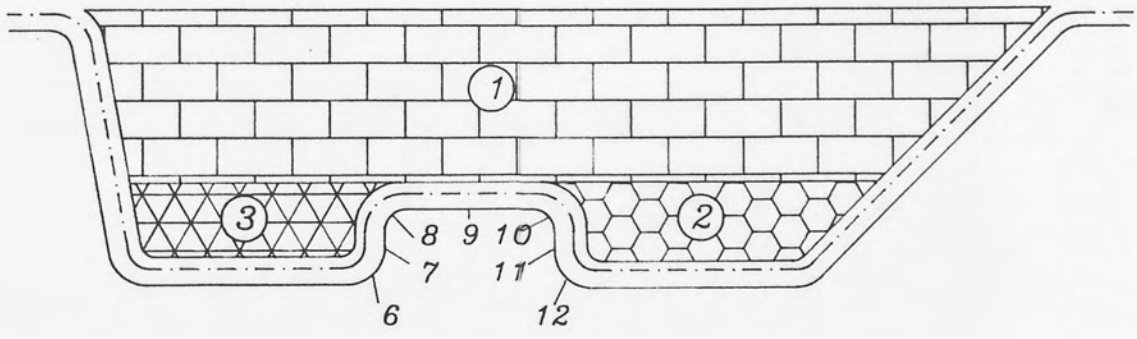

Figure 5.26(a)

Division of Pocket into Smaller Areas.

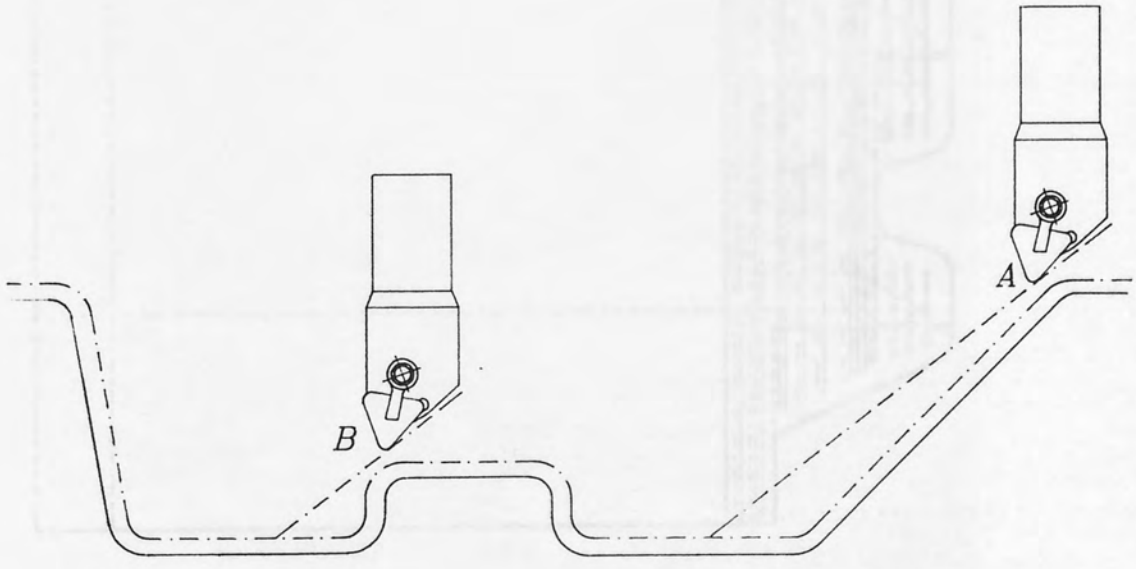

Figure 5.26(b)

Position of Dig_in Lines.

TOOL LIBRARY_1 RH.FINISH RAD=0.40 ANG= 70.0 WID= 18.0 PROT= 50.0

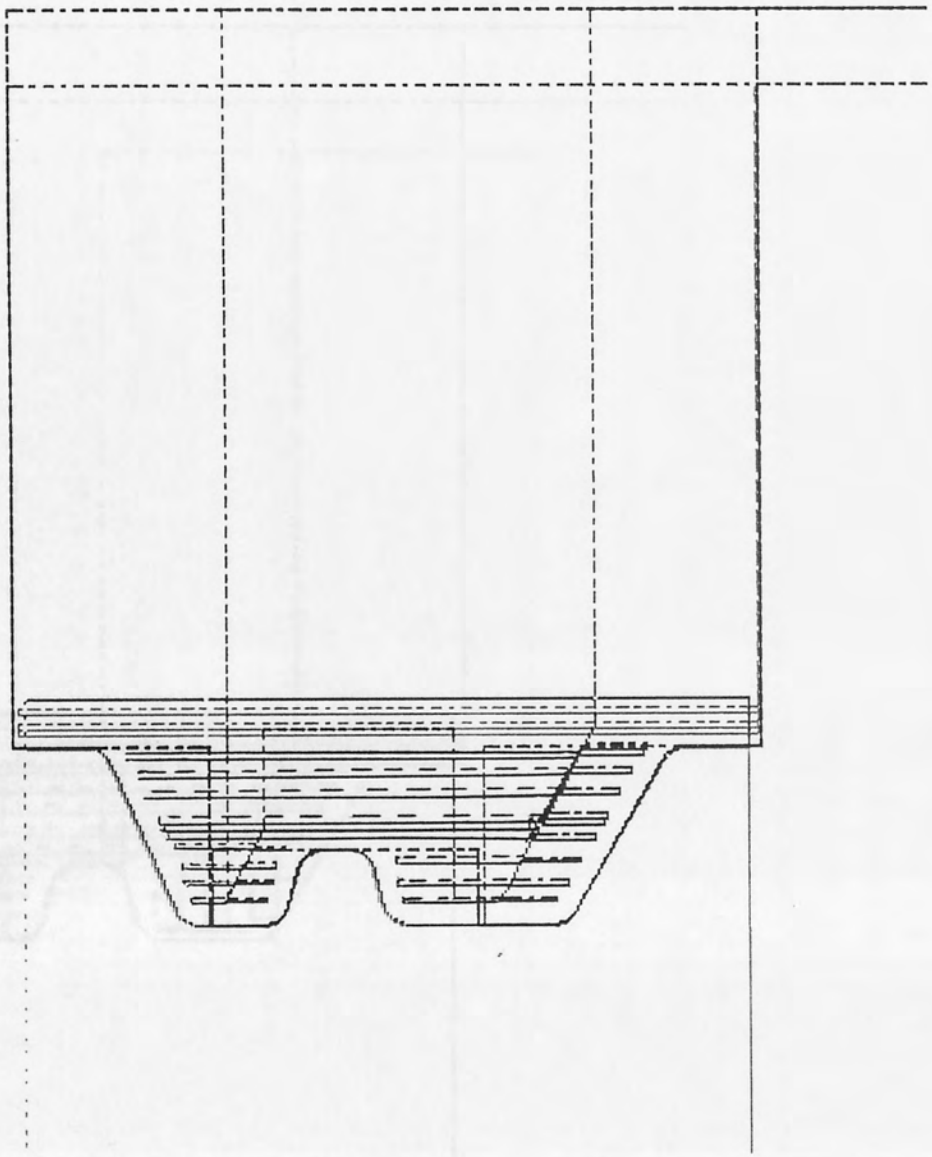

Figure 5.26(c)

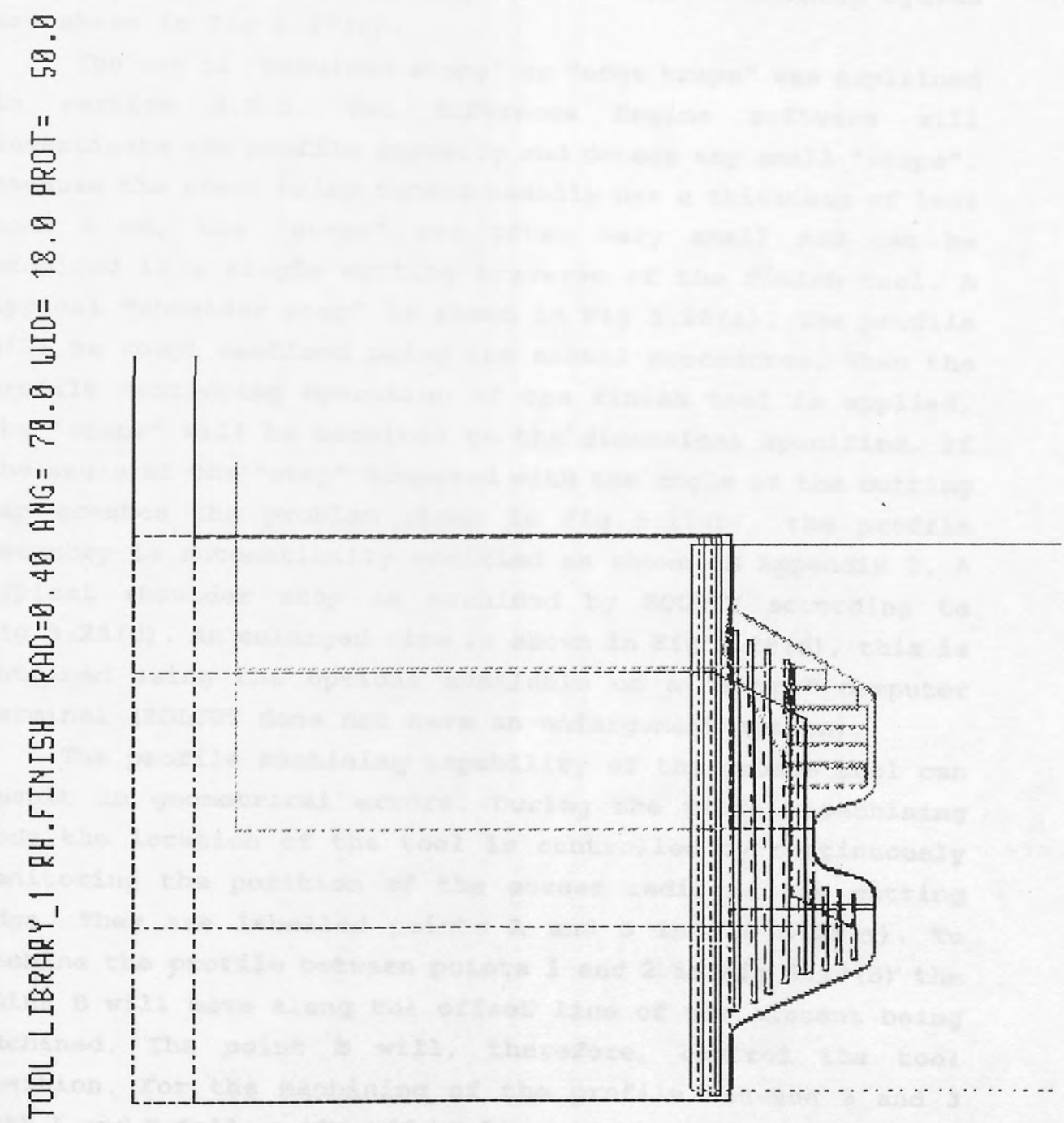

Figure 5.26(d)

cycle is shown in Fig 5.26(d). The tool paths for the groove cycle have been applied to machine area 2, with areas 1 and 3 being machined using the pocket cycle.

In the relatively rare case when there is more than one projection, see Fig 5.27(a), the Inference Engine will identify the areas 1, 2, 3 and 4 and identifies the projection with the largest diameter (i.e. element 8 in Fig 5.27(a)), thus the pocket tools then machines area 1. The rest of the recess will be left to be machined with the groove cycle as shown in Fig 5.27(b). Finally, after the finish tools have traversed across the profile, the combined machining cycles are shown in Fig 5.27(c).

The use of "shoulder stops" or "edge traps" was explained in section 3.2.5. The Inference Engine software will investigate the profile geometry and detect any small "steps". Because the sheet being formed usually has a thickness of less than 2 mm, the "steps" are often very small and can be machined in a single cutting traverse of the finish tool. A typical "shoulder stop" is shown in Fig 5.28(a). The profile will be rough machined using the normal procedures. When the profile contouring operation of the finish tool is applied, the "steps" will be machined to the dimensions specified. If the angle of the "step" compared with the angle of the cutting tip creates the problem shown in Fig 5.28(b), the profile geometry is automatically modified as shown in Appendix 2. A typical shoulder stop is machined by ROLCUT according to Fig 5.28(c). An enlarged view is shown in Fig 5.28(d), this is obtained using the options available on a "smart" computer terminal (ROLCUT does not have an enlargement option).

The profile machining capability of the groove tool can result in geometrical errors. During the profile machining mode the location of the tool is controlled by continuously monitoring the position of the corner radii of the cutting edge. They are labelled points A and B in Fig 5.29(a). To machine the profile between points 1 and 2 in Fig 5.29(b) the point B will move along the offset line of the element being machined. The point B will, therefore, control the tool position. For the machining of the profile between 2 and 3 both A and B fall on the offset line. When the profile between 3 and 4 is machined point A will move along the offset line

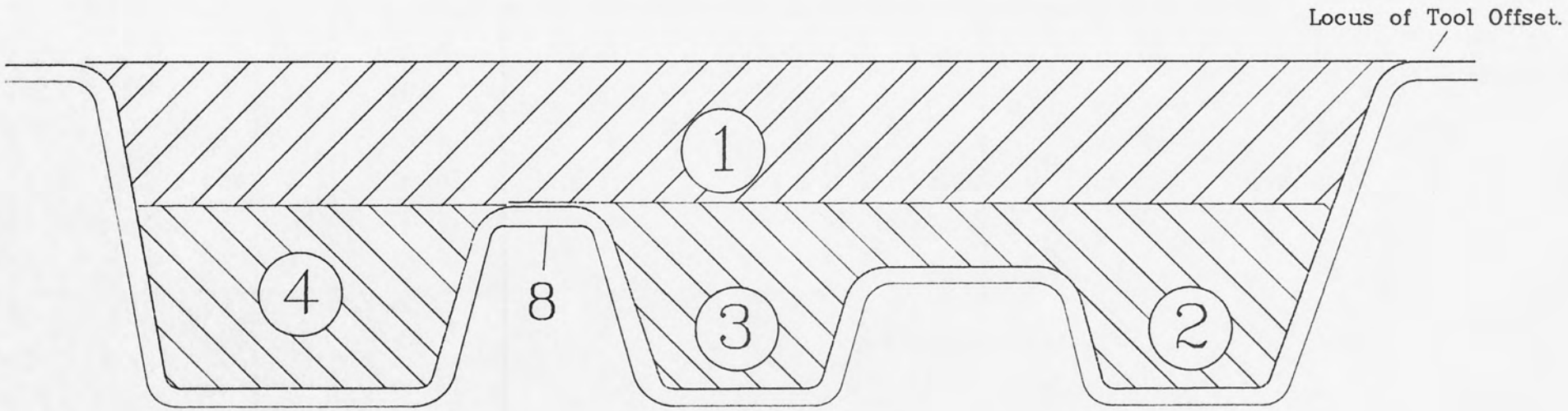

Figure 5.27(a)

Division of a pocket with more than one protrusion.

Figure 5.27(b)

TOOL LIBRARY_1 RH.FINISH RAD=0.40 ANG= 70.0 WID= 18.0 PROT= 50.0

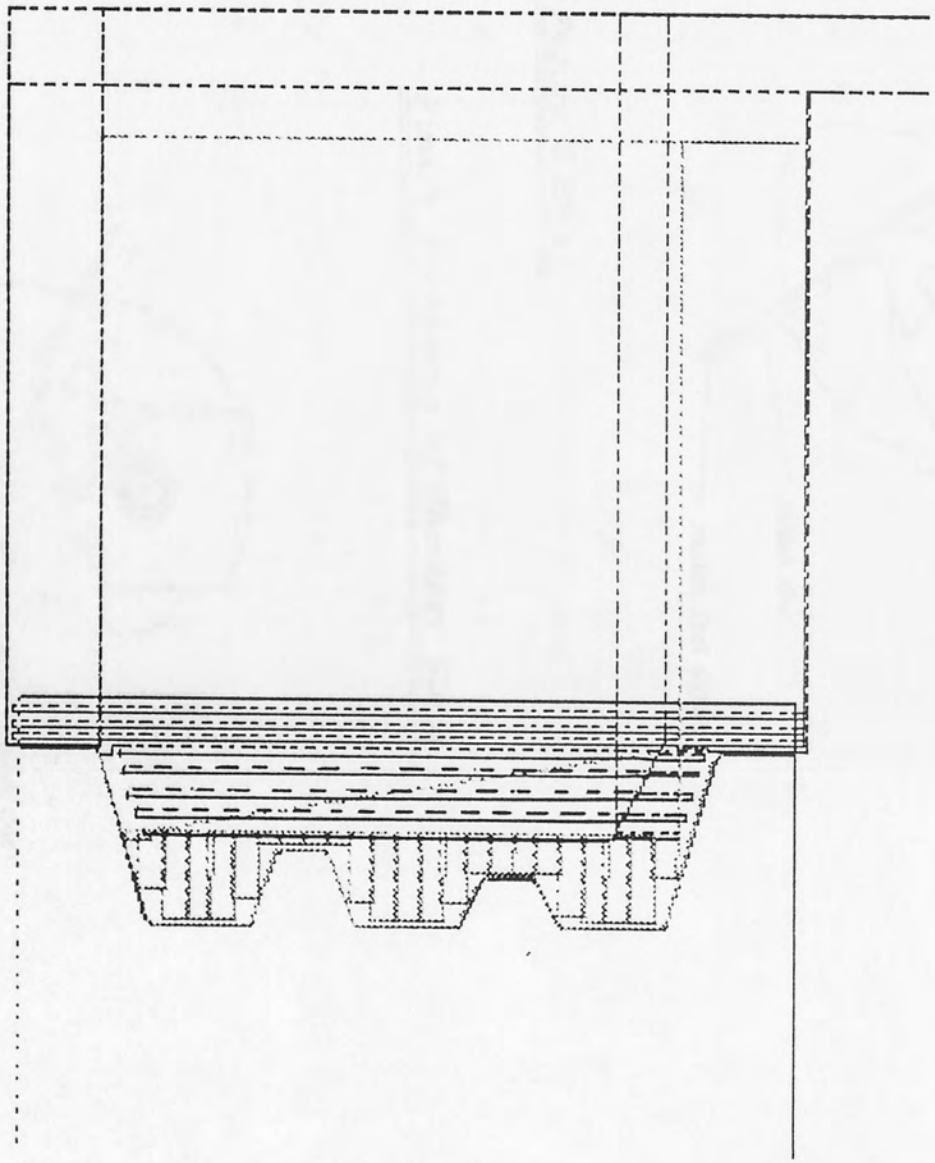

Figure 5.27(c)

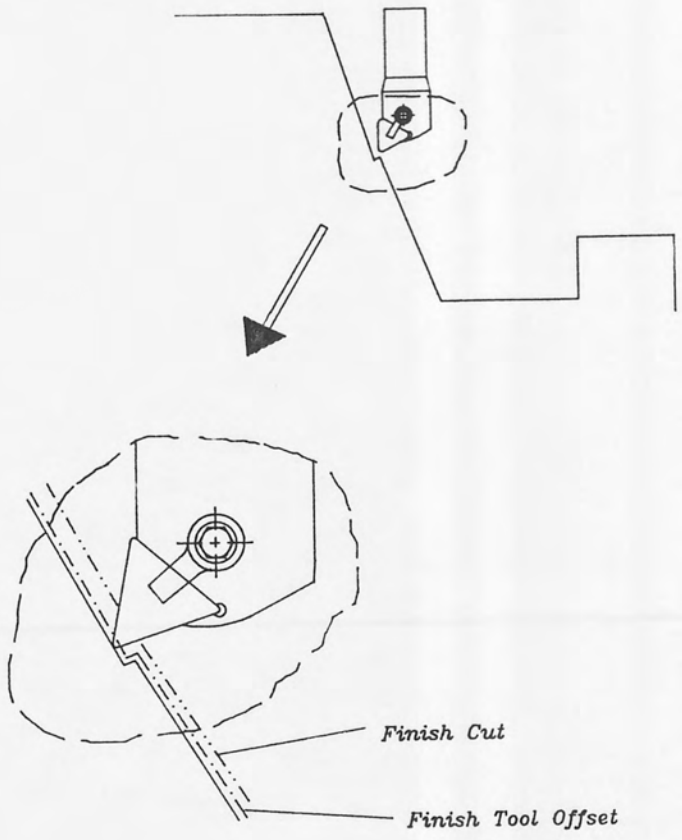

Figure 5.28(a)

Finish Machining of Shoulder Stops.

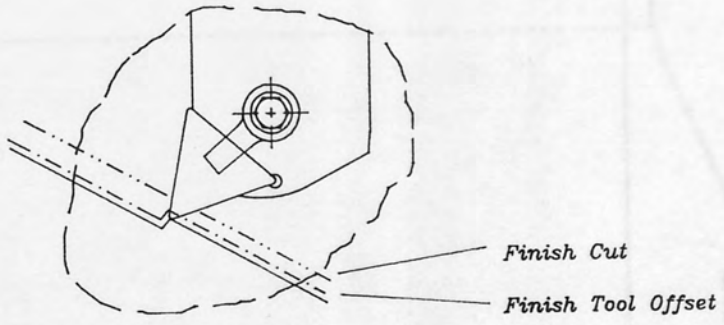

Figure 5.28(b)

Possible Problems Encountered When Machining Shoulder Stops.

TODL LIBRARY_2 RH.FINISH RAD=0.40 ANG= 70.0 LEN= 18.0 PROT= 50.0

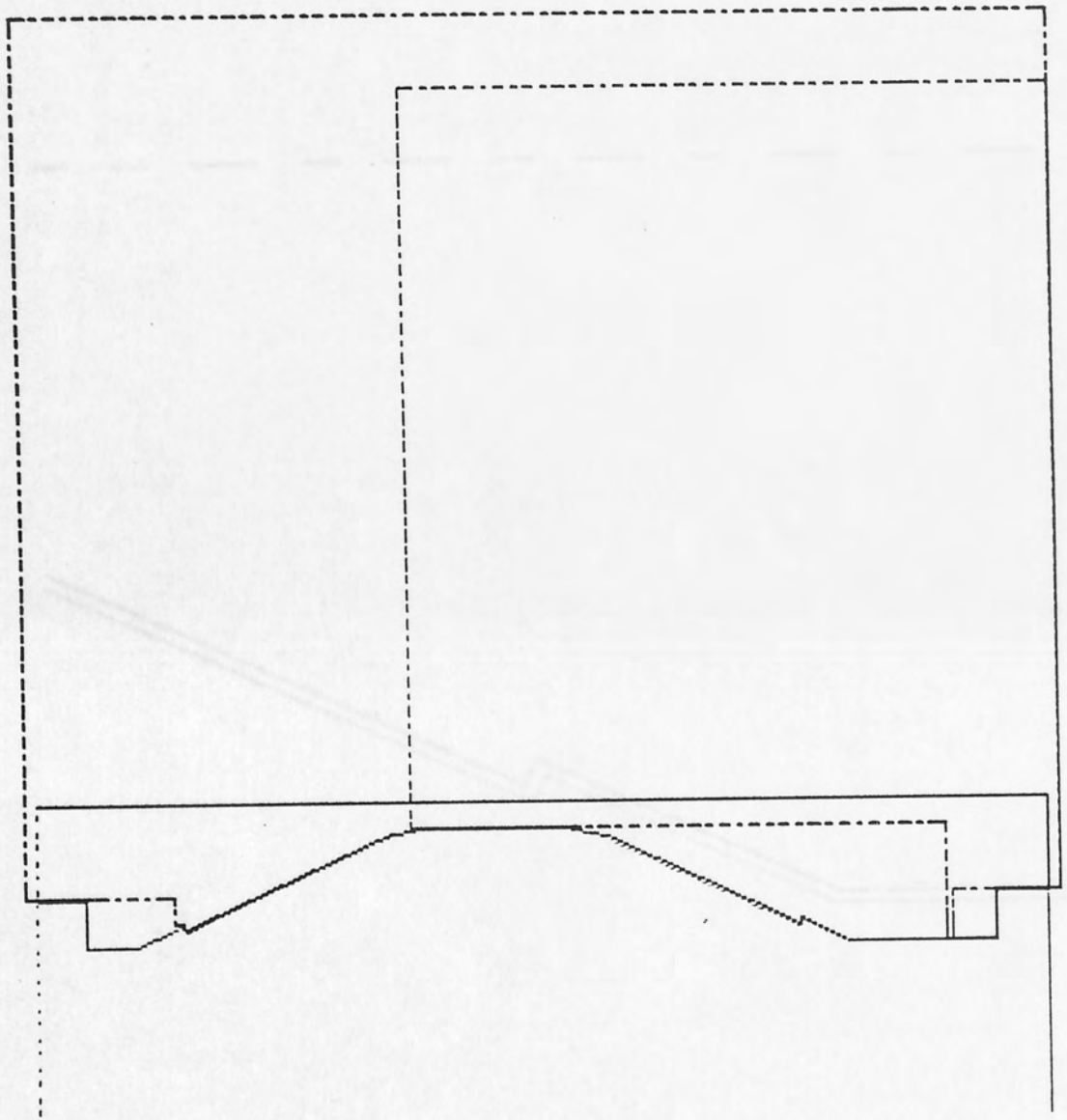

Figure 5.28(c)

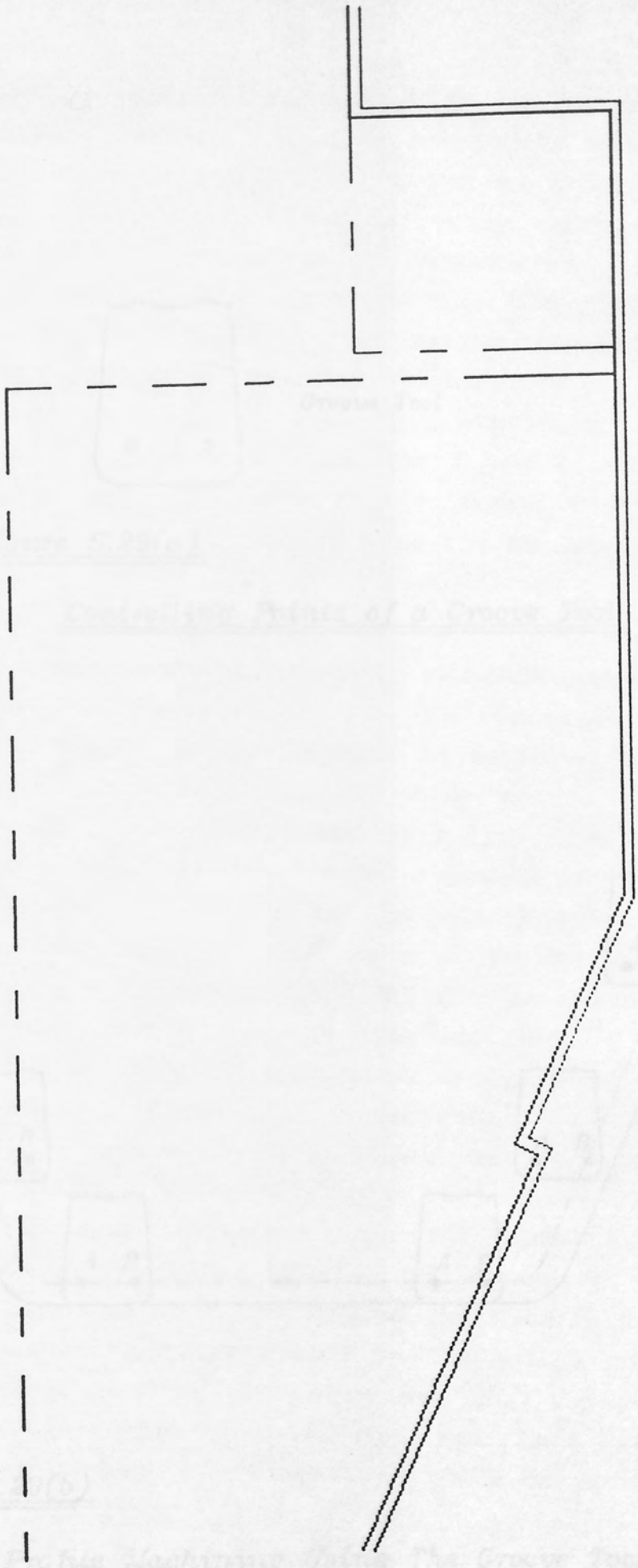

Figure 5.28(d)

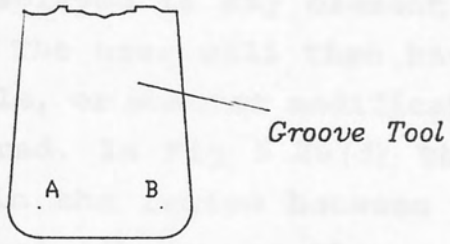

Figure 5.29(a)

Controlling Points of a Groove Tool.

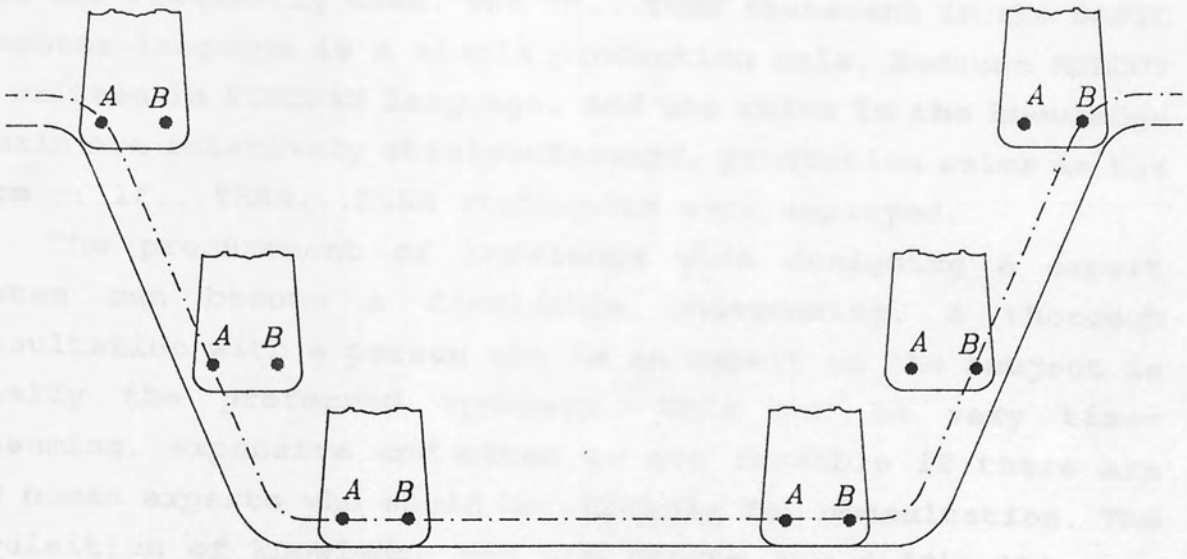

Figure 5.29(b)

Profile Machining Using The Groove Tool.

and so the tool position is controlled by this point. This method of tool positioning is usually completely successful, but the profile shown in Fig 5.29(c) indicates that problems can occur. The profile is machined correctly apart from the length between 1 and 2, which is left unmachined. A warning message will be displayed if any element in the profile has not been machined. The user will then have to decide if the profile is acceptable, or whether modifications to the profile geometry are required. In Fig 5.29(d) the profile has been slightly modified in the region between 1 and 2 and having also changed the tool library so that a groove tool with a narrower blade is available, the problem can be overcome.

5.5.3 ROLCUT Knowledge Base.

A general description of the Knowledge Base of an expert system is given in section 5.3.1. The representation of knowledge in the ROLCUT Knowledge Base is achieved by using production rules. This technique is very common and the software is easier to write compared with the other methods that are frequently used. The IF...THEN statement in the BASIC computer language is a simple production rule. Because ROLCUT is written in FORTRAN language, and the rules in the knowledge domain are relatively straightforward, production rules in the form of IF...THEN...ELSE statements were employed.

The procurement of knowledge when designing a expert system can become a formidable undertaking. A thorough consultation with a person who is an expert on the subject is usually the preferred approach. This can be very time-consuming, expensive and often is not feasible if there are few human experts who would be suitable for consultation. The acquisition of knowledge did not create any difficulties in this research project because advice and technical guidance from an experienced skilled machinist was available, which provided all the expertise that was required. This was most fortunate and, as a result, the quality of the expert system was considerably enhanced.

The rules in the Knowledge Base are not selected individually by the ROLCUT Inference Engine software, but groups of rules are selected as the discussion in section 5.5.2 explained. The rules in the Knowledge Base, therefore,

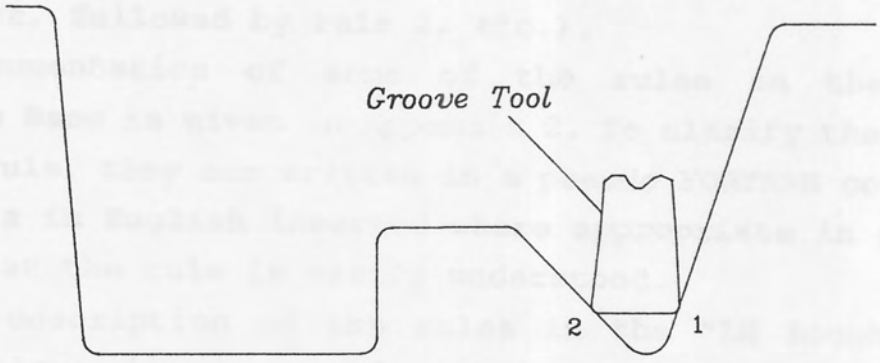

Figure 5.29(c)

Problems of Unmachined Areas when Grooving.

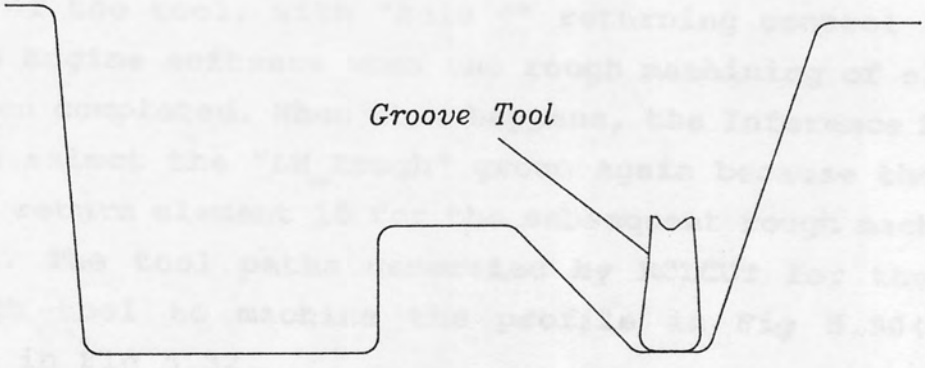

Figure 5.29(d)

Changes to Profile and Tooling

are arranged into groups with each given a name for identification purposes. When a group of rules has been selected, the rules within the group are always applied in the order in which they are placed in the group, (i.e. rule number 1 is first, followed by rule 2, etc.).

Documentation of some of the rules in the ROLCUT Knowledge Base is given in Appendix 2. To clarify the meaning of each rule, they are written in a pseudo FORTRAN code, with statements in English inserted where appropriate in order to ensure that the rule is easily understood.

The description of the rules in the "LH Rough" group which follows is an example of the presentation used in Appendix 2. Fig 5.30(a) and Fig 5.30(b) show the set-up for machining with the L.H. Rough tool and defines the names used in the pseudo FORTRAN coding. The tool paths for rough machining the largest diameter in the profile will have already been generated by the "Rough_OD" group of rules. Because this rule group uses the left hand rough tool to turn the outside diameter in the majority of cases, the position of the rough tool is as indicated in Fig 5.30(a). This will be the starting position for "TPOS" prior to the tool paths generated by the "Rough_OD" group. The rules are then shown in Fig 5.31(a) and Fig 5.31(b). The profile element in Fig 5.30(a) which will be machined first is element 11. The rules in the "LH_Rough" group are repeated for each cutting traverse of the tool, with "Rule 6" returning control to the Inference Engine software when the rough machining of element 11 has been completed. When this happens, the Inference Engine will soon select the "LH_Rough" group again because the next sort will return element 18 for the subsequent rough machining operation. The tool paths generated by ROLCUT for the left hand rough tool to machine the profile in Fig 5.30(a) is displayed in Fig 5.32.

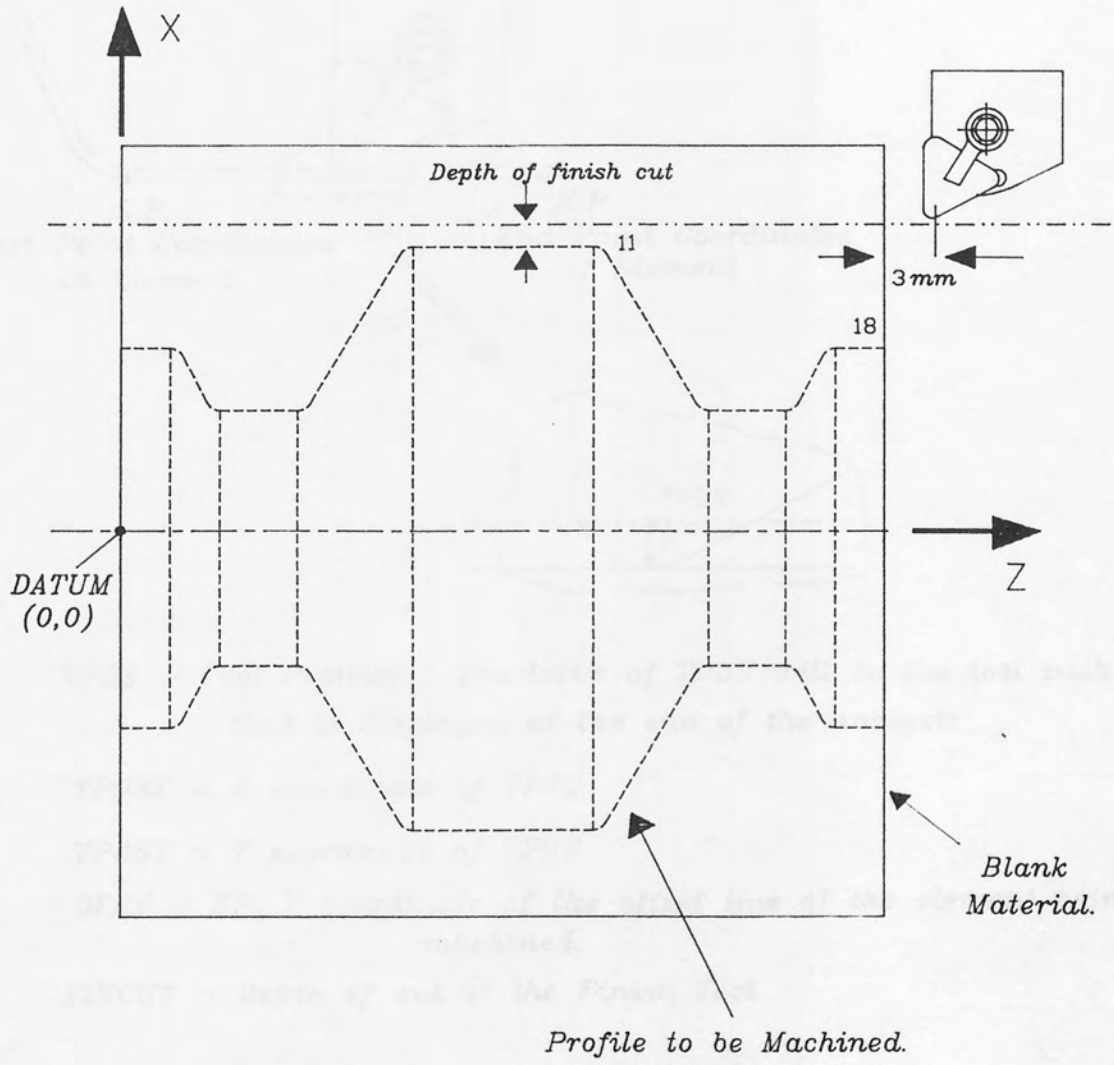

Figure 5.30(a)

Setup for the Machining of the Blank.

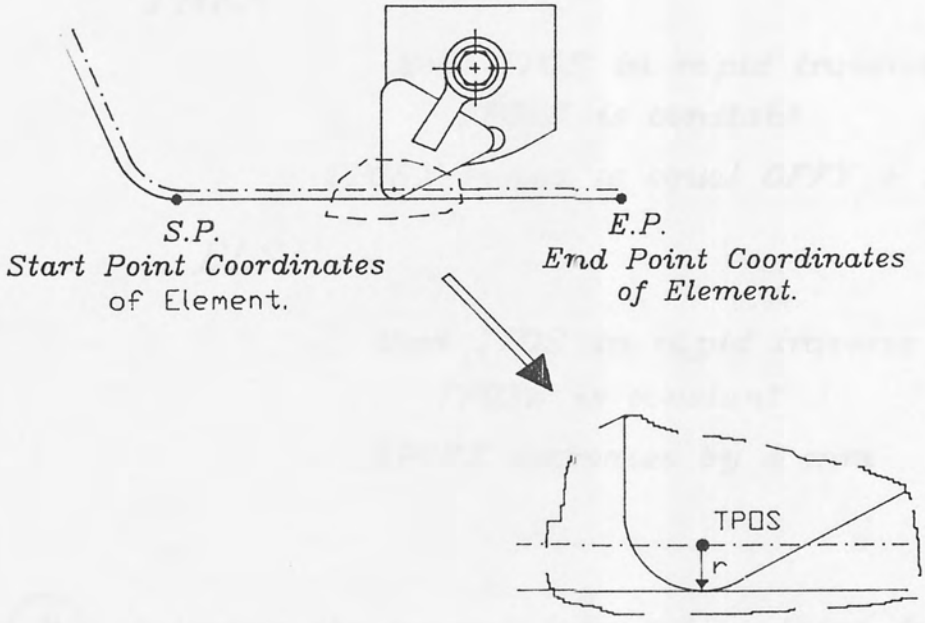

TPOS = Tool Position : The locus of TPOS will be the tool path that is displayed at the end of the analysis

TPOSX = X coordinate of TPOS.

TPOSY = Y coordinate of TPOS.

OFFY = SP. Y coordinate of the offset line of the element being machined.

FINCUT = Depth of cut of the Finish Tool.

Figure 5.30(b)

Definitions used in the Description of the Machining Rules.

(1) IF TPOSX is less than OFFX + 4 + FINCUT

THEN

Move TPOS in rapid traverse
TPOSZ is constant
TPOSX moves to equal OFFY + FINCUT

ELSE

Move TPOS in rapid traverse
TPOSZ is constant
TPOSX decreases by 4 mm

(2) Calculate the nearest Intersection Point from TPOS between an horizontal line through TPOS and a profile element offset line. Store the X coordinate of this point in a variable named "STOPTRAV"

(3) Move TPOS in FEED TRAVERSE

TPOSZ is decreased to equal STOPTRAV + FINCUT

Figure 5.31(a)

An Example of the Pseudo-FORTRAN Code.

(4) *Move TPOS in FEED TRAVERSE*

TPOSZ is constant

TPOSX is increased by 1mm.

(5) *Move TPOS in RAPID TRAVERSE*

TPOSX is constant

TPOSZ is increased to equal the X coordinate

of TPOS before Rule (3) was applied.

(6) *IF* *TPOSX IS EQUAL TO*
OFFX + FINCUT

THEN

Return to INFERENCE ENGINE
Software Control.

ELSE

Goto Rule (1)

Figure 5.31(b)

Example of Pseudo-FORTRAN Code Continued.

Figure 5.32

CHAPTER SIX.

PREVIOUS RESEARCH INTO THE COLD ROLL FORMING PROCESS.

6.1 Introduction.

The design work which is associated with the cold roll forming process was discussed in Chapter Three. The dependence on knowledge which is based entirely on past experience is clearly an unsatisfactory approach. A form-roll schedule is rarely correct when it is first tested on the rolling mill, and subsequent modifications can be very time-consuming. The cold-roll forming industry has expanded considerably over the last ten years and many of the companies have invested in computer technology. The problems of form-roll schedule design, however, have not been significantly reduced, although the need for improvements have become more evident. There is indubitably a desperate need for a more scientific approach, but the steady growth in popularity of the process has failed to stimulate a radical change in attitude in this country. Scientific methods are conspicuously absent from the design work, and the introduction of computer-aided techniques has failed to make any important changes. Computerisation has been successful in creating automatic draughting or computer-aided manufacturing facilities, but it has failed to make a notable contribution to flower pattern design methods.

There are a few scientific research projects in the area of cold-roll forming. Apart from the research carried out at the University of Tokyo, influential and impressive research projects are extremely difficult to find. Professor Kiuchi and the fellow researchers have made an outstanding contribution to cold-roll forming research and have succeeded in stimulating interest in this relatively unknown sheet metal forming process. Unfortunately, they have not been able to achieve innovations in flower pattern design methods, but the approach used by Kiuchi et al has built a solid foundation for future research projects.

Cold-roll forming has a large number of parameters which influence the process. The number of different combinations of values for the parameters is virtually infinite, which makes research projects based on empirical studies likely to achieve only a limited success. The final shape of the metal sheet will obviously be dependent on the residual strains which have been generated due to its passage through the rolling mill. The accurate evaluation of the residual strains, or even a close approximation, is a very complicated problem to solve. It is, therefore, difficult to select the approach which is most likely to yield the biggest advancement, a purely experimental project or a purely theoretical one. This uncertainty is possibly responsible for there being a dearth of scientific research in the area, combined with the fact that cold-roll forming has been a relatively unknown process until recent years. Fortunately, there has been research projects in other areas, such as press tool design, which have proposed theories that are also applicable to cold-roll forming. This is particularly useful when creating a mathematical model of the cold-roll forming process, where general theories on the bending of thin sheet metal are valid.

The discussion on the previous research into the cold-roll forming process has been divided into two categories. It is generally found that each research project is based mainly on experimental studies using a C.R.F. mill, or theoretical studies which model the bending process using a computer.

6.2 Previous Experimental Work.

The majority of published research papers in the area of cold-roll forming describe experimental investigations using a rolling mill and a number of different form-roll schedules. Usually the objective is either to devise an optimum schedule for a specific section geometry, or to study a production defect such as longitudinal curvature. Different form-roll combinations are tested on the mill and the effect on the geometry and surface texture of the sheet is observed. Because form-rolls are expensive to manufacture, the total number of form-rolls used in the project is usually reduced to a minimum. The conclusions from this type of investigation, therefore, are susceptible to criticism because they will

always be incomplete. A comprehensive study of mill setting techniques can be more easily implemented, so investigations of this type are frequently carried out.

Jimma and Ona[26] studied a number of production defects that occurred when rolling wide sheet to form corrugated products. The section geometry of a typical wide profile product is shown in Fig 6.1. This product is widely used in the building industry for roofing and wall panels. A common defect with wide profile rolling is that the edge flanges will not be straight in the longitudinal direction. A regular wave pattern is often exhibited along the edge of the sheet a defect often called "edge buckling". It was found that the total length of the edge flange was most influential because the defect was not evident until a certain length was exceeded.

A similar defect to edge buckling can occur in a longitudinal direction along the web or flange of a wide profile. Jimma and Ona suggested that the longitudinal strain in the sheet was an important cause of this defect, together with the total length of the web or flange. A large flange or web length increased the likelihood of this defect occurring. By increasing the speed of the form-rolls at the last few stages of the mill, the severity of the defect was reduced. It was claimed that this technique applied a tensile force on the sheet which reduced the strains causing the wave deformation.

Jimma and Ona have carried out a number of investigations of this nature. In a study of asymmetric sections[27] they attempted to establish a method for reducing the continuous twist in the finish rolled section. This defect is common in asymmetric section geometry and extremely difficult to overcome. It was suggested that the form-rolls of the last few stages in the mill should be rotated to counter the twist in the section. The spindles of both the top and bottom form-rolls were moved upwards on one side only, without changing the size of the gap between them. This remedy would be inappropriate for many mills because the bottom spindles are not adjustable.

Conclusions of this nature are typical from this type of investigation. They provide very limited assistance in general flower pattern design. To investigate the effects of varying

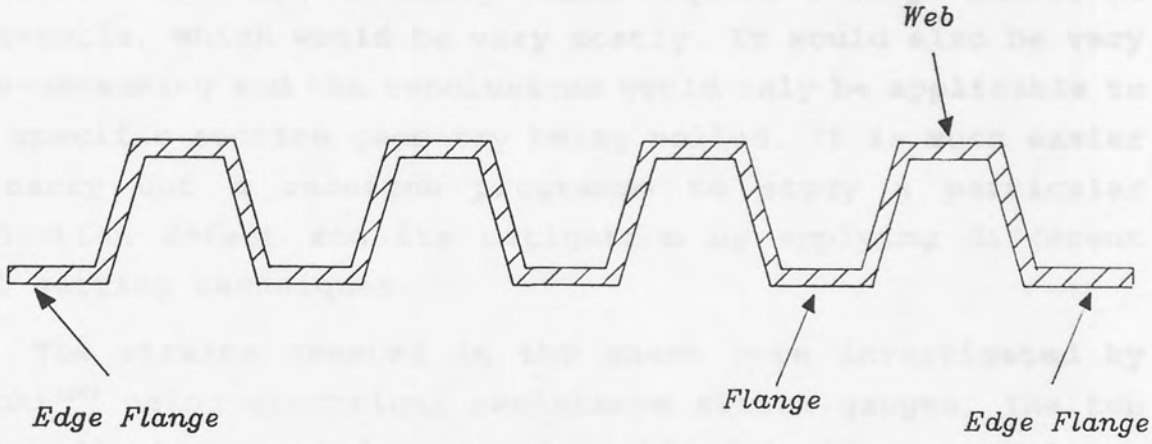

Cross-Section of a Wide Profile Product.

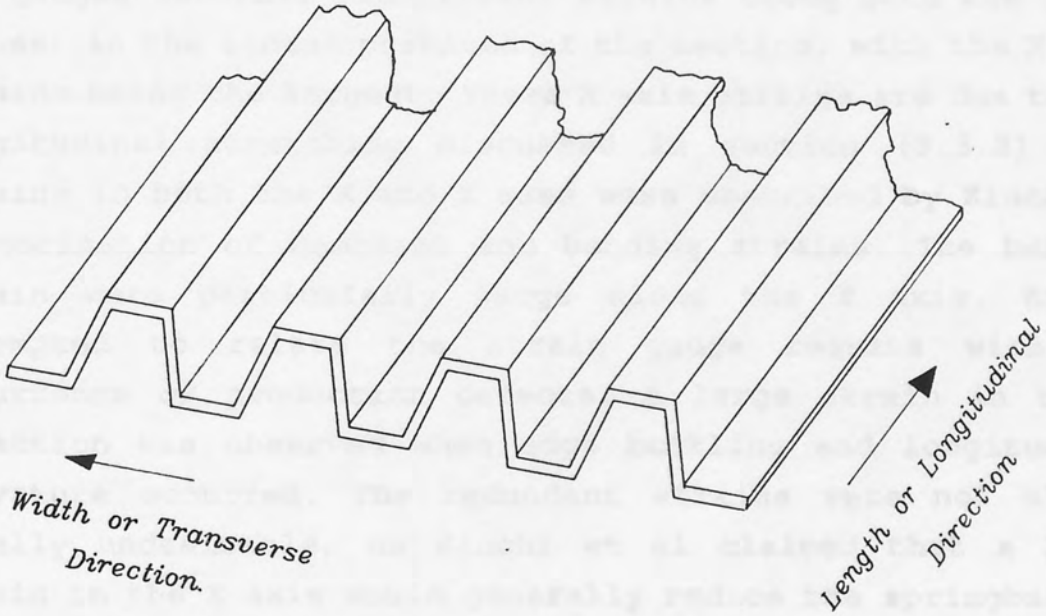

Figure 6.1

Typical Section Geometry of a Wide Profile.

the form-roll schedule fully would require a large number of form-rolls, which would be very costly. It would also be very time-consuming and the conclusions would only be applicable to the specific section geometry being rolled. It is much easier to carry out a research programme to study a particular production defect and its mitigation by applying different mill setting techniques.

The strains created in the sheet were investigated by Kiuchi[28] using electrical resistance strain gauges. The top form-rolls had special recesses machined in their profile as Fig 6.2 shows. This allows the gauges to pass through the stages of the mill without being crushed. Kiuchi emphasized the presence of strains in the section which did not contribute to the desired forming process. A bending strain in the bend regions of the section is the only strain which is required, but in cold-roll forming there are a number of additional strains. Kiuchi called them "Redundant Strains" because they are generally not required. Kiuchi reported that the gauges recorded significant strains along both the X and Y axes, in the linear portions of the section, with the X axis strains being the largest. These X axis strains are due to the longitudinal stretching discussed in section (3.3.2). The strains in both the X and Y axes were described by Kiuchi as a combination of membrane and bending strains. The bending strain were particularly large along the Y axis. Kiuchi attempted to relate the strain gauge results with the occurrence of production defects. A large strain in the X direction was observed when edge buckling and longitudinal curvature occurred. The redundant strains were not always totally undesirable, as Kiuchi et al claimed that a large strain in the X axis would generally reduce the springback at the bend regions.

By attaching lengths of thin aluminum wire to the sheet, an approximation of the contact surface forces between the sheet and form-rolls was obtained by measuring the deformation of the wire. An analysis of the major forces involved in the bending process was then carried out. It is important that the presence of different forces is recognized, but to measure them individually with a good degree of accuracy will obviously be very difficult. Kiuchi et al studied the

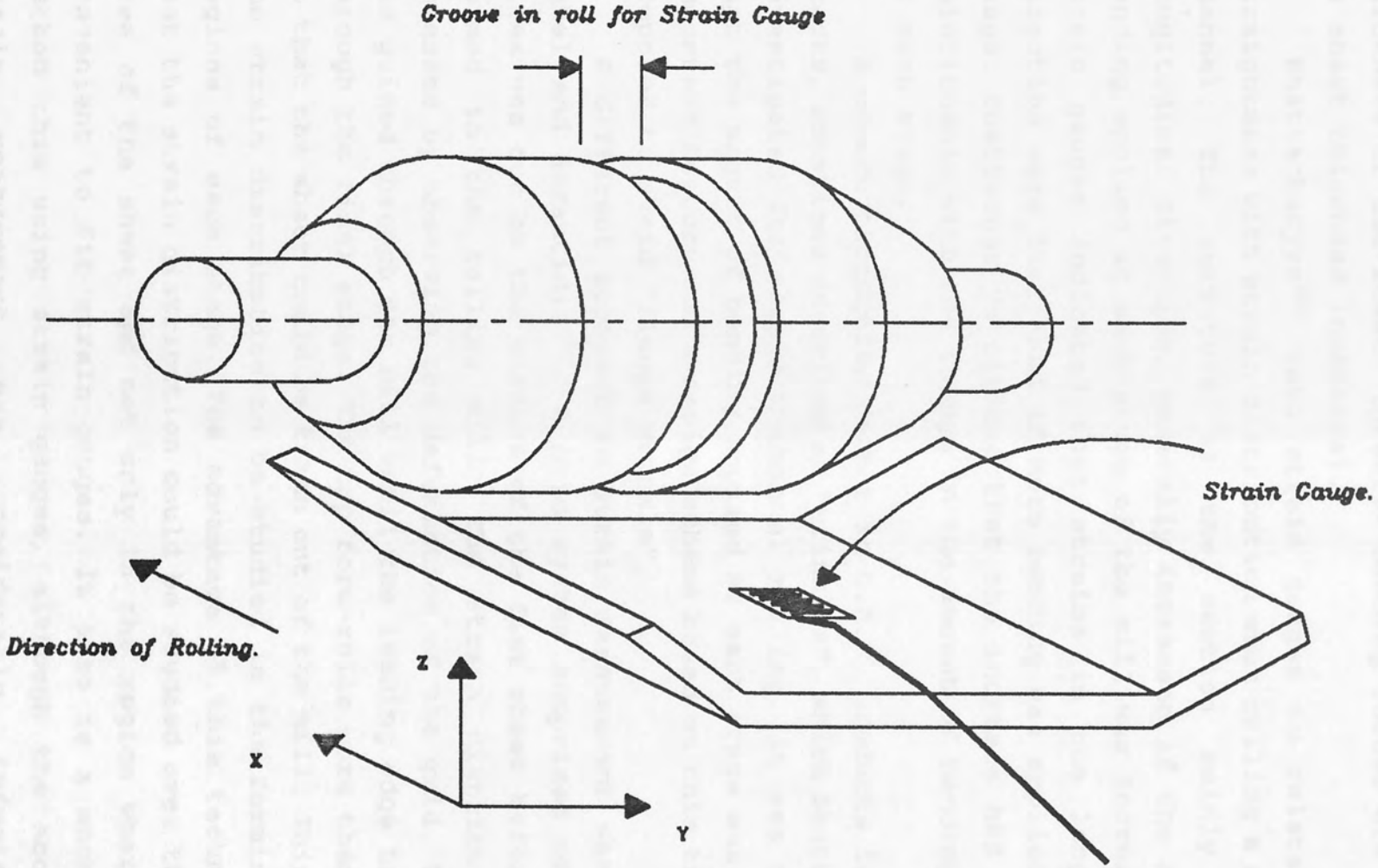

Figure 6.2

Material Strain Measurement Using Strain Gauges.

longitudinal curvature defect when rolling simple U-channel sections and recorded the forces which were present. It was claimed that the forces were substantially influenced by the pinch difference, the web-length (a longer web length increases the length of drive surface portion) and the thickness of the sheet, (greater bending forces are required as sheet thickness increases).

Bhattacharyya[29] used strain gauges to relate product straightness with strain distribution when rolling a simple U-channel. The curvature of the section mainly in the longitudinal direction, generally increased if the amount of bending applied at each stage of the mill was increased. The strain gauges indicated that strains in the longitudinal direction were increased if more bending was applied at each stage. Bhattacharyya claimed that the increase had a linear relationship with the change in the amount of bending applied at each stage.

A common production defect in C.R.F. products is surface cracks, sometimes described as "wrinkles", which Bhattacharyya investigated for simple U-channel rolling. It was suggested that the amount of bending applied at each stage was the most important feature and a design scheme based on this theory was proposed to avoid "flange wrinkle".

A different approach to strain measurement was used by Nobel and Sarantidis[30]. A grid system comprised of scribed lines was cut on the surface of the flat sheet before it was formed in the rolling mill. The strain distribution was assessed by observing the deformation of the grid. The sheet was guided through the mill until the leading edge had passed through the final stage. The top form-rolls were then removed so that the sheet could be taken out of the mill. This allowed the strain distribution to be studied in the forming length regions of each stage. The advantage of this technique was that the strain distribution could be studied over the entire area of the sheet and not only in the region where it was convenient to fit strain gauges. It also is a much cheaper method than using strain gauges, although the accuracy of strain measurement was considerably inferior. The investigation concluded that the mill pitch had no influence on the bending process unless it was reduced to a value which

was less than the largest forming length in the schedule. The effect of varying the pass height was also observed. The value of the maximum longitudinal strain recorded was found to be dependent on the pass height. The results generally supported the theory proposed in section 3.3.

The effect of using a lubricant was studied by Starchenko[31]. It was found that the bending forces required to form the sheet were reduced if a lubricant was used. The life of the form-rolls was also extended due to a reduction in wear caused by form-roll slippage.

Jimma and Ona[32] used 42 different schedules when rolling a simple channel section to investigate flange wrinkle. Three different sheet materials were investigated, with the objective of devising an optimum form-roll schedule for the section being rolled.

The limitation of this type of investigation is that the conclusion will only be applicable to the condition which existed during the investigation. If a different section geometry is rolled, the material specification of the sheet is altered, or maybe the mill setting is significantly different, then the schedule proposed by Jimma and Ona will obviously no longer be the optimum. Jimma and Ona used a large number of schedules, but many more schedules would have to be tested before an optimum schedule could arguably be suggested.

Experimental investigations of the type described in this section can be summarised as very time-consuming, tedious to carry out and the final conclusions have limited value. Apart from a few statements that have been made, to confirm something which is often already widely suspected to be true, the human effort involved appears to have rarely been rewarded.

6.3 Previous Theoretical Research.

The shape of the sheet after it has been rolled is dependent on the residual strains which are generated due to its passage through the mill. A mathematical model of the cold roll forming process must, therefore, be based on evaluating the strains in the section. Unfortunately, this is an

extremely difficult task. The bending process creates a complex three-dimensional shape in the forming length region at each stage of the mill. The stress distribution is complicated, with some regions suffering severe plastic deformation whilst others have only small residual stresses induced. Plastic deformation will result in material work hardening and when Griffin[33] studied this phenomenon using a simple tensile test it was found that the yield stress of typical C.R.F. products may increase by more than half of its original value.

The initial material properties of the sheet are also a troublesome feature when attempting to model the stresses accurately. Kato[34] tested nineteen different materials in an investigation involving sheet which was used in the cold-roll forming of tubes. The effect of impurities on the mechanical properties of the material was evident. If changes in material properties occur that cannot be predicted, then the evaluation of the stresses using a mathematical model cannot be made accurately. A mathematical model of the bending process must be based on the mean material property values. If material properties of a particular sheet, vary considerably from the mean values then inaccuracies in the model are unavoidable.

6.3.1 The Redundant Strains.

In the experimental investigation using strain gauges, discussed in section 6.1, Kiuchi emphasized the existence of forces on the sheet which did not contribute to the bending forces required to achieve the desired sheet geometry. In Fig 6.3 a small element taken from the bend region is analysed. Only the transverse bending strain, ε_{yb}, is required to form the bend, but the cold-roll forming process creates a number of other strains which Kiuchi called "Redundant Strains". Their influence on the final shape of the section can be considerable. The longitudinal strain, ε_{xx}, is often claimed to be the main cause of edge buckling, longitudinal curvature and twist.

The mill setting techniques which were discussed in section 3.4 will generally change the strain distribution including the values of the redundant strains. An important mill adjustment is the pass height, which will have a profound

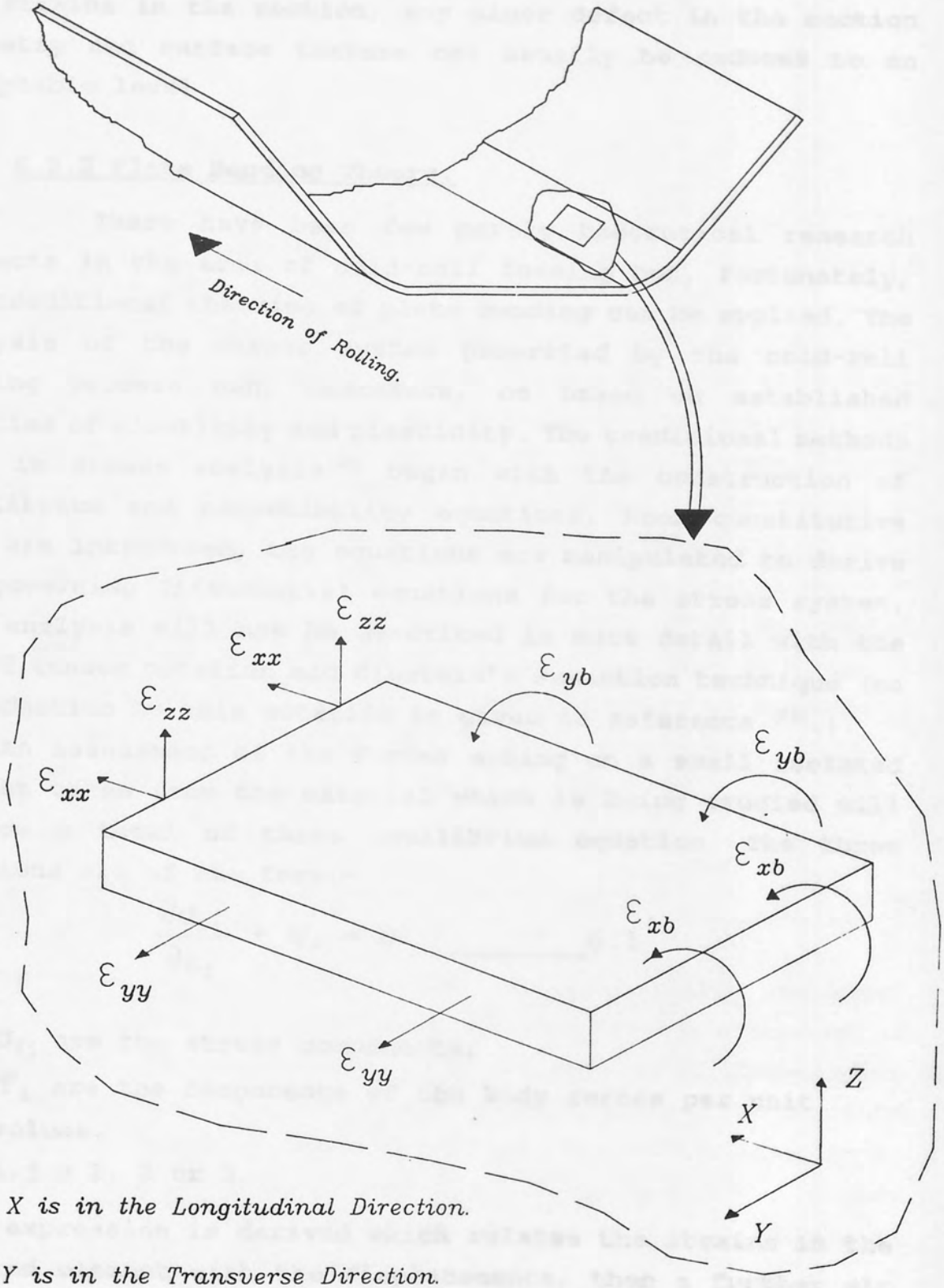

Figure 6.3

Kuichi's Redundant Strains.

effect on the value of ε_{xx}. By using such techniques to change the strains in the section, any minor defect in the section geometry and surface texture can usually be reduced to an acceptable level.

6.3.2 Plate Bending Theory.

There have been few purely theoretical research projects in the area of cold-roll forming but, fortunately, the traditional theories of plate bending can be applied. The analysis of the stress system generated by the cold-roll forming process can, therefore, be based on established theories of elasticity and plasticity. The traditional methods used in stress analysis[35] begin with the construction of equilibrium and compatibility equations. When constitutive laws are introduced, the equations are manipulated to derive the governing differential equations for the stress system. This analysis will now be described in more detail with the use of tensor notation and Einstein's summation technique (an introduction to this notation is given in reference [36].).

An assessment of the forces acting on a small isolated element taken from the material which is being studied will provide a total of three equilibrium equation. The three equations are of the form:-

$$\frac{\partial \sigma_{ij}}{\partial x_j} + \Psi_i = 0 \qquad \text{6.1}$$

where

σ_{ij} are the stress components,

Ψ_i are the components of the body forces per unit volume.

and $i, j = 1, 2$ or 3.

If an expression is derived which relates the strains in the isolated element with the displacements, then a further six equations are derived. The six equations for small displacements are of the form:-

$$\varepsilon_{ij} = \tfrac{1}{2}\left(\frac{\partial u_i}{\partial x_j} + \frac{\partial u_j}{\partial x_i} \right) \qquad \text{6.2}$$

The constitutive laws will relate the stress components in the isolated element with the corresponding strain components. If

the material obeys Hooke's Law and is both isotropic and homogeneous, the six equations, given in the form below, will apply if the deformation remains within the elastic limit.

$$\sigma_{ij} = \frac{2\mu\upsilon}{(1-2\upsilon)}\,\delta_{ij}\varepsilon_{kk} + 2\mu\varepsilon_{ij} \qquad 6.3$$

Equations 6.1 and 6.2 will apply to any material. The mechanical properties of the material are represented in the analysis by equation 6.3.

Most of the sheet used for cold-roll forming operations is either low carbon steel or a common non-ferrous alloy. The assumption that it will obey Hooke's Law and is isotropic and homogeneous will be correct in the majority of cases. If the equations in 6.2 are substituted into the set of equations in 6.3 and the result is substituted into the equations in 6.1, after considerable manipulation a set of equations is derived which will be in terms of displacements only. They are called the governing differential equations of the system or Navier's equations and they fully describe the problem to be solved. If the deformation remains within the elastic limit, the six Navier equations are of the form :-

$$\frac{1}{(1-2\upsilon)}\,\frac{\partial^2 u_j}{\partial x_i \partial x_j} + \frac{\partial^2 u_j}{\partial x_i \partial x_j} + \frac{1}{\mu}\,\psi_i = 0 \qquad 6.4$$

The geometrical and force boundary condition which are known are used to solve these equations. Because the number of unknowns is usually greater that the number of independent equations in the analysis, the system is often indeterminate and an exact solution cannot be found. The Navier equations, therefore, can only be solved for extremely trivial system equations. It is, therefore, necessary to make assumptions to enable a solution to be derived.

If the stresses induced exceed the elastic limit of the material, the Navier equations become more complex since a portion of the displacement is irrecoverable. However, the governing differential equations for plastic deformation are similar to equation 6.4, but a modified body force term is introduced to represent the irrecoverable component of the deformation field. Although a quasi-linear approach is used,

the complexity of the solution is significantly increased.

6.3.3 Obtaining an Approximate Solution.

Limit analysis[37] is a mathematical analysis that is commonly used to evaluate the stress and strain distribution when forming metal. It provides a technique that enables a solution to be found for the extremely complex differential equations. Although it will rarely be an exact solution, it will be a sufficiently accurate approximation in most cases. When used to find stresses or strains in a material, the limit analysis will frequently involve energy calculations. The governing differential equations to be solved are usually rewritten in terms of the energy applied to the system. If a limit analysis is applied, the objective is to obtain a solution which is a very close approximation to the exact answer. It will be extremely fortuitous if the exact solution is found. To obtain an approximate solution, the rigid conditions which apply to the governing differential equations of the system are relaxed. If a "lower bound" limit analysis is applied, the conditions used to establish the compatibility equations and the stress-strain relationships are not rigidly applied. The geometric boundary conditions used to solve the governing differential equations of the system are also relaxed. The method involves the selection of stress fields which are admissible to the system and the one which provides the maximum energy is used to obtain the approximate solution.

An "upper bound" limit analysis is similar to the "lower bound" but it is the equilibrium equations that are relaxed instead of the compatibility equations. When solving the governing differential equations, the boundary force conditions are not rigidly applied. If this method is used, a family of displacement fields which is compatible to the system is selected and the one which provides the minimum energy is used to obtain the approximate solution. Limit analysis techniques are widely used in stress analysis because of the need to obtain a good approximate solution. The finite element method, which has become so popular due to the availability of computers capable of doing the required calculations, uses the limit analysis technique.

If the stress system is assumed to be either a plane stress or plane strain system, then the mathematical analysis becomes much easier. A simple description of a plane stress or plane strain systems is given by Hearn[38]. Hill[39] described a plane strain analysis applied to a system subjected to bending moments and showed that the neutral axis can be moved towards the centre of curvature without creating significant inaccuracies in the analysis. If a plane strain condition is assumed, the radius of curvature can vary considerably. The plane stress analysis is contrary to this, the radius of curvature must not be less than three times the thickness of the sheet and the neutral axis is assumed to remain at the middle of the sheet. Unlike a plane strain analysis, the plane stress condition can only be assumed for thin sections.

Although a plane stress or plane strain theory could be used, in the case of bending and stretching of plates, the plane stress assumption reduces the mathematical complexity of the analysis. The sheet material which is used in cold-roll forming operation is generally classified as thin, with the major proportion of the sheets having a thickness of less than 5 mm. The size of the bend radius of cold roll formed sections vary considerably. However, it is feasible to assume that a plane stress analysis could be used in the mathematical model without creating significant inaccuracies provided that the ratio of the bend radius to thickness was not too small.

6.3.4 Previous Theoretical Research Projects.

Masuda[40] devised a mathematical model to represent the cold-roll forming of tube. A plane stress condition was assumed so that σ_z, τ_{zx} and τ_{zy} where equated to zero. All membrane strains were considered as negligible, so that only bending strains were assessed. A rigid-perfectly plastic material was assumed and the Lévy-Mises equations were applied to obtain the stress-strain relationship. The material yield point was determined by the von Mises criterion and Poisson's ratio was fixed at 0.5 for both elastic and plastic deformation. The geometry of the deformed sheet was defined by approximating the radius of curvature of the sheet along the X and Y axes. This enabled the bending stresses of the sheet in the X and Y to be evaluated.

The analysis provided an estimation of the strain distribution in the sheet from which the total energy consumed in the forming operation was calculated. Experimental tests were carried out to verify the mathematical analysis by measuring the bending forces applied by the form-rolls. Correlation between the two sets of results was very poor with an error of approximately 30 per cent. This is an example of an analysis which was erroneous because of the assumptions that were made. Assumptions must be made to allow the governing differential equation to be solved, but care must be exercised to ensure that features which are most influential are included in the analysis. The membrane stresses were not considered by Masuda, although other researchers[41] have since shown that they are very important.

Bhattacharyya[42] constructed a theoretical model for a simple U-channel section. A rigid-perfectly plastic condition was assumed and the following formula to find the plastic work done per unit length of bend, which is discussed by Hill[39], was applied in the bend region of the channel.

$$W_b = \frac{1}{4} \sigma_y t^2 \theta$$

where

t is the material thickness,

θ the angle of bend

σ_y is the yield stress of the material.

An assumption was made that bending in the flange or web was negligible. It was stated that a bend region must already exist in the sheet, so the analysis is not applicable to the forming length of the first stage of the mill.

Bhattacharyya developed the work done equation by analysing a small element of the sheet in the flange and calculating the work done due to the stretching of each element. The total work done due to stretching per unit length was obtained by integrating over the area of each individual element. The total plastic work done per unit length was calculated by adding the work due to bending in the bend region and the work due to stretching in the flange. The web was assumed to remain undeformed.

$$W_t = W_b + W_s = \frac{1}{4}\ \sigma_y\ t^2\ \theta + \frac{1}{6}\ \sigma_y\ a^3\ t \left[\frac{d\theta}{dz}\right]^2$$

where

a is the flange length

z is measured longitudinally along the forming length.

The total work done is found by integrating over the forming length L (see Fig 3.2).

$$W_t = \sigma_y\ t \int_{z=0}^{z=L} \left[\frac{t\theta}{4} + \frac{a^3}{6} \left(\frac{d\theta}{dz} \right)^2 \right] dz$$

Bhattachayya solved this equation by applying the principal of stationary total potential energy directly. This states that for all geometrical configurations that a mechanical system could possibly attain, the true one that corresponds to an equilibrium of forces is that which has a stationary total potential energy. The variational calculus was applied to find the condition for stationary total potential energy and it was found that the W^T equation satisfied Euler's equation directly. For an introduction to the variational calculus refer to Richards[43]. When the boundary conditions at the start of the forming length are applied where X=0 and $\theta = 0$, a solution to the governing differential equations of the system is obtained. After some manipulation, the following equations are derived :-

$$\theta = \frac{\theta_p z}{L} + \frac{3tz}{8(a^3)}\ (z-L)$$

and

$$L = a \sqrt{\left(\frac{8a\theta_p}{3t} \right)}$$

where

θ_p is the prescribed increase in bending angle at the stage

θ is the angle of bend at the point z along the forming length.

It would appear that the expression defining θ will provide a reasonably accurate approximation of the shape of the sheet in the forming length region. If the boundary conditions are applied at the opposite end of the forming length, where X=L and the angle of the flange is θ_p the solution to the θ equation becomes a complex number. The assumption that bending can be ignored in the flange and web region has created significant anomalies. Bhaatacharyya recognised the limitations of the analysis, but claimed that the equations to determine the forming length were a good approximation. This was verified by experimental investigations.

Kiuchi[44] developed a mathematical model for the cold-roll forming of circular tubes by applying an upper bound limit analysis. The following expression was used as the assumed displacement field :-

$$S(X) = \mathrm{Sin}\left[\frac{\pi}{2} \left(\frac{X}{L_s} \right)^n \right]$$

where

X = the distance somewhere between the i^{th} and the $(i+1)^{th}$ stage

L_s = the distance between the neighbouring stages.

n = an unknown value.

The S(X) value is used to calculate the geometry of the sheet using the expressions given in Fig 6.4. Kiuchi divided the sheet into small elements and devised an expression for the membrane strain in each element based on simple trigonometry. The bending strains were estimated using a similar method to that adopted by Masuda[40], with the calculation of the sheet curvature along the X and Y axes expressing the degree of bending. The assumed displacement expression, S(X), was an independent variable in both the membrane strain and bending strain equations. The magnitude of the strain in each element was evaluated by the summation of the strain due to bending and the strain due to stretching. The constitutive laws to relate the strains to the stresses were taken from a technique developed by Yamada[45] for plane analysis using the finite

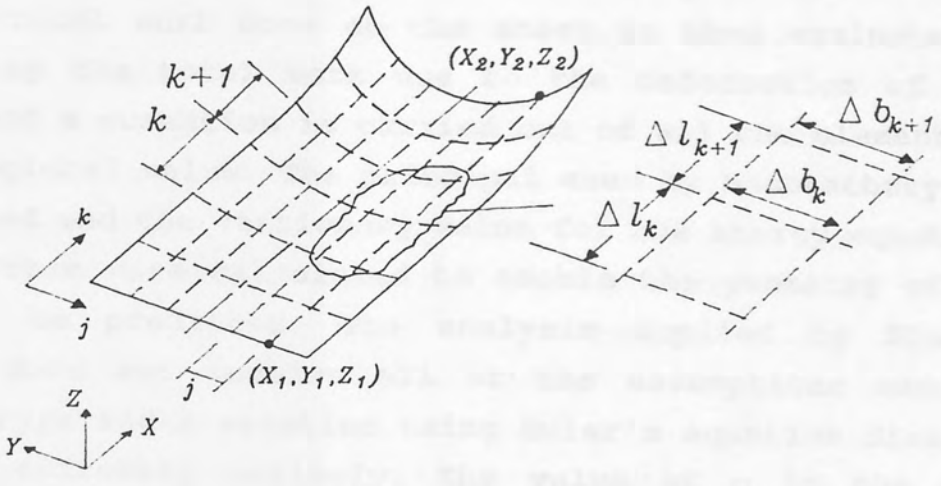

$$S(X) = Sin \left[\frac{\pi}{2} \left\{ \frac{X}{L} \right\}^{n} \right]$$

$$Y = Y_1 + [Y_2 - Y_1]\ S(X)$$

$$Z = Z_1 + [Z_2 - Z_1]\ S(X)$$

The membrane strains for step k,j are given by :-

$$(d\varepsilon_{xm})_{k,j} = (\Delta l_{k+1} - \Delta l_k) / \Delta l_k$$

$$(d\varepsilon_{ym})_{k,j} = (\Delta b_{k+1} - \Delta b_k) / \Delta b_k$$

The bending strains for the step k,j are given by :-

$$(d\varepsilon_{xb})_{k,j} = \eta \left[\frac{1}{(\rho_x)_{k,j}} - \frac{1}{(\rho_x)_{k-1,j}} \right]$$

$$(d\varepsilon_{yb})_{k,j} = \eta \left[\frac{1}{(\rho_y)_{k,j}} - \frac{1}{(\rho_y)_{k-1,j}} \right]$$

Figure 6.4

Derivation of Geometry and Strains According to Kiuchi.

element method. Yamada's equations allow an element to enter the plastic region, with Hooke's law being applied in the elastic region.

The total work done on the sheet is then evaluated by calculating the total work due to the deformation of each element and a summation is carried out of all the elements to obtain a global value. The principal used by Bhattacharyya[42] was applied and the stationary value for the energy equations of the system were calculated to enable the geometry of the sheet to be predicted. The analysis applied by Kiuchi, however, does not involve all of the assumptions made by Bhattacharyya and a solution using Euler's equation directly would be extremely unlikely. The value of n in the S(X) expression was continually incremented until a stationary value for the total work expression was obtained using the Neldler-Meade Simplex minimisation technique[46]. Having found the value of n which results in a minimum total potential energy, the geometry of the sheet is defined using this value of n and the resulting stresses are evaluated.

The main objective of Kiuchi's model was to design form-roll schedules for tube rolling. It was necessary, therefore, to devise a method for defining the amount of bending applied at each stage of the mill. Kiuchi developed a software program which determined the amount of bending by ensuring that the total work done at each stage of the mill was approximately equal. Firstly, the stationary values are found from the work equations so that a value for the variable n can be established. If the total work done by the stage, calculated using the n value, is significantly smaller or larger than that of the first stage, the amount of bending applied by the stage is adjusted accordingly and a new n value is found. As an alternative to having equal work done at each stage, the amount of bending can be determined by having an equal longitudinal force at each stage. The direct stress components in the sheet that act in the X direction were analysed to obtain an approximation of the total force acting in the longitudinal direction.

Kiuchi's theoretical model was original and innovative when it was first introduced. It is claimed that it has successfully designed a number of form-roll schedules for tube

rolling. It is not difficult to criticize the model, however, because there is only one variable in the expression which describes the deformed surface. If the finite element method is used there is likely to be several hundreds. A theory must be proposed to define the amount of bending applied at each stage, but the validity of the theory used by Kiuchi is questionable. Although it was claimed that the model had assisted in the design of successful schedules, there is a lack of experimental data to support the theoretical model. Numerical values of stress and strain produced by the theoretical model were not compared with corresponding experimental values obtained, for example, using electrical resistance strain gauges.

The theoretical model developed by Panton[11] was very similar to the Kiuchi model. A new assumed displacement field was developed following a series of experimental investigations.

$$S(X) = e^{-a[(L-y)/y]^b}$$

The number of unknowns had been increased to two, which provided the possibility of obtaining a more accurate prediction of the sheet geometry. The model was not restricted to tube rolling because Panton devised an equation to evaluate the strain in the linear portions of the section. The bend region of the section was analysed using the S(X) displacement field in a similar way to Kiuchi's tube rolling analysis. The linear portions of the section were analysed to determine the longitudinal strains using equations based on simple trigonometric ratios. Longitudinal strains only were assessed in the linear portions of the section. The method which determines the values of the unknowns a and b in the S(X) displacement equation was identical to the method used by Kiuchi. Panton verified the theoretical model with experimental data obtained from rolling a simple U-channel. The strain distribution was measured using a grid system similar to Nobel and Sarantidis[30], with rows of small circular dots being cut on the flat sheet prior to rolling. Panton

claimed that there was a reasonable correlation between the experimental data and the results obtained from the theoretical model. The numerical values from the theoretical model were generally greater, but this would be expected since the rolled specimens were removed from the mill before the deformation of the grid was measured. The springback that will have occurred would tend to reduce the measured values. The most significant limitation in Panton's theoretical model is that a high level of accuracy could not be attained. Only longitudinal strains are considered in the linear portions of the section and only two unknowns were involved in the assumed displacement field which was used to analyse the strains in the bend region. An error in the prediction of the shape of the bend region would also cause errors in the calculated strains in the linear portions. The calculation of longitudinal strain was based on simple and concise calculations will only occur if the section geometry is not significantly more complicated than a U-channel. There is a limitation on the complexity of the section geometry if the evaluation of extremely long trigonometrical expressions is to be avoided.

In certain cases Panton's model is capable of providing a reasonably good estimate of the strain distribution in the sheet. There are cases, however, where considerable inaccuracies would be unavoidable. The section geometry would have to be relatively simple for reasonable accuracy to be attained. If the linear portions of the section was subjected to bending, which will always occur in the forming length of the first stage, even a simple U-channel could not be accurately analysed.

CHAPTER SEVEN.

THE FINITE ELEMENT METHOD.

7.1 Introduction.

The theoretical models of the cold roll forming process discussed in section 6.2 all applied the limit analysis technique. There are a number of established methods which use limit analysis to derive a solution to unwieldly sets of equations by providing a close approximation to the exact solution. Three limit analysis techniques are described below which are commonly applied to a material stress analysis problems.

a) Finite Difference Technique.

This method substitutes simple, localised algebraic expressions for the differential operators in the governing differential equation which are valid at certain points or nodes throughout the body. A large number of nodes may be required to accurately represent the behaviour of the system. Possibly, however, its biggest disadvantage is that the method is difficult to computerise.

b) Boundary Element Method.

This method transforms the governing differential equations into equivalent sets of integral equations. In this technique the integrals are solved analytically before any discretisation or approximations are made. The mathematics is usually extremely demanding, but the method can be computerised easily. Since the number of algebraic equations to be solved is reduced, the method has become more popular in recent years. However, the technique cannot easily model thin sheet materials.

c) Finite Element Method.

This method divides the region which is to be studied into a number of small elements. Each element approximately reproduces the behaviour of the region of the material which it is representing and continuity is enforced at certain points between neighbouring elements.

When the elements are assembled together they provide a good approximation to the real system. This is the most popular limit analysis technique, but has a major disadvantage due to the large number of unknowns in the analysis. The mathematics is relatively easy, however, and the method is highly compatible with computerisation. Wood[47] analysed the material behaviour of a number of sheet metal forming processes using the finite element methods. His conclusions confirmed that a finite element solution could be used to predict such material behaviour.

There are many different ways in which the limit analysis principles can be applied apart from the three common techniques that have been listed. Kiuchi used an upper bound limit analysis in his theoretical model which was discussed in section 6.3.4, but it was not a finite difference, boundary element or finite element method. The governing differential equation for a theoretical model of the cold roll forming process will be highly complex. To find an approximate solution using a limit analysis technique is obviously a feasible approach, but the decision which limit analysis technique would be the most suitable is more difficult.

The cold roll forming process has a number of characteristics which are extremely difficult to model mathematically. The material will extend into the plastic zone, creating the usual difficulties when stress is not linearly proportional to strain. The material non-linearity may be combined with geometric non-linearity to create the an additional problem. This occurs when large material displacement takes place due to severe loading conditions and there is a likelihood that it may occur in the cold roll forming process. The bend regions of the section are subjected to severe deformation, but this area is relatively small compared with the total area of the section. It is most likely that large areas of the forming length will experience material non-linearity only. The combined effect of these features makes the cold roll forming process particularly difficult to model accurately.

7.2 Commercial Stress Analysis Packages.

In recent years, powerful computer systems have become widely available at a reasonable cost and with diligent technical support from the vendor. Largely due to this, the finite element method has become the most popular way of analysing material stress analysis problems. It was not surprising, therefore, that only finite element packages were found in a survey to identify the commercial computer software packages which were most suitable for modelling the cold roll forming process. The method has many advantages over rival limit analysis techniques but, unless the problem is simple the solution must be formulated on a powerful computer.

There are few commercial finite element package available which offer non-linear analysis. At Aston University the PAFEC[48] package is available on a Vax 8500 cluster system. It is not capable of modelling the cold roll forming process using the two-dimensional elements. However, PAFEC could model the process using three-dimensional brick type elements, but it was found that the processing time was far too great and problems occurred due to the much smaller dimension through the thickness of the plate. Other packages studied in the survey which were capable of analysing the plastic region using two dimensional elements tended to be rather expensive, and suggested that a long processing time was inevitable if the mesh required a large number of elements. A number of software companies which did not have a suitable package offered to modify an existing package to allow the analysis to be performed and proposed to customise the package in order to reduce the processing time slightly. The general conclusions of the survey confirmed that the finite element method could model the cold roll forming process accurately, but the complexity of the problem would result in large computer processing times.

Commercial finite element packages are designed to be general purpose programs and, therefore, would not be ideal for carrying out a specialist analysis. This was one of the major disadvantages of purchasing a commercial finite element package solely to model the cold roll forming

process. The vast majority of the facilities would not be used.

The main reason why a commercial finite element package was not used in this research project, however, was based purely on financial considerations. The cost involved in purchasing the software would be substantial and a powerful mainframe computer must be used. The vast majority of the cold roll forming companies in this country are classified as "small" and a large financial investment in new computerised methods would be impossible for most of them.

In an attempt to overcome the disadvantages of commercial packages, a finite element program was written in this research project to model the cold roll forming process. The problem of financing the purchase of software would be avoided and a specially tailor-made package may not require an extremely powerful computer. The program would be much smaller than a commercial package because it would not have the features of a general purpose program. There will also be a possibility of making significant reductions in processing times.

The finite element method was chosen in preference to other limit analysis techniques because there was evidence that it could do the task successfully. Also, there is literature readily available on the finite element method and the techniques for computerising it. From the outset, however, the magnitude of the endeavour was not underestimated. The theory of finite elements is not simple, and the translation of the theory into a computer language requires the understanding of additional concepts.

7.3 Rudiments of the Finite Element Method.

It is most fortunate that the analysis which is applicable to a linear stress-strain law can also be applied when the constitutive law is non-linear. When the strain has entered the plastic zone a linear analysis can be repeatedly applied using one of the techniques described in Chapter Eight. It is important, therefore, that the linear analysis is fully understood before progressing to the more complex non-linear theories. In this section a

brief outline will be given of the concepts that are applied for a purely linear analysis using the finite element method. The sheet which is being deformed in cold roll forming is a continuum and it will have an infinite number of ways it can deform, depending upon the loading. The governing differential equations for a continuum are insoluble in most practical cases, which is why a limit analysis is required to obtain a good approximate solution.

The finite element method gets its name from the first step in the analysis. The system is divided up into a number of small elements, a process called discretisation, with each element intersecting with its neighbour at special points on the boundary called "nodes". The properties of each element are assumed to be concentrated or lumped at the nodes and this includes the unknowns which the analysis will be evaluating. If the unknowns are displacements, for example, then the objective of the analysis will be to approximate the displacement of any arbitrary point within the element in terms of the displacements at the nodal points.

When the principal of minimum total potential energy is used with the displacements as the unknowns, a solution is approximated using the "displacement method". The strains are calculated from the approximation of displacements and the stresses are found by applying a constitutive law. A disadvantage of this approach is that the stresses are not as accurately evaluated as the displacements. The differential of the estimated displacement values to obtain the corresponding strains will create unavoidable inaccuracies.

If nodal stresses are used as the unknowns in the analysis, then the principle of total complementary energy is used. This will provide an approximation of the stresses directly and is usually called the "Equilibrium Method".

There are certain cases where an analysis is carried out with both the nodal displacements and stresses being unknown. In this case there are two approaches which are applicable. If an "Hybrid" analysis is applied the modified principle of stationary total complementary energy is used. Alternatively, a "Mixed" analysis may be chosen where the

modified "Reissner Variational Principle" is employed.

Both the Mixed and Hybrid methods involve a more complicated analysis than either the displacement or equilibrium methods and are rarely used. The displacement method is the most popular method. All the commercial finite element packages in the survey which were potentially capable of modelling the cold roll forming process used the displacement method. After considering the possibility of using the equilibrium method, the displacement method was chosen for the model developed in this research project.

7.3.1 The Total Potential Energy.

The total potential energy which fully describes a system deformed within the elastic region can be described by the following equation.

$$V = \frac{1}{2}\int_{Vol} [\varepsilon]^T[\sigma]\ dVol - \int_{Vol} [\delta]^T[\mathbf{p}]\ dVol - \int_{S} [\delta]^T[\mathbf{q}]\ dS - [\delta]^T[\mathbf{R}]$$

where $[\sigma]$ and $[\varepsilon]$ are the stress and strain vectors respectively, $[\delta]$ are the displacements at any point, $[\mathbf{p}]$ is the body forces per unit volume, $[\mathbf{q}]$ are the applied surface tractions over the surface area S and $[\mathbf{R}]$ are the concentrated loads.

The governing differential equation of the system can be obtained by minimising the above equation and reference should be made to Zienkiewicz[49] for a detailed derivation. The first integral is the internal strain energy of the system and represents the work done by the system to resist the external work which is being applied. The second term represents the work done by the body forces such as gravity or magnetic fields. This can be ignored if the energy equation represents the sheet metal which is being deformed in a cold roll forming process, since its contribution will be small compared with the other terms. The last two terms

represent the external work done, which, in the cold roll forming process, will be the work done by the forces imparted to the sheet by the rolls. A uniformly distributed load acting over a surface area S, is described using the [q] matrix and a concentrated point load using the [R] matrix. When the finite element technique is applied, the total potential energy of a system will be the sum of the energy contributions of the individual elements. In the analysis which is explained later, both the external work done terms are represented by one matrix $[F_e]$ which expresses the forces acting at the nodes of the element. In section 7.3.4 a different expression is developed for the internal strain energy term and includes the definition of the element stiffness matrix $[K^e]$. The result is that the total potential energy of an element can be described using the following matrix format.

$$V^e = \tfrac{1}{2} [\delta^e]^T [K^e] [\delta^e] - [\delta^e]^T [F_e]$$

where

$[\delta^e]$ is a vector of nodal displacement of the element.

The following analysis identifies the parts of this equation which will require numerical evaluation. If an "Upper Bound" limit analysis is applied the displacement field which produces the minimum total potential energy is the one which is selected. To find the extrema of the V_e expression, differential calculus can be applied in the normal manner.

$$\frac{dV_e}{d[\delta^e]} = 0 = [K^e] [\delta^e] - [F^e]$$

This is equated to zero to find a stationary value.
It is apparent that only $[K^e]$ and $[F^e]$ will have to be evaluated since $[\delta^e]$ are the unknown nodal displacements which are to be calculated. A far more elegant version of this proof is given by Richards[43] using the principal of virtual work. The $[K^e]$ matrix which represents the element stiffness will always be a square symmetric matrix. The values in $[F^e]$ are called the "generalized forces" of the element and they are assumed to act at the element nodal points.

7.3.2 Displacement Model.

The basic principles of limit analysis were discussed in section 6.3.1. The displacement method is an upper bound limit analysis, thus a family of displacement fields must be chosen which is compatible with the system. A more complicated displacement function can be formulated by using natural coordinates and, because the analysis is considerably enhanced, it is worth the extra effort. Experience has shown that greater accuracy can be achieved using a more complexed element, rather than a large number of simpler ones. If natural or curvilinear coordinates are used, an element which has its geometry described using the coordinates X and Y is converted into a ξ and η coordinate system, with both ξ and η varying from +1 to −1. This is shown diagrammatically in Fig 7.1. To explain the transformation into the X, Y domain of an arbitrary point on an element which has its geometry described in the ξ, η domain, an example of an eight node quadrilateral element is used. With reference to the PAFEC Theory Manual[50], the following is an expression to evaluate the X coordinate of a point which is currently described using ξ, η coordinates.

$$x = \alpha_1 + \alpha_2\xi + \alpha_3\eta + \alpha_4\xi\eta + \alpha_5\xi^2 + \alpha_6\eta^2 + \alpha_7\xi^2\eta + \dot{\alpha}_8\eta^2\xi$$

In matrix form this becomes

$$x = [1,\ \xi,\ \eta,\ \xi\eta,\ \xi^2,\ \eta^2,\ \xi^2\eta,\ \eta^2\xi]$$
$$[\alpha_1,\ \alpha_2,\ \alpha_3,\ \alpha_4,\ \alpha_5,\ \alpha_6,\ \alpha_7,\ \alpha_8]^T$$

or

$$x = [\mathbf{P}]\,[\alpha_x]^T \qquad (7.1)$$

The Y and Z coordinates are defined in a similar way. The Z coordinate is only necessary when a three dimensional analysis is required. An expression to describe the displacement of an arbitrary point on the element is also required. A common type of finite element, called an "isoparametric" element, uses a similar expression to define both the displacement and the coordinate transformation to the X, Y domain. In Fig 7.2 an isoparametric finite element is shown. The X coordinate at

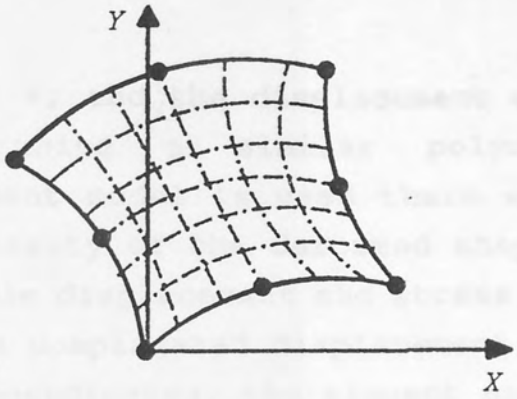

The X–Y Domain.

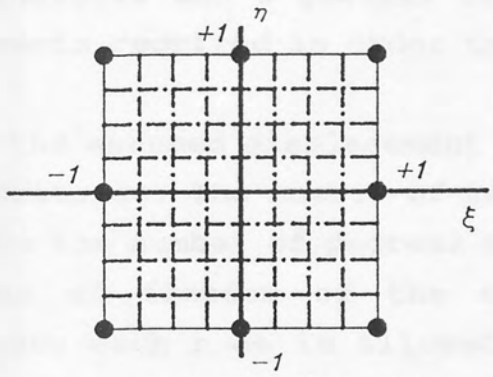

The ξ – η Domain

Figure 7.1

Conversion from Cartesian to Natural Coordinates.

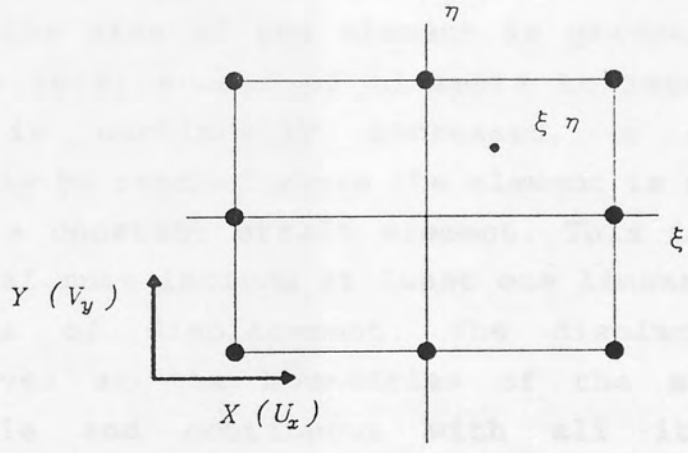

Transformation of Axes.

$$X_p = \alpha + \alpha\ \xi + \alpha\ \eta + \alpha\ \eta\xi + \alpha\ \eta^2 + \alpha\ \xi^2 + \alpha\ \eta^2\xi + \alpha\ \eta\xi^2$$

Variation of Displacement in the X Direction

$$U_x = \alpha + \alpha\ \xi + \alpha\ \eta + \alpha\ \eta\xi + \alpha\ \eta + \alpha\ \xi + \alpha\ \eta^2\xi + \alpha\ \eta\xi^2$$

Figure 7.2

Displacement Fields.

the point P, and the displacement at P in the X axis, are defined using a similar polynomial. If a simple displacement model is used there will be a limitation on the complexity of the deformed shape of the element. Only very simple displacement and stress fields can be modelled. If a more complicated displacement model is chosen, using natural coordinates, the element properties such as stress or strain can vary within the region of the element. This allows a more elegant analysis and a general reduction in the total number of elements required in order to model the system accurately.

The suitability of the assumed displacement polynomial depends on a number of criteria. The number of terms in the polynomial must relate to the number of degrees of freedom. In Fig 7.2 the degrees of freedom of the eight-noded element is sixteen because each node is allowed to deform along the X and Y axes. Therefore the polynomial to define the displacement in the X axis has eight terms to allow for the eight degrees of freedom in the X axis.

It is essential that the element will remain completely free of strain if rigid body movement occurs. To achieve this the polynomial must have a constant term.

If the size of the element is gradually reduced, so that the total number of elements to represent the real system is continually increased, a situation must eventually be reached where the element is so small that it will be a constant strain element. This implies that the polynomial must include at least one linear term in all of its axes of displacement. The displacement and its derivatives at the boundaries of the element must be compatible and continuous with all its neighbouring elements. This is necessary in order to avoid gaps or overlapping occurring at the element boundaries.

The polynomial in Fig 7.2 satisfies these conditions, where α_1 is the constant term and $\alpha_2\xi$ and $\alpha_3\eta$ are the two linear terms. If the displacements are the unknowns, they and some of their derivatives must be continuous within the element and compatible with neighbouring elements at the nodal point. There are displacement polynomials, however, which do not achieve these conditions and these are called

"non-conforming" elements. Such elements have been used to successfully model a number of engineering problems, including sheet bending processes. Zeinkiewicz[49] provides a detailed discussion on non-conforming elements.

Using equation (7.1) a matrix of X coordinates at the nodes of an element, $[\mathbf{x}_e]$, can be found. This also introduces the $[\mathbf{A}]$ matrix which is defined below.

$$[\mathbf{x}_e] = [\mathbf{A}]\,[\alpha_x]$$

where

$$[\mathbf{A}] = \left\{ [\mathbf{P}_1], [\mathbf{P}_2], [\mathbf{P}_3], [\mathbf{P}_4], [\mathbf{P}_5], [\mathbf{P}_6], [\mathbf{P}_7], [\mathbf{P}_8] \right\}^T$$

$[\mathbf{A}]$ is an 8 x 8 square matrix.

$$[\mathbf{x}_e] = [x_1, x_2, x_3, x_4, x_5, x_6, x_7, x_8]$$

and $$x_1 = [\mathbf{P}_1]\,[\alpha_x]$$

It is necessary to obtain an expression for displacements in terms of the nodal displacements since it is assumed that the properties of an element are concentrated at its nodes. By substituting for $[\alpha_x]$, and after some manipulation, the X coordinate of any point on the element is found in terms of the nodal X coordinate by using the following equation.

$$x = [\mathbf{P}]\,[\mathbf{A}]^{-1}[\mathbf{x}_e] \qquad (7.2)$$

A similar expression gives the Y and Z coordinates at any point in the element.

There will be occasions when the evaluation of $[A]^{-1}$ will cause considerable problems. To avoid this difficulty a more elegant solution can be obtained by using interpolation polynomials. Either the Serendipity family or the Lagrange family can relate geometry or displacement of an arbitrary point on the element with the nodal values at the element boundary.

An example of an eight-node quadrilateral element is shown in Fig 7.3. The N_i expressions are from the serendipity family. Generally,

$$x = \sum_{i=1}^{i=n} N_i x_i$$

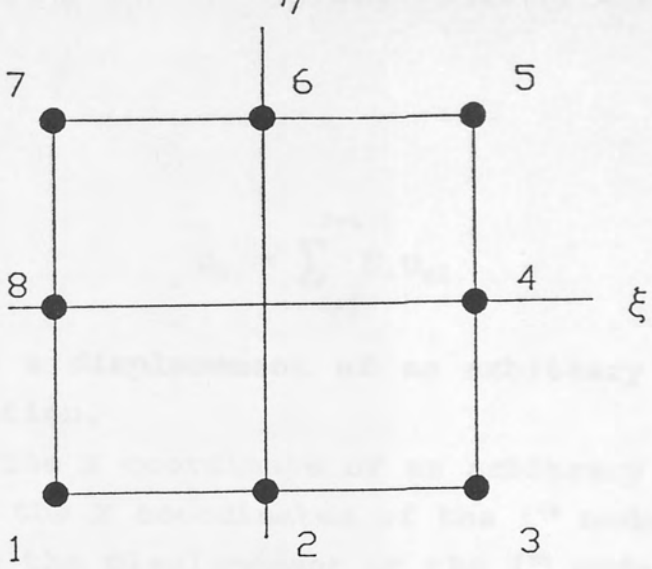

For Corner Nodes $i = 1, 3, 5$ and 7

$$N_i = \frac{1}{4}(1 + \xi_i \xi)(1 + \eta_i \eta)(\xi_i \xi + \eta_i \eta - 1)$$

For Midside Nodes where $\xi = 0$ ($i = 4, 8$)

$$N_i = \frac{1}{2}(1 + \xi^2)(1 + \eta_i \eta)$$

For Midside Nodes where $\eta = 0$ ($i = 2, 6$)

$$N_i = \frac{1}{2}(1 + \eta^2)(1 + \xi_i \xi)$$

Figure 7.3

Shape Functions for a Quadratic Element.

and

$$u_x = \sum_{i=1}^{i=n} N_i u_{xi}$$

where

u_x is a displacement of an arbitrary point in the X direction.

x is the X coordinate of an arbitrary point

x_i is the X coordinates of the i^{th} node.

u_{xi} is the displacement at the i^{th} node along the X axis.

and n = the number of nodes in each element.

For the theoretical model developed in this research project the displacement function is based on the Serendipity family.

The previous matrix equation (7.2) is now replaced with

$$x = [\mathbf{N}_i]\,[\mathbf{x}_i]$$

If the finite element is isoparametric, the N_i expressions can be used directly in the assumed displacement function. For an element which models displacement in X and Y only and therefore is a plane stress or a plane strain element, the following matrix identity is used.

$$[\delta] = \begin{bmatrix} u_x \\ u_y \end{bmatrix} = \sum_{i=1}^{i=n} \begin{bmatrix} N_i & 0 \\ 0 & N_i \end{bmatrix} \begin{bmatrix} u_{xi} \\ u_{yi} \end{bmatrix}$$

7.3.3 Derivation of Stress and Strain.

If the deformation is linear and within the elastic region the strains within the element are found using Cauchy's Infinitesimal Strain Tensor. The ε_{xx} value is calculated using the expression below :-

$$\varepsilon_{xx} = \frac{\partial u_x}{\partial x} = \frac{\partial}{\partial x}\left\{\sum_{i=1}^{i=n} N_i u_{xi}\right\}$$

Since N_i is a function of the curvilinear coordinates (ξ,η) and $\frac{\partial u_x}{\partial x}$ is required, the Jacobean [J], is applied[51]. The differential is found from the following manipulation.

$$[J] = \begin{bmatrix} \frac{\partial x}{\partial \xi} & \frac{\partial y}{\partial \xi} \\ \frac{\partial x}{\partial \eta} & \frac{\partial y}{\partial \eta} \end{bmatrix} = \sum_{i=1}^{i=n} \begin{bmatrix} \frac{\partial N_i}{\partial \xi} x_i & \frac{\partial N_i}{\partial \xi} y_i \\ \frac{\partial N_i}{\partial \eta} x_i & \frac{\partial N_i}{\partial \eta} y_i \end{bmatrix}$$

Using standard procedure, the [J] matrix is inverted

$$[J]^{-1} = \begin{bmatrix} \frac{\partial \xi}{\partial x} & \frac{\partial \eta}{\partial x} \\ \frac{\partial \xi}{\partial y} & \frac{\partial \eta}{\partial y} \end{bmatrix} = \frac{1}{\text{Det } |J|} \begin{bmatrix} \frac{\partial y}{\partial \eta} & -\frac{\partial y}{\partial \xi} \\ -\frac{\partial x}{\partial \eta} & \frac{\partial x}{\partial \xi} \end{bmatrix}$$

Therefore, where $\frac{\partial N_i}{\partial x}$ is a function of ξ and η is obtained from :-

$$\frac{\partial N_i}{\partial x} = \frac{\partial N_i}{\partial \xi} \frac{\partial \xi}{\partial x} + \frac{\partial N_i}{\partial \eta} \frac{\partial \eta}{\partial x}$$

Similarly

$$\frac{\partial N_i}{\partial y} = \frac{\partial N_i}{\partial \xi} \frac{\partial \xi}{\partial y} + \frac{\partial N_i}{\partial \eta} \frac{\partial \eta}{\partial y}$$

The strains for a plane stress or plane strain element are evaluated using the matrix equation shown below :-

$$[\varepsilon] = \begin{bmatrix} \varepsilon_{xx} \\ \varepsilon_{yy} \\ \varepsilon_{xy} \end{bmatrix} = \sum_{i=1}^{i=n} \begin{bmatrix} \frac{\partial N_i}{\partial x} & 0 \\ 0 & \frac{\partial N_i}{\partial y} \\ \frac{\partial N_i}{\partial y} & \frac{\partial N_i}{\partial x} \end{bmatrix} \begin{bmatrix} u_{xi} \\ u_{yi} \end{bmatrix}$$

or generally :-

$$[\varepsilon] = [\mathbf{B}]\ [\delta_e]$$

The N_i expression remains a function of ξ and η throughout the analysis and therefore the [B] matrix will also be a function of ξ and η.

To find the stresses a constitutive law must be applied to relate the strains to the corresponding stresses. For an isotropic and homogeneous material that obeys Hooke's law, the plane stress condition will have the following relationship.

$$[\sigma] = [\mathbf{D}]\ [\varepsilon]$$

where

$$[\mathbf{D}] = \frac{E}{1-\upsilon^2}\begin{bmatrix} 1 & \upsilon & 0 \\ \upsilon & 1 & 0 \\ 0 & 0 & \frac{(1-\upsilon)}{2} \end{bmatrix}$$

Ahmad and Irons[52] discuss the [D] matrix and its applications in detail.

7.3.4 Derivation of the Element Stiffness Matrix.

In section 7.3.1 it was stated that the total internal strain energy of an element which is deformed within the elastic range is expressed by the following integral :-

$$S.E = \frac{1}{2}\int_{Vol} [\varepsilon]^T[\sigma]\ dVol$$

In section 7.3.3 an expression for [ε] and [σ] have been derived, so the integral can now be evaluated and the strain energy for the plane elastic element can be found.

Generally,

$$[\varepsilon] = [\mathbf{B}][\delta^e] \qquad \text{and} \qquad [\sigma] = [\mathbf{D}][\varepsilon]$$

therefore,

$$S.E = \frac{1}{2} \int_{Vol} [\delta^e]^T [\mathbf{B}]^T [\mathbf{D}] [\mathbf{B}] [\delta^e] \; dVol$$

or

$$S.E = \frac{1}{2} [\delta^e]^T \left[\int_{Vol} [\mathbf{B}]^T [\mathbf{D}] [\mathbf{B}] \; dVol \right] [\delta^e]$$

hence

$$S.E = \frac{1}{2} [\delta^e]^T [\mathbf{K}^e] [\delta^e]$$

where $$[\mathbf{K}^e] = \int_{Vol} [\mathbf{B}]^T [\mathbf{D}] [\mathbf{B}] \; dVol$$

If the element is of uniform thickness, dV can be expressed as :-

$dV = t.dx.dy$ where t= element thickness

Because the [B] matrix is a function of ξ and η, not x and y, the relationship $dx.dy = |\mathbf{J}| \; d\xi.d\eta$ can be applied. The stiffness of the element can, therefore, be obtained by evaluation of the integral below.

$$[\mathbf{K}^e] = \int_{-1}^{+1} \int_{-1}^{+1} [\mathbf{B}]^T [\mathbf{D}] [\mathbf{B}] \; |\mathbf{J}| \; t \; d\xi \; d\eta$$

The above stiffness integral for the element must be evaluated numerically. A very common method, which is often chosen because of its accuracy, is the Gauss-Lagrandre quadrature. There are other techniques which can be applied,[49] but this one is easily translated into computer

coding which makes it very popular in finite element programming. Considering the integral shown below where ϕ is some arbitrary function of ξ and η

$$I_n = \int_{-1}^{+1} \int_{-1}^{+1} \phi(\xi,\eta)\ d\xi\ d\eta$$

The Gauss-Lagrandre method approximates this integral by evaluating the following summation

$$I_n = \sum_{i=1}^{i=ng} \sum_{j=1}^{j=ng} a_i a_j\ \phi(\xi_i,\eta_j)$$

where

a_i, a_j are weighting factors

and ng = the total number of integration points.

Points are selected within the region of the integral and their coordinates in ξ_i and η_j are substituted into the $\phi(\xi_i,\eta_j)$ function. The points are called "Integration", "Sampling" or "Gauss" points. The number of Gauss points used will depend on the order of the polynomial to be solved and on the accuracy required. Nine Gauss points will provide a good results for material in a state of plane stress or plane strain. The Gauss points are defined by a Gauss-Lagrandre rule. The "2-point" and "3-point" rules are shown diagrammatically in Fig 7.4. The 2-point rule selects 4 Gauss points, the first point having coordinates of $\left\{-\frac{1}{\sqrt{3}}, -\frac{1}{\sqrt{3}}\right\}$. The 3-point rule takes nine Gauss points, the first point having coordinates of $\{-\sqrt{0.6}, -\sqrt{0.6}\}$. The value of the weighting factors, a_i and a_j is dependent on the rule which is being applied and the Gauss point which is being processed.

A detailed account of the Gauss-Legrandre method is given by Banerjee and Butterfield[53]. It is a particularly suitable method for the finite element analysis of a material stress problem because the selection of Gauss points allows the stresses to be assessed at locations

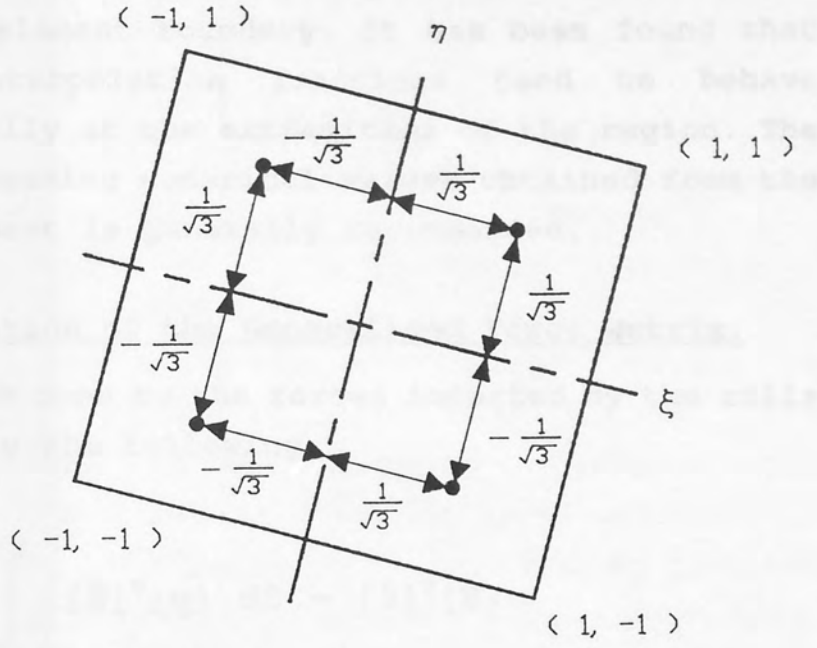

Two Point Gauss Rule

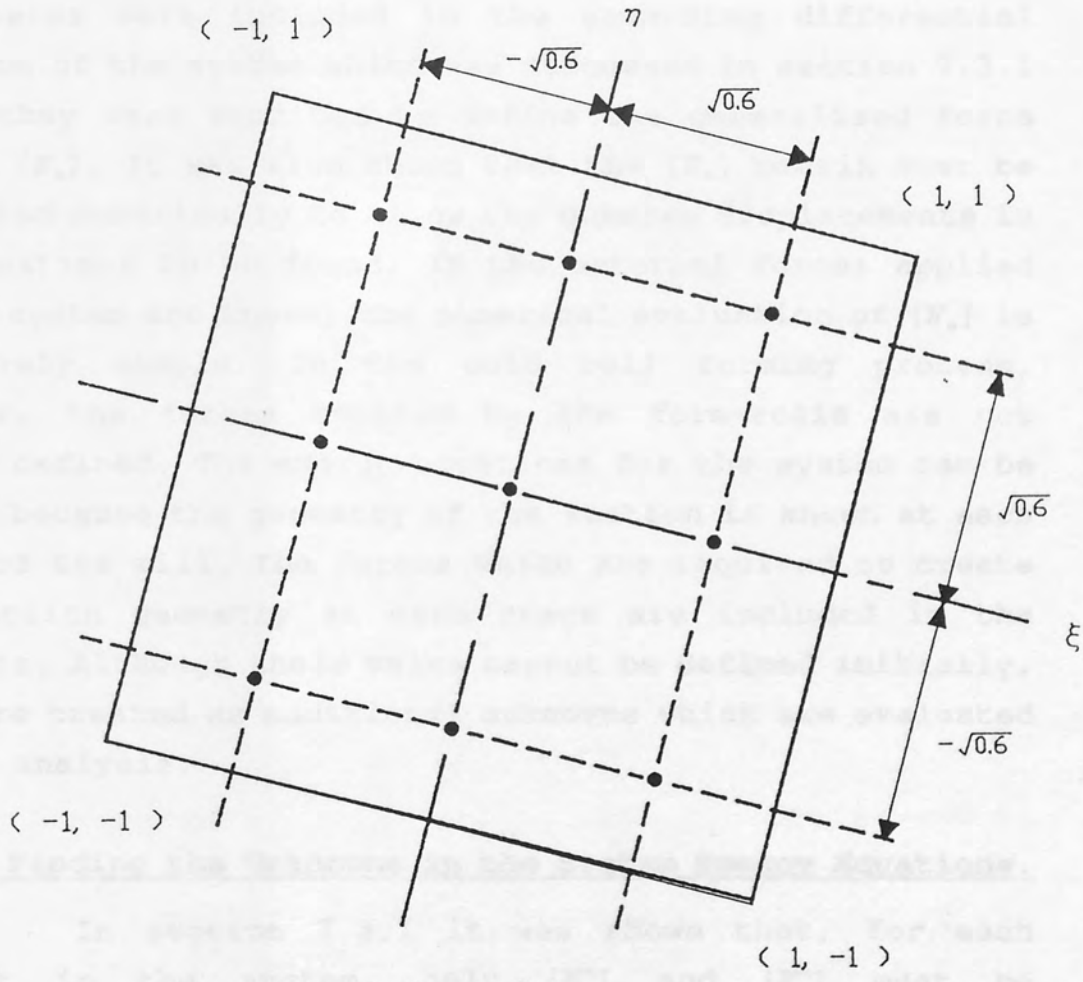

Three Point Gauss Rule

Figure 7.4

The Gaussian Integration Points.

within the element, instead of using stresses at the nodes situated on the element boundary. It has been found that the Lagrange interpolation functions tend to behave slightly erratically at the extremities of the region. The avoidance of processing numerical values obtained from the nodes of the element is generally recommended.

7.3.5 Derivation of the Generalised Force Matrix.

The work done by the forces imparted by the rolls are represented by the following.

$$\Omega = - \int_S [\delta]^T[\mathbf{q}] \, dS - [\delta]^T[\mathbf{R}]$$

Both terms were included in the governing differential equation of the system which was discussed in section 7.3.1 where they were combined to define the generalised force matrix $[\mathbf{F}_e]$. It was also shown that the $[\mathbf{F}_e]$ matrix must be evaluated numerically to allow the unknown displacements in the equations to be found. If the external forces applied to the system are known, the numerical evaluation of $[\mathbf{F}_e]$ is relatively simple. In the cold roll forming process, however, the forces applied by the form-rolls are not easily defined. The energy equations for the system can be solved because the geometry of the section is known at each stage of the mill. The forces which are required to create the section geometry at each stage are included in the analysis. Although their value cannot be defined initially, they are treated as additional unknowns which are evaluated in the analysis.

7.3.6 Finding the Unknowns in the System Energy Equations.

In section 7.3.1 it was shown that, for each element in the system, only $[\mathbf{K}^e]$ and $[\mathbf{F}^e]$ must be numerically evaluated. The stiffness matrices of the individual elements can then be assembled into one global matrix which represents the stiffness of the whole system. Similarly a global generalised force matrix is generated.

The system can then be represented by :-

$$0 = [\mathbf{K}]\,[\delta] - [\mathbf{F}]$$

where

$[\delta]$ = the unknown displacements of the system

$[\mathbf{K}]$ = global stiffness of the system

$[\mathbf{F}]$ = global generalised forces of the system

The unknowns in the analysis, which will largely be displacements in the case of cold roll forming, are evaluated by solving the system energy equations. The global stiffness matrix $[\mathbf{K}]$ is obtained by assembling all the individual element stiffness matrices, $[\mathbf{K}^e]$, to form one stiffness matrix that represents the whole system. One method of assembling the $[\mathbf{K}]$ matrix is to use a Boolean matrix, $[\mathbf{C}]$, as shown below :-

$$[\mathbf{K}] = [\mathbf{C}]^T\,[\tilde{\mathbf{K}}]\,[\mathbf{C}]$$

where

$[\mathbf{K}]$ is the global stiffness matrix,

$[\mathbf{C}]$ is the compatibility or Boolean matrix,

$[\tilde{\mathbf{K}}]$ is defined by :-

$$[\tilde{\mathbf{K}}] = \begin{bmatrix} [\mathbf{K}^1] & 0 & 0 & \ldots\ldots & 0 \\ 0 & [\mathbf{K}^2] & 0 & \ldots\ldots & 0 \\ 0 & 0 & [\mathbf{K}^3] & \ldots\ldots & 0 \\ \multicolumn{5}{c}{\ldots\ldots\ldots\ldots\text{etc}\ldots\ldots\ldots\ldots} \\ 0 & 0 & 0 & \ldots\ldots & [\mathbf{K}^n] \end{bmatrix}$$

where n = number of elements

Unless the system is very simple, the $[\mathbf{C}]$ matrix will be very large, its order depending on the number of unknowns in the analysis. If the numbering of all the nodes in the system is carried out by obeying a simple rule, all the stiffness components will reside in a narrow band down the leading diagonal of the $[\mathbf{K}]$ matrix. The width of the band is governed by the nodal numbering system. Examples of two contrasting nodal numbering systems are given in Fig 7.5.

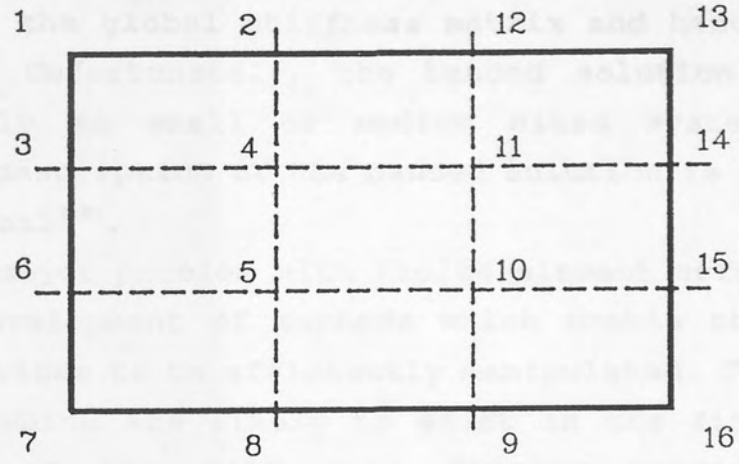

Size of the Bandwidth is controlled by 12−2=8 the greatest difference between two nodal numbers in any one of the elements in the structure.

(a) "Close Control" of Nodal Numbering

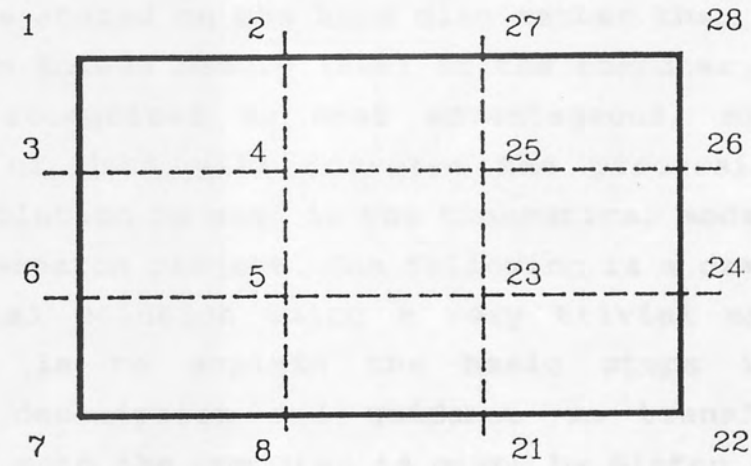

Size of the Bandwidth is controlled by 27−2=25

(b) Nodal Numbering without "Close Control"

Figure 7.5

Size of Bandwidth determined by Nodal Numbering.

A technique known as the "Banded Solution" can be applied to invert the global stiffness matrix and hence solve the unknowns. Unfortunately, the banded solution only works efficiently on small or medium sized systems. A more detailed description of the banded solution is given in the PAFEC Manual[48].

The major problem with finite element software design is the development of methods which enable the extremely large matrices to be efficiently manipulated. The number of unknowns which are likely to exist in the finite element analysis of the cold roll forming process will be unavoidably large. A banded solution is generally regarded as being too inefficient for a system where the number of unknowns in excess of one thousand.

There are a number of alternative ways of assembling the global stiffness matrix so that it is reduced in size, but a method developed by Irons[54] called the "Frontal Solution" is commonly used. It is a very efficient technique which allows a large proportion of the stiffness data to be stored on the hard disc rather than residing in the Random Access Memory (RAM) of the computer. Generally, this is recognized as most advantageous, although the transfer of data will increase the processing time. A frontal solution is used in the theoretical model developed in this research project. The following is a description of the frontal solution using a very trivial example. The objective is to explain the basic steps involved. A detailed description and guidance on transforming the technique onto the computer is given by Hinton and Owen[55].

The rectangular plate shown in Fig 7.6(a) is analysed using a simple element mesh and having one degree of freedom at each node.

Step 1.

The elemental stiffness and force matrices for element number 1 are transferred from the backing store (i.e. the computer hard disc) and placed in an array in the RAM. To assist in the visualisation, a pseudo description of the transfer is shown diagrammatically in Fig 7.6(b). This shows the location of the local element values

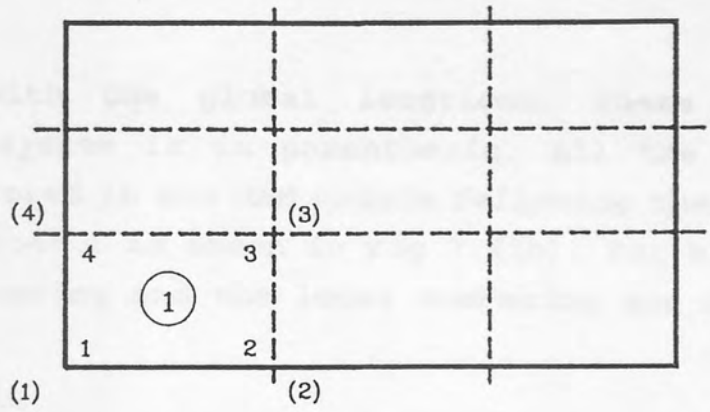

Energy Equation for the first element is –:

$$\begin{bmatrix} k_{11}^{1} & k_{12}^{1} & k_{13}^{1} & k_{14}^{1} \\ k_{21}^{1} & k_{22}^{1} & k_{23}^{1} & k_{24}^{1} \\ k_{31}^{1} & k_{32}^{1} & k_{33}^{1} & k_{34}^{1} \\ k_{41}^{1} & k_{42}^{1} & k_{43}^{1} & k_{44}^{1} \end{bmatrix} \begin{bmatrix} \delta_1^1 \\ \delta_2^1 \\ \delta_3^1 \\ \delta_4^1 \end{bmatrix} = \begin{bmatrix} F_1^1 \\ F_2^1 \\ F_3^1 \\ F_4^1 \end{bmatrix}$$

Figure 7.6(a)

Discretisation of a Rectangular Plate.

$$\begin{bmatrix} (K_{11}) & (K_{12}) & (K_{13}) & (K_{14}) \\ k_{11}^{1} & k_{12}^{1} & k_{13}^{1} & k_{14}^{1} \\ (K_{21}) & (K_{22}) & (K_{23}) & (K_{24}) \\ k_{21}^{1} & k_{22}^{1} & k_{23}^{1} & k_{24}^{1} \\ (K_{31}) & (K_{32}) & (K_{33}) & (K_{34}) \\ k_{31}^{1} & k_{32}^{1} & k_{33}^{1} & k_{34}^{1} \\ (K_{41}) & (K_{42}) & (K_{43}) & (K_{44}) \\ k_{41}^{1} & k_{42}^{1} & k_{43}^{1} & k_{44}^{1} \end{bmatrix} \begin{bmatrix} (\delta_1) \\ \delta_1^1 \\ (\delta_2) \\ \delta_2^1 \\ (\delta_3) \\ \delta_3^1 \\ (\delta_4) \\ \delta_4^1 \end{bmatrix} = \begin{bmatrix} (F_1) \\ F_1^1 \\ (F_2) \\ F_2^1 \\ (F_3) \\ F_3^1 \\ (F_4) \\ F_4^1 \end{bmatrix} \begin{matrix} \\ -Eqn.\ 1 \\ \\ -Eqn.\ 2 \\ \\ -Eqn.\ 3 \\ \\ -Eqn.\ 4 \end{matrix}$$

Figure 7.6 (b)

Transfer of Local to Global Matrices.

compared with the global locations, where the global numbering system is in parenthesis. All the information which is stored in the RAM matrix following the transfer of element number 1 is shown in Fig 7.6(b). For element 1 the global numbering and the local numbering are identical in this case.

Step 2.

A search of the matrix is carried out to identify the variables or degrees of freedom which will not receive additional information when the equations of all the other elements in the system have been transferred from the backing store. In the example shown in Fig 7.6(a), only node 1 will be selected after element 1 has been transferred.

Step 3.

Because node 1 was selected in step 2, the first row and the first column of the RAM matrix are reduced to zero. If node 3 had been selected instead, the third row and column would be reduced to zero. In order to achieve this, the Gaussian Reduction is applied in the normal way (see reference[55]). The result is shown in Fig 7.7, with the single dash symbol indicating that all the value will be different following the Gaussian Reduction. Equation 1 in Fig 7.7, is then stored in the backing store and the locations which it occupied in the RAM matrix are assigned to zero. This results in the first row and the first column of the RAM matrix having zero values and being available for use by the next variable which is not already occupying a place in the RAM matrix.

Step 4.

The equation for element 2 is then transferred from the backing store into the RAM. In order to assist the visualisation a pseudo description of the transfer is shown in Fig 7.8. The way in which the stiffness components of the new element are added in to the matrix in the RAM requires special attention. It is this part of the frontal solution which makes the method rather abstruse.

1) Observing that k_{11}^{2} is an addition to K_{44} on the global numbering system. In the RAM matrix the K_{44} position is given the new value of $(k_{44}^{1'} + k_{11}^{2})$

$$\begin{bmatrix} k_{11}^{1} & k_{12}^{1} & k_{13}^{1} & k_{14}^{1} \\ 0 & k_{22}^{1'} & k_{23}^{1'} & k_{24}^{1'} \\ 0 & k_{32}^{1'} & k_{33}^{1'} & k_{34}^{1'} \\ 0 & k_{42}^{1'} & k_{43}^{1'} & k_{44}^{1'} \end{bmatrix} \begin{bmatrix} \delta_1^1 \\ \delta_2^1 \\ \delta_3^1 \\ \delta_4^1 \end{bmatrix} = \begin{bmatrix} F_1^1 \\ F_2^{1'} \\ F_3^{1'} \\ F_4^{1'} \end{bmatrix} \begin{matrix} \text{——} (1) \\ \text{——} (2) \\ \text{——} (3) \\ \text{——} (4) \end{matrix}$$

Figure 7.7

Energy Equations after the Gaussian Reduction of node 1

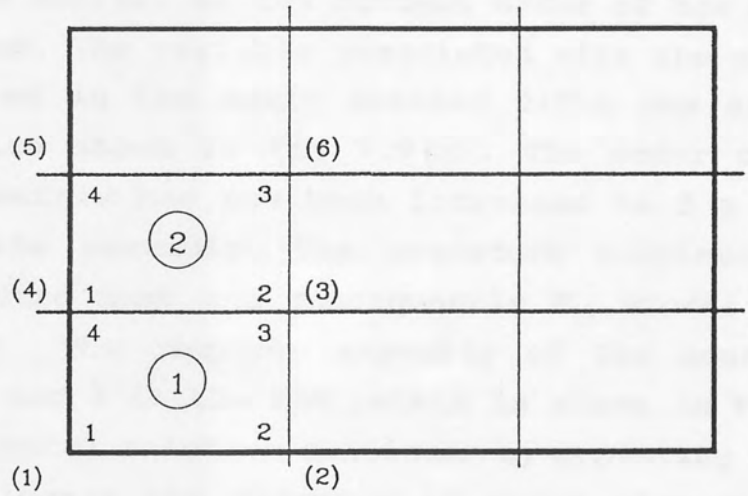

Energy Equations for Element 2 are –:

$$\begin{bmatrix} k_{11}^{2} & k_{12}^{2} & k_{13}^{2} & k_{14}^{2} \\ k_{21}^{2} & k_{22}^{2} & k_{23}^{2} & k_{24}^{2} \\ k_{31}^{2} & k_{32}^{2} & k_{33}^{2} & k_{34}^{2} \\ k_{41}^{2} & k_{42}^{2} & k_{43}^{2} & k_{44}^{2} \end{bmatrix} \begin{bmatrix} \delta_1^2 \\ \delta_2^2 \\ \delta_3^2 \\ \delta_4^2 \end{bmatrix} = \begin{bmatrix} F_1^2 \\ F_2^2 \\ F_3^2 \\ F_4^2 \end{bmatrix}$$

Figure 7.8

Energy Equations for Element 2.

2) Similarly k^2_{12} is an addition to K_{43} on the global numbering system. In the RAM matrix the K_{43} position is given the value $(k^{1'}_{43} + k^2_{12})$

3) When the next stiffness component k^2_{13} is selected. Which is an addition to K_{46} on the global numbering system, there is currently no global K_{46} position (see Fig 7.6(b)). Because the fourth row has a zero value in the first column, the k^2_{13} value is stored at the global K_{46} position. This implies that the first row and column become associated with the variable at global node number 6 as shown in Fig 7.9(a).

4) When k^2_{14} is selected, which is an addition to K_{45} on the global numbering system, again there is no K_{45} position in the RAM matrix and there is no available space in the current RAM matrix, so the current order of the RAM matrix is increased. The variable associated with the global node 5 is located in the newly created fifth row and column. This is also shown in Fig 7.9(a). The order of the RAM stiffness matrix has now been increased to 5 x 5 at this stage of the assembly. The procedure continues with k^2_{21} being selected next and consequently K_{34} stores the value $(k^{1'}_{34} + k^2_{21})$. The complete assembly of the equations for elements 1 and 2 in the RAM matrix is shown in Fig 7.9(b)

The frontal solution continues by repeating Step 2 and Step 3 following the assembly of every element into the RAM. After element 2 has been assembled, node 4 is selected in Step 2 and equation 4 in Fig 7.9(b) is transferred to the backing store in Step 3, after the Gaussian reduction has been applied. The RAM matrix will then have zero values in the fourth row and the fourth column.

Every element in the system is assembled and reduced by observing the rules described in steps 2, 3 and 4. The diagrammatical representation given in Fig 7.10(a) shows the situation after elements 1, 2 and 3 have been assembled and reduced. The line A:A in Fig 7.10(a) is called the "Front" and all the nodes which are on the front are said to be "active". When element 4 is assembled the front will take up the position given in Fig 7.10(b). The size of the front, called the "Frontwidth", increases to take into account the extra variables at the nodes which

$$\begin{bmatrix} 0 & 0 & 0 & 0 & 0 \\ & (K_{22}) & (K_{23}) & (K_{24}) & \\ 0 & k_{22}^{1'} & k_{23}^{1'} & k_{24}^{1'} & 0 \\ & (K_{32}) & (K_{33}) & (K_{34}) & \\ 0 & k_{32}^{1'} & k_{33}^{1'} & k_{34}^{1'} & 0 \\ (K_{46}) & (K_{42}) & (K_{43}) & (K_{44}) & (K_{45}) \\ k_{13}^{2} & k_{42}^{1'} & k_{43}^{1'} + k_{12}^{2} & k_{44}^{1'} + k_{11}^{2} & k_{14}^{2} \end{bmatrix} \begin{bmatrix} 0 \\ (\delta_2) \\ \delta_2^1 \\ (\delta_3) \\ \delta_3^1 \\ (\delta_4) \\ \delta_4^1 \end{bmatrix} = \begin{bmatrix} 0 \\ (F_2) \\ F_2^1 \\ (F_3) \\ F_3^1 \\ (F_4) \\ F_4^{1'} + F_1^2 \end{bmatrix} \begin{matrix} -Eqn.\ 1 \\ \\ -Eqn.\ 2 \\ \\ -Eqn.\ 3 \\ \\ -Eqn.\ 4 \end{matrix}$$

Figure 7.9(a)

Global Stiffness Matrix with Element 2 partially assembled.

$$
\begin{bmatrix}
(K_{66}) & (K_{62}) & (K_{63}) & (K_{64}) & (K_{65}) \\
k_{33}^{2} & 0 & k_{32}^{2} & k_{31}^{2} & k_{34}^{2} \\
(K_{26}) & (K_{22}) & (K_{23}) & (K_{24}) & (K_{25}) \\
0 & k_{22}^{1'} & k_{23}^{1'} & k_{24}^{1'} & 0 \\
(K_{36}) & (K_{32}) & (K_{33}) & (K_{34}) & (K_{35}) \\
k_{13}^{2} & k_{32}^{1'} & k_{33}^{1'}+k_{22}^{2} & k_{34}^{1'}+k_{21}^{2} & k_{24}^{2} \\
(K_{46}) & (K_{42}) & (K_{43}) & (K_{44}) & (K_{45}) \\
k_{13}^{2} & k_{42}^{1'} & k_{43}^{1'}+k_{12}^{2} & k_{44}^{1'}+k_{11}^{2} & k_{14}^{2} \\
(K_{56}) & (K_{52}) & (K_{53}) & (K_{54}) & (K_{55}) \\
k_{43}^{2} & 0 & k_{42}^{2} & k_{41}^{2} & k_{44}^{2}
\end{bmatrix}
\begin{bmatrix} \\ \delta_6 \\ \\ \delta_2 \\ \\ \delta_3 \\ \\ \delta_4 \\ \\ \delta_5 \end{bmatrix}
=
\begin{bmatrix}
(F_6) & \\
F_3^{2} & -Eqn.\ 6 \\
(F_2) & \\
F_2^{1'} & -Eqn.\ 2 \\
(F_3) & \\
F_3^{1'}+F_2^{2} & -Eqn.\ 3 \\
(F_4) & \\
F_4^{1'}+F_1^{2} & -Eqn.\ 4 \\
(F_4) & \\
F_4^{1} & -Eqn.\ 5
\end{bmatrix}
$$

Figure 7.9(b)

The Global Stiffness Matrix after the Assembly of Element 2.

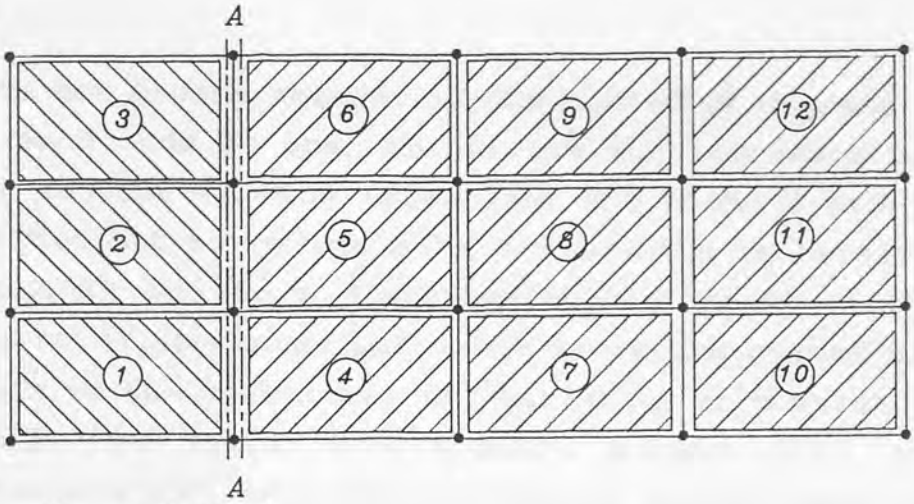

Figure 7.10(a)

Position of FRONT after assembly and reduction of the first three elements.

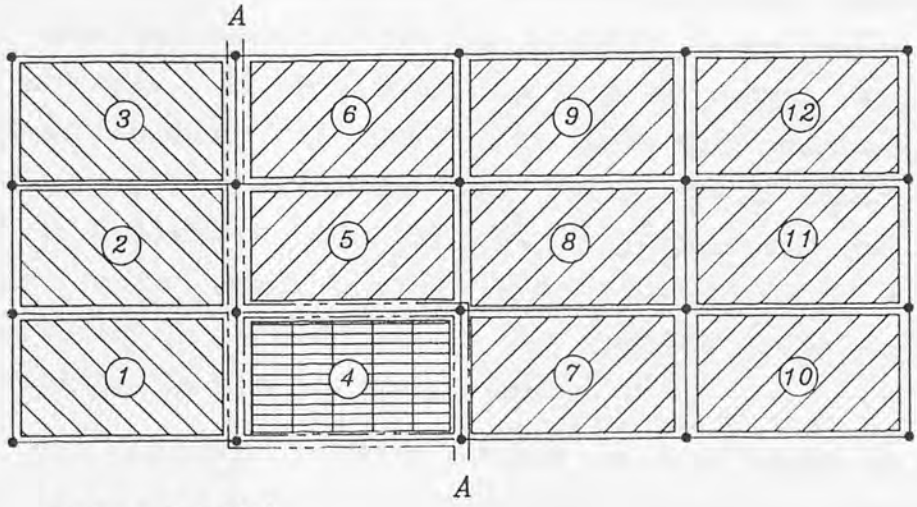

Figure 7.10(b)

Position of FRONT after assembly of element 4.

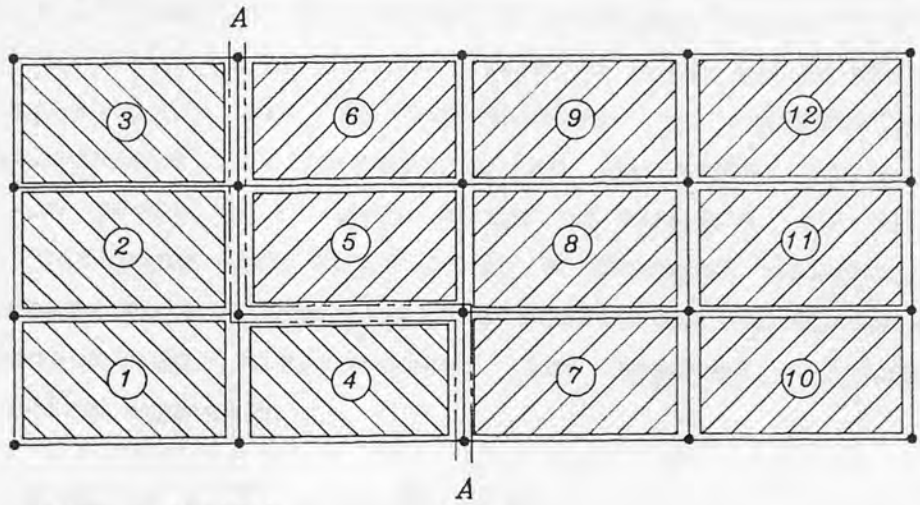

Figure 7.10(c)

Position of FRONT after assembly and reduction of element 4.

have now become active. If the number of degrees of freedom at each node is one, the frontwidth increases by 2 due to the element 4 being assembled. The steps 2 and 3 are then carried out to reduce and eliminate the necessary equations and this is shown diagrammatically in Fig 7.10(c). This procedure continues until the front has passed through the whole of the structure. The variables or degrees of freedom which the front has already passed over are called "deactivated" and the variables which have yet to be assembled and reduced are called "inactive".

Step 5.

The unknowns variables are evaluated using a simple "back-substitution". The last reduced equation which has been transferred to the backing store will have only one unknown, so this variable can be found. The previous reduced equation to this will have two unknowns, one of them being the variable just found, so a second variable can be evaluated. All of the variables can be evaluated using this back-substitution technique, simply by processing the equations in the reverse order to the order of storage in the backing store.

The external forces acting on the sheet in the cold roll forming process are difficult to measure accurately so they cannot be used to solve the global energy equations. The presence of the forces are represented in the analysis by the [**F**] matrix discussed in section 7.3.5. The geometry of the sheet, however, is known at each stage of the mill. Consequently, it is necessary to prescribe known displacements at certain nodes in order to enable the section geometry at each stage of the mill to be defined. When carrying out Step 5 in a frontal solution, it is necessary to include an additional reaction force each time a prescribed displacement is applied. Consider the following equation :-

$$k_{12}\,\delta_2 + k_{13}\,\delta_3 + k_{14}\,\delta_4 = F_2$$

If δ_2 is a prescribed value and all the other values have already been evaluated by the back-substitution procedure,

then an extra unknown force must be added.

$$k_{12}\delta_2 + k_{13}\delta_3 + k_{14}\delta_4 = F_2 + R$$

The value of R will equal the force required to cause the prescribed displacement. Forces which have been added in Step 5 are treated as the unknowns and are evaluated by the back-substitution procedure.

The frontal solution is particularly suitable for problems that entails a non-linear analysis because an iteration process will be involved. When the frontal solution is used it is not necessary to carry out all the calculations for each iteration. There is no assemble procedure of the stiffness matrix for each iteration, alterations to the force matrix are only necessary followed by the full back-substitution applied in Step 5. The iterative calculations take about 80 per cent of the time necessary for a full frontal analysis, so the time saving is considerable. If a frontal solution is used, then the numbering (or "ordering") of the elements in the mesh is an important feature. The frontwidth must be kept as small as possible because it directly influences the size of the RAM that is required. The ordering in Fig 7.6(a) ensures that the maximum frontwidth will be six.

CHAPTER EIGHT.

ELASTIC-PLASTIC ANALYSIS.

8.1 Introduction.

The mathematical model of the cold roll forming process must be capable of producing a good approximation for the plastic strain distribution which is generated in the formed sheet. The analysis of the stresses in the elastic region is relatively simple due to the linear relationships that usually exist. In the plastic zone, however, the analysis is far more difficult. Unfortunately, the plastic strains are of paramount importance in the cold roll forming process, so an elastic-plastic model is essential. This chapter discusses the different techniques that are used to assess the state of stress when some form of non-linearity occurs.

8.2 Geometric and Material Non-linearity.

There are two basic types of non-linearity that can occur during metal deformation. The derivation of Green's Strain Tensor, is based purely on a geometrical analysis[43]. The properties of the material are not considered, so the equation, which is shown below, is an assessment of the geometrical linear and non-linear strains.

$$E_{ij} = \frac{1}{2}\left[\frac{\partial u_i}{\partial x_j} + \frac{\partial u_j}{\partial x_i}\right] + \frac{1}{2}\frac{\partial u_i}{\partial x_j}\frac{\partial u_j}{\partial x_i}$$

If the strains are small, it is most likely that a linear relationship will exist between the strain and displacement and Cauchy's Infinitesimal Strain Tensor is applicable.

$$\varepsilon_{ij} = \frac{1}{2}\left[\frac{\partial u_i}{\partial x_j} + \frac{\partial u_j}{\partial x_i}\right]$$

It is apparent, therefore, that the product term in Green's Strain Tensor is negligible compared with the other terms and

hence the strain is proportional to displacement. The formulation of a solution is made significantly easier if Cauchy's Infinitesimal Strain Tensor is used. For the cold roll forming process, geometric non-linearity was only considered to occur in the small bend regions of the section. The strains in the larger linear portions of the section, which generally will be considerably less than in the bend region, was assessed using Cauchy's Infinitesimal Strain Tensor. When a non-linear geometrical analysis is applied the [**B**] matrix (refer to section 7.3.3) will be dependent on the magnitude of the displacements and a reformulation of the process is required to account for this change. It is possible, however, to consider geometric non-linearity using a fairly simple method if it is assumed that the effect of the stresses on the stiffness matrix, [**K**], is small. A technique described by PAFEC[50] applies the load in small increments and calculates the displacements for each load increment using Cauchy's Infinitesimal Strain Tensor. The displacement due to the load increment is added to the original coordinates to define the new geometry and the [**B**] matrix is recalculated. The next load increment is then applied and the calculations are repeated. Although it is unlikely that the state of stress, generated when modelling the C.R.F. process, will have no influence on the stiffness, the method is simple to implement and is commonly used when a large plate, with its edges simply supported, undergoes a large deformation due to an out-of-plane central load. This is the method which is applied by the theoretical model developed in this research project.

Material non-linearity occurs when the constitutive equation that defines the relationship between stress and strain becomes non-linear. Therefore,

$$[\sigma] = [\mathbf{D}]\ [\varepsilon] \text{ is not a linear function.}$$

This condition can be assessed without a completely new formulation of the problem. An iterative process can be applied where the constitutive law is adjusted at each iteration. A method of adjusting the [**D**] matrix at each iteration is described by Yamada[45] and Marcel and King[56]. It involves altering the stiffness of the system so that the [**D**] matrix becomes a function of the strains, (refer to section 7.3.4 where an expression for [**K**] is given for a linear elastic system). The method is shown

diagrammatically in Fig 8.1 for a simple uniaxial stress system. The [**D**] matrix is modified so that a linear stress-strain relationship is generated, hence it will form a tangent to the stress-strain law after each iteration. The major disadvantage of this method is that the [**K**] matrix has to be recalculated at every iteration, which is extremely time-consuming.

A method described by Argyris[57] does not involve the repeated alteration of the [**K**] matrix. An initial strain is introduced in to the constitutive law.

Generally :-

$$[\sigma] = [\mathbf{D}] \{[\varepsilon] - [\varepsilon_o]\}$$

where $[\varepsilon_o]$ is the initial strain.

The initial strain is adjusted at each iteration so that the true stress-strain relationship is defined at each interval. The difference between the strain calculated by a simple linear law and the actual strain is evaluated in the form of residual forces which are redistributed throughout the system. The method is particularly suitable for brittle metal deformation.

An alternative technique to the initial strain method is to incorporate an initial stress into the system stress-strain relationship.

$$[\sigma] = [\mathbf{D}] [\varepsilon] + [\sigma_o]$$

where $[\sigma_o]$ represents the initial stress.

In principal it is similar to the initial strain method because the initial stress is adjusted at each iteration so that the true stress-strain relationship is defined at each interval. Each time $[\sigma_o]$ is changed, additional residual forces are created on the system which must be considered in the next iteration. The iterative calculations begin with the evaluation of the following equation which is based on a linear stress-strain law.

$$[\delta] = [\mathbf{K}_o]^{-1} [\mathbf{F}_o]$$

where

$[\mathbf{K}_o]$ is the initial stiffness of the system, which remains constant throughout the analysis.

$[\mathbf{F}_o]$ represents the initial increment in loading on the system.

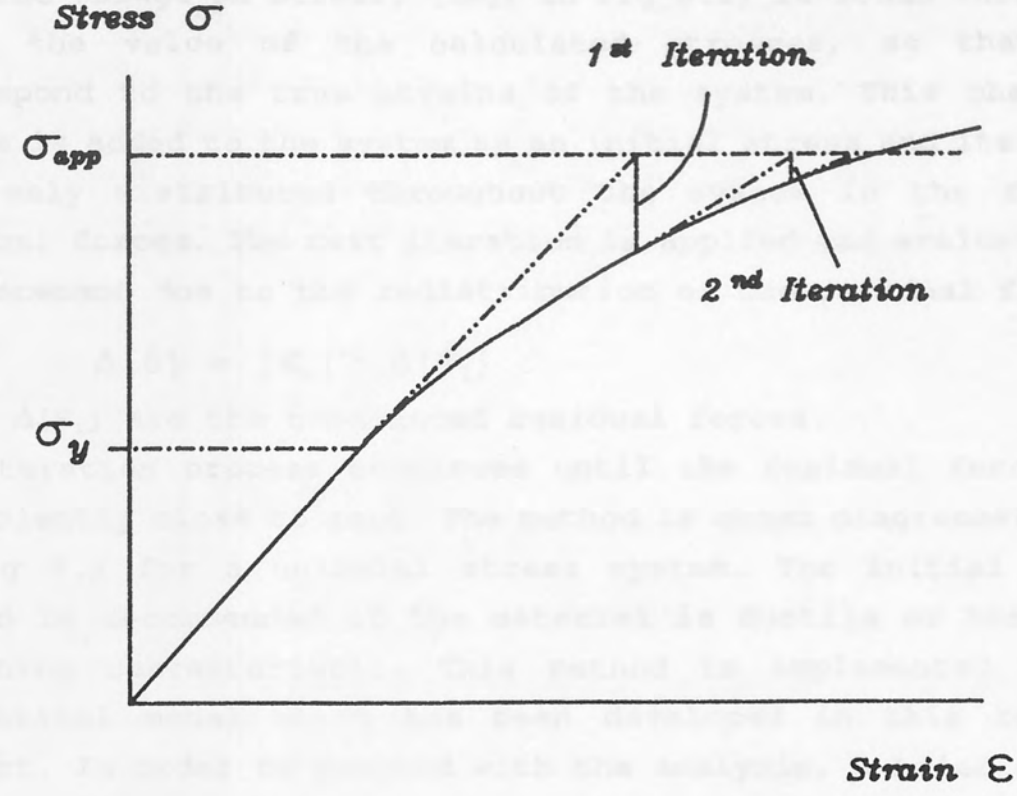

Figure 8.1

Variable Stiffness Solution.

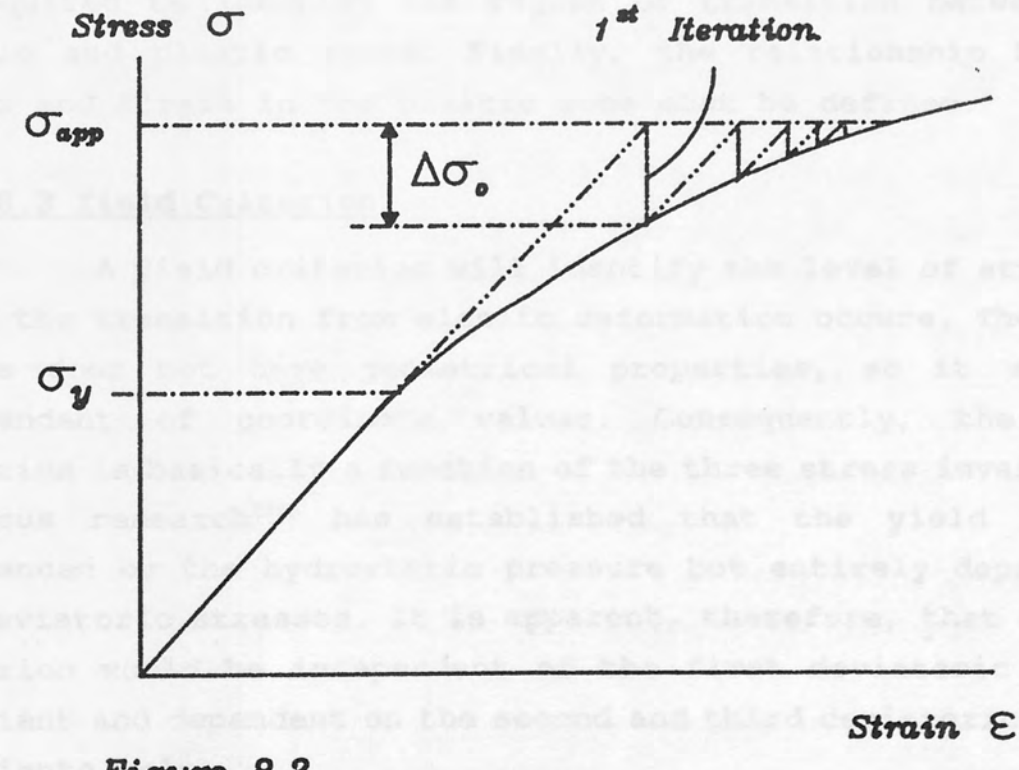

Figure 8.2

Initial Stiffness Method.

The change in stress, $[\Delta\sigma_o]$ in Fig 8.2, is found which will alter the value of the calculated stresses, so that they correspond to the true strains of the system. This change in stress is added to the system as an initial stress and its effect is evenly distributed throughout the system in the form of residual forces. The next iteration is applied and evaluates the displacement due to the redistribution of the residual forces.

$$\Delta[\delta] = [\mathbf{K}_o]^{-1} \Delta[\mathbf{F}_1]$$

where $\Delta[\mathbf{F}_1]$ are the unbalanced residual forces.
The iteration process continues until the residual forces are sufficiently close to zero. The method is shown diagrammatically in Fig 8.2 for a uniaxial stress system. The initial stress method is recommended if the material is ductile or has a low hardening characteristic. This method is implemented in the theoretical model which has been developed in this research project. In order to proceed with the analysis, a brief outline of the mathematical theory of plasticity is discussed.

There are three requirements for a mathematical theory of plasticity. Firstly, it is necessary to define the relationship between stress and strain in purely elastic conditions, achieved by applying Hooke's law. Then a postulation of a yield criterion is required to identify the region of transition between the elastic and plastic zones. Finally, the relationship between stress and strain in the plastic zone must be defined.

8.3 Yield Criterion.

A yield criterion will identify the level of stress at which the transition from elastic deformation occurs. The yield stress does not have geometrical properties, so it will be independent of coordinate values. Consequently, the yield criterion is basically a function of the three stress invariants. Previous research[39] has established that the yield is not influenced by the hydrostatic pressure but entirely depends on the deviatoric stresses. It is apparent, therefore, that a yield criterion would be independent of the first deviatoric stress invariant and dependent on the second and third deviatoric stress invariants only.

There are only two frequently applied yield criterion for metal deformation problems. Either the Tresca or von Mises criterion is chosen because the other techniques are not supported by experimental results. It is generally found that von Mises criterion will correlate more closely with experimental data than Tresca and consequently it is the more often used theory.

Hence

$$F(\sigma_{ij}, k) = 0$$

or

$$k(\kappa) = f(J_2', J_3') \qquad \text{8.1}$$

where

$k(\kappa)$ is a material parameter to be determined experimentally which maybe a function of a hardening parameter κ.

J_2' = second deviatoric stress invariant.

J_3' = third deviatoric stress invariant.

A visualisation of the von Mises yield criterion is shown in Fig 8.3(a). The principal stress axis where the three corresponding principal stresses are equal is called the "space diagonal". A plane which has the space diagonal as a perpendicular and where the sum of the principal stresses is zero, is called the "π" plane. The von Mises criterion can be represented on the π plane by a circle, as shown in Fig 8.3(b), where the area inside the circle defines a stress level which results in elastic deformation. When the level of stress reaches the periphery of the circle and continues to increase, then plastic deformation will occur. Other yield criteria, like Tresca's theory for example, will be a shape other circular when plotted on the π plane. The von Mises yield criterion can be represented as an infinitely long cylinder which has the space diagonal as its axis as Fig 8.3(a) shows.

According to the von Mises theory, the transition to plastic deformation will occur when the second deviatoric stress invariant reaches a critical value.

$$(J_2')^{0.5} = k(\kappa)$$

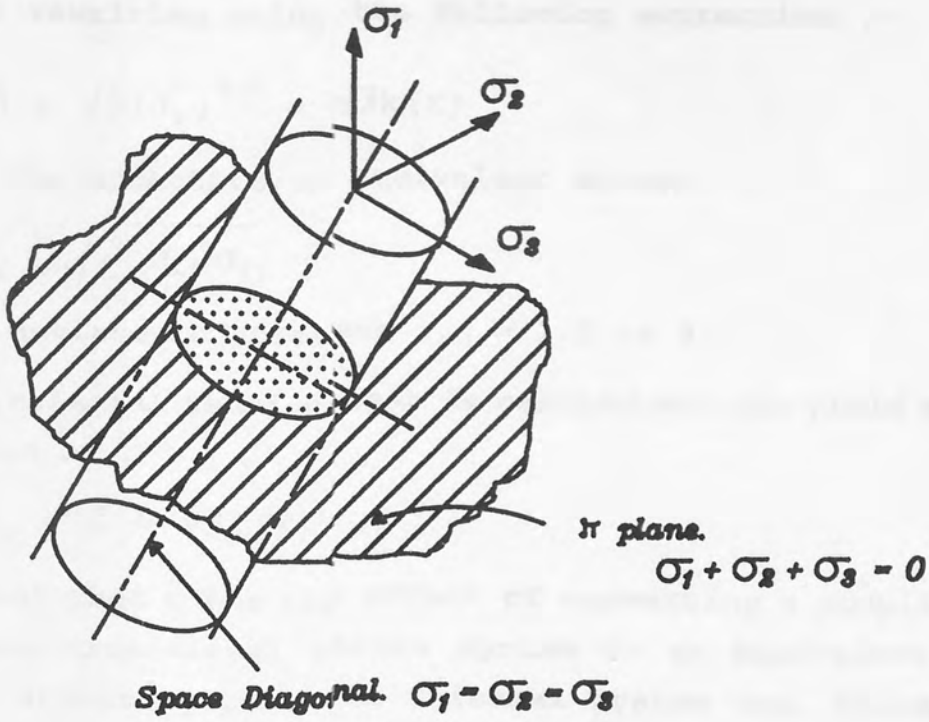

Figure 8.3(a)

The yield surface on stress space axes.

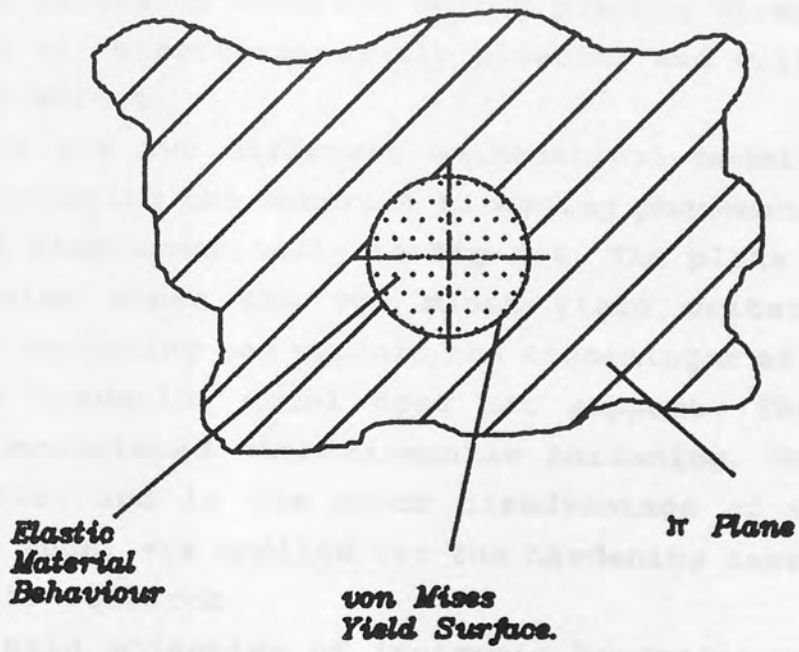

Figure 8.3(b)

Projection of the yield surface on the π plane

This can be rewritten using the following expression :-

$$\bar{\sigma} = \sqrt{3}\,(J_2')^{0.5} = \sqrt{3k(\kappa)}$$

where $\bar{\sigma}$ is the effective or equivalent stress

$$\bar{\sigma} = \sqrt{\frac{3}{2}\,\sigma_{ij}'\,\sigma_{ij}'}$$

where σ_{ij}' = deviatoric stresses i,j = 1,2 or 3.

If a simple uniaxial tension test is carried out the yield stress will be given by :-

$$\sigma_y = \bar{\sigma} = \sqrt{3k(\kappa)}$$

It is apparent that $\bar{\sigma}$ has the effect of converting a complicated two- or three-dimensional stress system to an equivalent one-dimensional stress system. The uniaxial system can, therefore, be investigated to establish a yield stress level.

It has previously been stated that the yield stress will be a function of κ, the property that defines the degree of hardening. When a material is deformed in the plastic region it is most likely to receive an increase in its hardness value. Not all materials possess this characteristic, their hardness value remaining virtually constant during plastic straining. They are described as "elastic-perfectly plastic" and will not exhibit a hardening effect.

There are two different mathematical models which can be used for studying the material hardening phenomenon and they are described diagrammatically in Fig 8.4. The plots on the π plane are circular since the von Mises yield criterion was used. Kinematic hardening can explain the Bauschinger effect, which the isotropic hardening model does not support. The mathematical analysis associated with kinematic hardening, however, is far more complex and is the major disadvantage of this model. An isotropic model was applied for the hardening assessment carried out in this research.

The main objective of isotropic hardening calculations is to assess the rate of change of the hardness parameter, κ, during plastic deformation. Any change in hardness will directly effect the yield stress value and, therefore, should be considered by the yield criterion. There are two common theories which can be applied. The work hardening theory makes the parameter, κ, equal

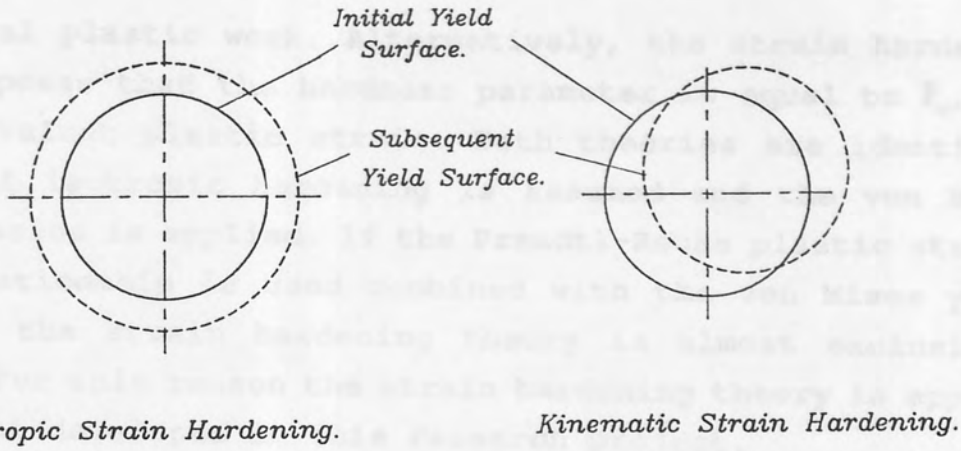

Figure 8.4

Typical Strain Hardening Models.

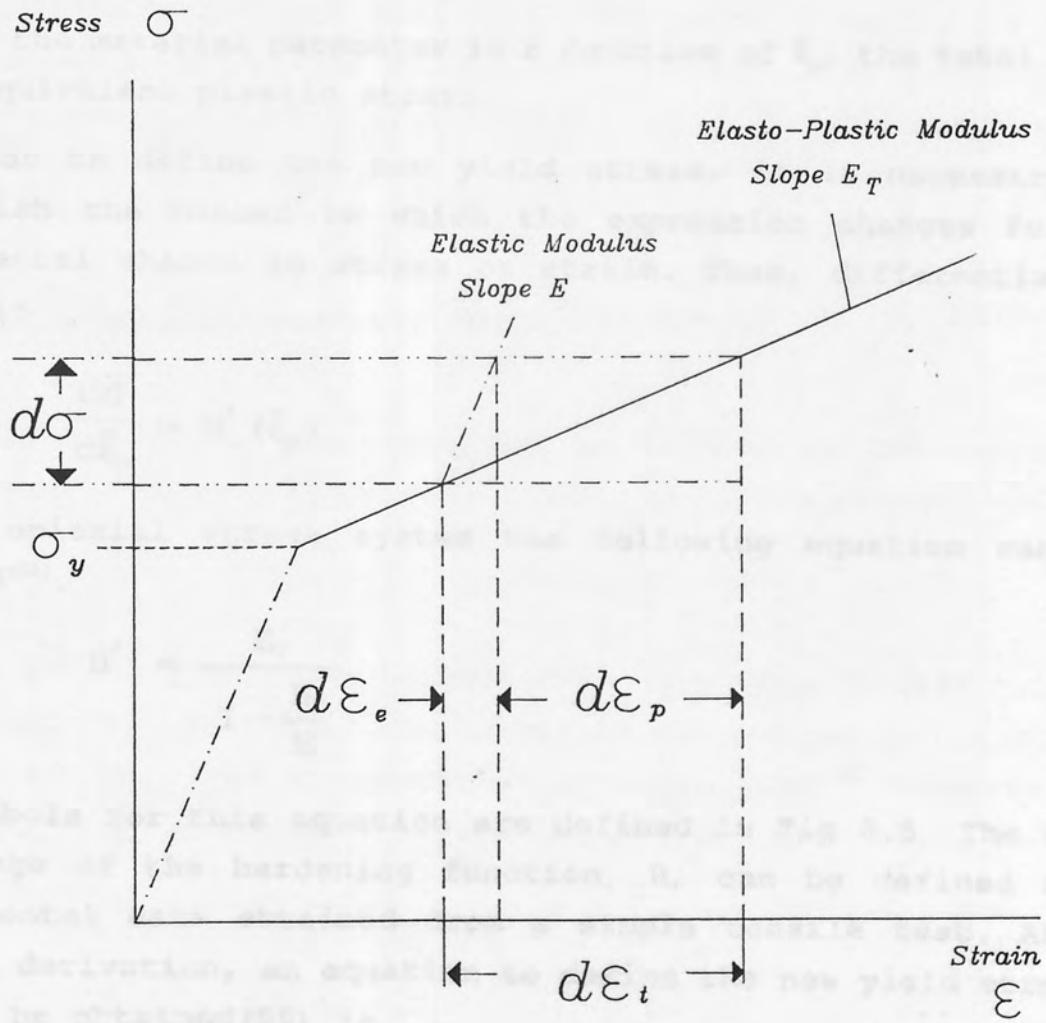

Figure 8.5

Definition of Hardening Parameters using a Uniaxial Stress–Strain Plot.

to the total plastic work. Alternatively, the strain hardening theory proposes that the hardness parameter is equal to $\bar{\varepsilon}_p$, the total equivalent plastic strain. Both theories are identical, however, if isotropic hardening is assumed and the von Mises yield criterion is applied. If the Prandtl-Reuss plastic stress-strain relationship is used combined with the von Mises yield criterion, the strain hardening theory is almost exclusively chosen[58]. For this reason the strain hardening theory is applied by the model developed in this research project.

Following a plastic deformation that has propagated material strain hardening, the hardening law $k(\kappa)$ can be expressed in terms of the effective stress as follows :-

$$\bar{\sigma} = H(\bar{\varepsilon}_p)$$

where

H the material parameter is a function of $\bar{\varepsilon}_p$, the total equivalent plastic strain.

In order to define the new yield stress, it is necessary to establish the manner in which the expression changes for an incremental change in stress or strain. Thus, differentiating gives :-

$$\frac{d\bar{\sigma}}{d\bar{\varepsilon}_p} = H'(\bar{\varepsilon}_p)$$

For a uniaxial stress system the following equation can be derived[52].

$$H' = \frac{E_T}{1 - \frac{E_T}{E}}$$

The symbols for this equation are defined in Fig 8.5. The rate of change of the hardening function, H, can be defined from experimental data obtained from a simple tensile test. After further derivation, an equation to define the new yield stress, σ_y, can be obtained(59) :-

$$\sigma_y = \sigma_y^\circ + H'\bar{\varepsilon}_p$$

where

σ_y° is the yield stress in a simple tensile test before any hardening due to plastic deformation

and

$$\bar{\varepsilon}_p = \int d\varepsilon_p = \int \frac{3}{2} \left(d\varepsilon_{ij}' \, d\varepsilon_{ij}'\right)$$

$d\varepsilon_p$ is defined in Fig 8.5

The new yield stress is found, therefore, having allowed for any changes caused by strain hardening. This analysis was used in the theoretical model developed in this research project and a more detailed description of the technique is given by Hinton and Owen[59].

8.4 The Stress-Strain Relationship.

The relationship between strain and stress in the elastic region is usually linear because most engineering materials obey Hooke's law. For the plastic region, a more complicated relationship exists which is much more difficult to evaluate. Any increment in strain can be divided into two separate parts, the elastic strain component and the plastic strain component.

$$d\varepsilon_{ij} = (d\varepsilon_{ij})_e + (d\varepsilon_{ij})_p$$

where $i, j = 1, 2$ or 3.

The elastic strain component can be related to corresponding increments in stress components using the linear relationship :-

$$[\varepsilon_{ij}]_e = [\mathbf{D}]^{-1} \, [\sigma_{ij}]$$

Because of the non-linear behaviour it is much more difficult to relate the plastic strain components to the corresponding stress components. An approach described by Mendelsson[58] involves the formulation of a function called the plastic potential, Q.

$$Q = Q(\sigma_{ij}, k)$$

or

$$\frac{\partial Q}{\partial \sigma_{ij}} \propto (d\varepsilon_{ij})_p \qquad \text{where } i, j = 1, 2 \text{ or } 3.$$

A special condition called a "normality condition" occurs when the plastic potential equals the yield stress function. Recall from section 8.3

$$F(\sigma_{ij}, k) = 0$$

Hence

$$F(\sigma_{ij}, k) = Q(\sigma_{ij}, k)$$

At the normality condition it can be shown that the following relationship exists[60].

$$(d\varepsilon_{ij})_p = d\lambda \frac{\partial F}{\partial \sigma_{ij}}$$

where $d\lambda$ is a proportionality constant called the "plastic multiplier".

Subsequently, the following expression is developed for the incremental stress-strain relationship using an elasto-plastic material .

$$[d\varepsilon_{ij}] = [\mathbf{D}]^{-1}[d\sigma_{ij}] + d\lambda \frac{\partial F}{\partial \sigma_{ij}} \qquad \text{8.2}$$

This equation is usually manipulated to obtain a matrix format that is compatible to computerisation. An expression for $d\lambda$ and $\frac{\partial F}{\partial \sigma_{ij}}$ is required in matrix format to allow the numerical evaluation of the equation.

From equation 8.1 the general yield stress condition is expressed as :-

$$F(\sigma_{ij}, k) = f(\sigma_{ij}) - k(\kappa) = 0$$

Differentiating using Taylor's Theorem :-

$$\partial F = \frac{\partial F}{\partial \sigma_{ij}} d\sigma_{ij} + \frac{\partial F}{\partial \kappa} d\kappa = 0$$

or alternatively,

$$[\mathbf{a}]\, d\sigma_{ij} - A d\lambda = 0$$

where $[\mathbf{a}] = \frac{\partial F}{\partial \sigma_{ij}}$

and $A = -\frac{1}{d\lambda} \frac{\partial F}{\partial \kappa} d\kappa$

It can be shown that this expression for A equals the strain hardening parameter, H', discussed in section 8.3[60]

$$A = H'$$

From section 8.3

$$f(\sigma_{ij}) = \bar{\sigma} = \sqrt{3}\,(J_2')^{0.5}$$

therefore,

$$[\mathbf{a}] = \frac{\partial\{\sqrt{3}\,(J_2')^{0.5}\}}{\partial\sigma_{ij}}$$

thus,

$$[\mathbf{a}]^T = \frac{\sqrt{3}}{2\,(J_2')^{0.5}}\,[\sigma_{xx}',\ \sigma_{yy}',\ \sigma_{zz}',\ 2\tau_{xy},\ 2\tau_{xz},\ 2\tau_{yz}]$$

defining

$$[\mathbf{d}_D] = [\mathbf{D}]\ [\mathbf{a}] \qquad \text{8.3}$$

where [D] is the elastic stress-strain relationship
After manipulation, the following equation is derived[58]:-

$$d\lambda = \left\{ \frac{1}{(A+[\mathbf{a}]^T[\mathbf{D}]\,[\mathbf{a}])} \right\}\ [\mathbf{a}]^T[\mathbf{d}_D]\,[d\varepsilon_{ij}] \qquad \text{8.4}$$

Substituting this $d\lambda$ identity into equation 8.3, after some manipulation the following stress-strain relationship is derived :-

$$[d\sigma_{ij}] = [\mathbf{D}_{ep}]\ [d\varepsilon_{ij}] \qquad \text{8.5}$$

where $$[\mathbf{D}_{ep}] = [\mathbf{D}] - \frac{[\mathbf{d}_D]\ [\mathbf{d}_D]^T}{\{A + [\mathbf{d}_D]^T\ [\mathbf{a}]\}}$$

Alternatively by rearranging equation 8.5 the following expression is derived[59] :-

$$[d\sigma_{ij}] = [\mathbf{D}]\ [d\varepsilon_{ij}] - d\lambda[\mathbf{d}_D]$$

or

$$= [d\sigma_e] - d\lambda[\mathbf{d}_D] \qquad \text{8.6}$$

where $[d\sigma_e]$ = elastic stress increment.

The accuracy of the above equations will be dependent on the size of the increment. Only small load increments are recommended although Hinton and Owen[59] describe a method where larger increments can be taken without a considerable reduction in accuracy.

8.5 Iterative Procedure for an Elasto-Plastic Material.

Having obtained the equations in a form which is compatible to computerisation, the computer coding can be written to allow the iterative technique to be carried out. This method was used in the theoretical model developed in this research project and the nine steps which are performed for each increment in load are explained below.

For the r^{th} iteration and the n^{th} increment in load.

Step 1.

Apply the residual forces, calculated during the r-1 iteration, $[dP_{r-1}]^n$ to the nodes of the system and determine the corresponding elastic strain increments at each Gaussian point $[d\varepsilon_e]$.

Generally,

$$[dP_{r-1}]^n = [\mathbf{K}]\ [d\delta]$$

hence,

$$[d\varepsilon_e] = [\mathbf{B}]\ [d\delta]$$

The total displacement of the structure is given by :-

$$[\delta^r] = [\delta^{r-1}] + [d\delta]$$

The corresponding elastic stress increments, $[d\sigma_e^r]$ are evaluated using :-

$$[d\sigma_e^r] = [\mathbf{D}]\ [d\varepsilon_e]$$

Step 2.

Add the increment of elastic stress, $[d\sigma_e^r]$, to the stress already existing at each Gauss point in the system $[\sigma^{r-1}]$ and, therefore, obtain the new stress state, $[\sigma_e^r]$

Step 3.

Select the first, or subsequent Gauss point. Test whether the stress at the Gauss point has exceeded the yield stress before the current iteration load was applied. Thus evaluate the following statement :-

$$\bar{\sigma}^{r-1} < \sigma_y^\circ + H' \bar{\varepsilon}_p^{r-1}$$

If the statement is false, the Gauss point has not previously yielded and step 4 is applied.

If the statement is true a further test is carried out to ascertain whether the stress at the Gauss point is decreasing by evaluation of the following statement :-

$$\bar{\sigma}^r < \bar{\sigma}^{r-1}$$

If the statement is true, the stress state is elastically unloading at the Gauss point. When this occurs Step 3 is repeated and the next Gauss point is selected.

If the statement is false, the Gauss point has previously yielded and the level of stress is continuing to increase. In this case the stress increment, $[d\sigma_e^r]$, is reduced onto the yield surface using the method described in steps 5 to 9 below. To explain the procedure a uniaxial system is shown in Fig 8.6(a). The π plane representation is shown in Fig 8.6(b).

Step 4.

Test whether the application of the current load increment has resulted in the stress at the Gauss point exceeding the yield stress. Therefore, evaluation of the expression below is required :-

$$\bar{\sigma}^r < \sigma_y^\circ$$

If the statement is false step 3 is applied, which means that the next Gauss point is selected. Otherwise, the proportion of $[d\sigma_e^r]$ which must be reduced onto the yield surface is calculated. The following equation is evaluated :-

$$[d\sigma_{ep}^r] = R\,[d\sigma_e^r]$$

where $$R = \frac{\bar{\sigma}^r - \sigma_y}{\bar{\sigma}^r - \bar{\sigma}^{r-1}}$$

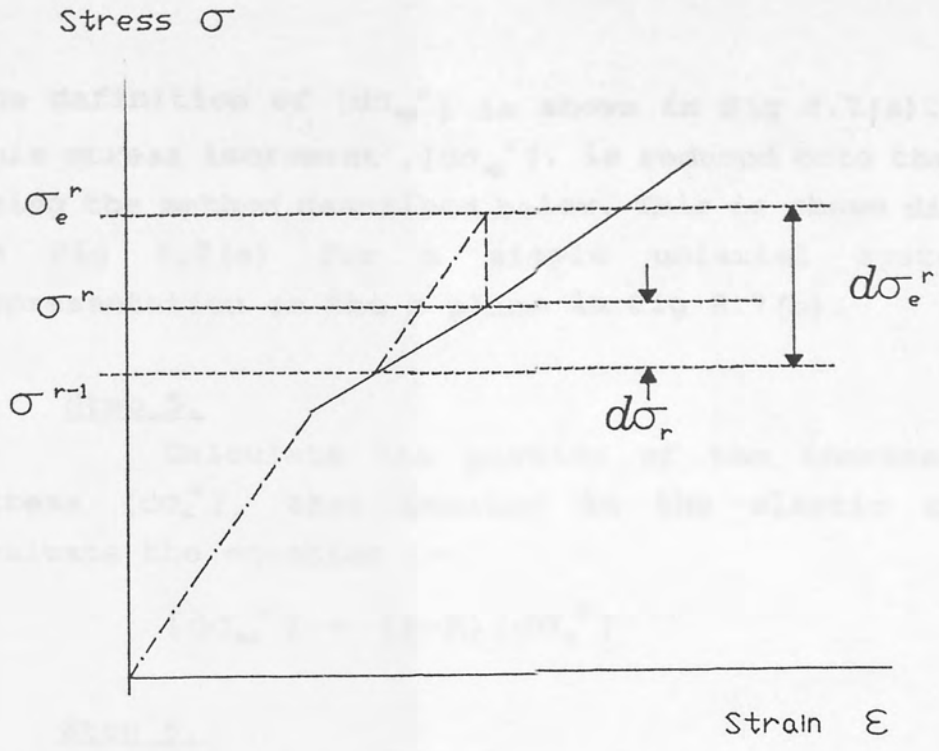

Figure 8.6(a)

Uniaxial Stress–Strain graph for a load increment applied from the plastic region.

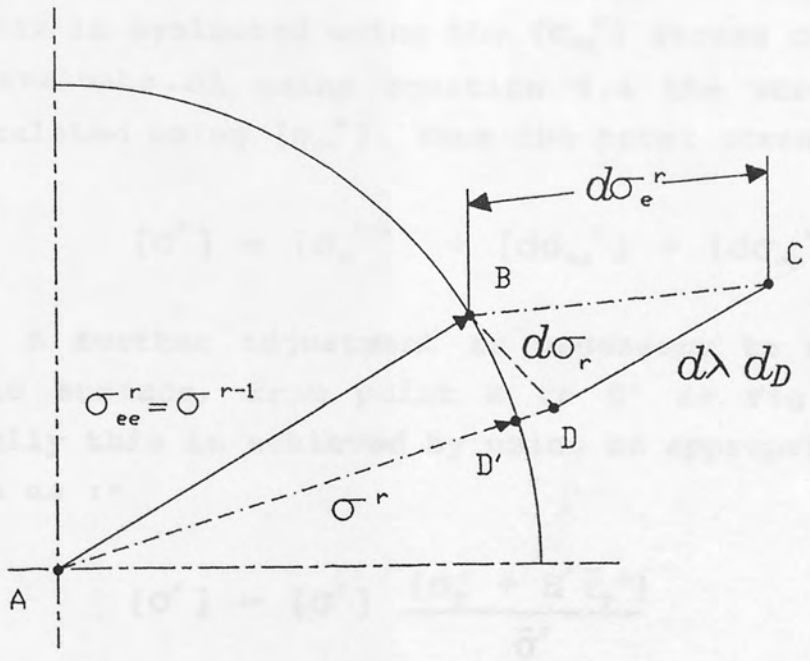

Figure 8.6 (b)

Stresses on the π plane for a load increment applied from the plastic region

The definition of $[d\sigma_{ep}^{r}]$ is shown in Fig 8.7(a). Consequently, this stress increment, $[d\sigma_{ep}^{r}]$, is reduced onto the yield surface using the method described below. This is shown diagrammatically in Fig 8.7(a) for a simple uniaxial system, with the representation on the π plane in Fig 8.7(b).

Step 5.

Calculate the portion of the increment of elastic stress $[d\sigma_{e}^{r}]$, that remains in the elastic region. Hence, evaluate the equation :-

$$[d\sigma_{ee}^{r}] = (1-R)[d\sigma_{e}^{r}]$$

Step 6.

Reduce $[d\sigma_{ep}^{r}]$ onto the yield surface. First calculate the value of $[d\sigma^{r}]$ using equation 8.6

$$[d\sigma^{r}] = [d\sigma_{e}^{r}] - d\lambda[\mathbf{d}_{D}]$$

Refer to Fig 8.7(b) for the definition of the symbols. Equation 8.3 is used to evaluate $[\mathbf{d}_{D}]$. In this equation, the [a] matrix is evaluated using the $[\sigma_{ee}^{r}]$ stress components. In order to evaluate $d\lambda$ using equation 8.4 the stress components are calculated using $[\sigma_{ee}^{r}]$. Thus the total stress is given by :-

$$[\sigma^{r}] = [\sigma_{e}^{r-1}] + [d\sigma_{ee}^{r}] + [d\sigma_{ep}^{r}] - d\lambda[\mathbf{d}_{D}]$$

A further adjustment is necessary to move $[\sigma^{r}]$ onto the yield surface, from point E to E′ as Fig 8.7(b) indicates. Usually this is achieved by using an appropriate scaling factor such as :-

$$[\sigma^{r}] = [\sigma^{r}] \frac{\{\sigma_{y}^{\circ} + H'\bar{\varepsilon}_{p}^{r}\}}{\bar{\sigma}^{r}}$$

where the total equivalent plastic strains, $\bar{\varepsilon}_{p}^{r}$ are found from :-

$$\bar{\varepsilon}_{p}^{r} = \bar{\varepsilon}_{p}^{r-1} + \frac{d\lambda[\mathbf{A}]^{T}[\sigma_{ee}]}{\bar{\sigma}^{r}}$$

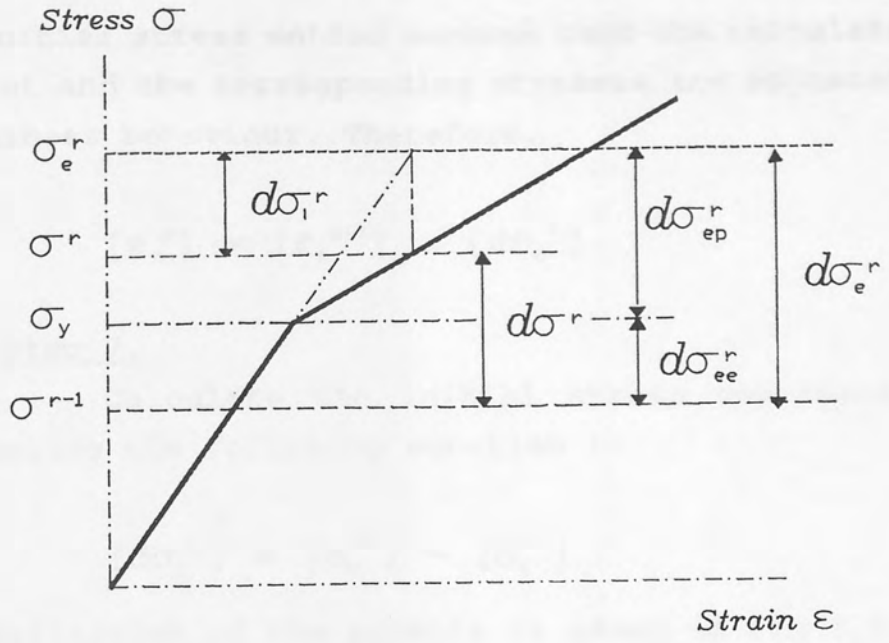

Figure 8.7(a)

Uniaxial Stress–Strain graph for a load increment applied from the elastic region.

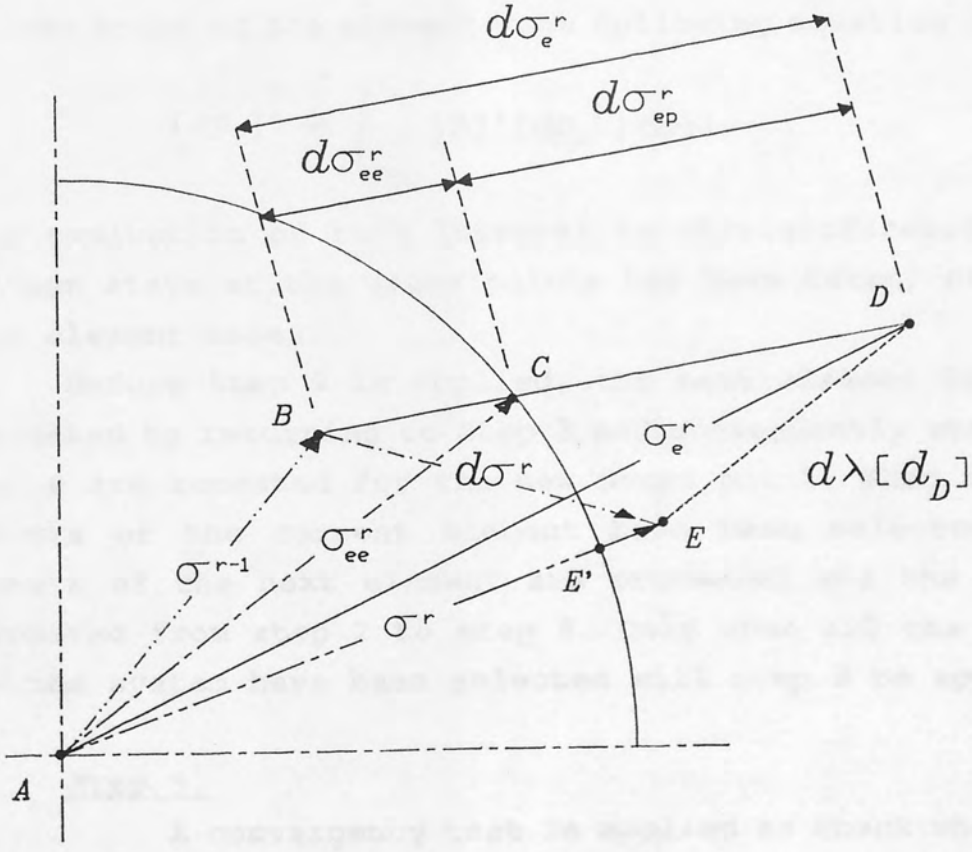

Figure 8.7(b)

Stresses on the π plane for a load increment applied from the elastic region

The initial stress method assumes that the calculated strains are correct and the corresponding stresses are adjusted to allow for non-linear behaviour. Therefore,

$$[\varepsilon_e^r] = [\varepsilon_e^{r-1}] + [d\varepsilon_e^r]$$

Step 7.

Calculate the initial stress components, $[d\sigma_i^r]$, by evaluating the following equation :-

$$[d\sigma_i^r] = [\sigma_e^r] - [\sigma_r^r]$$

The definition of the symbols is given in Fig 8.7.

Step 8.

Calculate the residual nodal forces, $[P_r]^n$, that are generated by $[d\sigma_i^r]$. The principle of virtual work is applied to balance the internal work due to $[d\sigma_i^r]$ with the external work due to $[dP_r]^n$ at each node. In order to find the residual forces at the nodes of the element, the following equation is evaluated.

$$[dP_r]^n = \int_{Vol} [\mathbf{B}]^T [d\sigma_i^r] \, dVol$$

The evaluation of this integral is straightforward because the stress state at the Gauss points has been taken, rather than at the element nodes.

Before Step 9 is applied, the next element Gauss point is selected by returning to Step 3 and consequently steps 3,4,5,6,7 and 8 are repeated for the new Gauss point. When all the Gauss points of the current element have been selected, the Gauss points of the next element are processed and the procedure is repeated from step 2 to step 8. Only when all the Gauss points in the system have been selected will step 9 be applied.

Step 9.

A convergency test is applied to check whether another iteration, r+1, is required. For each degree of freedom, if the ratio of the norm of the total displacement and that of the change in displacement is within a predetermined tolerance zone then the iteration process is terminated. The user has the option

of defining the size of the tolerance zone, but a default value of 3 per cent applies. Hence the following expressions are evaluated :-

$$\frac{\sqrt{\{\sum_{i=1}^{i=N} (dU_x)^2\}}}{\sqrt{\{\sum_{i=1}^{i=N} (U_x)^2\}}} < 0.03$$

where N = total number of nodes in the system.

Similar expressions are calculated using the displacements V_y, W_z, θ_x, θ_y and θ_z. If any of these expressions results in the ratio being greater than the tolerance value, the convergence statement is false and a further (r+1) iteration is required. The procedure is repeated from Step 1 using the residual forces, $[dP_r]^n$, calculated in Step 8.

If this convergence statement is true, the next increment in load F^{n+1} is added to the small residual forces $[dP_r]^n$ and the procedure is repeated from Step 1.

The size of the load increment, F^n, is entirely dependent on the type of system which is being analysed. For the theoretical model developed in this research project, an increment of 5 per cent was used as a default value, but this is discussed further in chapter 9. A visualisation of the iteration process using the π plane is shown in Fig 8.8. The first two iterations of a load increment are illustrated and the small discrepancy at each iteration, indicated by X, is corrected using the equations shown in step 6.

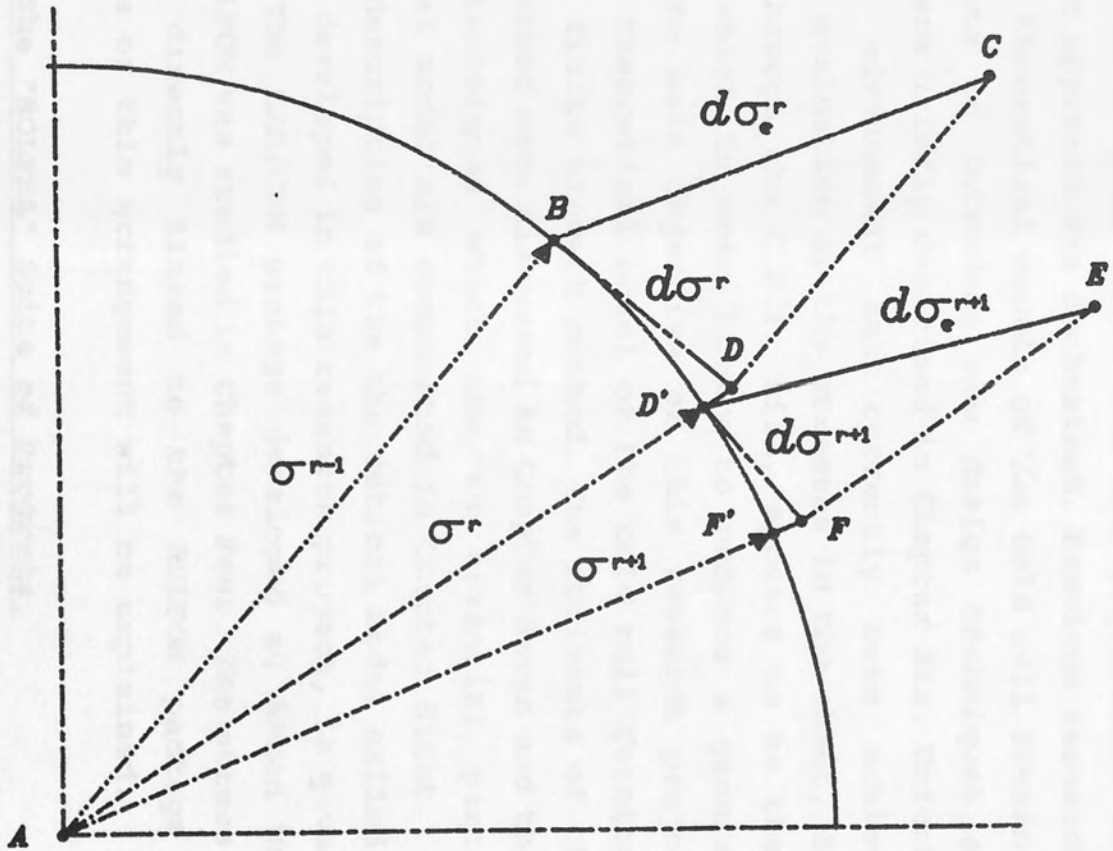

Figure 8.8 ***Iteration Process on the π Plane.***

Chapter Nine.

Finite Element Analysis of the Cold Roll Forming Process.

9.1 Introduction.

The problems of form-roll schedule design was discussed in Chapter Three and the requirement for a more scientific approach was emphasised. Previous researchers have developed theoretical models of the cold roll forming process in attempts to introduce new design techniques and their efforts were briefly described in Chapter Six. Unfortunately, no major advancement has currently been achieved. The numerical evaluation of the stresses in the sheet, due to its passage through the C.R.F. mill, appears to be the area of research which is most likely to produce a general design theory. The main objective of this research project is to develop a theoretical model of the cold roll forming process using the finite element method. The rudiments of the finite element method were discussed in Chapter Seven and the elasto-plastic techniques which are an essential part of the theoretical model are documented in Chapter Eight.

The description of the theoretical model called "ROLFEA" which was developed in this research project, is given in this chapter. The CAD/CAM package developed at Aston University called ROLFOM was studied in Chapter Four. The stress analysis model is directly linked to the ROLFOM package and the advantages of this arrangement will be explained.

9.2 The "ROLFEA" Suite of Programs.

The suite of programs for ROLFEA is shown in Fig 9.1. The CONTROL module selects the program required by the user interactively. In the case of the finite element program, because the time to run the program is quite considerable, the program is activated on a queuing system. This is achieved by the CONTROL module once the queue to be used has been established. The details of each program accessed by the CONTROL module will now be discussed.

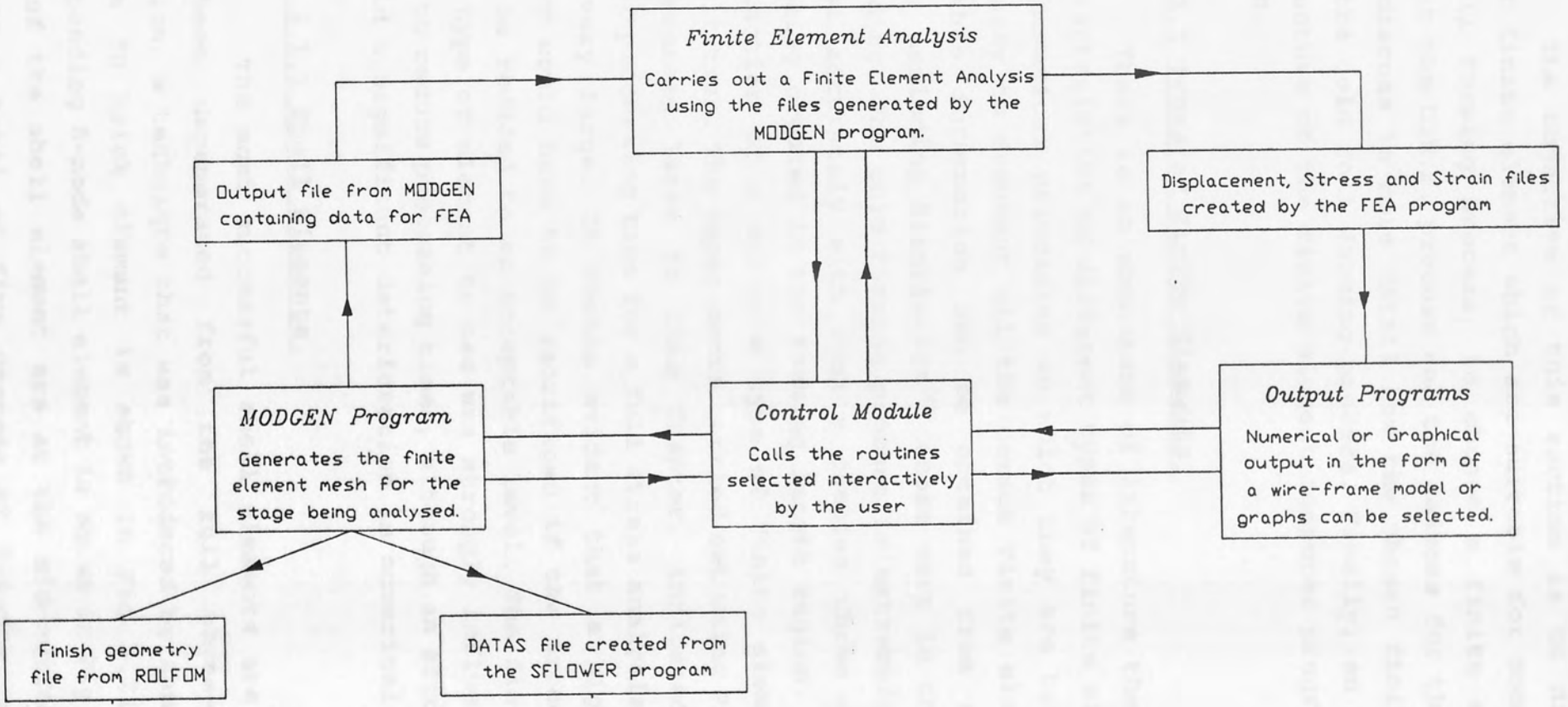

Figure 9.1 Configuration of the ROLFEA suite of programs.

9.3 The Finite Element Program.

The objective of this section is to discuss the types of finite element which are suitable for modelling the cold roll forming process, to choose a finite element to represent the C.R.F. process and the reasons for that choice, and to discuss in more detail how the chosen finite element models the cold roll forming process. Finally, an outline of the structure of the finite element computer program will be provided.

9.3.1 Types of Finite Elements.

There is an abundance of literature that explains the characteristics of different types of finite elements and the mathematical principles on which they are based. It is unnecessary to document all the common finite elements here since this information can be obtained from many other sources, including Zienkiewicz[49] whose work in this area is outstanding. The cold forming process is extremely difficult to model accurately with such a complex three dimensional shape being created in the forming length region. This makes the selection of a suitable type of finite element a very difficult task. The experiments carried out using PAFEC, which are discussed later in this Chapter, indicated that the computer processing time for a full stress analysis was likely to be very large. It became evident that a high level of accuracy would have to be sacrificed if the processing time was to be reduced to an acceptable level. The final decision on the type of element to use was strongly influenced by the desire to reduce processing times, although an effort was made to avoid a significant deterioration in numerical accuracy.

9.3.1.1 Shell Elements.

The most successful shell elements are those that have been degenerated from the full three-dimensional condition, a technique that was introduced by Ahmad[61]. A 24-node 3D brick element is shown in Fig 9.2(a) and the corresponding 8-node shell element is shown in Fig 9.2(b). The nodes of the shell element are at the mid-surface and each node has a total of five degrees of freedom, as shown in

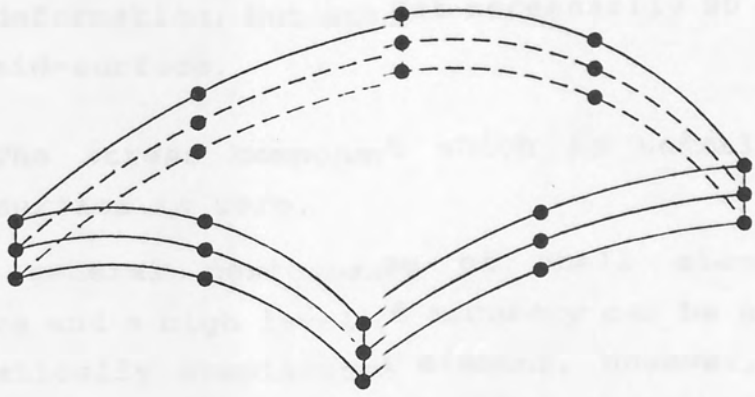

Figure 9.2(a) Twenty Four noded 3D brick element.

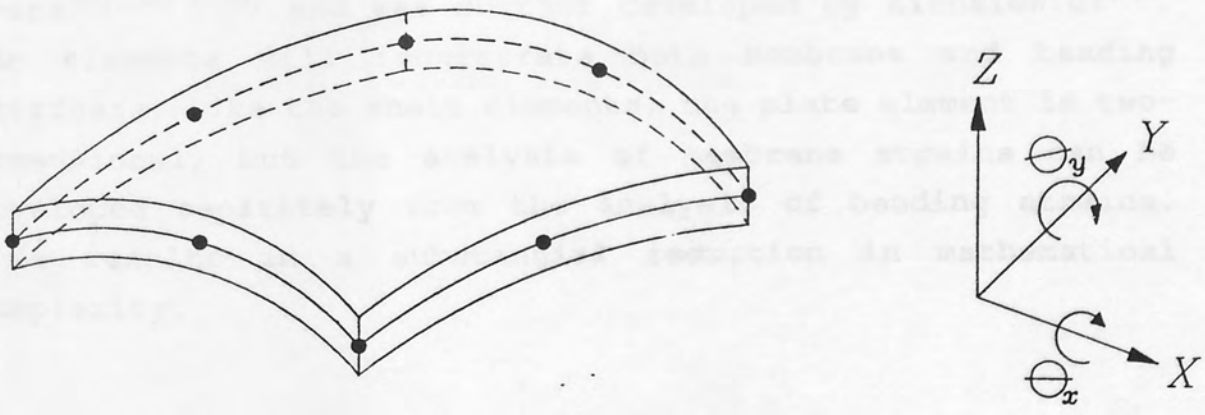

Figure 9.2(b) Eight noded shell element.

Fig 9.2(b). Generally, there is on rotation about the Z axis. The following assumptions are made for a shell analysis :-

1) The normals to the mid-surface remain straight after deformation, but are not necessarily 90 degrees to the mid-surface.

2) The stress component which is normal to the mid-surface is zero.

The general performance of shell elements is very impressive and a high level of accuracy can be expected. It is a mathematically complicated element, however, and computer processing time is likely to be very large. The high computational costs are the major disadvantage of these shell elements.

9.3.1.2 Flat Plate Elements.

The flat plate element is substantially less complicated than a shell element and consequently the computational costs will invariably be less. In Fig 9.3 the curved surface of a shell is modelled using flat plate elements. The technique was first introduced by Rockey and Evans[61],[62] & [63] and was further developed by Zienkiewicz[64]. The elements will incorporate both membrane and bending stiffness. Like the shell elements, the plate element is two-dimensional, but the analysis of membrane strains can be developed separately from the analysis of bending strains. This results in a substantial reduction in mathematical complexity.

(1) Membrane Strain Analysis.

The degrees of freedom that are allowed in the membrane analysis of a flat plate element are shown in Fig 9.4. There are two displacements, U_x and V_y, at each node and, consequently, this will introduce two forces F_x and F_y. The mathematics are based on a plane stress condition, and the displacements are calculated from the system energy equation in the usual manner (ref. 7.3.6).

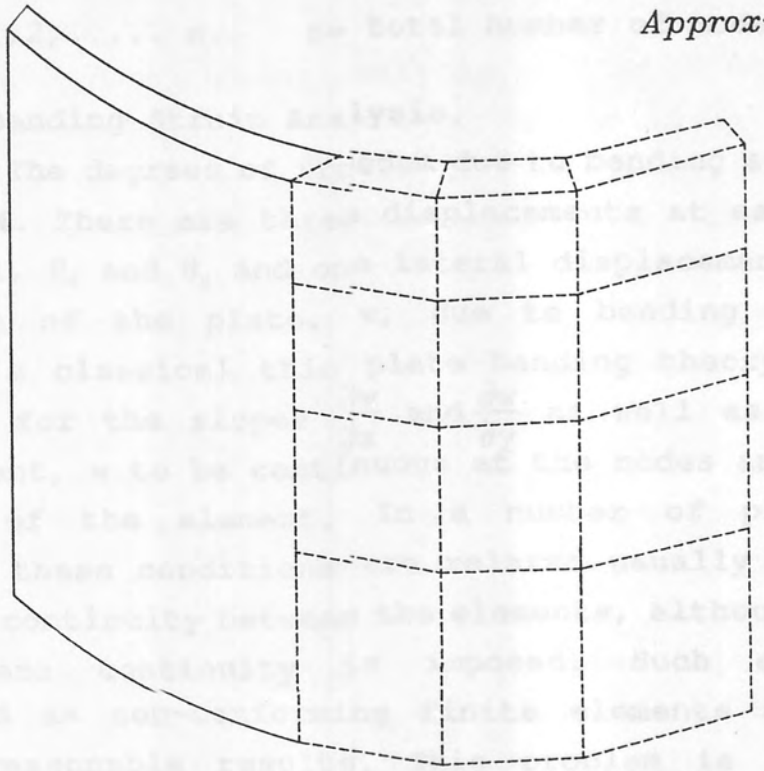

Figure 9.3 Discretisation of a Curved Surface.

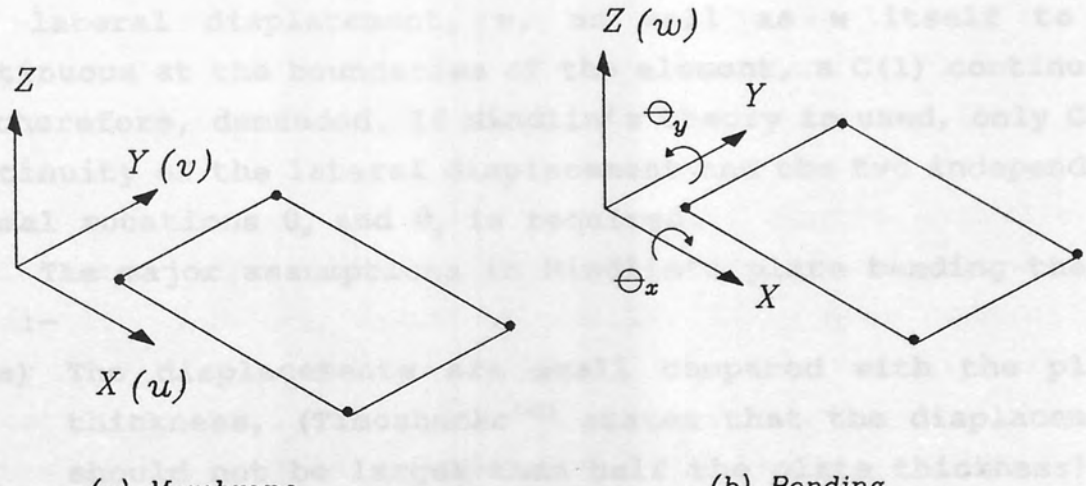

(a) Membrane (b) Bending

Figure 9.4

Degrees of Freedom in a Flat-Plate Element

$$\begin{bmatrix} F_{xi} \\ F_{yi} \end{bmatrix} = [K_m] \begin{bmatrix} U_{xi} \\ V_{yi} \end{bmatrix}$$

$[K_m]$ = plane stress stiffness matrix

where

i = 1,2,..... n. n= total number of nodes.

(2) Bending Strain Analysis.

The degrees of freedom due to bending are also shown in Fig 9.4. There are three displacements at each node, two rotational, θ_x and θ_y and one lateral displacement, w. If the deflection of the plate, w, due to bending is based on Kirchhoff's classical thin plate bending theory then it is desirable for the slopes $\frac{\partial w}{\partial x}$ and $\frac{\partial w}{\partial y}$ as well as the lateral displacement, w to be continuous at the nodes and around the boundary of the element. In a number of plate bending elements, these conditions are relaxed usually by violating the slope continuity between the elements, although not at the nodes where continuity is imposed. Such elements are classified as non-conforming finite elements and some can provide reasonable results. This problem is discussed in detail by Zienkiewicz[49].

Continuity can be ensured if Mindlin's bending theory is applied. Kirchoff's bending theory requires the derivatives of the lateral displacement, w, as well as w itself to be continuous at the boundaries of the element, a C(1) continuity is therefore, demanded. If Mindlin's theory is used, only C(0) continuity of the lateral displacement and the two independent normal rotations θ_x and θ_y is required.

The major assumptions in Mindlin's plate bending theory are :-

(a) The displacements are small compared with the plate thickness, (Timoshenko[65] states that the displacement should not be larger than half the plate thickness).

(b) The stress normal to the plate mid-surface is negligible.

(c) The normals to the mid-surface of the sheet remain straight, but not necessarily normal to the mid-surface, after deformation.

Having made these assumptions, the mathematical complexity is considerably simplified. As a result of assumption (a), Cauchy's Strain Tensor can be applied and the potential energy due to membrane deformation and bending deformation can be assessed independently. The total potential energy is simply a summation of the potential energy due to bending and stretching[43].

When a finite element analysis is used to model the cold roll forming process, the deformation due to bending of each element is assumed to be small in comparison with the sheet thickness. There is appreciable movement of the elements in the linear portions of the section during the bending process, but the majority is entirely rigid body movement created by the forming in the bend region. The deformation in the bend region is applied gradually along the forming length and the total displacement at each stage of the mill is often quite large. In a finite element model, the elements close to the stage will experience considerable deformation, exceeding half the thickness of the sheet in most cases. The finite element analysis developed in this work, however, applies the displacements to these elements in increments. A full stress analysis is taken at each increment of displacement, which enables assumption (a) to be applicable.

The importance of applying the loading increments is illustrated in Fig 9.5(a). Element number 108 has its edge, AB, moved through 15 deg due to the bending applied by the n^{th} stage. The total displacement of the element at this stage cannot be classified as a "small" displacement. When load increments are applied, the displacement is relatively small for each increment in load, and a full stress analysis is implemented before the next load increment is applied. The assumption that displacements are small has more credibility under these circumstances. Generally, the bending process illustrated in Fig 9.5(b) is analogous to the true bending mechanism in cold roll forming. As the sheet approaches the stage it is formed progressively to the geometry of the form-roll profiles. The forming is not a rapid process, unlike the bending applied by a press tool.

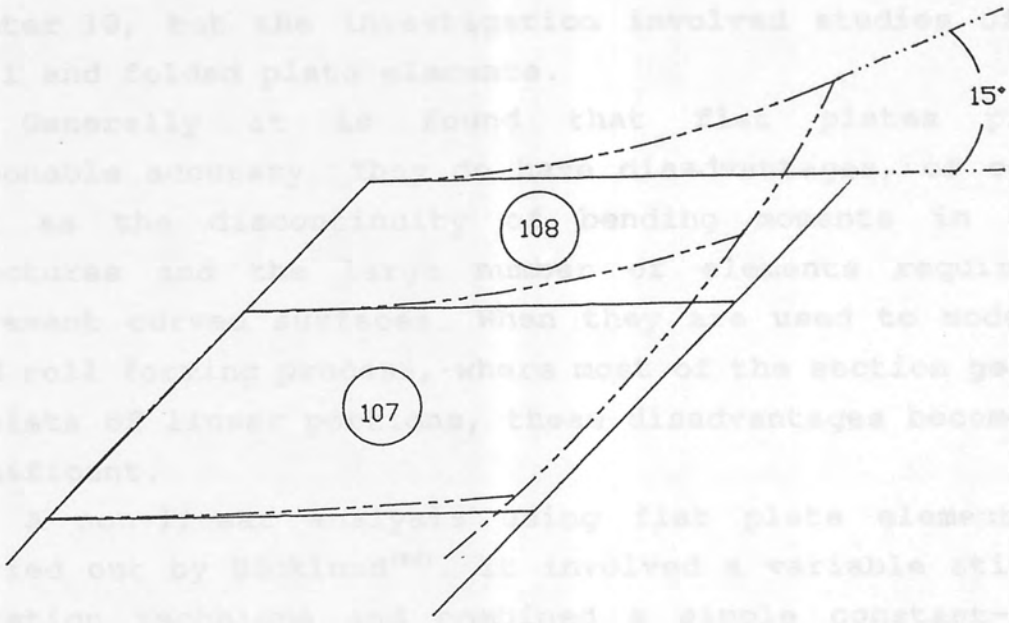

Figure 9.5(a)

Typical prescribed displacement at the first stage.

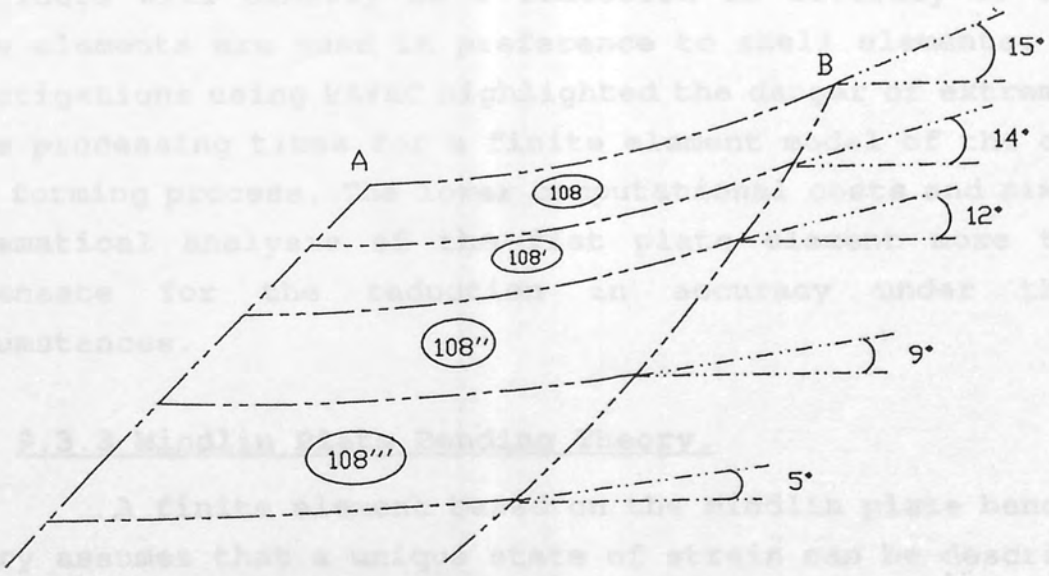

Figure 9.5(b)

Actual bending process up to the stage at AB

9.3.2 Selection of a suitable Finite Element.

To assist in the selection of a finite element to model the cold roll forming process, a series of investigations was carried out using a PAFEC finite element analysis package. Details of the results are given in Chapter 10, but the investigation involved studies of both shell and folded plate elements.

Generally it is found that flat plates provide reasonable accuracy. They do have disadvantages, of course, such as the discontinuity of bending moments in curved structures and the large number of elements required to represent curved surfaces. When they are used to model the cold roll forming process, where most of the section geometry consists of linear portions, these disadvantages become less significant.

A non-linear analysis using flat plate elements was carried out by Bäcklund[66]. It involved a variable stiffness iteration technique and combined a simple constant-strain plane stress element, and a constant-moment plate bending element. The final results indicated that even this relatively simple finite element can be used successfully in modelling reasonably curved structures.

There will clearly be a reduction in accuracy if flat plate elements are used in preference to shell elements. The investigations using PAFEC highlighted the danger of extremely large processing times for a finite element model of the cold roll forming process. The lower computational costs and simple mathematical analysis of the flat plate element more than compensate for the reduction in accuracy under these circumstances.

9.3.3 Mindlin Plate Bending Theory.

A finite element based on the Mindlin plate bending theory assumes that a unique state of strain can be described using the nodal displacements w, θ_x, θ_y. The displacements are shown in Fig 9.6, where the line AB defines the normal to the mid-surface before deformation took place. The displacement in the XZ plane is defined by the following equation :-

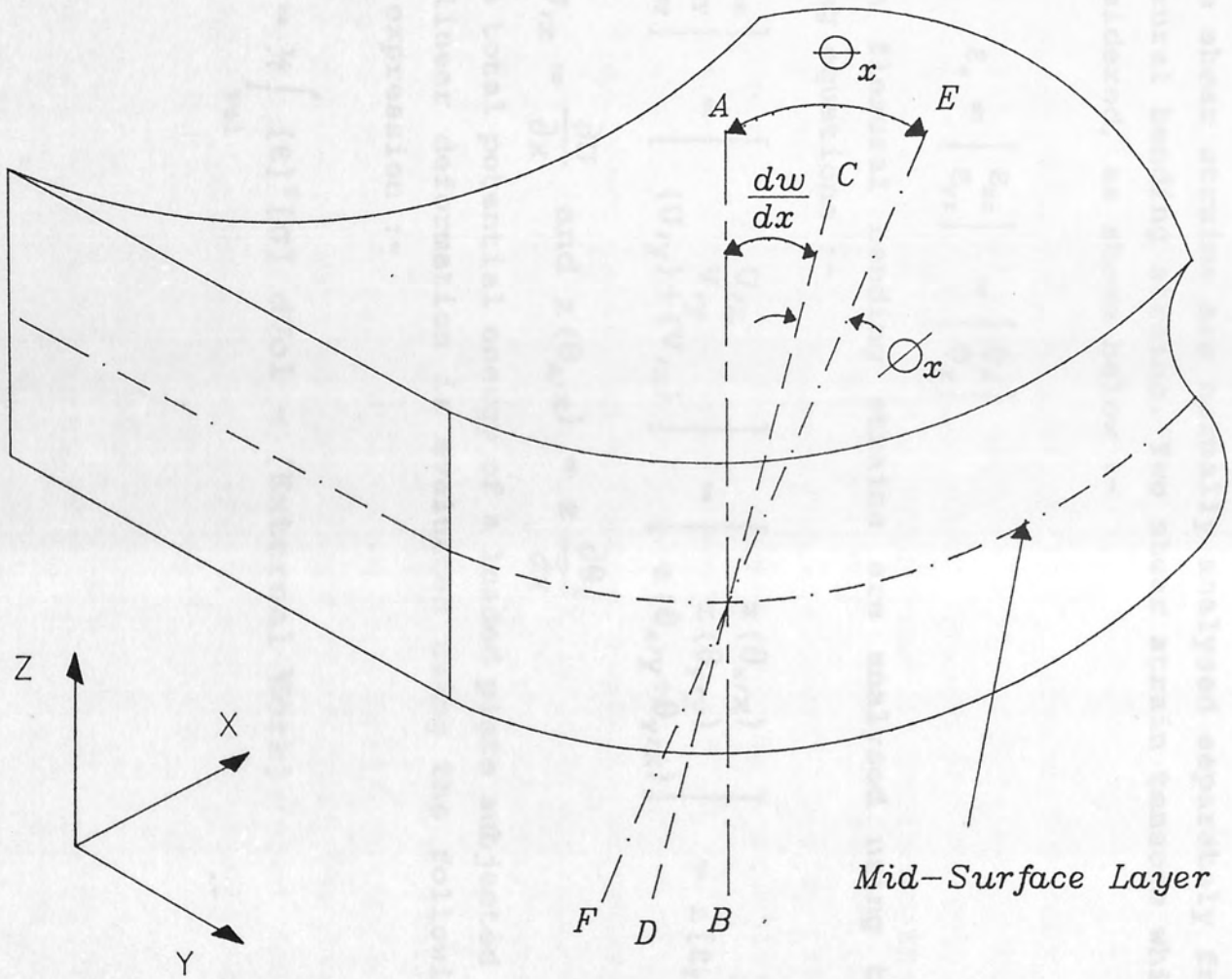

Figure 9.6 Plate Bending incorporating Shear Angles.

$$\theta_x = \frac{\partial w}{\partial x} + \phi_x$$

A similar equation defines the displacement in the YZ plane.

From a description of the Mindlin plate bending theory given by Nikiuchi[67] the displacement of a point at an increment in Z from the mid-surface will be fully described in the following equations :-

$$\begin{aligned} U(x,y,z) &= z\theta_x \\ V(x,y,z) &= z\theta_x \\ w(x,y,z) &= w \end{aligned}$$

where $\theta_x = \theta_x(x,y)$, $\theta_y = \theta_y(x,y)$ and $w=w(x,y)$

The shear strains are normally analysed separately from the flexural bending strains. Two shear strain tensors which are considered, as shown below :-

$$\varepsilon_s = \begin{bmatrix} \varepsilon_{xz} \\ \varepsilon_{yz} \end{bmatrix} = \begin{bmatrix} \phi_x \\ \phi_y \end{bmatrix}$$

The flexural bending strains are analysed using the following equations :-

$$\begin{bmatrix} \varepsilon_{xx} \\ \varepsilon_{yy} \\ \varepsilon_{xy} \end{bmatrix} = \begin{bmatrix} U_{,x} \\ V_{,y} \\ (U_{,y}) + (V_{,x}) \end{bmatrix} = \begin{bmatrix} z\,(\theta_{x,x}) \\ z\,(\theta_{y,y}) \\ z\,(\theta_{x,y} + \theta_{y,x}) \end{bmatrix} = z\,[\varepsilon_f]$$

where $U_{,x} = \dfrac{\partial U}{\partial x}$ and $z\,(\theta_{x,x}) = z\,\dfrac{\partial \theta_x}{\partial x}$

The total potential energy of a loaded plate subjected to purely linear deformation is evaluated using the following general expression :-

$$V_T = \tfrac{1}{2} \int_{Vol} [\varepsilon]^T [\sigma]\ dVol - [External\ Work]$$

For a loaded plate analysed using Mindlin's plate bending theory the following applies :-

$$V_T = \tfrac{1}{2}\int_{Area}\int_{-t/2}^{+t/2} z\,[\varepsilon_f]^T[\sigma_f]\;dz\;dA + \tfrac{1}{2}\int_{Area}\int_{-t/2}^{+t/2} [\varepsilon_s]^T[\sigma_s]\;dz\;dA - \int_{A_1} wq\;dA$$

where

q = normal load distributed on the surface area A_1 of the plate.

$$[\sigma_f] = [\sigma_{xx}\ \sigma_{yy}\ \sigma_{xy}]^T$$

$$[\sigma_s] = [\sigma_{xz}\ \sigma_{yz}]^T$$

This V_T equation does not include the individual forces and moments acting on the plate, such as a transverse shear force or a moment acting along an edge. If applied forces and moments of this nature do exist, they must be included in the analysis as part of the external work, being treated in a similar manner to the normally distributed load q. Thick plates are normally divided into layers and the V_T equation is used to calculate the potential energy in each layer. The model of the cold roll forming process is associated with bending thin sheet metal and a layered analysis is generally not essential. If a layered approach is not applied, the mathematics will be simplified (by introducing stress resultants instead of actual stresses) and ultimately the computer processing time will be reduced. For these reasons, the layered approach was not used in this research project.

The following expression defines the stress resultants (i.e. moments and shear forces) that are generated due to plate deformation according to Mindlin's plate bending theory-

$$[\mathbf{M}] = \begin{bmatrix} M_{xx} \\ M_{yy} \\ M_{xy} \end{bmatrix} = \begin{bmatrix} \int z\sigma_{xx}\,dz \\ \int z\sigma_{yy}\,dz \\ \int z\sigma_{xy}\,dz \end{bmatrix}$$

$$[Q] = \begin{bmatrix} Q_x \\ Q_y \end{bmatrix} = \begin{bmatrix} \int \tau_{xz}\, dz \\ \int \tau_{yz}\, dz \end{bmatrix}$$

where the integral through the thickness is between the limits $\pm\frac{t}{2}$

The total potential energy of the system, V_T, can therefore be expressed using the following equation :-

$$V_T = \tfrac{1}{2}\int_{Area} [\varepsilon_f]^T[M]\ dA + \tfrac{1}{2}\int_{Area} [\varepsilon_s]^T[Q]\ dA - \tfrac{1}{2}\int_{A_1} wq\ dA$$

For an isotropic and homogeneous material subjected to purely elastic behaviour, the following relationships apply[68].

$$[M] = [D_f]\ [\varepsilon_f]$$
$$[Q] = [D_s]\ [\varepsilon_s]$$

where

$$[D_f] = \frac{Et^3}{12(1-\upsilon^2)} \begin{bmatrix} 1 & \upsilon & 0 \\ \upsilon & 1 & 0 \\ 0 & 0 & \frac{(1-\upsilon)}{2} \end{bmatrix}$$

and $$[D_s] = \frac{Et}{2(1+\upsilon)\alpha} \begin{bmatrix} 1 & 0 \\ 0 & 1 \end{bmatrix}$$

where

α = warping factor (usually given the value of $^6/_5$)
E = Young's Modulus of Elasticity
υ = Poisson's Ratio

Therefore, the total potential energy of the system is described by the following equation.

$$V_T = \tfrac{1}{2}\int_{Area} [\varepsilon_f]^T[D_f][\varepsilon_f]\ dA + \tfrac{1}{2}\int_{Area} [\varepsilon_s]^T[D_s][\varepsilon_s]\ dA - \tfrac{1}{2}\int_{A_1} wq\ dA$$

The Mindlin plate bending theory can be applied to a plate where the loading could generate high shear stresses or negligible shear stresses. Hence, it is equally applicable to shear-weak and shear-stiff plates. This is true because the shear energy term, which involves the displacement due to shear, can be reduced to zero. The shear energy term will then be as follows.

$$\text{Shear Energy} = \tfrac{1}{2}\int_{\text{Area}} [\varepsilon_s]^T [D_s] [\varepsilon_s] \; dA$$

and $$\theta_x \propto \frac{\partial w}{\partial x} \qquad \theta_y \propto \frac{\partial w}{\partial y}$$

Experimental results have indicated, however, that anomalies in the analysis occur if the shear stresses are negligible compared with the bending stresses. The system stiffness is over-estimated by the Mindlin theory if $\phi_x = \phi_y = 0$. If the plate thickness is less than 2 mm, the shear stresses are generally assumed to be negligible compared with the other stresses, this will apply to the vast majority of the sheet used in the cold roll forming industry. Fortunately, this limitation in the Mindlin theory can be overcome if a reduced or selective integration technique is used to calculate the stiffness of the system (ref. section 7.3.4, Gaussian Quadrature technique). This method will fully integrate a polynomial expression if a sufficient number of Gauss points are considered. This is called a "full integration" and the number of Gauss points required can be found from the following equation. :-

$$p = (2n-1)$$

where

p = order of the polynomial

n = the point rule number.

A plane stress condition will involve the integration of a quintic polynomial, hence a three point rule is applicable and will involve a total of nine Gauss points. A quintic polynomial also occurs in general plate bending theory, so the three point rule will result in a full integration being

performed.

If a three point rule is used when Mindlin theory is applied to thin plates subjected to negligible shear angles, the calculated stiffness will be too great. A "reduced integration" using a two point rule, where only four Gauss points are taken, will improve the accuracy of the stiffness calculations. Hinton[68] emphasised that irregularities may occur if the two point rule was applied, due to the production of spurious zero energy modes. A superior technique, therefore, is the "selective integration" method, which uses the two point rule on the shear energy integral and the three point rule on the bending moment integral. This overcomes the irregularities of solely using the two point rule and the over-estimation of stiffness when using the three point rule. Consequently, the Mindlin plate theory incorporating a selective integration technique was used in the finite element model developed in this research.

9.3.4 Generation of the Global Stiffness Matrix.

A finite element analysis using Mindlin's plate bending theory will result in the following matrix equation being applied to assess the degree of bending in each element :-

$$[\mathbf{F}_i^b] = [\mathbf{K}_e^b]\,[\delta_i^b]$$

where

$i = 1, 2, \ldots N$ N = number of nodes per element

$[\mathbf{K}_e^b]$ = element bending stiffness

$$[\mathbf{F}_i^b] = \begin{bmatrix} T_{xi} \\ T_{yi} \\ F_{zi} \end{bmatrix} \qquad [\delta_i^b] = \begin{bmatrix} \theta_{xi} \\ \theta_{yi} \\ w_i \end{bmatrix}$$

and T_{xi} is the torque related to the displacement θ_{xi} at the i^{th} node.

Folded plate finite element theory introduces an additional degree of freedom which allows a rotation about the Z axis. The θ_{zi} displacement is due to a twisting force acting in the plane of the element. It is usually assumed to be negligible compared with the other forces when the stiffness of the system is calculated. Consequently, one row and one

column of the element stiffness matrix will consist entirely of zeros to correspond with the θ_{zi} in the displacement matrix. The θ_{zi} cannot be omitted from the folded plate analysis because its presence is important when the element stiffness matrices are assembled to form the global stiffness matrix, as explained later. The displacements and the forces at each node of a flat plate element are defined in Fig 9.7.

It is sometimes convenient to represent the stiffness matrix using a number of sub-matrices which represent individual nodes of the element. For the stiffness which relates the displacement at node s with the corresponding forces at node r, there will be a sub-matrix to represent the membrane forces and a sub-matrix to represent the bending forces. The result is that many of the components in the stiffness matrix which solely represent node r and node s are zero, as Fig 9.8 shows. The sixth row and sixth column in Fig 9.8 are included due to the presence of the θ_{zi} displacement.

The element stiffness matrix will use a local coordinate system, the axes being in the plane of the element. To allow the assembly of a system or global stiffness matrix, using the individual element stiffness matrix, the local coordinate system of each element must be transformed to create a common global system. This is also necessary if equilibrium equations which describe the global system are to be generated. In Fig 9.9(a), the local coordinate system for an arbitrary element uses the axes X′,Y′,Z′ and the global coordinate system uses axes X,Y,Z. Transformation between each set of axes is achieved using simple direction cosines. The element stiffness matrix referred to the global axes is derived using the diagonal [**T**] matrix and this is shown in Fig 9.9(b)

For the sub-matrix $[\mathbf{K}_{rs}]$ shown in Fig 9.8, the transformation is obtained by using the [**L**] matrix as shown below :-

$$[\mathbf{K}_{rs}] = [\mathbf{L}]^{T} [\mathbf{K}'_{rs}] [\mathbf{L}]$$

The matrix manipulation tends to be easier if the sub-matrices are processed and, consequently, this was the method used in this research project. Transformation to the global axis was achieved using the [**L**] matrix rather than the [**T**] matrix.

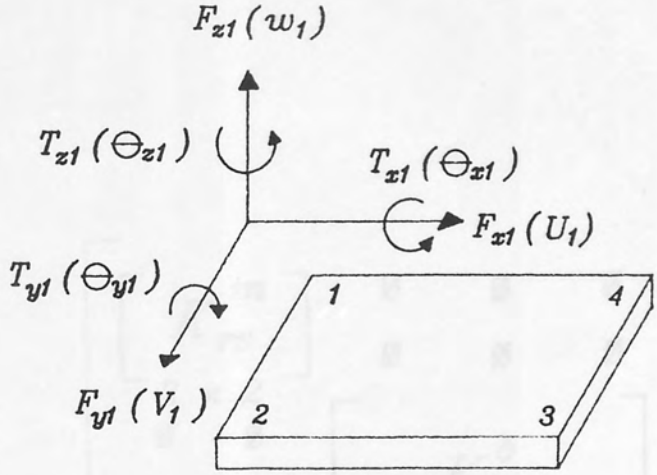

The stiffness of the element is defined by :-

$$\left[F_i\right] = \left[K_e\right] \quad \left[\delta_i\right]$$

or

$$\begin{bmatrix} [F_1] \\ [F_2] \\ [F_3] \\ [F_4] \end{bmatrix} = \left[K_e\right] \begin{bmatrix} [\delta_1] \\ [\delta_2] \\ [\delta_3] \\ [\delta_4] \end{bmatrix}$$

where

$$[F_1] = \begin{bmatrix} F_{x1} \\ F_{y1} \\ F_{z1} \\ T_{x1} \\ T_{y1} \\ T_{z1} \end{bmatrix} \qquad [\delta_1] = \begin{bmatrix} U_1 \\ V_1 \\ w_1 \\ \Theta_{x1} \\ \Theta_{y1} \\ \Theta_{z1} \end{bmatrix}$$

Figure 9.7

The Local Forces and Displacements Acting on an Element.

$$\left[K_{rs}\right] = \begin{bmatrix} \underset{2\times 2}{\left[K_{rs}^{m}\right]} & \begin{matrix} \emptyset & \emptyset & \emptyset & \emptyset \\ \emptyset & \emptyset & \emptyset & \emptyset \end{matrix} \\ \begin{matrix} \emptyset & \emptyset \\ \emptyset & \emptyset \\ \emptyset & \emptyset \\ \emptyset & \emptyset \end{matrix} & \begin{bmatrix} & K_{rs}^{b} & \end{bmatrix}_{3\times 3} \begin{matrix} \emptyset \\ \emptyset \\ \emptyset \\ \emptyset \end{matrix} \end{bmatrix}$$

where

$\left[K_{rs}^{m}\right]$ stiffness components due to bending forces.

$\left[K_{rs}^{b}\right]$ stiffness components due to membrane forces.

Figure 9.8

A Typical Local Stiffness Sub-Matrix.

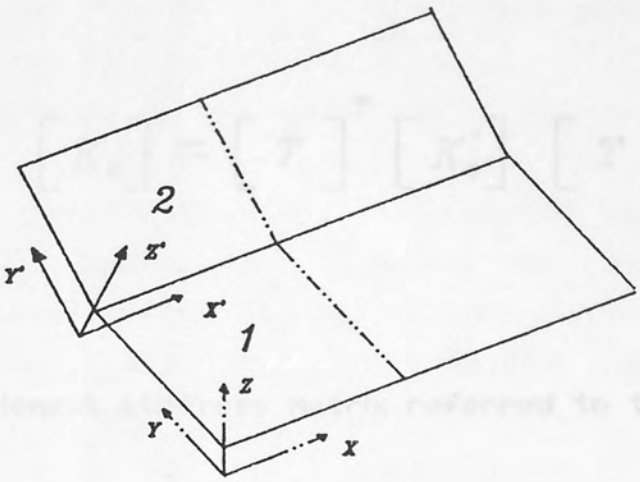

$$[\delta_i'] = [L]\ [\delta_i]$$

where

$[\delta_i']$ is the element displacement matrix referred to the local axes.

$[\delta_i]$ is the corresponding displacement matrix referred to the global axes.

i = number of nodes in a element.

$$[L] = \begin{bmatrix} [\lambda] & 0 \\ 0 & [\lambda] \end{bmatrix} \qquad [\lambda] = \begin{bmatrix} \text{Cos}\,\Theta_{x'x} & \text{Cos}\,\Theta_{x'y} & \text{Cos}\,\Theta_{x'z} \\ \text{Cos}\,\Theta_{y'x} & \text{Cos}\,\Theta_{y'y} & \text{Cos}\,\Theta_{y'z} \\ \text{Cos}\,\Theta_{z'x} & \text{Cos}\,\Theta_{z'y} & \text{Cos}\,\Theta_{z'z} \end{bmatrix}$$

where

$\text{Cos}\,\Theta_{x'x}$ is the angle between the global x and the local x' axis.

Similarly,

$$[F_i'] = [L]\ [F_i]$$

Figure 9.9(a)

Transformation of Displacements and Forces from Local to Global axes.

$$\left[K_e\right] = \left[T\right]^T \left[K_e'\right] \left[T\right]$$

where

$\left[K_e\right]$ = element stiffness matrix referred to the global axes.

$\left[K_e'\right]$ = element stiffness matrix referred to the local axes.

and

$$\left[T\right] = \begin{bmatrix} [L_1] & 0 & 0 & \cdot & \cdot \\ 0 & [L_2] & 0 & \cdot & \cdot \\ 0 & 0 & [L_3] & \cdot & \cdot \\ \cdot & , & \cdot & \text{etc} & \cdot \\ \cdot & , & \cdot & \cdot & [L_n] \end{bmatrix}$$

where n = number of element nodes.

Figure 9.9(b)

Transformation of the Stiffness Matrix.

Following the transformation of the coordinate system, the assembly of the global stiffness matrix can be carried out using one of the standard methods. The frontal solution technique is described in detail in 7.3.6 and is used in this research project.

After the unknowns in the analysis have been evaluated, in the case of the ROLFEA program the unknowns will primarily be displacements, their values will correspond to the global coordinate system. Before the stresses can be computed, however, it is essential that the calculated displacements are converted back to their local coordinate systems. The following equation is applied to carry out this conversion :-

$$[\delta'] = [\mathbf{L}]^T [\delta]$$

where

$[\delta']$ local coordinate displacements.

$[\delta]$ global coordinate displacements.

$[\mathbf{L}]$ is the coordinate transformation matrix.

$[\mathbf{L}]^T = [\mathbf{L}]^{-1}$

A peculiarity occurs at the nodes which are located on the boundaries between coplanar folded plate elements. Because there are six degrees of freedom at each node, there will be six displacements or forces which have to be evaluated and there must be six equilibrium equations in order to enable the unknowns to be calculated. At the boundary between two coplanar elements, the six equilibrium equations can be derived, but the equations corresponding to θ_z are not independent. When this occurs, the stiffness matrix will be singular and, therefore, cannot be inverted. A number of alternatives can be applied to overcome this difficulty. A solution suggested by Rockey[62] deletes the equilibrium equation which corresponds to the θ_z displacement and this is the method used in this research project. A search is carried out to identify all the nodes which are located at the boundaries of coplanar elements. These nodes are then subjected to an additional restraint which effectively reduces the θ_z displacement to zero.

9.3.5 Finite Element Program Structure.

The structure of the finite element analysis is typical of most large FORTRAN software packages. The usual hierarchical structure is adopted, with the selection of sub-programs, or sub-routines, being controlled by a Main or Executive program. There are only nine sub-routines, which ensures that their selection by the Main program is relatively simple. This has resulted in most of the sub-routines being rather large, but it has simplified the software structure considerably.

The mathematics carried out by the program is largely matrix manipulation, which normally is the case with finite element programs. The number of matrices involved is unavoidably large and a system of dynamic dimensioning ensures good housekeeping. This means that all the arrays are dimensioned by the Main program prior to being used by the sub-routines. A schematic representation of the finite element software structure is given in Fig 9.10. The Main program has control over the entire analysis and calls each sub-routine whenever it is required. Its primary purpose is to inquire whether the iterative loop has satisfied the convergence test (applied by the CONVERGENCE sub-routine). Depending on the result of the convergency test, the Main program will either continue with the next iteration if the test is not satisfied, or it will apply the next load increment using the INCREMENTS sub-routine.

9.4 Automatic Finite Element Mesh Generation.

The ROLFEA programs are fully integrated with the ROLFOM package. The section geometry at each stage of the mill is defined in a file called "F"/SECNO which is generated by ROLFOM's "FLOWER" program. The format of this data is rearranged by the "SFLOWER" program to suit the GINO-F routines, which will enable the flower pattern drawings to be plotted. The data in this rearranged format are also required by the mesh-generating program. Hence, the SFLOWER program has been altered to allow this reformatted data to be captured and stored in a temporary file called "ROLDATA". When the mesh generation program is executed by ROLFEA, the user is

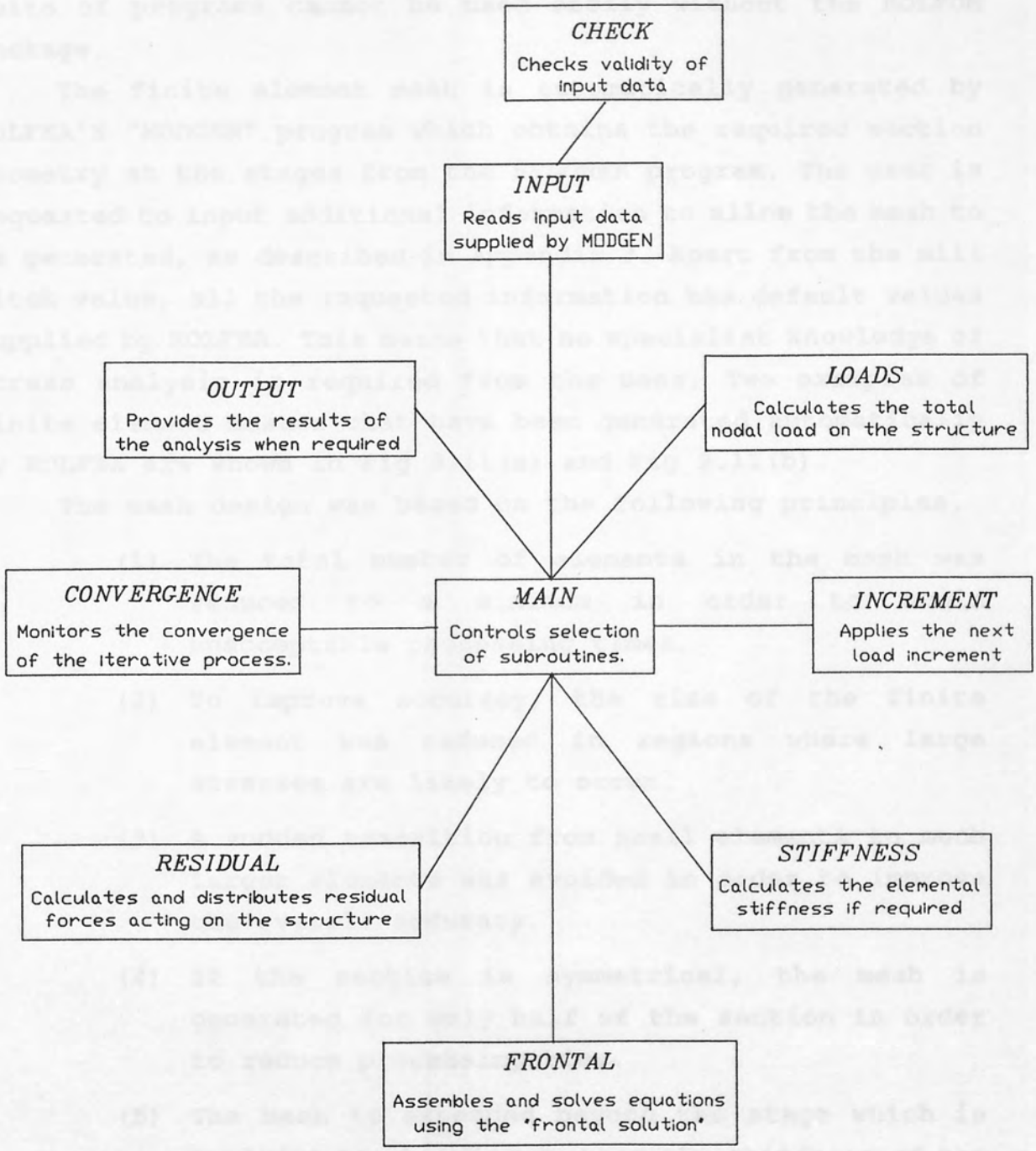

Figure 9.10

Layout of the Finite Element Analysis Program.

propositioned on whether the "ROLDATA" file has been created. If the "ROLDATA" file does not exist, the ROLFEA system will automatically create one by invoking the "SFLOWER" program. Unlike ROLCUT, which can be used as a totally separate entity that only requires access to the GINO-F library, the ROLFEA suite of programs cannot be used easily without the ROLFOM package.

The finite element mesh is automatically generated by ROLFEA'S "MODGEN" program which obtains the required section geometry at the stages from the SFLOWER program. The user is requested to input additional information to allow the mesh to be generated, as described in Appendix 3. Apart from the mill pitch value, all the requested information has default values supplied by ROLFEA. This means that no specialist knowledge of stress analysis is required from the user. Two examples of finite element meshes that have been generated automatically by ROLFEA are shown in Fig 9.11(a) and Fig 9.11(b).

The mesh design was based on the following principles.

(1) The total number of elements in the mesh was reduced to a minimum in order to avoid unacceptable processing times.

(2) To improve accuracy, the size of the finite element was reduced in regions where large stresses are likely to occur.

(3) A sudden transition from small elements to much larger elements was avoided in order to improve the overall accuracy.

(4) If the section is symmetrical, the mesh is generated for only half of the section in order to reduce processing time.

(5) The mesh is extended beyond the stage which is applying the bending so that the stiffness of the sheet upstream of this stage is considered in the analysis.

An important characteristic is shown in Fig 9.11(a) where the position of the first stage is shown. The mesh is extended beyond the stage in the upstream direction to allow for the effect of the stiffness in the sheet after it has

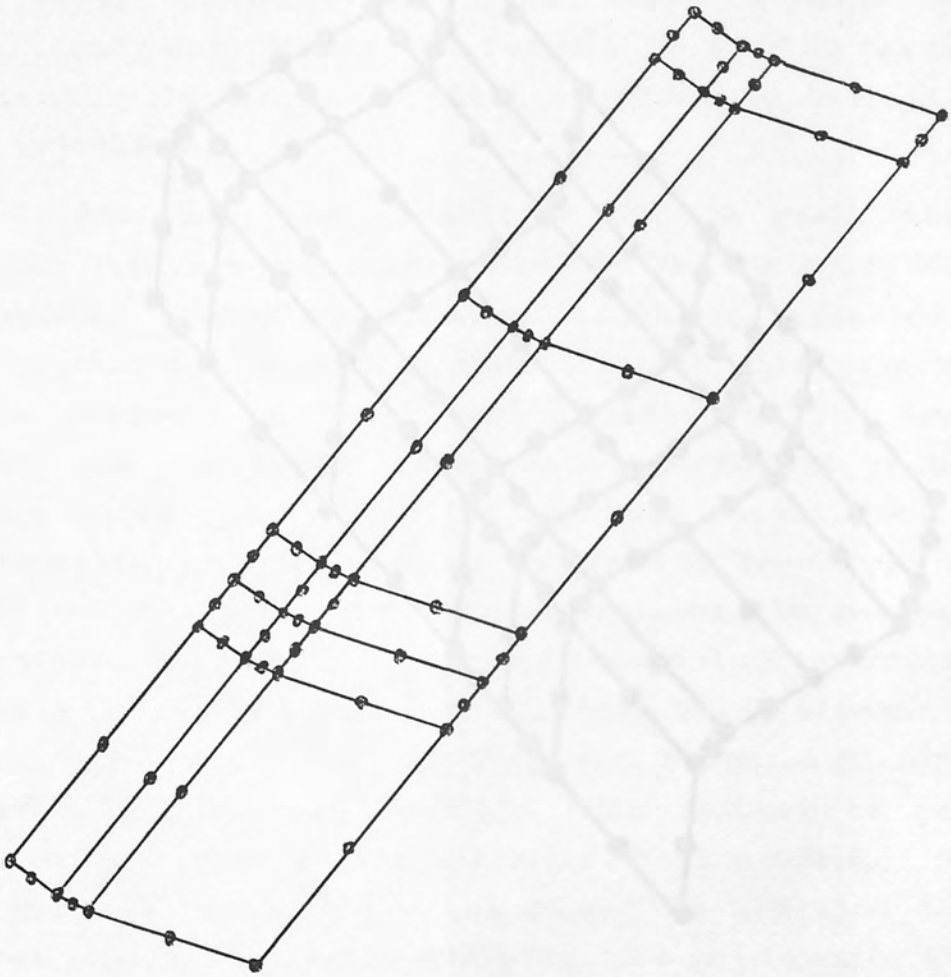

Figure 9.11(a) Mesh generated by ROLFEA.

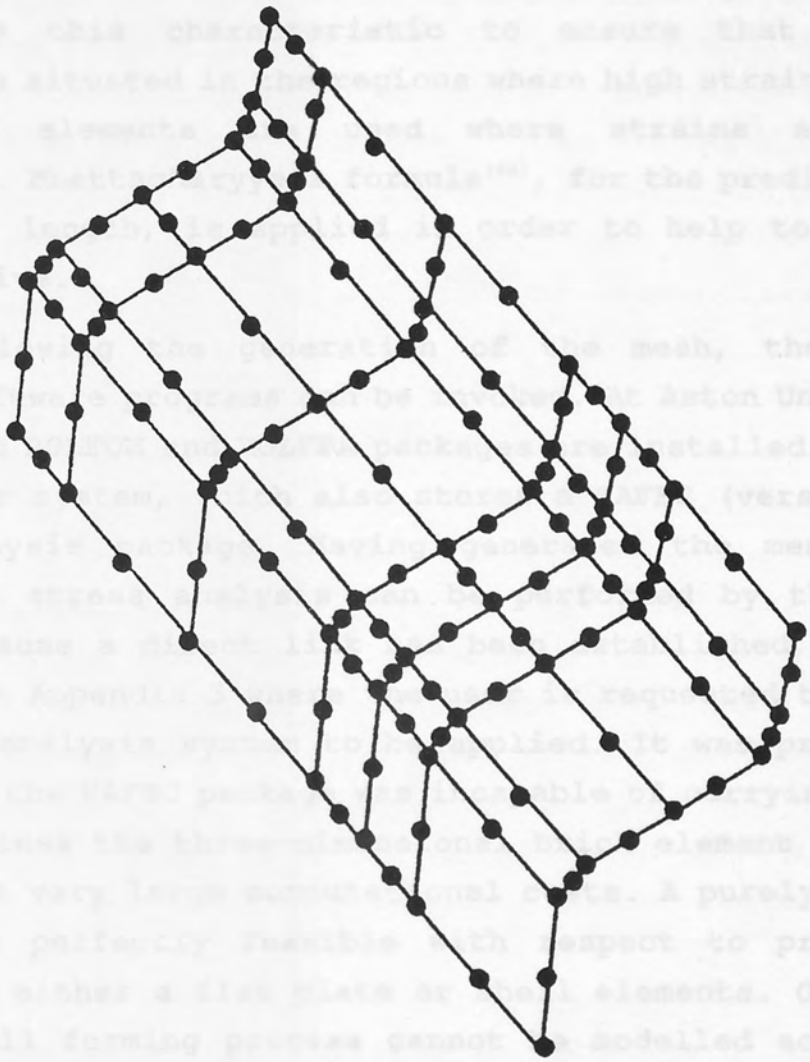

Figure 9.11(b) Top-hat mesh generated by ROLFEA.

passed through the form-rolls.

The existence of a forming length, described in 3.2.2, is widely known. Deformation of the sheet and, therefore, the creation of a strain distribution due to the n^{th} stage, will normally not extend to the n^{th}-1 stage. The mesh design uses this characteristic to ensure that smaller elements are situated in the regions where high strains exists and larger elements are used where strains are less significant. Bhattacharyya's formula[42], for the prediction of the forming length, is applied in order to help to achieve this objective.

Following the generation of the mesh, the stress analysis software programs can be invoked. At Aston University the combined ROLFOM and ROLFEA packages are installed on a VAX 8500 cluster system, which also stores a PAFEC (version 5.1) stress analysis package. Having generated the mesh using MODGEN, the stress analysis can be performed by the PAFEC package because a direct link has been established. This is indicated in Appendix 3 where the user is requested to select the stress analysis system to be applied. It was previously stated that the PAFEC package was incapable of carrying out an analysis unless the three-dimensional brick element is used, which incurs very large computational costs. A purely elastic analysis is perfectly feasible with respect to processing time, using either a flat plate or shell elements. Of course the cold roll forming process cannot be modelled accurately without an elasto-plastic analysis. The main reason why a link was installed between ROLFEA (ROLFOM) and PAFEC was to demonstrate that a link with a commercial stress analysis package can easily achieved. The observations discussed in section 10.4 suggest that a purely elastic analysis of the cold roll forming process can be useful in certain circumstances. Further information is required from the user if the PAFEC package is used, and this is also described in Appendix 3.

The ROLFEA package does not study all of the stages in the schedule in one analysis. Each stage is studied individually, which means that the MODGEN program generates a mesh for a single stage. This ensures that extremely large processing times are avoided.

9.5 ROLFEA's Modelling Characteristics.

The residual strains which are calculated by the elasto-plastic analysis programs are stored in a file and are used when analysing the next upstream stage of the mill. These residual strains are influential when the strain distribution created in the following stage is analysed. The finish section will possess residual strains which have been created by the combined effect of all the stages it has passed through and the analysis applied by ROLFEA allows for this situation. This means that the full analysis of a roll design schedule must begin with the first stage and progress sequentially to the final stage.

9.6 The Graphical Output Programs.

After the stress analysis for a stage has been completed, the user has a number of options regarding the display of the results. A list of nodal values for displacements can be obtained, as well as the magnitude of the residual strains and stresses at the Gauss points. Alternatively, a graphical output of the results may be chosen. The data output routines are written in FORTRAN and the high quality graphics are produced by the GINO-F library. The curve plotting is achieved by the GINO-F programs using the CURTO2 routine.

The user is requested to select the type of output from the list which is displayed in Appendix 3. Additional information is requested by the program so that the required graphical output can be produced. This additional information is also shown in Appendix 3. The nodal displacements, for example, can be displayed either as a plan view or as an end elevation, depending on the information which is given. If the PAFEC system is used, the graphical output is provided by the PIGS program and a FORTRAN routine has been written so PIGS is invoked automatically by ROLFEA. Generally, the output from ROLFEA compares favourable with PIGS and the curve plotting is arguably superior.

A wire-frame model of the sheet showing the forming length region can be generated, with the viewpoint of the display being defined by the user. Prior to the application

of the prescribed displacements, the section geometry of the sheet is assumed to be the same as its geometry at the downstream stage, as shown in Fig 9.11(b). A wire-frame model option can be used to visually check that the prescribed displacements are as intended. This option can be selected following the mesh generation; an example of the output is shown in Fig 9.12(a).

Having calculated the nodal displacements, the geometry of the deformed sheet can be superimposed onto the original structure. Each side of a element is generated by using the CURTO2 routine to provide a visualisation of the geometry of the deformed sheet. An example is shown in Fig 9.12(b) where a flanged U-channel is being analysed. This facility can provide a more accurate visualisation of the bending process than is possible if the wire-frame option in ROLFOM is used.

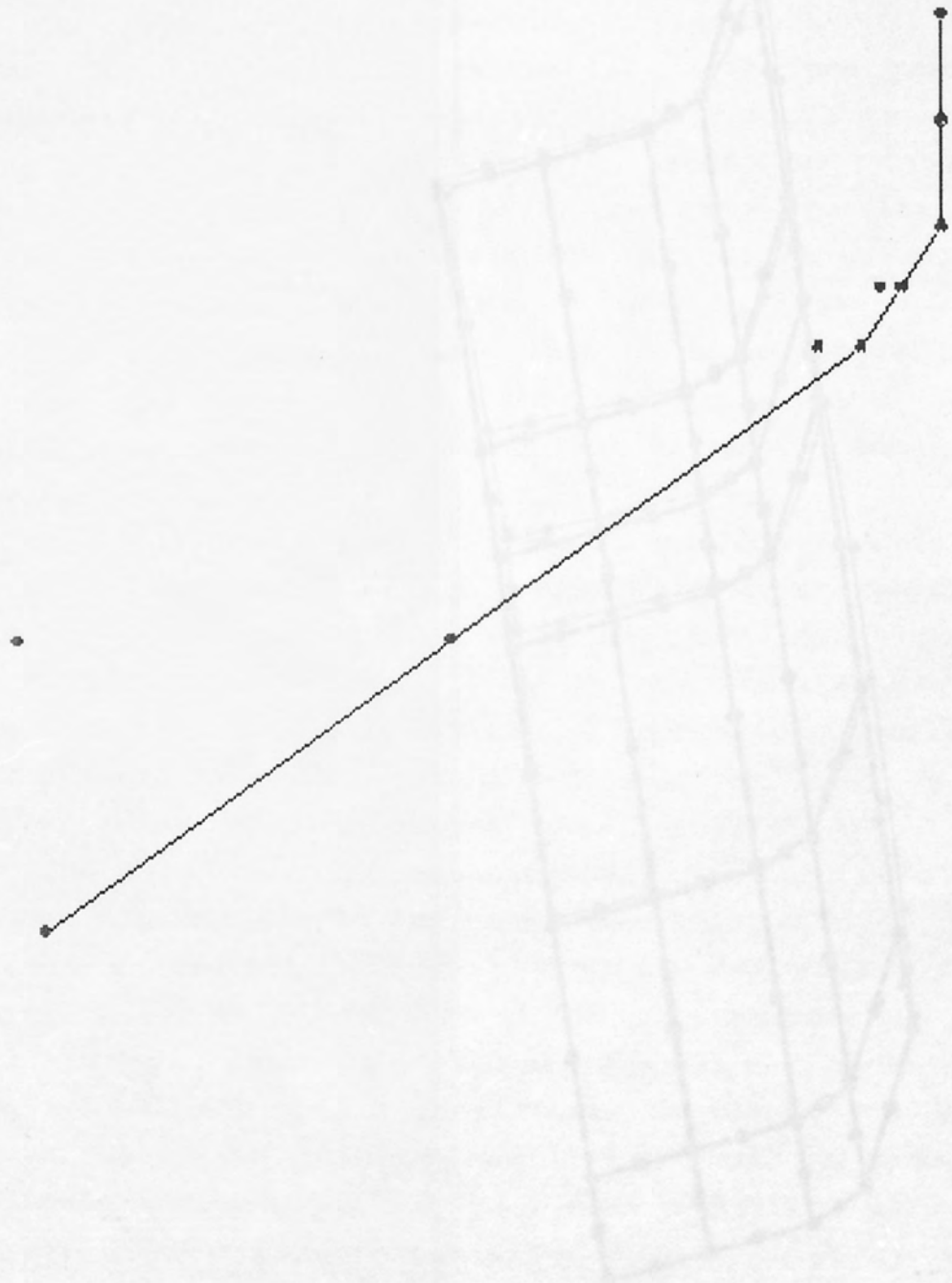

Figure 9.12(a) Prescribed displacement check by ROLFEA.

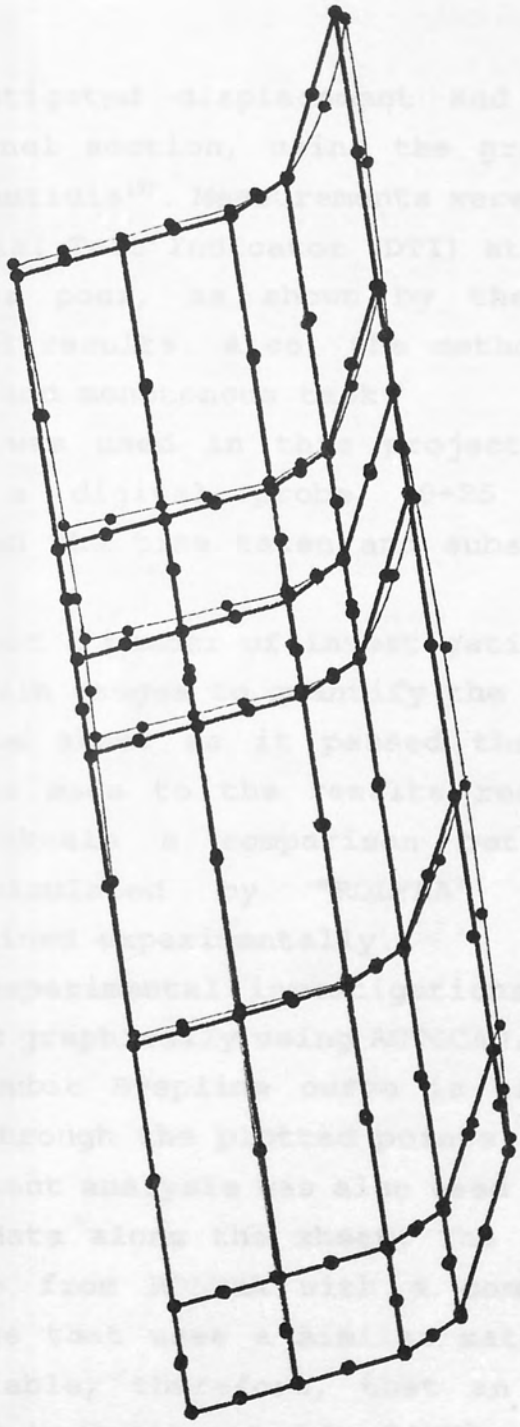

Figure 9.12(b) Deformation of mesh displayed by ROLFEA.

CHAPTER TEN.

RESULTS OF THE EXPERIMENTAL AND THEORETICAL INVESTIGATIONS.

10.1 Introduction.

Panton[11] investigated displacement and residual strain for a simple channel section, using the grid method previously adopted by Sarantidis[5]. Measurements were obtained using a Jig Borer and a Dial Test Indicator (DTI) attachment. However the accuracy was poor, as shown by the scatter obtained from the plotted results. Also, the method was an extremely time-consuming and monotonous task.

The same technique was used in this project but, to improve the accuracy, a digital probe (0-25 mm) was commissioned. This reduced the time taken and substantially improved the accuracy.

Fewtrell[70] carried out a number of investigations using electrical resistance strain gauges to quantify the strain at selected positions on the sheet as it passed through the C.R.F. mill. Reference is made to the results recorded by Fewtrell in order to obtain a comparison between the theoretical strains calculated by "ROLFEA" and the corresponding values obtained experimentally.

The data from the experimental investigations in this project has been displayed graphically using AUTOCAD. A choice between a quadratic or cubic B-spline curve is offered to obtain the "best" curve through the plotted points.

The PAFEC finite element analysis was also used to obtain displacement and strain data along the sheet. The objective was to correlate results from ROLFEA with a commercially available software package that uses a similar mathematical analysis. It was regrettable, therefore, that an elastic-plastic analysis could not be implemented by PAFEC, and there was no other finite element package available during this research programme. The use of PAFEC did contribute some worthwhile information, however, which influenced the choice of finite element and the type of loading used by ROLFEA.

Kiuchi[44] investigated deformation and strain in the cold roll forming of circular tube and Bhattacharyya's[42] mathematical model of the deformation length was based on a simple U-channel section. Generally, the majority of research into cold roll forming has been on a very simple section geometry. Although the cross-section of most C.R.F. products only consists of linear and circular portions, the complexity of the overall geometry still controls the intricate nature of a mathematical analysis. If a simple U-channel section is modelled using finite elements, only half of the section will require analysis, due to symmetry. The important geometrical parameters for a channel reduces to four, the sheet thickness, radius of the bend region, and the flange and base lengths. With the exception of the bend radius, the values of each parameter can easily be adjusted during an experimental test, which is an additional advantage. If a section geometry with a much larger number of geometrical parameters is chosen, mathematical modelling becomes far more demanding. For this reason a simple U-channel section was studied during this research programme.

10.2 Experimental Measurement of Deformation.

The grid method was chosen to assess the residual strains, on the sheet. A pattern of dots were machined onto the flat sheet prior to rolling using a Bridgeport Interact NC milling machine. The dimensions of the pattern are shown in Fig 10.1, and a detailed description of the manufacturing procedure is given by Panton[11].

The flat sheet is fed into the rolling mill and the mill is stopped when its leading edge has passed through the last stage. By removing all the top form-rolls and lifting the sheet from the mill, the forming lengths of each stage will be present. A specimen which has been formed over three stages of the mill is shown diagrammatically in Fig 10.2. After measuring the position of the dots in three dimensions the geometry of the forming lengths can be assessed.

The measuring process was carried out on a Societe Genevoise jig borer (model 2P) which has precision movement of the table in the horizontal plane. Unfortunately, an accurate measurement in the vertical plane is not provided by the jig

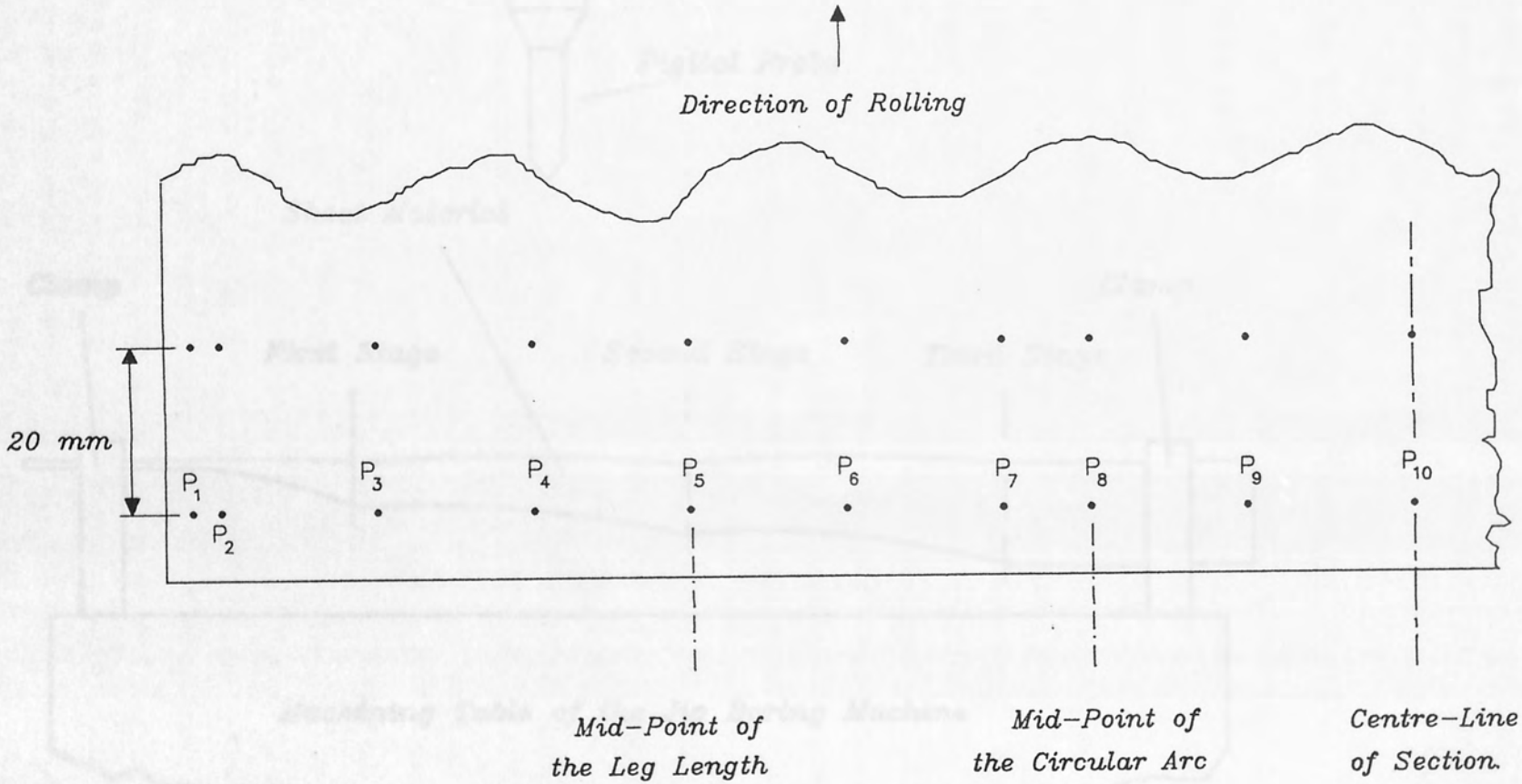

Figure 10.1 *Position of the scribed points.*

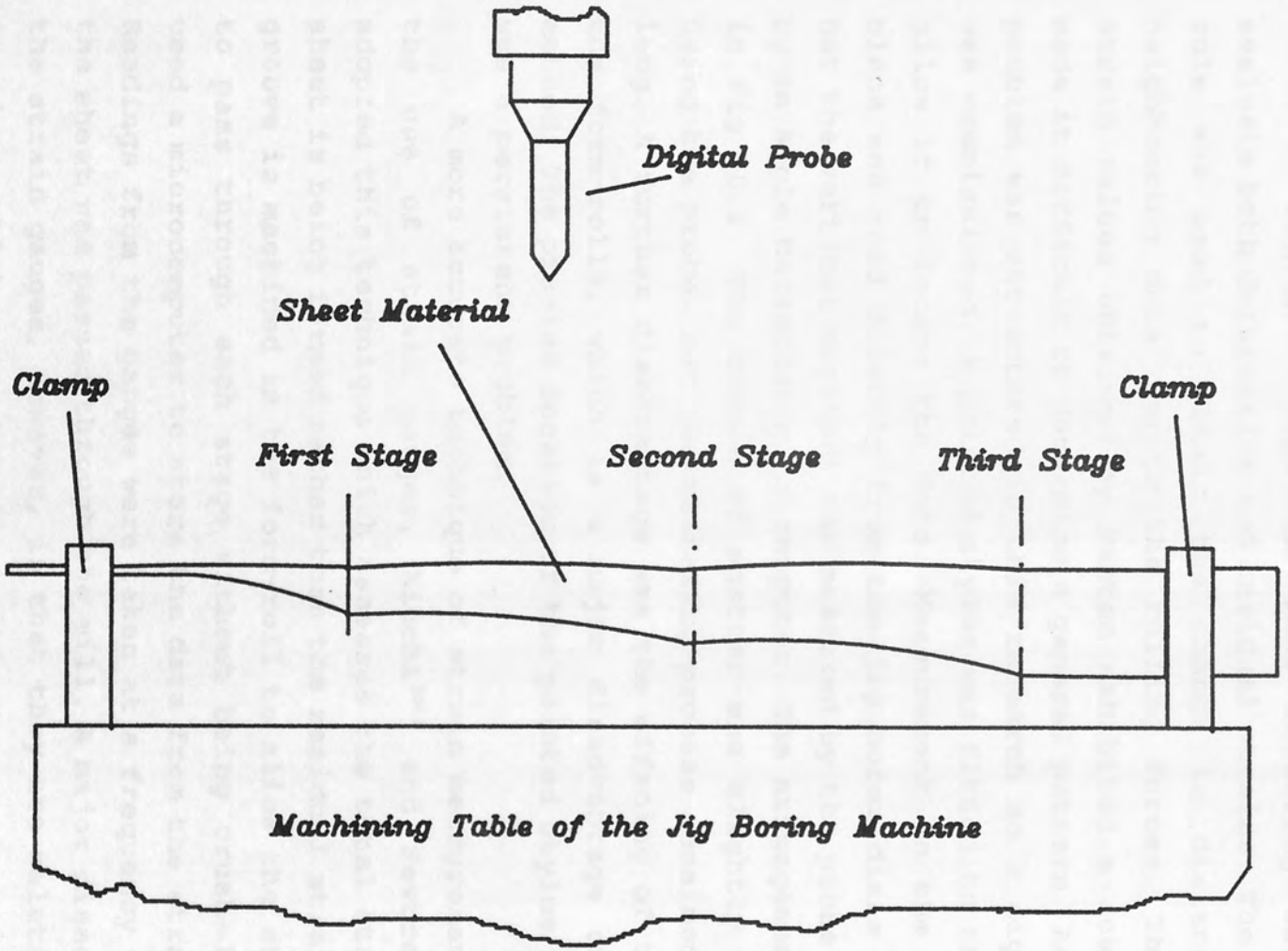

Figure 10.2

Setup for Measuring the Deformation of the Scribed Grid.

borer, so an assembly incorporating a DTI and slip gauges was required. A toolmaker's microscope was bolted to the spindle housing of the jig borer and used to focus on the dots. There position was then recorded by taking readings off the table dials and noting the size of the slip pile. The results suggested that this measuring technique was perfectly adequate for studying deformation, although it was evident that measuring accuracy in the vertical plane was poor.

10.3 Experimental Measurement of Strain.

Panton[11] used the same measuring technique to evaluate both deformation and residual strains. The Pythagoras rule was used to obtain the change in distance between neighbouring dots due to the rolling forces. The residual strain values obtained by Panton exhibited a scatter which made it difficult to determine a general pattern. An identical problem was encountered in this research so a digital probe was commissioned. A pointed stylus was fitted to the probe to allow it to locate the dots. Measurement in the horizontal plane was read directly from the jig borer dials as before, but the vertical movement was measured by the probe and stored by an Apple Macintosh microcomputer. The arrangement is shown in Fig 10.2. The degree of scatter was slightly reduced by using the probe, but the measuring process remained extremely long. A further disadvantage was the effacing of the dots at the form-rolls, which is a major disadvantage of the grid method. The precise location of the pointed stylus in the dots was a persistent problem.

A more accurate technique of strain measurement involves the use of strain gauges. Kiuchi[28] and Fewtrell[70] have adopted this technique which assesses the total strain as the sheet is being formed rather than the residual strain. A small groove is machined in the form-roll to allow the strain gauge to pass through each stage without being crushed. Fewtrell used a microcomputer to store the data from the strain gauges. Readings from the gauges were taken at a frequency of 80 Hz as the sheet was passed through the mill. A major disadvantage of the strain gauges, however, is that they are relatively large in size, which makes it impossible to study strain in the small bend regions. It has been acknowledged by form-roll

designers for many years that the bend regions of a section is of major importance.

10.4 Theoretical deformation and strain simulation.

Version 6.1 of the PAFEC finite element package is capable of implementing an elastic-plastic analysis for a small number of its finite elements. It is most unfortunate, however, that none of the finite elements that can assess an elastic-plastic stress/strain relationship are suitable for modelling the bending of thin sheet metal. Consequently a purely elastic analysis was carried out, which yielded some useful information. The semi-loof shell element first developed by Irons[52] was used because it allows a relatively large degree of out-of-plane bending. In addition, two flat plate elements (PAFEC element numbers 45210 and 44210), which uses a much simpler mathematical analysis, provided a comparison between the different element types.

Certain material parameters must be known before a theoretical analysis can be carried out, therefore a number of simple tensile tests were performed on specimens taken from a CR3 sheet. The stress-strain curve allows Young's Modulus for the material to be calculated and also indicates the approximate yield load in simple tension. This information was used by PAFEC and ROLFEA to simulate the cold roll forming process.

10.5 Deformation using toolmaker's microscope.

The displacement at the edge of the sheet shown in Fig 10.3 confirms that the majority of bending occurs close to the stage, so the forming length is considerably shorter than the mill pitch.

On its approach to the forming length of the first stage the edge of the flat sheet does not remain flat. The gradual bend must be a reaction to the bending in the forming length region and highlights the importance of this phase of the rolling process. The sheet does not have a bend region until it has passed through the first stage. After a bend region has been formed in the sheet, further bending, such as that applied at the second stage in Fig 10.3, is carried out

Specimen A

Flange Length = 50mm Base Length = 35mm Inside Radius = 6mm Thickness = 3mm

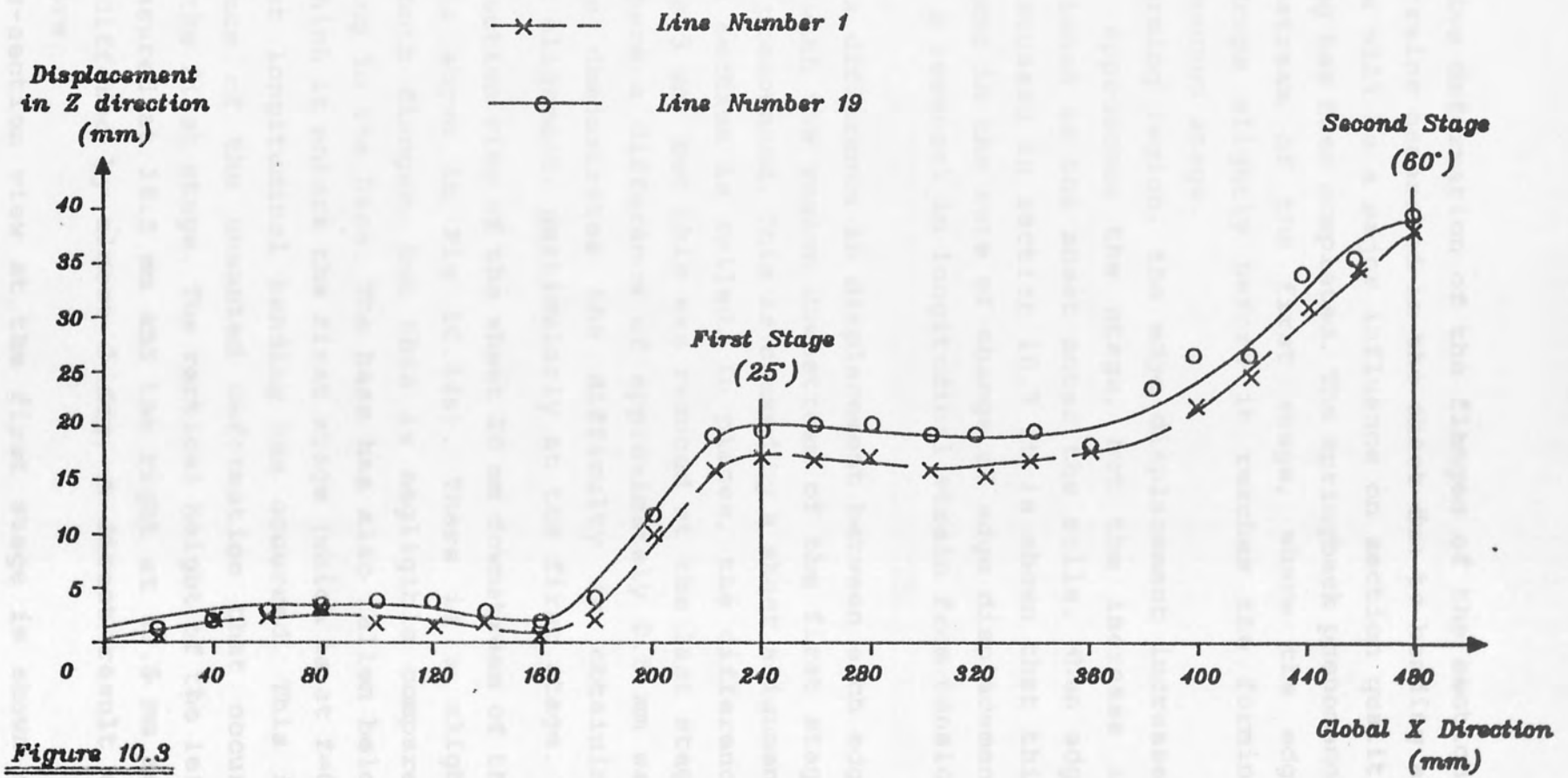

Figure 10.3

Edge displacement of specimen A using the Toolmaker's Microscope.

without extensive deformation of the flanges of the section. The residual strains generated in the sheet due to bending at the first stage will be a major influence on section quality when the rolling has been completed. The springback phenomenon is evident upstream of the first stage, where the edge displacement drops slightly before it reaches the forming length of the second stage.

In the forming region, the edge displacement increases rapidly as it approaches the stage, but the increase is suddenly diminished as the sheet enter the rolls. When edge strains are discussed in section 10.7 it is shown that this sudden adjustment in the rate of change of edge displacement coincides with a reversal in longitudinal strain from tension to compression.

There is a difference in displacement between each edge of the sheet, with the region downstream of the first stage being the most pronounced. This is caused by a sheet alignment error when the section is rolled. In places, the difference was as great as 3 mm, but this was reduced at the last stage of the mill where a difference of approximately 0.5 mm was measured. This demonstrates the difficulty in obtaining accurate sheet alignment, particularly at the first stage.

A cross-section view of the sheet 20 mm downstream of the first stage is shown in Fig 10.4(a). There is a slight curvature in both flanges, but this is negligible compared with the bending in the base. The base has also fallen below the level at which it enters the first stage (which is at Z=0) indicating that longitudinal bending has occurred. This is further evidence of the unwanted deformation that occurs downstream of the first stage. The vertical height of the left flange was measured at 16.5 mm and the right at 19.5 mm and their angles differed by almost 2 deg, a direct result of alignment errors.

The cross-section view at the first stage is shown in Fig 10.4(b). All the linear parts of the section are now relatively straight. The base side has straightened because both top and bottom form-rolls are gripping the sheet in this region. The effect of poor sheet alignment remains since the difference in the flange lengths and their angle are approximately the same as for the cross-section shape 20 mm

Specimen A

Flange Length = 50mm Base Length = 35mm Inside Radius = 6mm

Thickness = 3mm Angle of bend at first stage = 25°

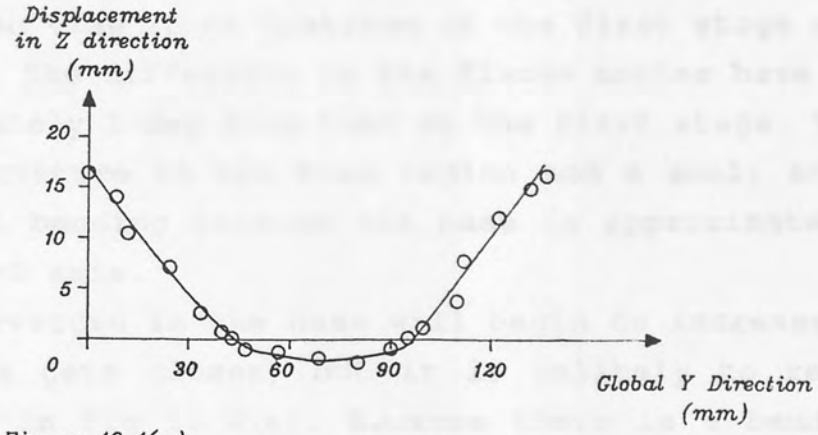

Figure 10.4(a)

Cross-Section shape 20mm downstream from the first stage of specimen A measured using the toolmaker's microscope.

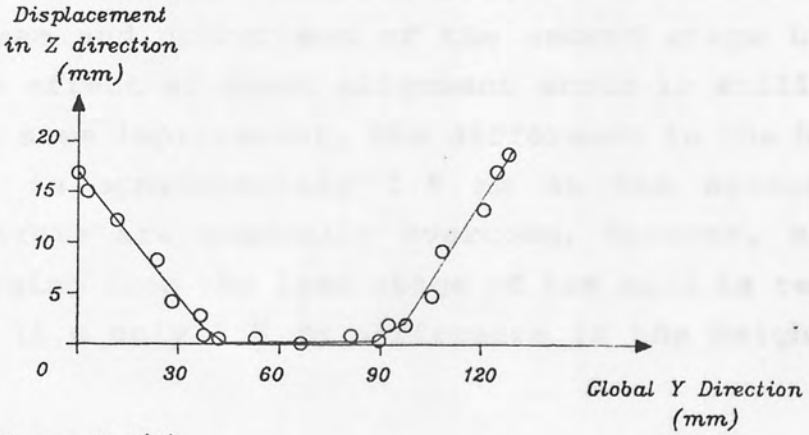

Figure 10.4(b)

Cross-Section shape at the first stage of specimen A measured using the toolmaker's microscope.

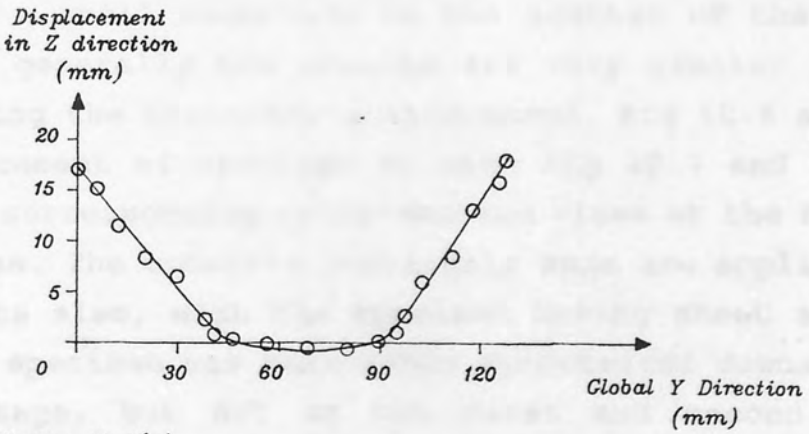

Figure 10.4(c)

Cross-Section shape 20mm upstream from the first stage of specimen A measured using the toolmaker's microscope.

downstream.

Only a small amount of springback is evident from the cross-section view 20 mm upstream of the first stage shown in Fig 10.4(c). The difference in the flange angles have changed by approximately 1 deg from that at the first stage. There is a slight curvature in the base region and a small amount of longitudinal bending because the base is approximately 1 mm below the Z=0 axis.

The curvature in the base will begin to increase as the second stage gets closer, but it is unlikely to reach the value shown in Fig 10.4(a). Because there is a bend region present, the flanges and base are not subject to the severe bending that occurs downstream of the first stage. Confirmation of this is shown in Fig 10.5(a), Fig 10.5(b) and Fig 10.5(c) where cross-section views at the second stage and 20 mm upstream and downstream of the second stage have been plotted. The effect of sheet alignment error is still present but there is some improvement, the difference in the height of the flanges is approximately 1.5 mm at the second stage. Alignment errors are gradually overcome, however, since the section emerging from the last stage of the mill is reasonably symmetrical (i.e only 0.5 mm difference in the height of the flanges).

10.6 Deformation using the probe.

Two different channel sections are investigated using the probe. The improvement in the measuring process resulted in a small reduction in the scatter of the plotted values, but generally the results are very similar to those obtained using the toolmaker's microscope. Fig 10.6 shows the edge displacement of specimen A, with Fig 10.7 and Fig 10.8 showing the corresponding cross-section views at the first and second stages. The comments previously made are applicable to these results also, with the specimen having sheet alignment errors. The specimen was reasonably symmetrical downstream of the last stage, but not at the first and second stages. Fig 10.9 shows the edge displacement of specimen B, since the flange length at the third stage of the section was 60 deg it allowed the cross-section view and edge displacement at the final stage to be recorded. The edge deformation in Fig 10.9

Specimen A

Flange Length = 50mm Base Length = 35mm Inside Radius = 6mm

Thickness = 3mm Angle Of Bend For Second Stage = 60°

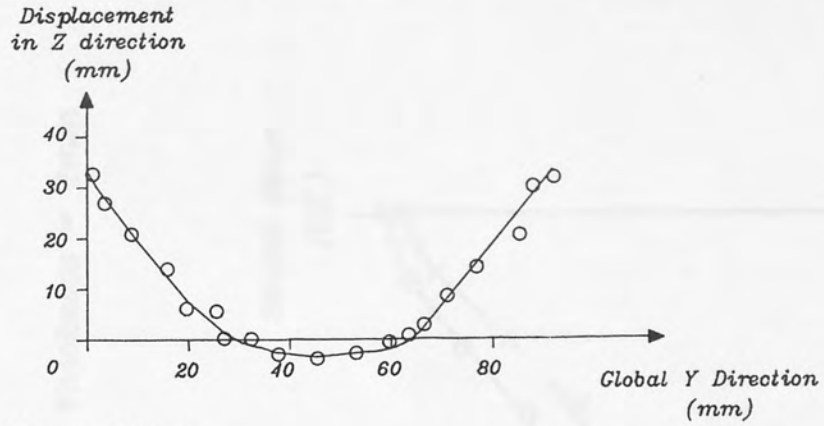

Figure 10.5(a)

Cross-Section shape 20mm downstream from the second stage of specimen A measured using the Toolmaker's Microscope.

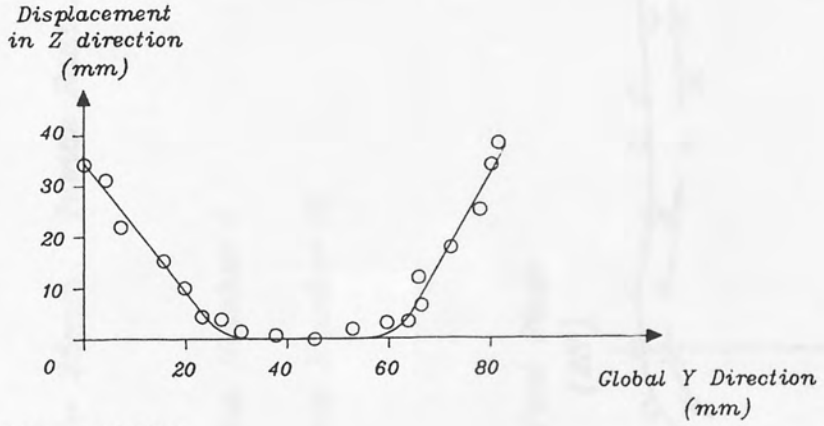

Figure 10.5(b)

Cross-Section shape at the second stage of specimen A measured using the Toolmaker's Microscope.

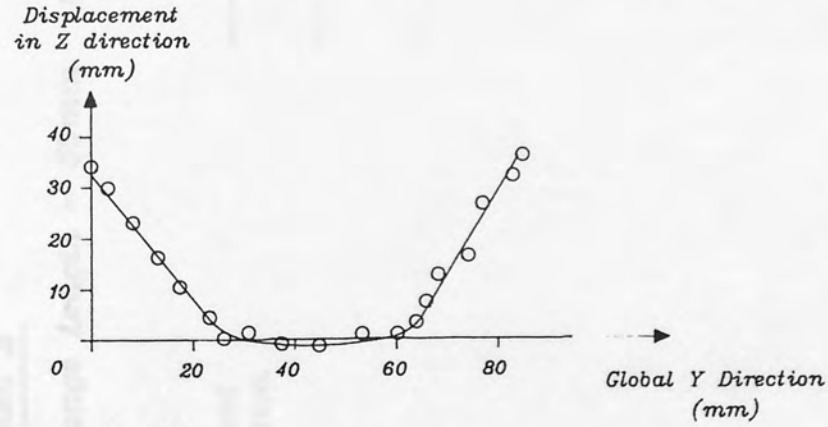

Figure 10.5(c)

Cross-Section shape 20mm upstream from the second stage of specimen A measured using the Toolmaker's Microscope.

Specimen A

Flange Length = 50mm Base Length = 35mm Inside Radius = 6mm Thickness = 3mm

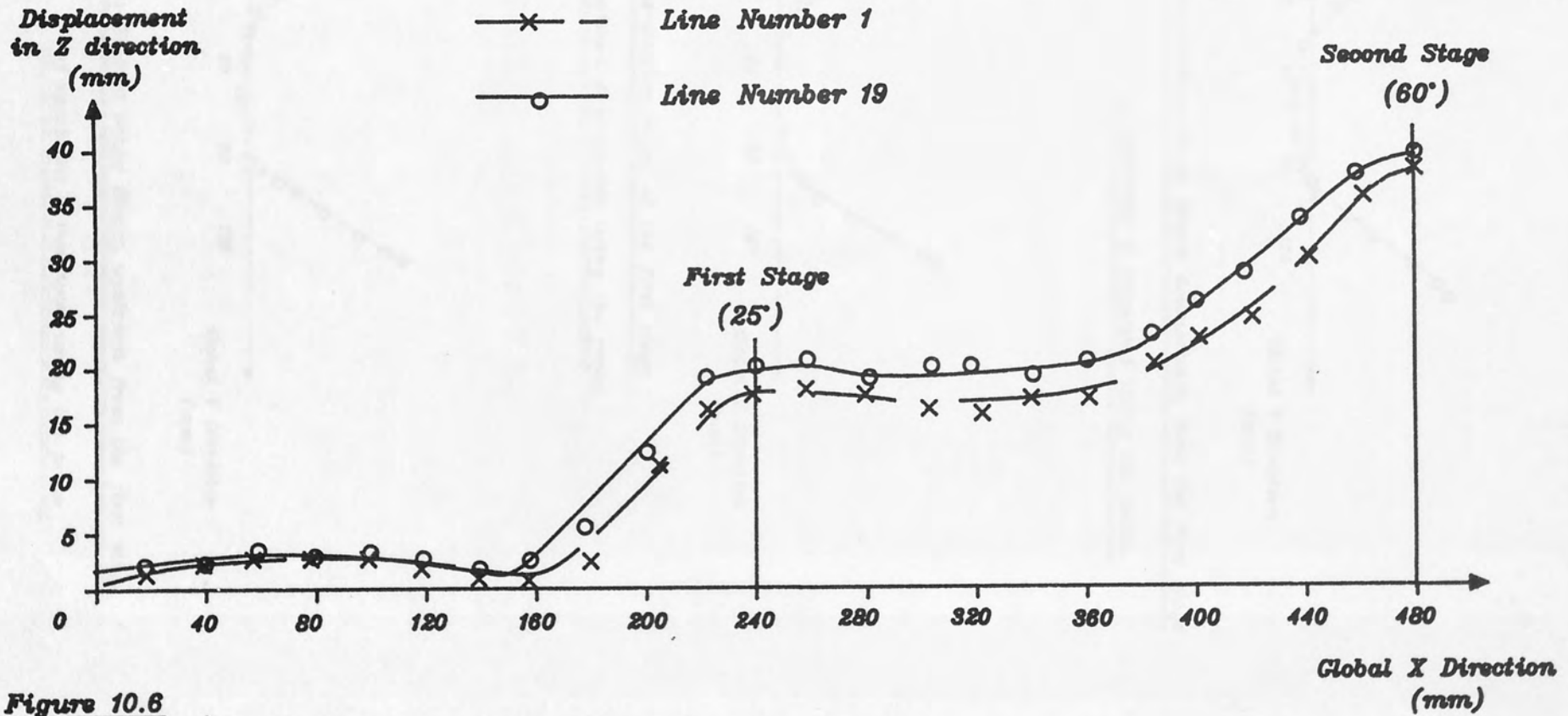

Figure 10.6

Edge displacement of specimen A using the probe.

Specimen A

Flange Length = 50mm Base Length = 35mm Inside Radius = 6mm

Thickness = 3mm Angle of bend at first stage = 25°

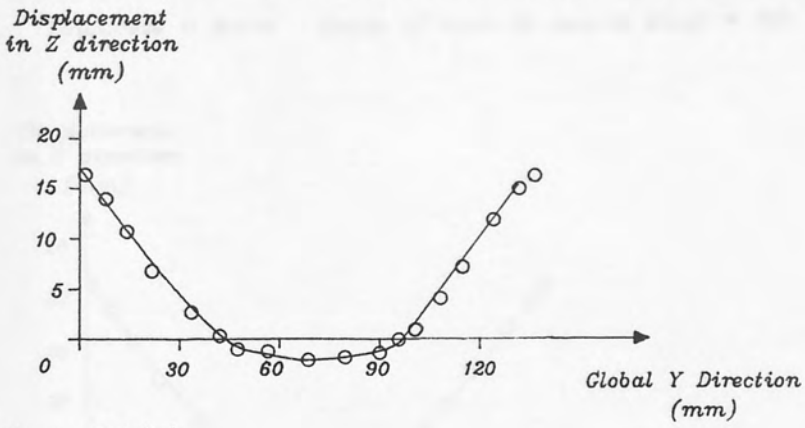

Figure 10.7(a)

Cross-Section shape 20mm downstream from the first stage of specimen A measured using the probe.

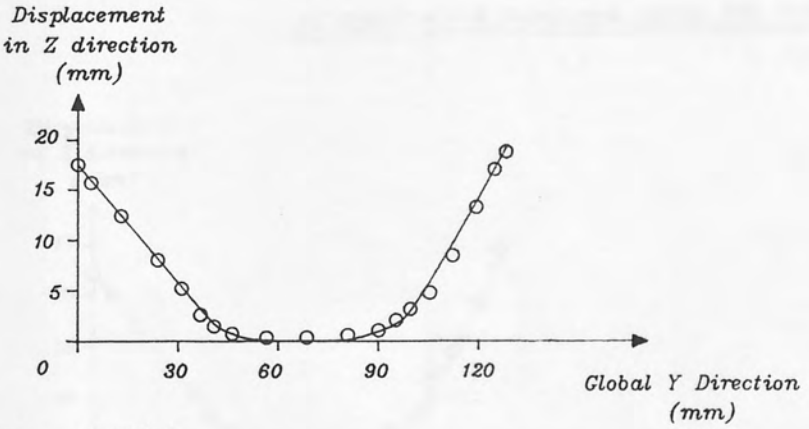

Figure 10.7(b)

Cross-Section shape at the first stage of specimen A measured using the probe.

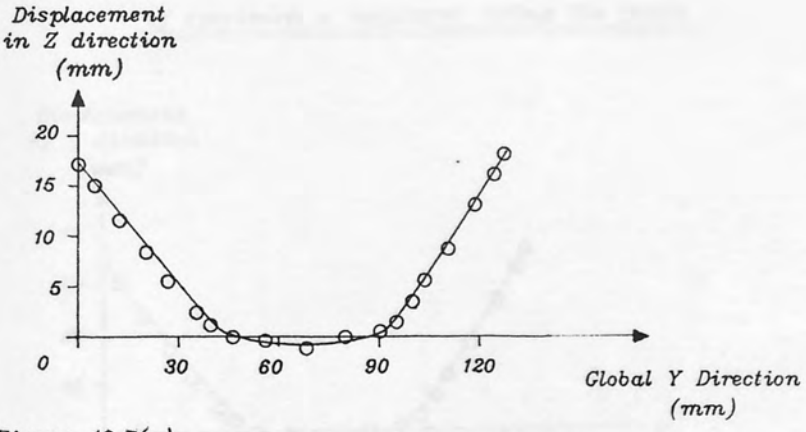

Figure 10.7(c)

Cross-Section shape 20mm upstream from the first stage of specimen A measured using the probe.

Specimen A

Flange Length = 50mm Base Length = 35mm Inside Radius = 6mm

Thickness = 3mm Angle of bend at second stage = 60°

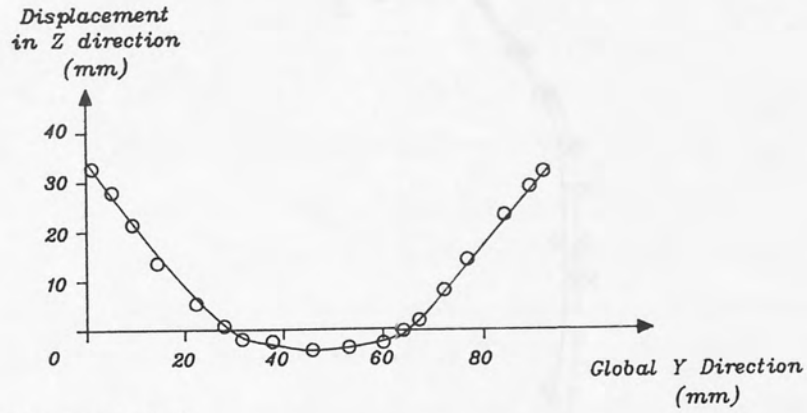

Figure 10.8(a)

Cross-Section shape 20mm downstream from the second stage of specimen A measured using the probe.

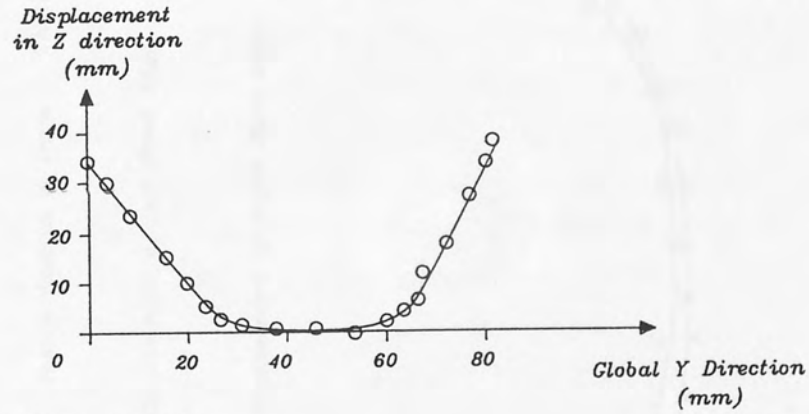

Figure 10.8(b)

Cross-Section shape at the second stage of specimen A measured using the probe.

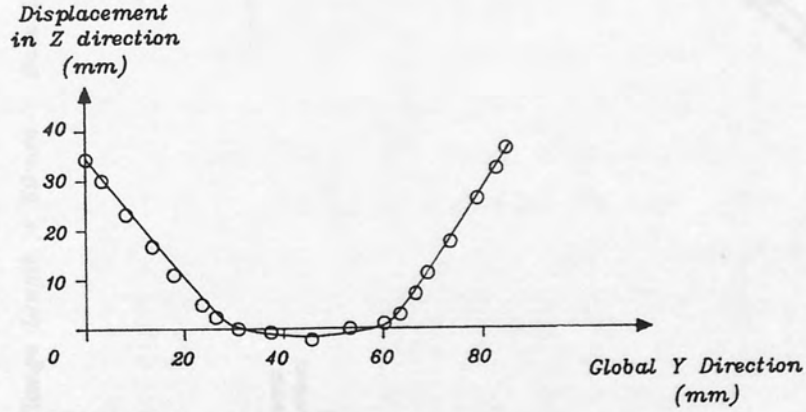

Figure 10.8(c)

Cross-Section shape 20mm upstream from the second stage of specimen A measured using the probe.

Specimen B

Flange Length = 50mm Base Length = 40mm Inside Radius = 1mm Thickness = 1.5mm

Displacement of Left Hand Edge.

Displacement of Right Hand Edge.

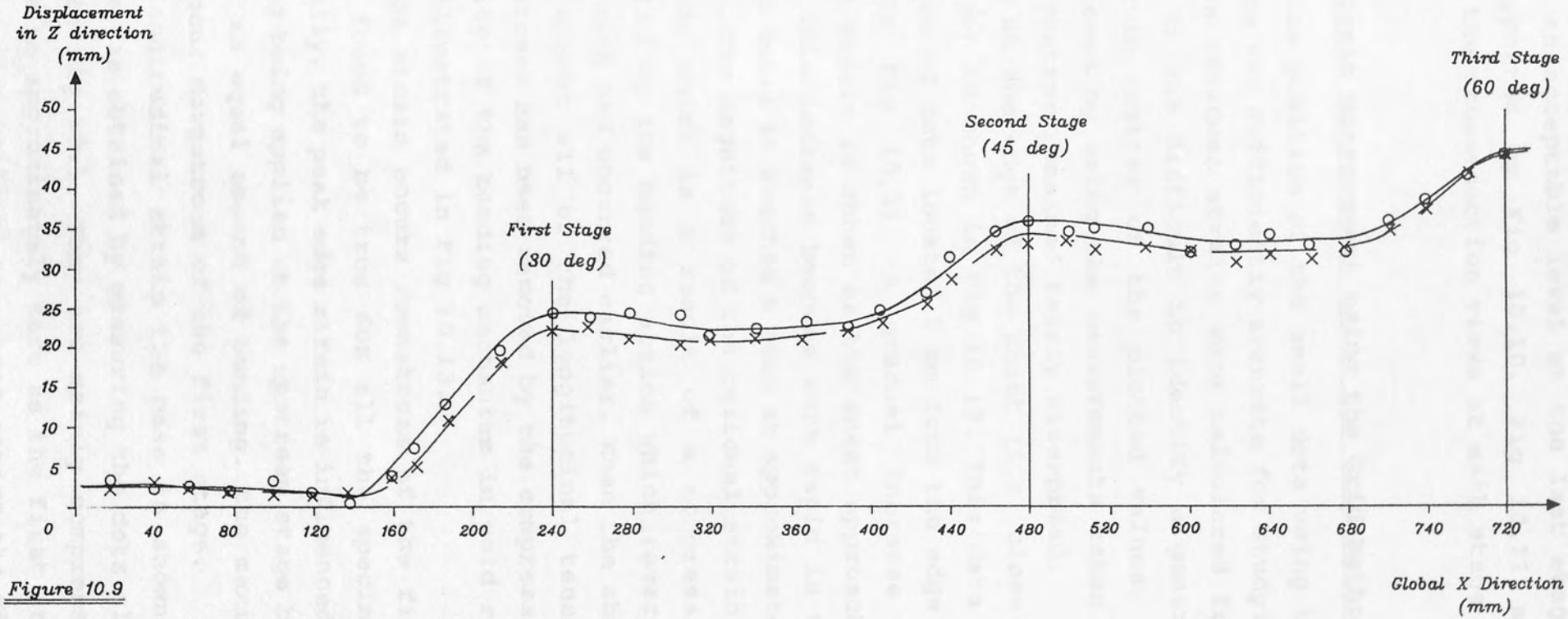

Figure 10.9

Edge displacement of specimen B using the probe.

clearly shows how the non-alignment error of the section is gradually reduced to an acceptable level at the last stage. This is further supported by Fig 10.10, Fig 10.11 and Fig 10.12 which show the cross-section views at each stage of specimen B.

10.7 Residual Strain measurement using the Grid Method.

Measuring the position of the small dots using the toolmaker's microscope was sufficiently accurate for studying deformation. When the residual strains were calculated from this data, however, it was difficult to identify a general pattern due to a wide scatter of the plotted values. An improvement was achieved by using the measurements taken by the probe, although scatter remained fairly widespread.

Residual strain at the edge of the sheet (i.e. close to the top of the flange) is shown in Fig 10.13. This data is obtained from the line of dots located 2 mm from the edge of the sheet (refer to Fig 10.1). A gradual increase in longitudinal tensile strain is shown as the sheet approaches the upstream stage. This increase becomes more rapid in the forming length region until it reaches a peak at approximately 40 mm from the stage. The magnitude of the residual strain is then rapidly reduced, which is a result of a compressive strain being generated by the bending action which reverses the tensile strain which had occurred earlier. When the sheet reaches the stage, almost all of the longitudinal tensile strain created downstream has been removed by the compressive forces. The complexity of the bending mechanism in cold roll forming is clearly illustrated in Fig 10.13.

The largest edge strain occurs downstream of the first stage and this was found to be true for all the specimens investigated. Generally, the peak edge strain is influenced by the amount of bending being applied at the upstream stage but, if all stages apply an equal amount of bending, the maximum edge strains will occur downstream of the first stage.

The residual longitudinal strain the base is shown in Fig 10.14. This data was obtained by measuring the dots along the line number 7 in Fig 10.1. They are mainly compressive strains which reduce to approximately zero as the first stage is approached but increase again as the sheet enters the first

Specimen B

Flange Length = 50mm Base Length = 40mm Inside Radius = 1mm

Thickness = 1.5mm Angle of bend at first stage = 30°

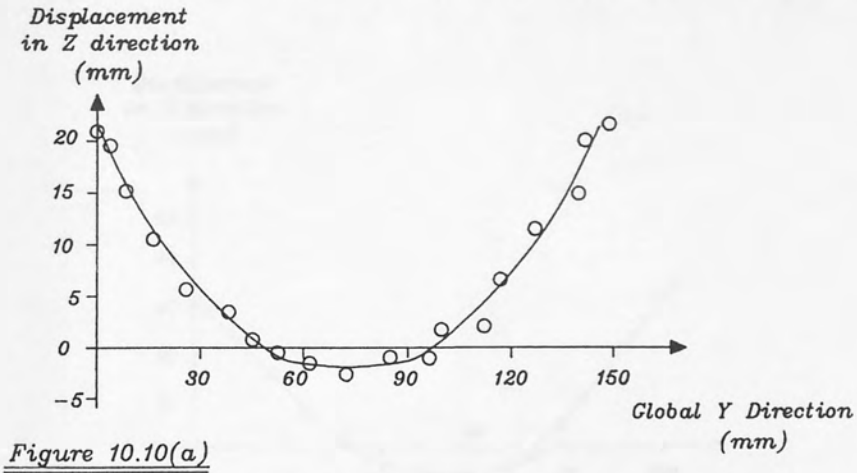

Figure 10.10(a)

Cross-Section shape 20mm downstream from the first stage of specimen B measured using the probe

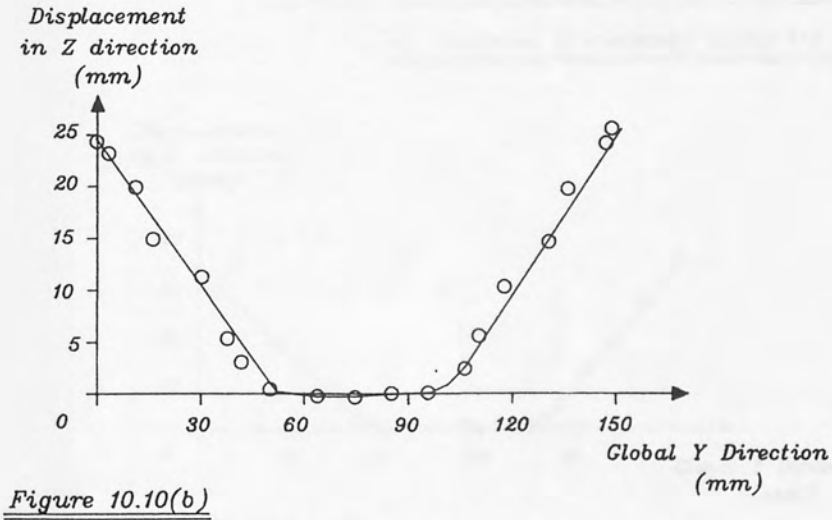

Figure 10.10(b)

Cross-Section shape at the first stage of specimen B measured using the probe

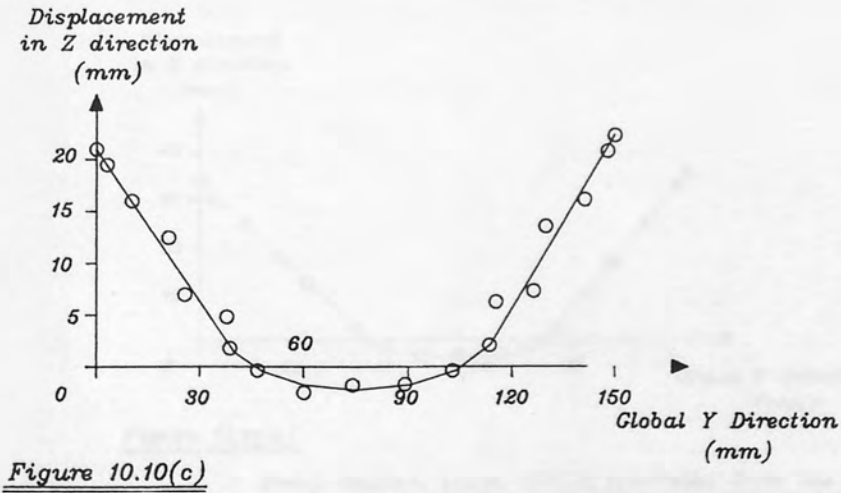

Figure 10.10(c)

Cross-Section shape 20mm upstream from the first stage of specimen B measured using the probe

Specimen B

Flange Length = 50mm Base Length = 40mm Inside Radius = 1mm

Thickness = 1.5mm Angle of bend for the second stage = 45°

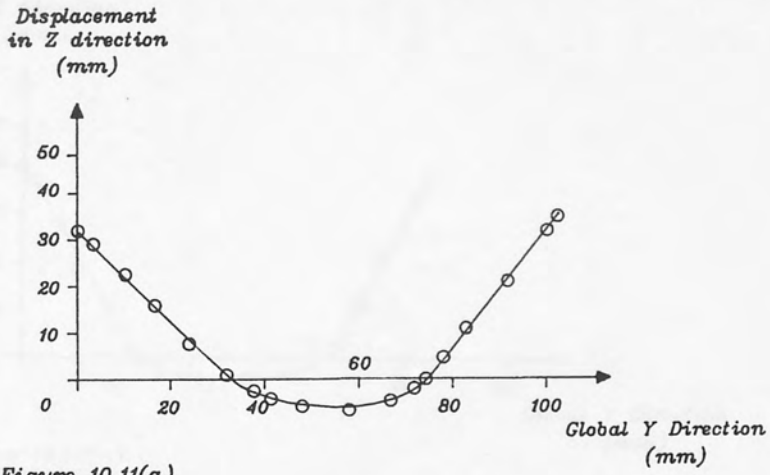

Figure 10.11(a)

Cross-Section shape 20mm downstream from the second stage of specimen B measured using the probe.

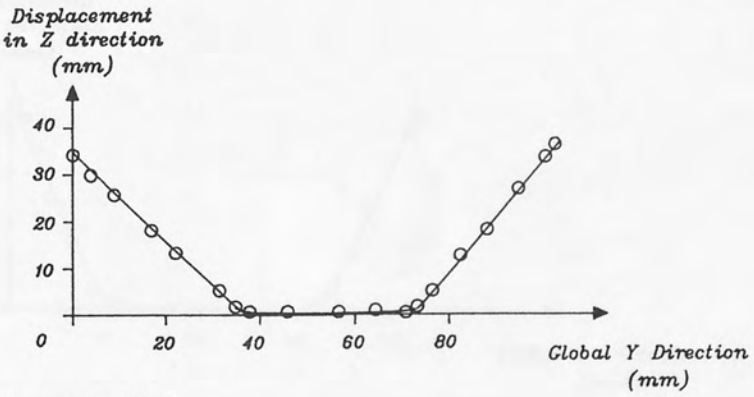

Figure 10.11(b)

Cross-Section shape at the second stage of specimen B measured using the probe.

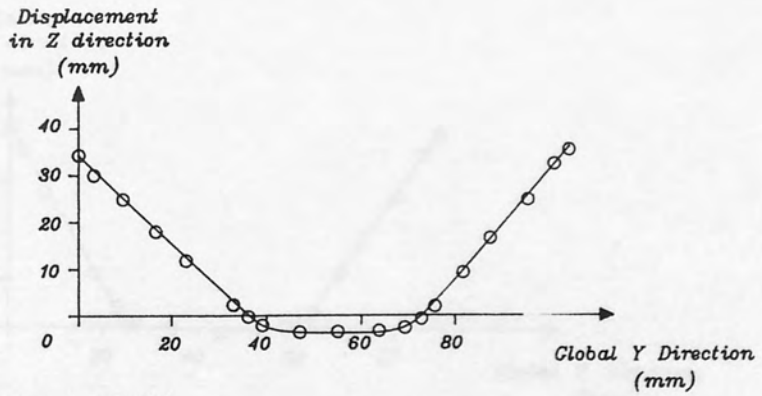

Figure 10.11(c)

Cross-Section shape 20mm upstream from the second stage of specimen B measured using the probe.

Specimen B

Flange Length = 50mm Base Length = 40mm Inside Radius = 1mm

Thickness = 1.5mm Angle of bend for the third stage = 60°

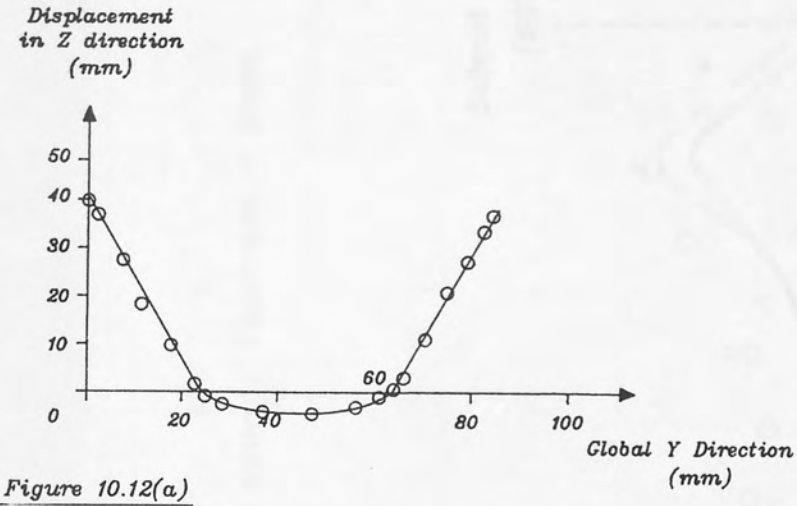

Figure 10.12(a)

Cross-Section shape 20mm downstream from the third stage of specimen B measured using the probe.

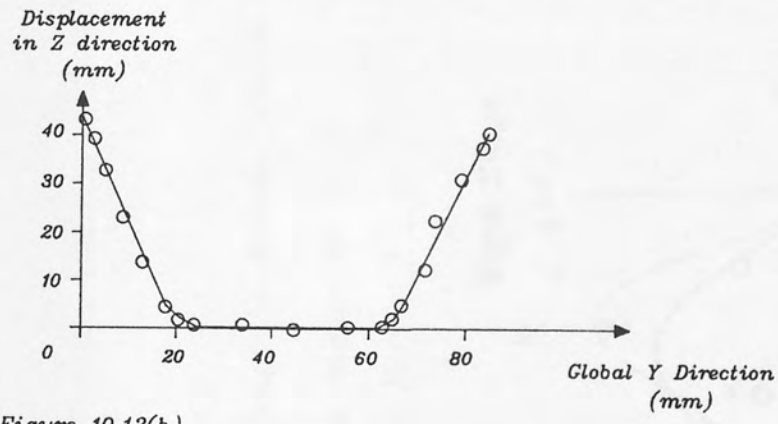

Figure 10.12(b)

Cross-Section shape at the third stage of specimen B measured using the probe.

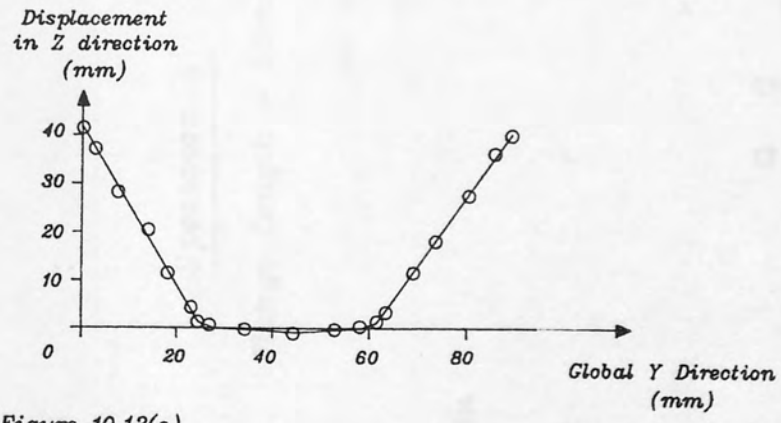

Figure 10.12(c)

Cross-Section shape 20mm upstream from the third stage of specimen B measured using the probe.

Specimen A

Flange Length = 50mm Base Length = 35mm Inside Radius = 6mm Thickness = 3mm

— x — Line Number 19

—o— Line Number 1

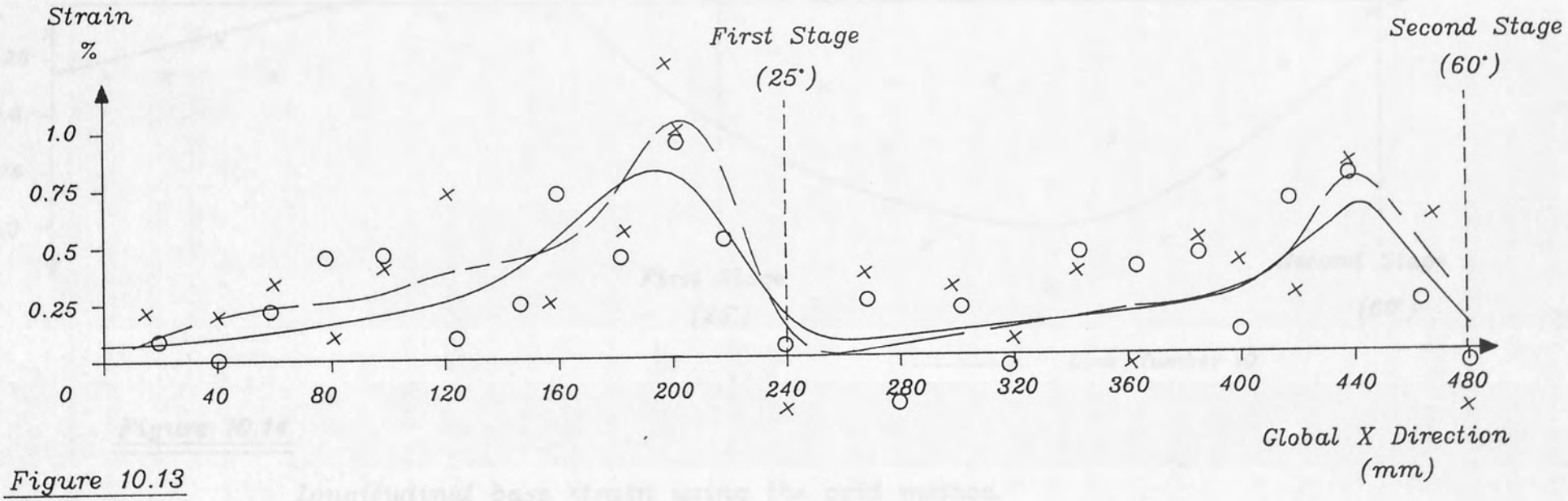

Figure 10.13

Longitudinal edge strains using the grid method.

Specimen A

Flange Length = 50mm Base Length = 35mm Inside Radius = 6mm Thickness = 3mm

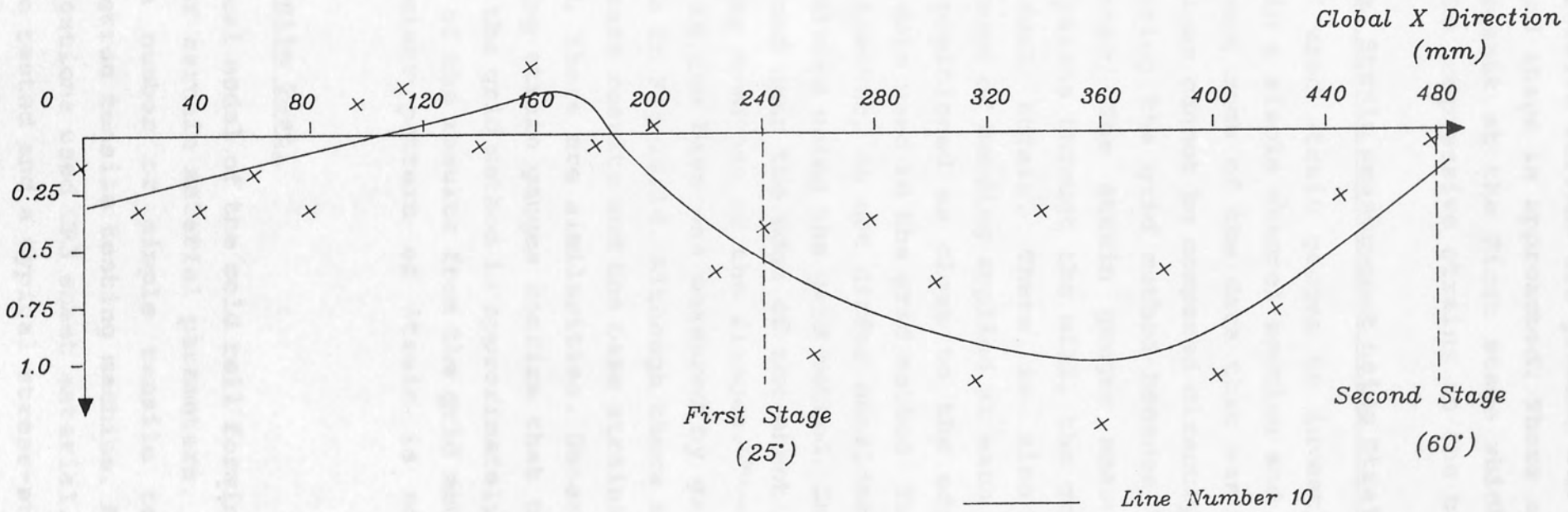

Figure 10.14

Longitudinal base strain using the grid method.

stage. A different pattern occurs downstream of the second stage where the compressive strains are greater but gradually diminish as the second stage is approached. There appears to be tensile forces present at the first stage which has the effect of reducing the compressive strains in the base.

10.8 Longitudinal Strain measurement using Strain Gauges.

Fewtrell[70] used strain gauges to investigate the longitudinal strain in a simple channel section and Fig 10.15 and Fig 10.16 represent some of the data that was recorded. Individual strain values cannot be compared directly with the strains calculated using the grid method because there are fundamental differences. The strain gauges measure total strain as the sheet passes through the mill, the grid method assesses only residual strain. There is also a small difference in the amount of bending applied at each stage and the gauges are not positioned as close to the edge of the sheet as the line of dots used in the grid method. The results shown in Fig 10.15, however, do not differ considerably from the edge strain calculated using the grid method. Gauge 1 and gauge 4 were positioned near the edge of the sheet and gauge 2 was located half way down one of the flanges.[70] Longitudinal strain in the base was measured by gauge 3 and the results are shown in Fig 10.16. Although there is a clear difference between these results and the base strains obtained from the grid method, there are similarities. Generally, the results obtained using strain gauges confirm that the strain pattern suggested by the grid method is approximately correct. However, the scatter of the results from the grid method is so widespread that a clear pattern of strain is not easily established.

10.9 Simple Tensile Test.

A theoretical model of the cold roll forming process requires the value of certain material parameters. To obtain this information, a number of simple tensile tests were performed using a Instron tensile testing machine. All of the experimental investigations used CR3 sheet material. A number of CR3 specimens were tested and a typical stress-strain plot

Specimen B

Flange Length = 50mm Base Length = 40mm Inside Radius = 1mm Thickness = 1.5mm

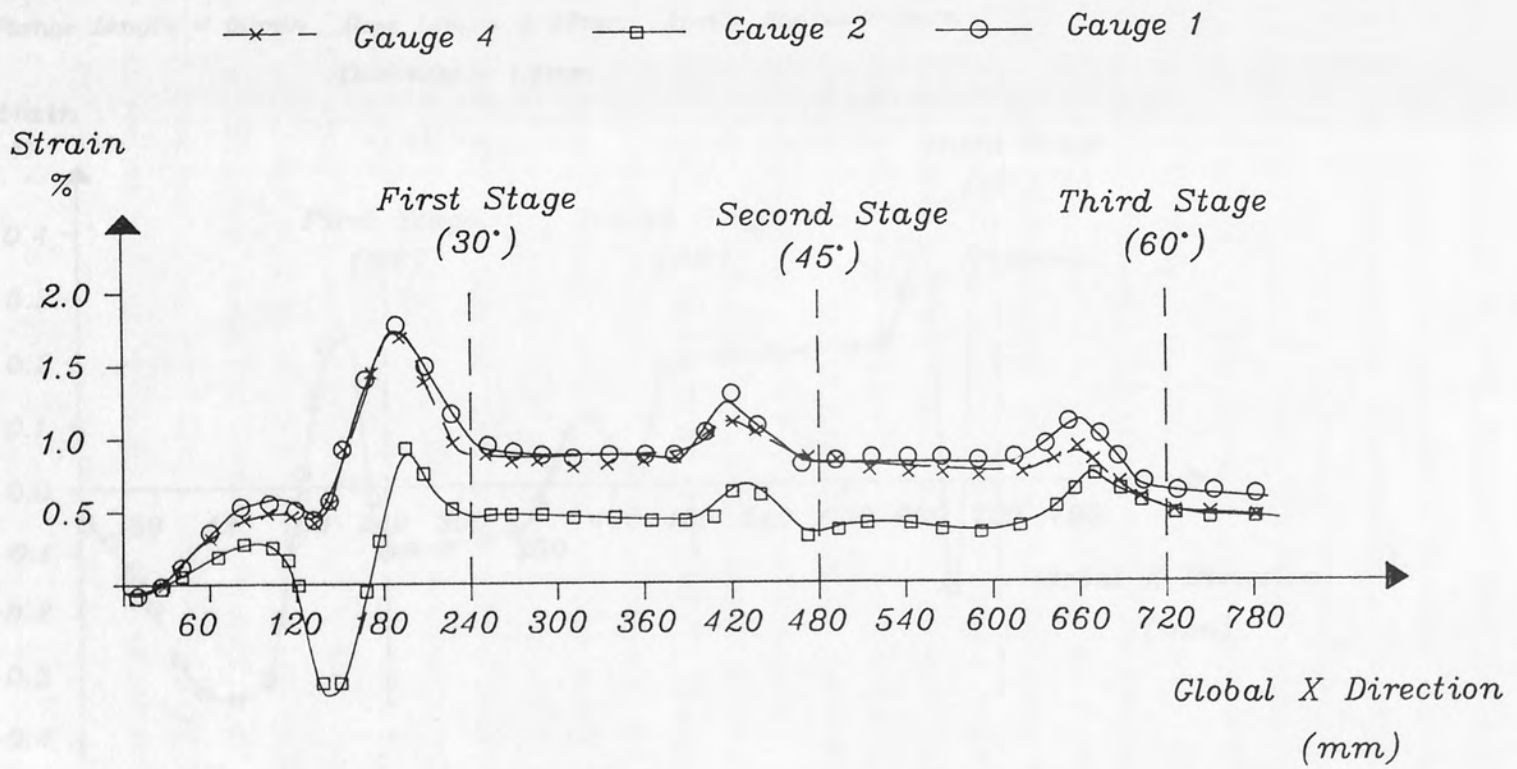

Figure 10.15

Longitudinal strains in the flange measured using strain gauges.

Specimen B

Flange Length = 50mm Base Length = 40mm Inside Radius = 1mm

Thickness = 1.5mm

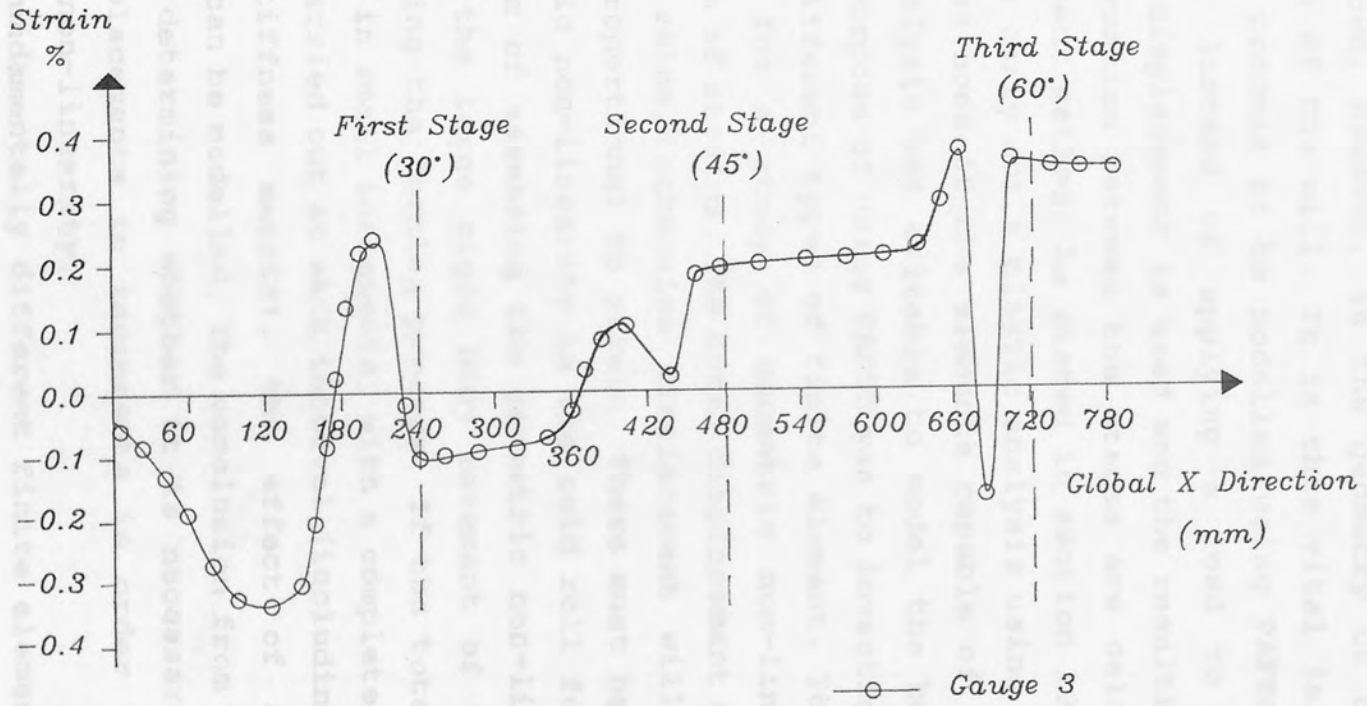

Figure 10.16

Longitudinal base strain measured using strain gauges.

is shown in Fig 10.17. From this information a value for Young's Modulus, the Tangential Modulus and an approximation of the yield load was obtained. The general pattern of the stress-strain graph suggests that the sheet material can be compared to an idealised elastic-plastic material, although not all the specimens tested fully supported this description.

10.10 Deformation and strain calculations using PAFEC.

Initially the bending forces acting on the sheet during the rolling process are unknown. An important parameter that is known, however, is the geometry of the section at every stage of the mill. It is this vital information that allows the process to be modelled using PAFEC without much difficulty. Instead of applying a load to the sheet, a prescribed displacement is used and the resulting strains and sheet deformation between the stages are calculated by the finite element method. As stated in section 10.1, it was not possible to carry out a plastic analysis using PAFEC (version 6.1) because none of the elements capable of carrying out a plastic analysis was suitable to model the bending of thin sheet The purpose of using PAFEC was to investigate the effect of using different types of finite element. It also provided the basis for a study of geometric non-linearity in the calculation of strains. The total displacement must not exceed a certain value, otherwise displacement will no longer be directly proportional to strain. There must be a possibility of geometric non-linearity in the cold roll forming process. The problem of assessing the geometric non-linearity is not helped by the large rigid body movement of the sheet that occurs during the forming process. If the total displacement is applied in small increments, with a complete finite element analysis carried out at each interval (including an adjustment of the stiffness matrix), the effect of geometric non-linearity can be modelled. The conclusion from the study would assist in determining whether it is necessary to apply the total displacements in increments in order to account for geometric non-linearity.

Two fundamentally different finite elements were in the PAFEC simulation. A shell element which implements a highly complex analysis was compared with the much simpler

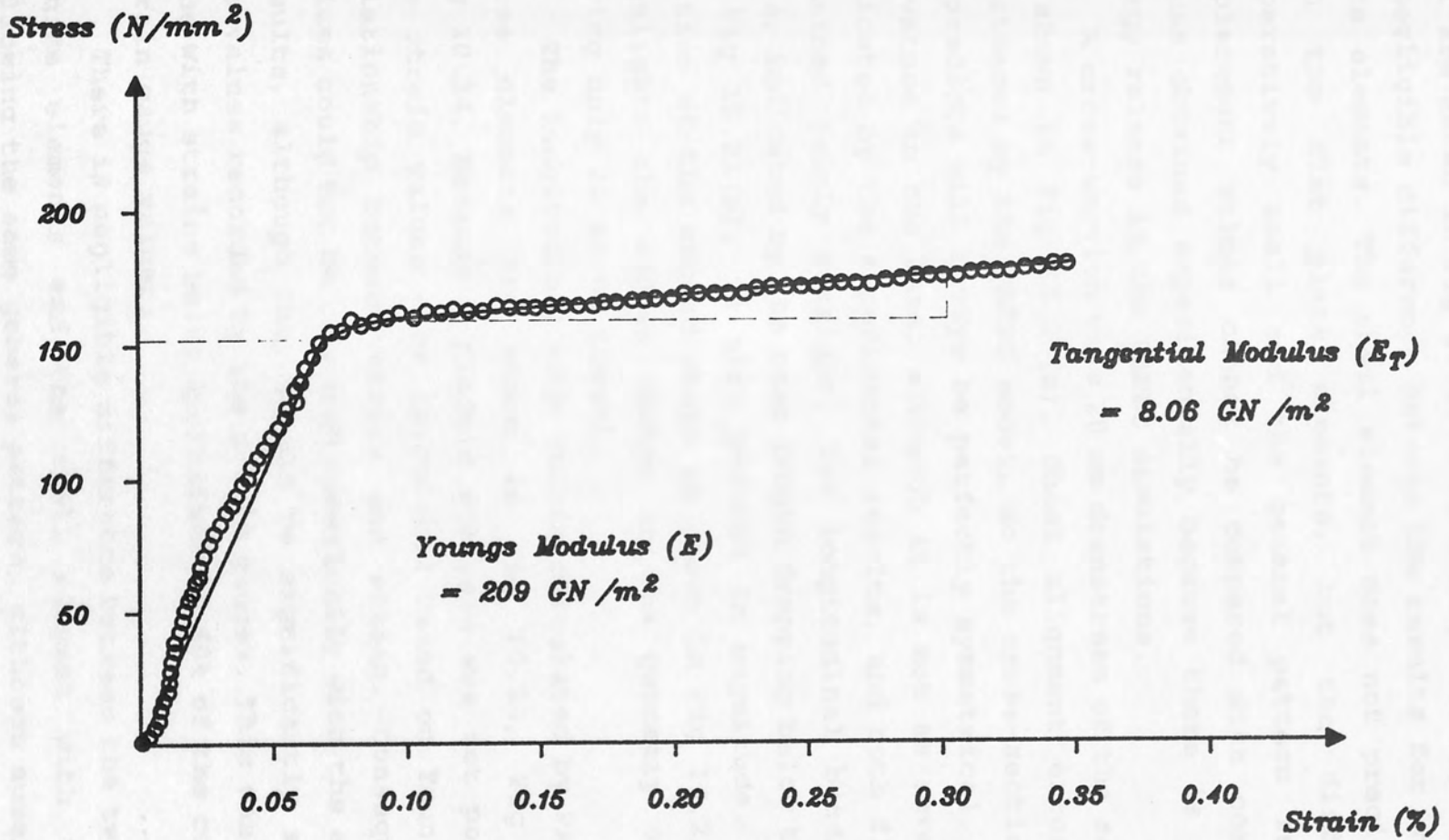

Figure 10.17

Stress – Strain Graph for CR3.

mathematical model that results from using flat plate elements. The 45210 flat plate element will assess shear deformation but the 44210 assumes that all shear forces are negligible. Both elements were used in the investigation.

The edge deformation over the first three stages of the mill are shown in Fig 10.18, Fig 10.19, and Fig 10.20. There is negligible difference between the results for the two flat plate elements. The shell element does not precisely agree with the flat plate elements, but the difference is comparatively small and the general pattern is similar. Displacement values cannot be compared with corresponding values obtained experimentally because there is no elastic energy release in the PAFEC simulations.

A cross-section view 20 mm downstream of the second stage is shown in Fig 10.21(a). Sheet alignment errors are not considered by the PAFEC model, so the cross-section geometry it predicts will always be perfectly symmetrical. There is a curvature in the base, although it is not as severe as that indicated by the experimental results, and both flanges have remained fairly straight. The longitudinal bending in the base, indicated by the base length dropping below the z=0 axis in Fig 10.21(a), is also reduced in magnitude. The cross-section at the second stage is shown in Fig 10.21(b), which highlights the sudden change in the geometry of the base during only 20 mm of travel.

The longitudinal edge strain calculated by PAFEC for the three elements are shown in Fig 10.22, Fig 10.23 and Fig 10.24. Because a plastic analysis was not possible, all the strain values were calculated based on Young's Modulus relationship between stress and strain. Consequently, the values could not be compared numerically with the experimental results, although they should be significantly smaller than the values recorded by the strain gauges. This was found to be true with strains being approximately 60% of the corresponding strain gauge values.

There is negligible difference between the two flat plate finite elements and the shell element with the results following the same general pattern, although numerically they are slightly greater in value.

Specimen B

Flange Length = 50mm Base Length = 40mm Inside Radius = 1mm Thickness = 1.5mm

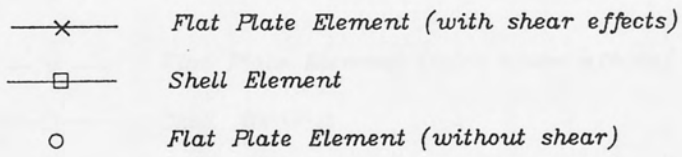

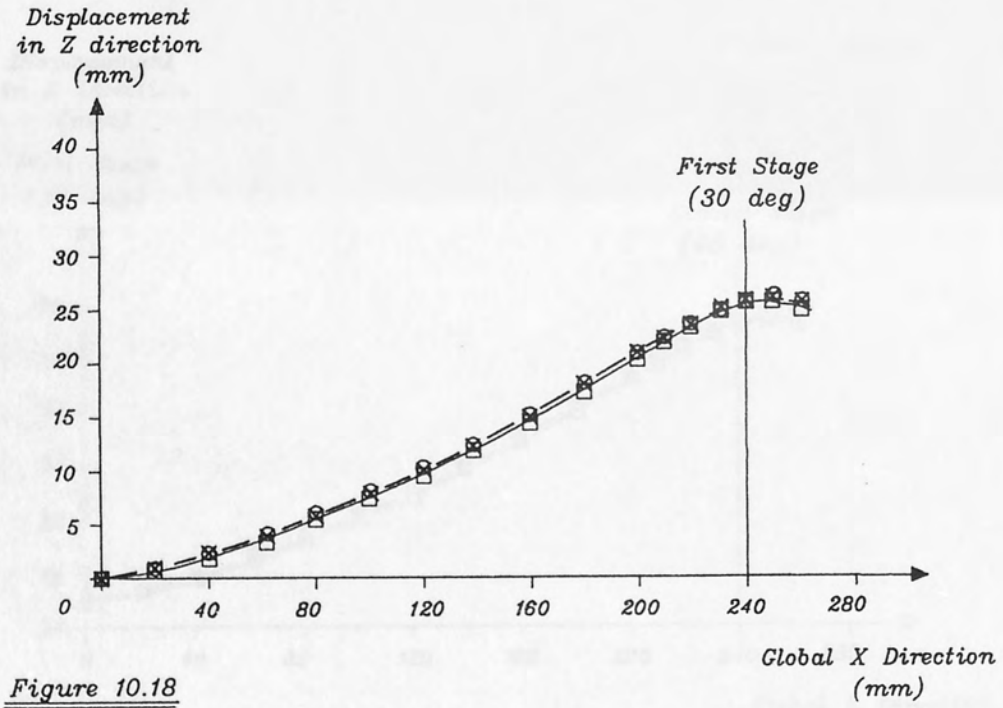

Figure 10.18

Edge displacement downstream of the first stage using three different PAFEC elements.

Specimen B

Flange Length = 50mm Base Length = 40mm Inside Radius = 1mm Thickness = 1.5mm

— × — *Flat Plate Element (with shear effects)*

—□— *Shell Element*

○ *Flat Plate Element (without shear)*

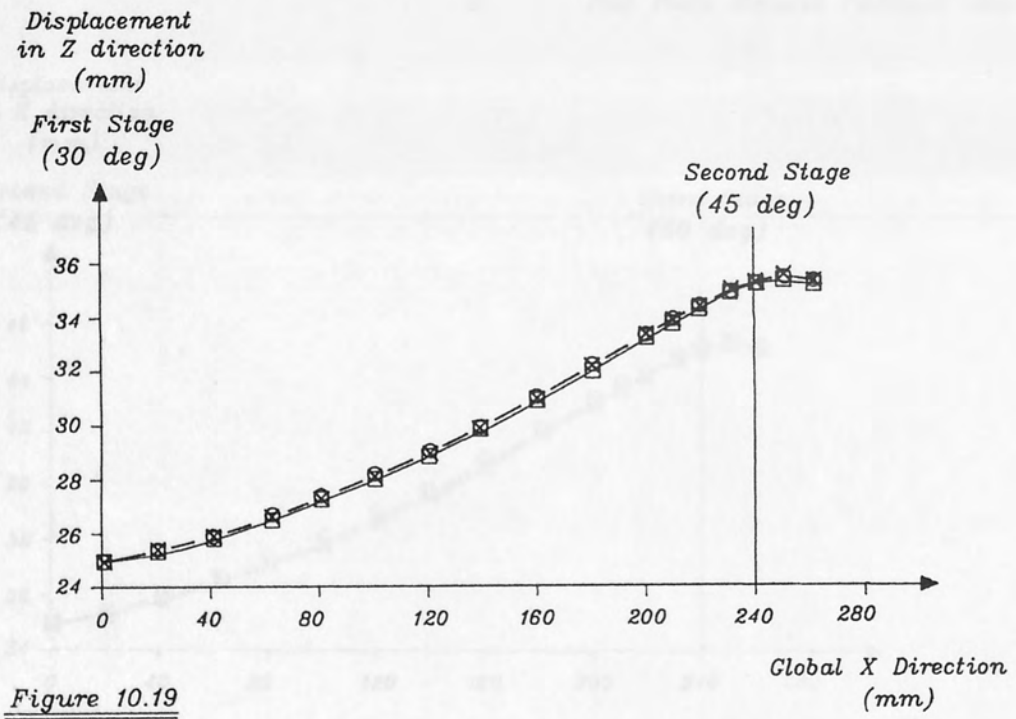

Figure 10.19

Edge displacement downstream of the second stage using three different PAFEC elements.

Specimen B

Flange Length = 50mm Base Length = 40mm Inside Radius = 1mm Thickness = 1.5mm

— × — Flat Plate Element (with shear effects)

—□— Shell Element

○ Flat Plate Element (without shear)

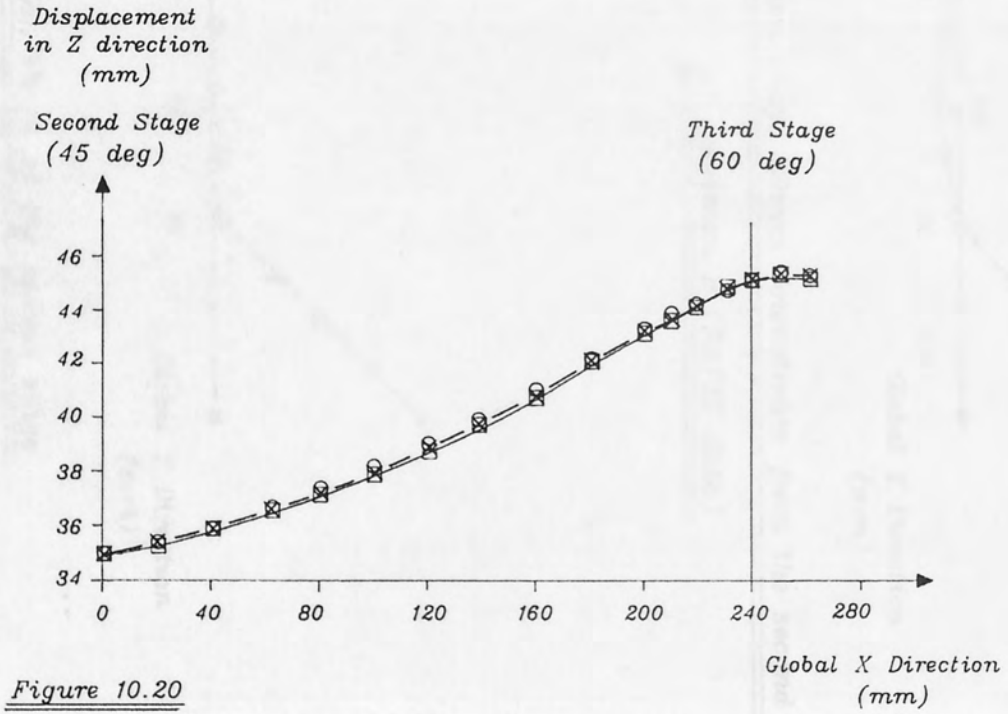

Figure 10.20

Edge displacement downstream of third stage using three different PAFEC elements.

Specimen B

Flange Length = 50mm Base Length = 40mm Inside Radius = 1mm

Thickness = 1.5mm Angle of bend for the second stage = 45°

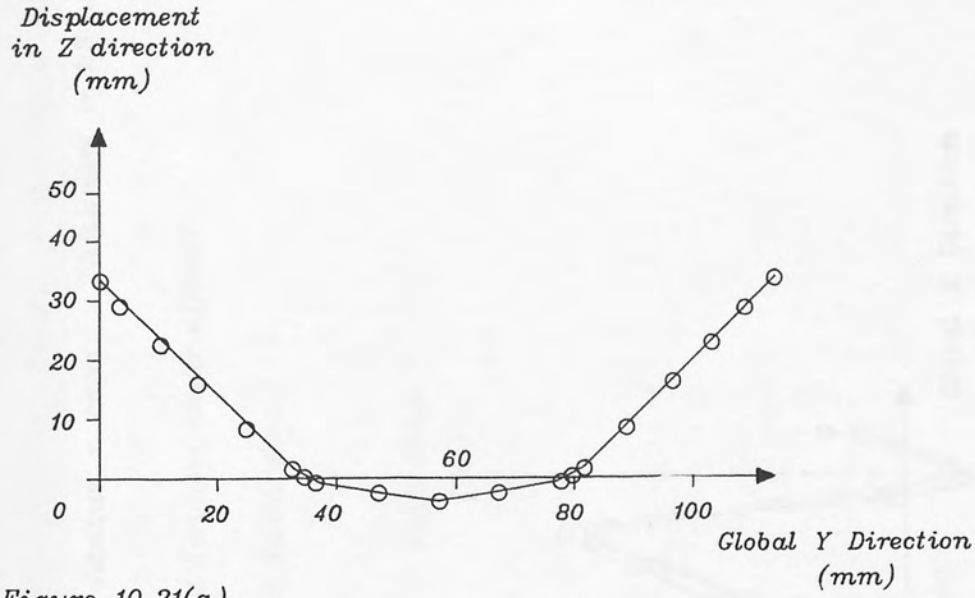

Figure 10.21(a)

Cross-Section shape 20mm downstream from the second stage of specimen B (PAFEC data)

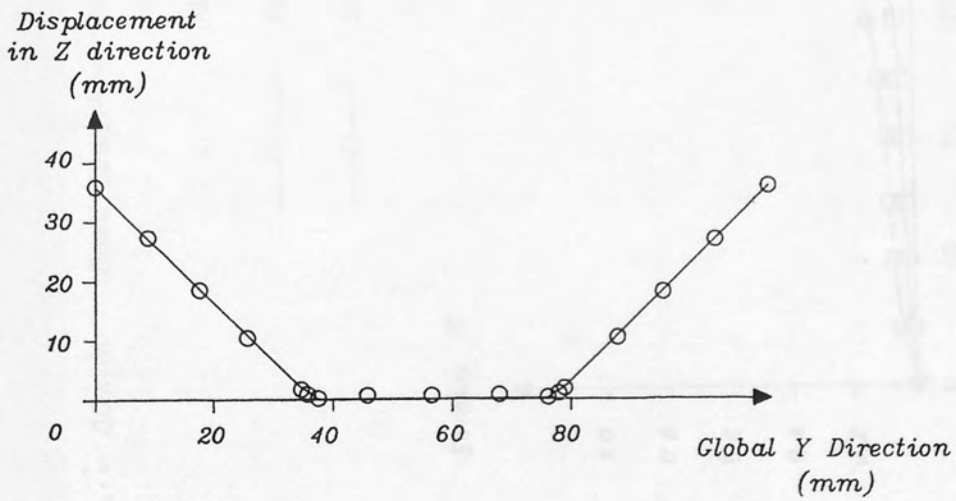

Figure 10.21(b)

Cross-Section shape at the second stage of specimen B (PAFEC data)

Specimen B

Flange Length = 50mm Base Length = 40mm Inside Radius = 1mm Thickness = 1.5mm

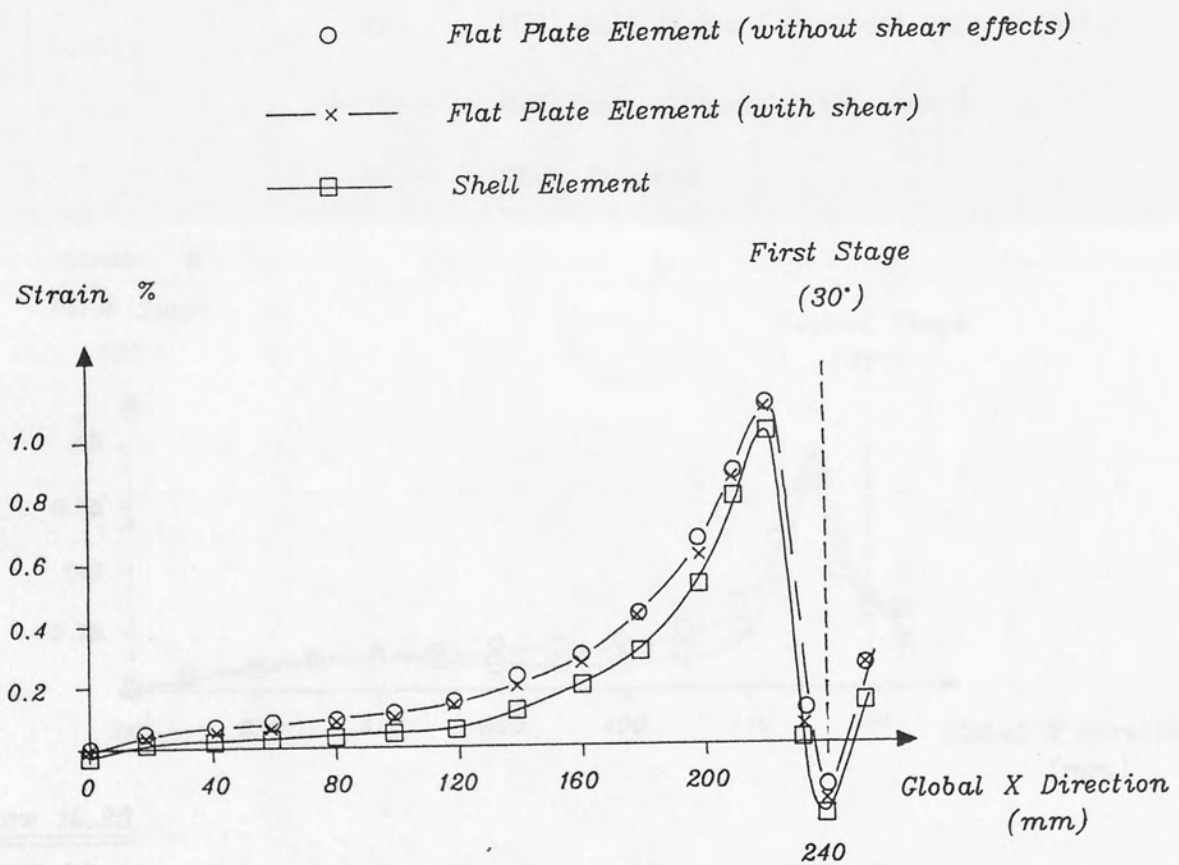

Figure 10.22

Longitudinal edge strain downstream of the first stage using PAFEC.

Specimen B

Flange Length = 50mm Base Length = 40mm Inside Radius = 1mm Thickness = 1.5mm

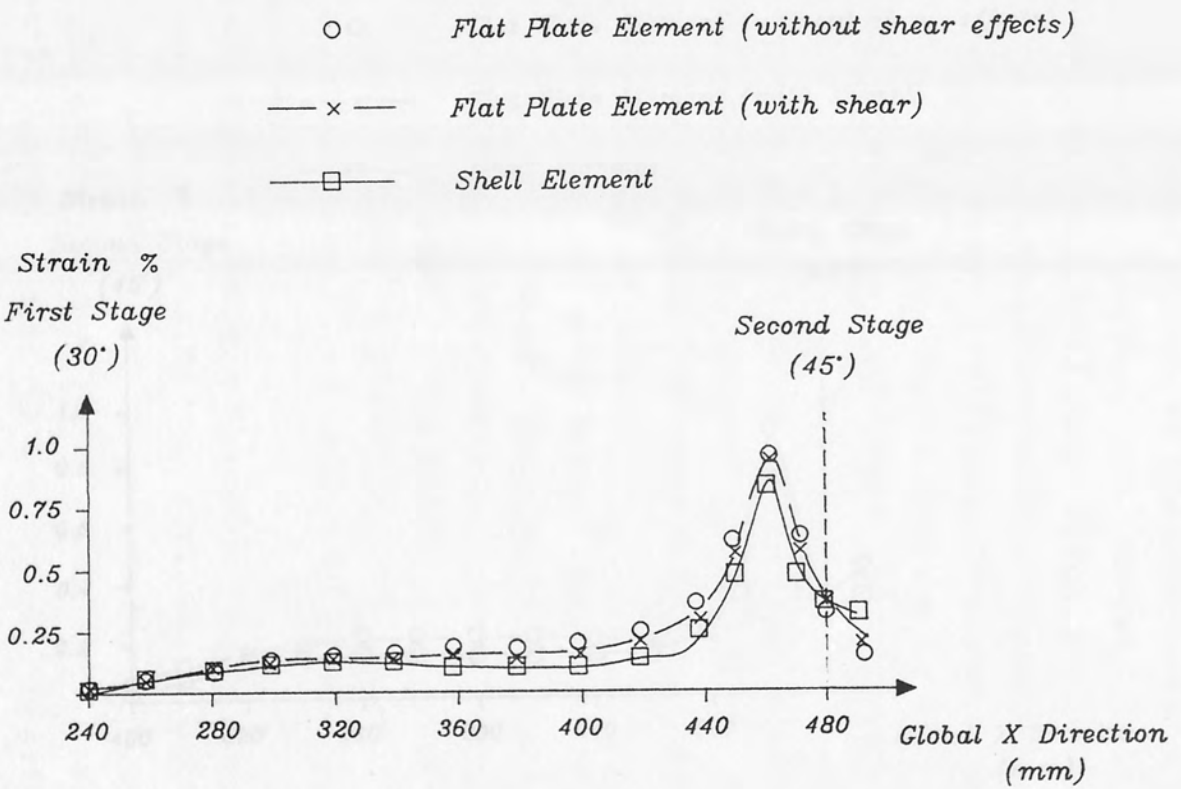

Figure 10.23

Longitudinal edge strain downstream of the second stage using PAFEC.

Specimen B

Flange Length = 50mm Base Length = 40mm Inside Radius = 1mm Thickness = 1.5mm

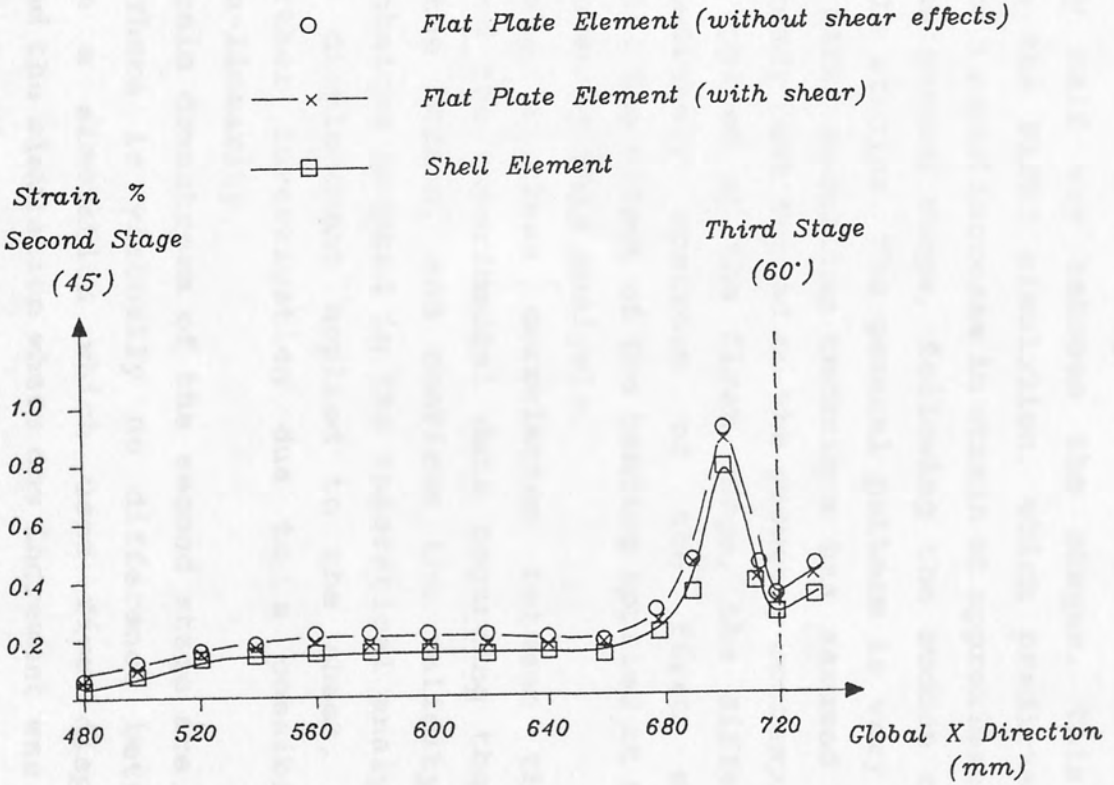

Figure 10.24

Longitudinal edge strain downstream of the third stage using PAFEC.

Longitudinal strain in the middle of the flange downstream of the second stage is shown in Fig 10.25. The general pattern compares closely with the strain gauge results. However, since no plastic analysis was available the values cannot be compared with the strain gauge results.

The longitudinal strain in the middle of the base is shown in Fig 10.26. The strain gauge results indicate that compressive strains are present immediately upstream of the first stage, and a rapid change to tensile strains occurs at approximately half way between the stages. This clearly differs from the PAFEC simulation, which predicts tensile strains before a rapid increase in strain at approximately 60 mm away from the second stage, following the sudden change to higher tensile strains. The general pattern is very similar. Because the PAFEC modelling technique has assumed that the sheet has already been formed to the geometry corresponding to the bending applied at the first stage, the difference in results immediately upstream of the first stage is understandable. The effect of the bending applied at the first stage is ignored by this analysis.

There was a close correlation between the PAFEC simulation and the experimental data regarding the general pattern of the strain, and confirms the validity of the modelling technique adopted in the theoretical analysis. The size of the displacement applied to the sheet, however, required further investigation due to a possibility of geometric non-linearity.

Edge strain downstream of the second stage are shown in Fig 10.23. There is virtually no difference between the results from a simulation which used five displacement increments and the simulation where one increment was applied. In both cases the flange was moved through 30 deg so that the edge of the sheet was displaced considerably but mostly by rigid body movement that does not effect the value of the edge strain.

The longitudinal strain at the mid-point of the bend region is shown in Fig 10.27. Taking small increments in displacement has made a large difference in the radius region, which is understandable because there will be no rigid body movement. Because there is not a substantial difference, the

Specimen B

Flange Length = 50mm Base Length = 40mm Inside Radius = 1mm Thickness = 1.5mm

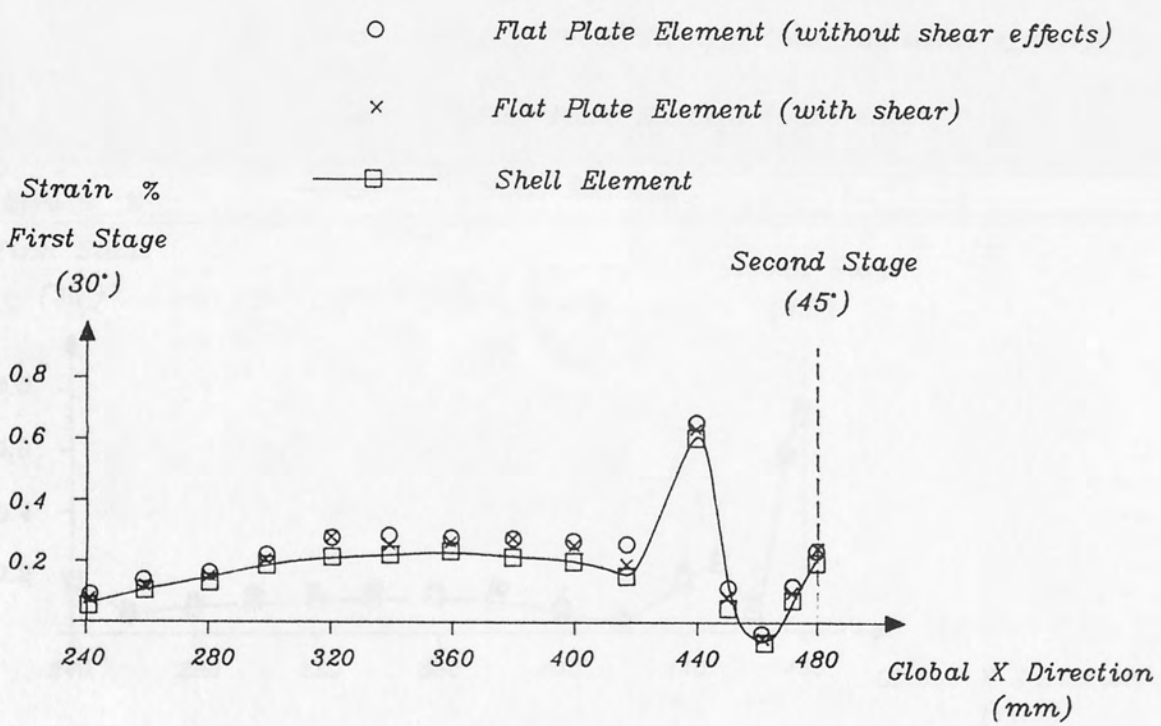

Figure 10.25

Longitudinal strain in the flange using PAFEC.

Specimen B

Flange Length = 50mm Base Length = 40mm Inside Radius = 1mm Thickness = 1.5mm

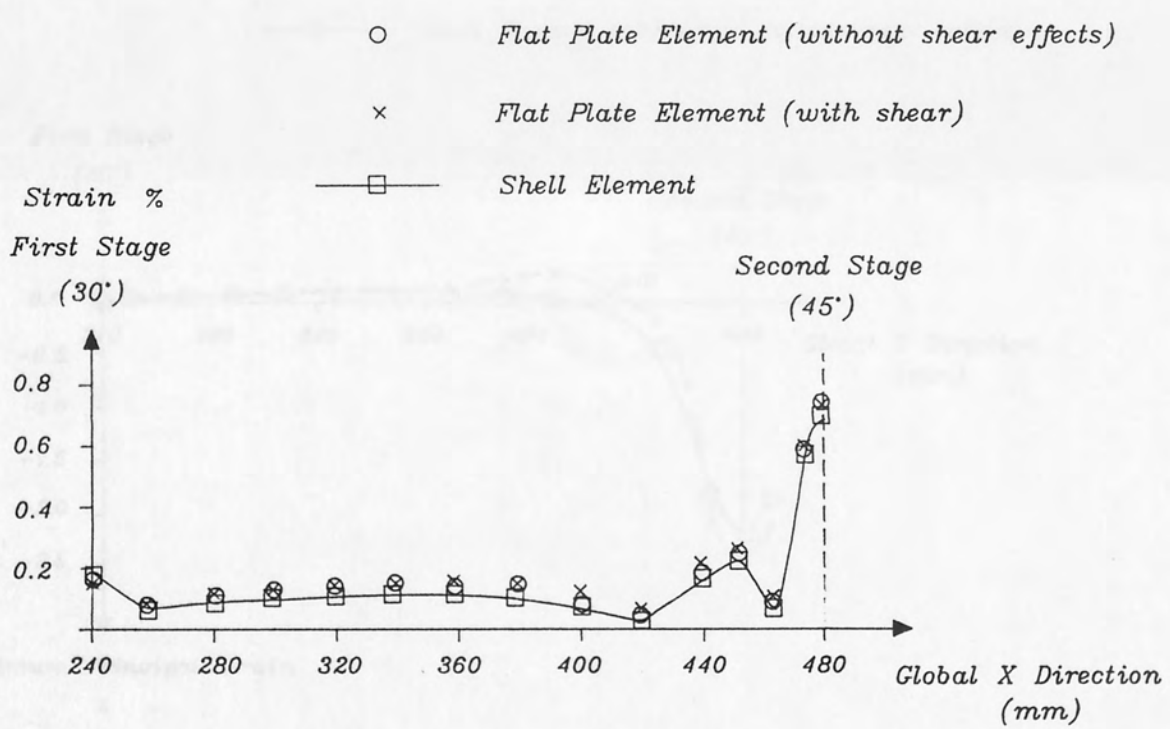

Figure 10.26

Longitudinal strain in the base using PAFEC.

Specimen B

Flange Length = 50mm Base Length = 40mm Inside Radius = 1mm Thickness = 1.5mm

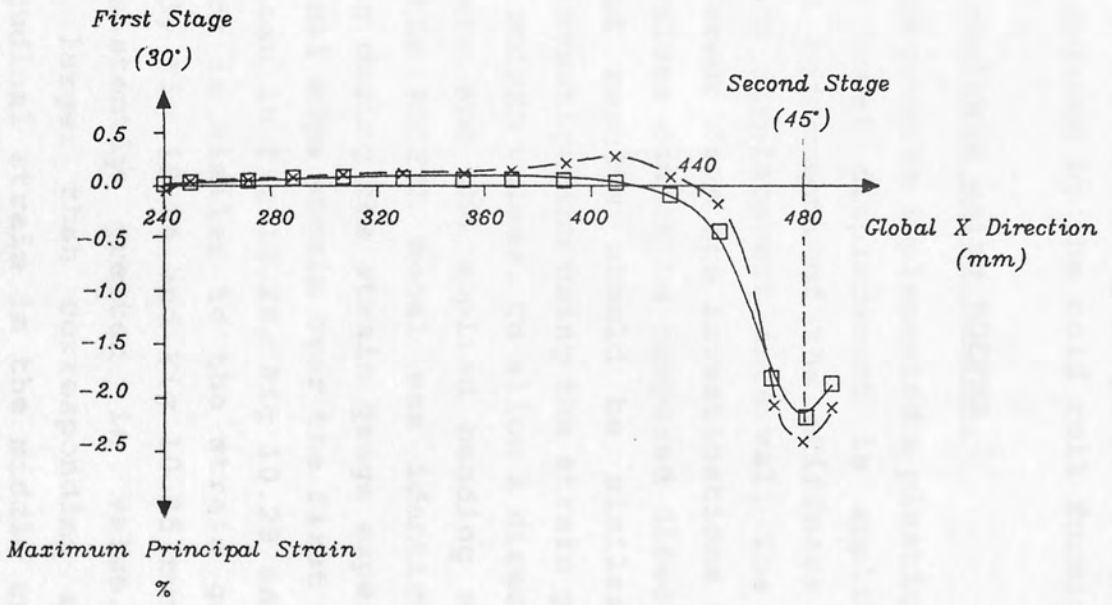

Figure 10.27

Strain in the radius downsteam of the second stage using PAFEC.

investigation has shown that the application of displacement in small increments is not essential, although it will increase accuracy in the bend regions.

The total number of finite elements involved in the analysis was minimised by using a very simple mesh design. This was necessary to avoid long computer processing times. The data shown in Fig 10.27, which used 65 elements recorded 2 min of processing time on the VAX 8500. The 44210 flat element which assumed that shear deformation was negligible and applied a much simpler mathematical analysis required approximately 1.5 min to process the same mesh. In both cases the section geometry was extremely simple in comparison to the shapes which are produced by the cold roll forming industry.

10.11 Strain analysis using ROLFEA.

The ROLFEA program implemented a plastic deformation analysis, and the total displacement is applied in small increments. A full adjustment of the stiffness matrices is carried out at each displacement interval. The analysis is fundamentally different from the investigations using PAFEC, so corresponding values cannot be compared directly, but the general pattern of results should be similar. The data obtained from the investigation using the strain gauges should correlate with the ROLFEA values. To allow a direct comparison the sheet parameters and the applied bending at the first three stages in the ROLFEA model was identical with the conditions existing during the strain gauge experiments.

The longitudinal edge strain over the first three stages of the mill are shown in Fig 10.28, Fig 10.29 and Fig 10.30. The general pattern is similar to the strain gauge results shown in Fig 10.23, Fig 10.24 and Fig 10.25 but the ROLFEA strains are consistently greater in value. They are approximately 25% larger than corresponding strain gauge values. The longitudinal strain in the middle of the flange downstream of the second stage are shown in Fig 10.31. Again, the general pattern of strain is very similar to Fig 10.15, which shows the strain gauge results, but corresponding strain is again approximately 25% greater. The longitudinal strains in the middle of the base shown in Fig 10.32 confirms that the ROLFEA calculations predict strains which are significantly

Specimen B

Flange Length = 50mm Base Length = 40mm Inside Radius = 1mm Thickness = 1.5mm

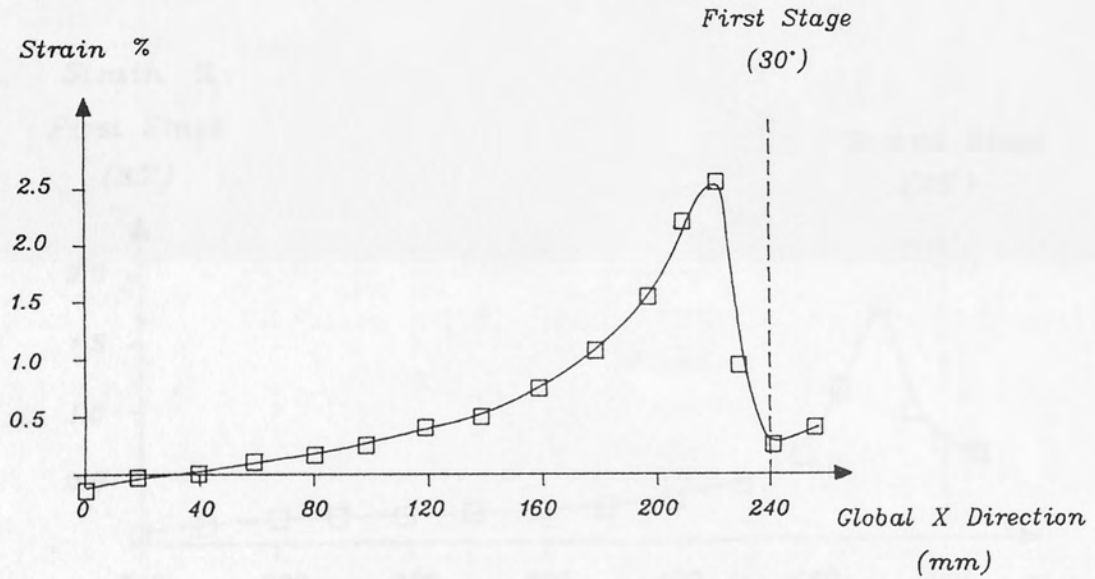

Figure 10.28

Total edge strain downstream of the first stage using ROLFEA.

Specimen B

Flange Length = 50mm Base Length = 40mm Inside Radius = 1mm Thickness = 1.5mm

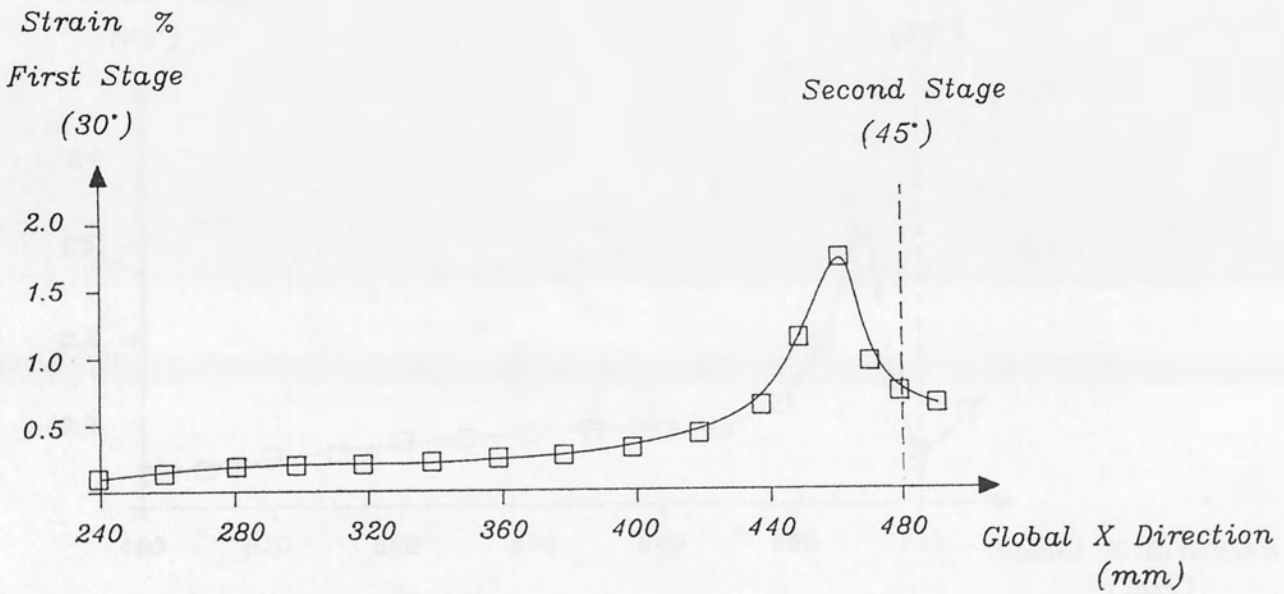

Figure 10.29

Total edge strain downstream of second stage using ROLFEA.

Specimen B

Flange Length = 50mm Base Length = 40mm Inside Radius = 1mm Thickness = 1.5mm

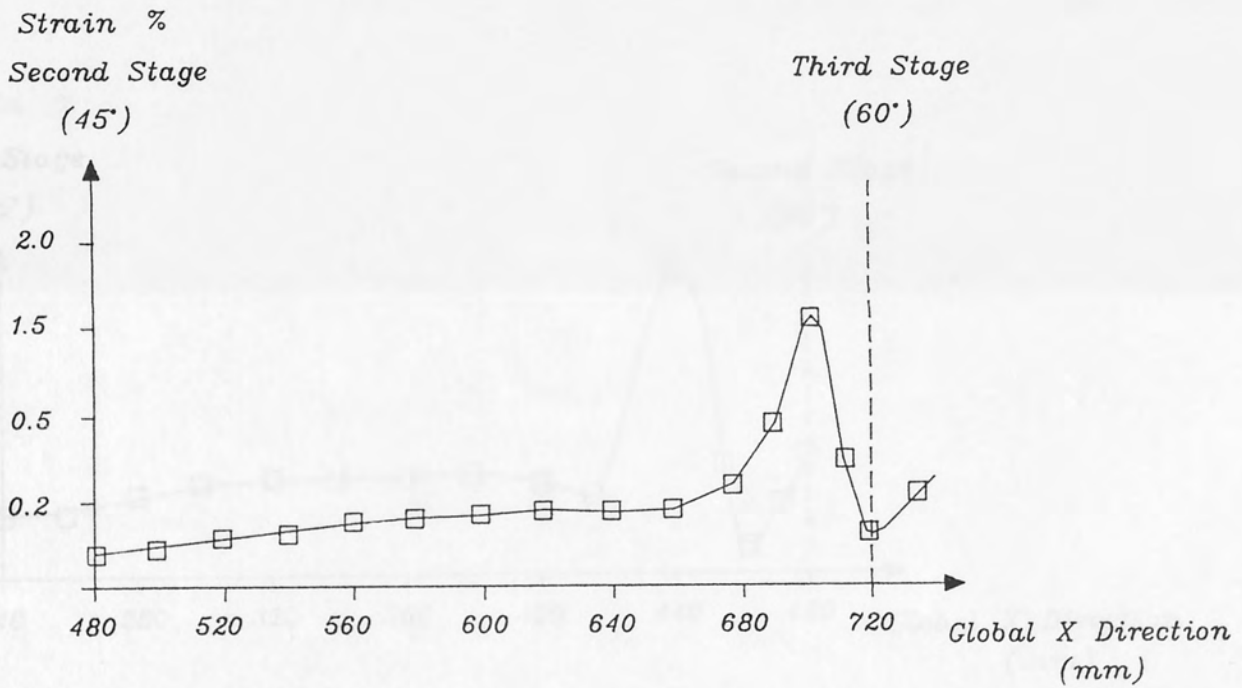

Figure 10.30

Total edge strain downstream of the third stage using ROLFEA.

Specimen B

Flange Length = 50mm Base Length = 40mm Inside Radius = 1mm Thickness = 1.5mm

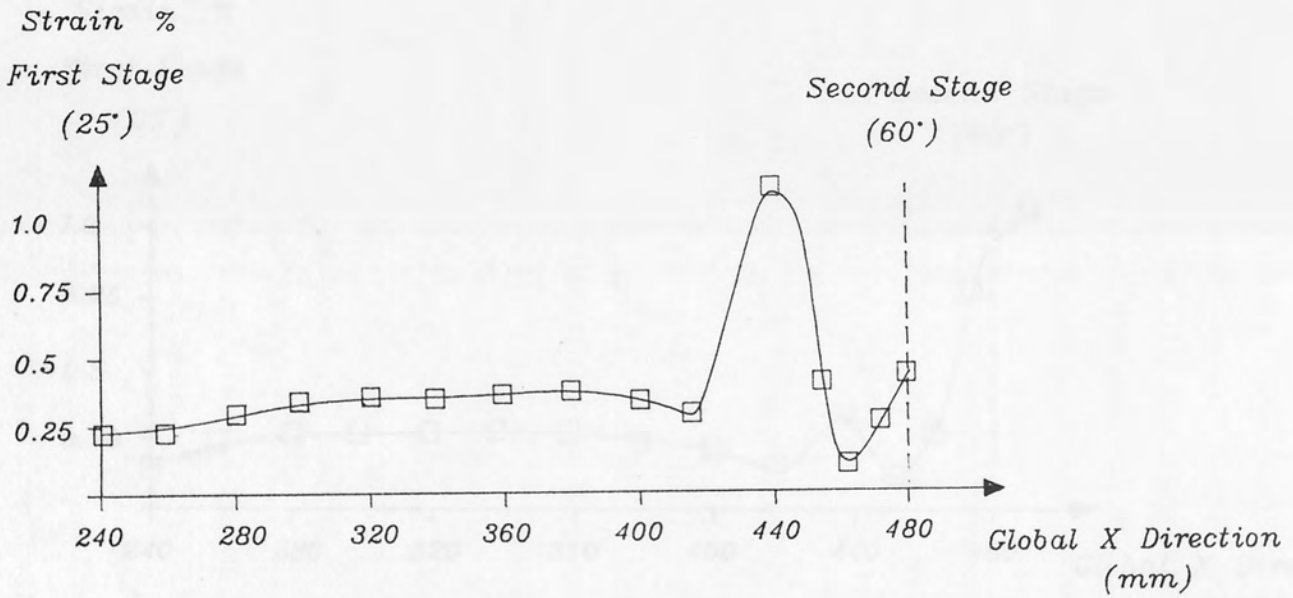

Figure 10.31

Total strain in the flange using ROLFEA.

Specimen B

Flange Length = 50mm Base Length = 40mm Inside Radius = 1mm Thickness = 1.5mm

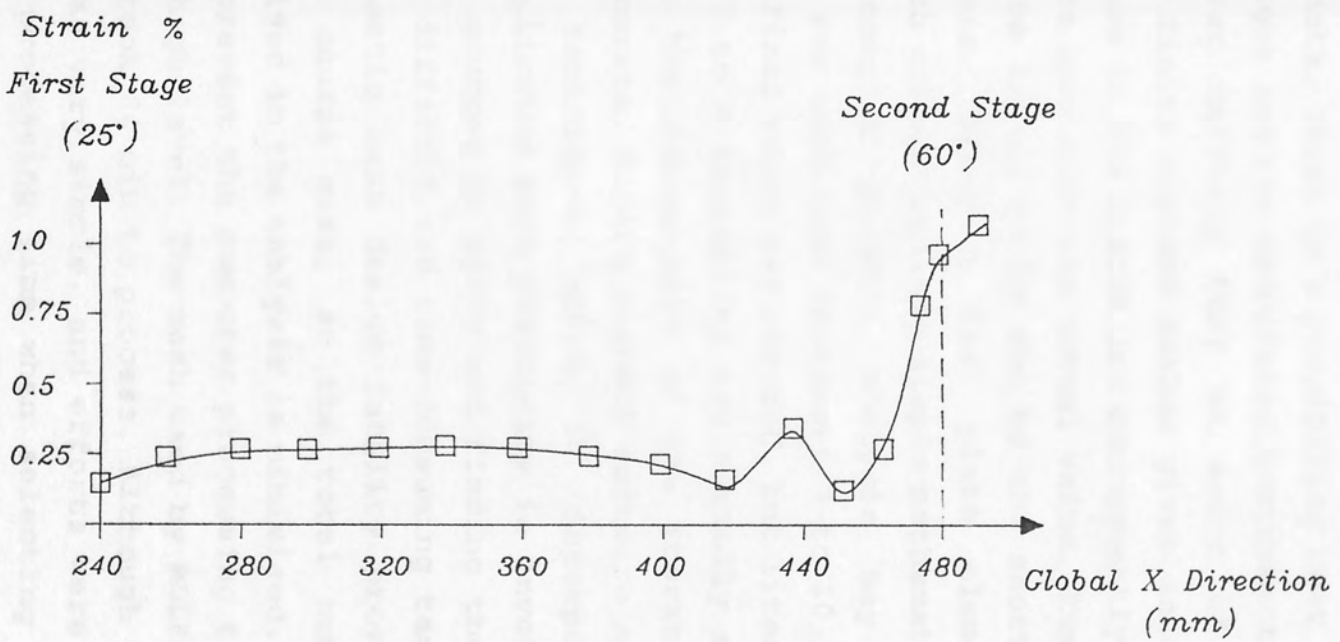

Figure 10.32

Total strain in the base using ROLFEA.

larger than experimental results, but the general pattern of the strain is very similar.

The close correlation in the general pattern of straining confirms that the modelling technique used by ROLFEA is accurate. It is difficult to ascertain the reasons for a consistently greater strain value prediction compared with the experimental data. There is a possibility that the accuracy of the strain gauges and the associated instrumentation was poor, but it is most unlikely that an error of 25% occurred. Normally, the finite element method gives an over-estimation of the stiffness in the system and consequently the calculated strains will be less that the actual value. The reason for the high values are likely to be due to the shortcomings in the ROLFEA analysis. Using a flat plate element, which is associated with a comparatively simple mathematical model, and applying a complex plastic analysis may have created inaccuracies. For each load increment 7 to 10 iterations were made before a final value was reached, but literary source[59,60] suggest that 3 to 4 iterations are normally adequate. It is possible that the convergence of the iteration process is slightly inaccurate. Finite element software and the numerous mathematical techniques which it incorporates becomes extremely complicated when plasticity is involved. There are many possible sources of error and finding the faults in the software is a difficult and time-consuming task.

The automatic mesh design facility provided by ROLFEA results in a course mesh, so the total number of finite elements involved in the analysis is minimised. Unfortunately, this did not prevent the computer processing time reaching an unacceptably high level. The mesh used by ROLFEA contained 18 elements and took 64 min to process. Although the geometry of the section was very simple, and efforts were made to reduce the computer processing time when selecting the analytical techniques used by ROLFEA, the processing time was much longer than expected.

Chapter Eleven.

Conclusions and Future Work.

11.1 Introduction.

The widespread application of computer-aided techniques throughout the engineering industry in the United Kingdom has imposed many radical changes. In the cold roll forming industry the introduction of CAD/CAM software has achieved major improvements where formerly archaic design and manufacturing methods have prevailed. The design of the rolls, however, has not been significantly effected by computerisation. The quality of the finished rolled product depends on the roll design and the operating conditions. There is no scientific design theory to guide the roll designer, or standard mill setting practices to assist the mill setter. The designer is totally dependent on the knowledge gleaned from previous efforts involving similar product geometry. A roll design must be tested on a mill, followed by the appropriate modifications which are usually required, before the design can be verified as satisfactory. This trial and error procedure is costly and inefficient, and no attempt is made to find the optimum design, only one that is satisfactory. A more scientific approach is required in order to allow the steady economic improvement in the cold roll forming industry to be maintained.

The objectives of this research project, which were outlined in Chapter One, have been successfully completed. The conclusions and suggestions for further work which now follow have been based on all aspects of the research programme.

11.2 Present CAD Systems.

The CAD software which is currently used in the cold roll forming industry is mainly for the rapid and efficient procurement of engineering drawings. They provide no assistance for the most important design decisions which have to be made. Flower pattern generation can provide a visualisation of the bending process, but to an inexperienced roll designer they are not very helpful.

11.3 Present CAD Systems : Future Work.

Development of existing CAD software to computerise the most important design decisions, such as the total number of stages or the magnitude of bending at each stage, would be a major task. Assistance could be provided, however, in many of the auxiliary design decisions where the problems are not so formidable. Investigations into methods for reducing form-roll slippage, the approximate prediction of springback, which segments of the section are to be used as drive surfaces and a method of determining an optimum pinch difference would be most worthwhile. Further study of sheet width calculations and a way of identifying regions of severe bending in a flower pattern drawing would also be beneficial. Present CAD software seems to have been restricted in the benefits it provides due to a shortcoming in the understanding of the cold roll forming process. It is most important that this is remedied.

11.4 CNC Lathe Programming using an Expert System.

The definition of tool paths for machining a profile on a CNC lathe requires a knowledge of the machining methods and the capability of lathe cutting tools. The level of knowledge required is related to the complexity of the machining, and the profiles on form-rolls are often quite intricate. Development of software in this project to carry out this task illustrated that work, formerly done by skilled humans, can successfully be computerised if the programming uses an expert system structure. Cutting tools are selected in the required order, and their movement is precisely defined by the calculation of a series of point coordinates. The ROLCUT program spends the majority of its processing time calculating point coordinates, which is a tedious and repetitive task for a human. In future years the expert systems extensively used in industry are likely to be engaged in doing time-consuming and monotonous tasks, combined with relatively trivial decision-making. This will allow highly skilled people to concentrate on jobs which require creative and resourceful analysis and would be uneconomic to computerise.

11.5 CNC lathe programming using an Expert System : Future Work.

The expert system program is written in the FORTRAN language and for graphical output the GINO-F library is used. Further development of the software to introduce additional features may require an advancement in the level of logic. One of the computer languages frequently used for expert systems, such as LISP or PROLOG, may be more suitable than FORTRAN if modifications of this nature are implemented. It may be necessary, therefore, to write a version of ROLCUT in a different language to FORTRAN to allow future advancements to be carried out.

Due to the costly driver programs required by GINO-F it is no longer a widely used graphics package. A substantial improvement would be achieved if ROLCUT was modified to allow one of the popular programs such as UNIRAS to supply the graphics.

11.6 The ROLCUT Program.

The ROLCUT program is capable of processing complicated profile geometry, including intricate shapes within a recess region. It allows the groove tool to perform profile machining cycles, therefore complicated shapes within narrow recesses are possible. There is a comprehensive check for tool collisions using the tool geometry data stored in the tool library. The user is provided with a visual inspection of the tool paths on the monitor, where any errors can easily be detected. A colour coding is adopted, and the rough, finish, pocket and groove tool paths can be displayed separately, allowing the path of each tool to be clearly shown. Small steps in the profile, usually to provide shoulder stops, are a relatively common feature and can be machined in one cut using a finish tool.

11.7 The ROLCUT Program : Future Work.

In order to increase machining efficiency, to improve the quality, and to extend further the range of profiles which can be machined, the following improvements to ROLCUT are suggested :-

1) The tools available in the tool library should be increased by extending the range of pocket tools (with different dig_in angles) and groove tools with different blade widths). Currently, the same groove tool is used to rough machine a recess and to perform the finish cut using the profile machining cycle. Using different groove tools for the rough and finish cycles would be a useful improvement.
2) The left hand pocket tool is used to cut into a recess region by moving along the dig_in line. In some cases, depending on the geometry of the recess region, it is beneficial to have a dig_in line for the right hand pocket tool to allow it to perform this operation. This is not allowed currently.

11.8 The C.R.F. Bending Process.

The investigations into the deformation and strain pattern in the rolled sheet illustrated a very complicated bending process. Even the linear portions of the section are subjected to forces that create residual strains. An arbitrary point on the sheet may experience both tensile and compressive strain during its travel through the forming length region of the stage. The residual strains that remain in the sheet upstream of the stage will depend on the overall effect of the tensile and compressive forces.

11.9 C.R.F. Bending Process : Future Work.

Further investigations are required into the strain generated in the sheet during the rolling operation. Particular emphasis should be made on the strain in the bend regions of the section. It would be beneficial if investigations involved complicated section geometry, since virtually all the published research refer to very simple geometry such as tubes or channel sections.

11.10 Deformation downstream of the first stage.

The investigations carried out in this research have highlighted the importance of the deformation caused by the bending applied at the first stage. In the simple channel section, the base is severely deformed and the residual strains that are generated will effect the quality of the finish rolled section. Because the sheet has no bend regions, the linear portions of the section usually suffer greater deformation due to curvature in the forming length of the first stage than at any other stage in the mill.

11.1 Deformation downstream of the first stage : Future Work.

A method of initially forming the bend radii in the sheet is required, which avoids the deformation of linear portions of the section to the extent that significant residual strains are created.

11.12 Sheet Alignment Errors.

All the rolled specimens used in the experimental investigations had sheet alignment errors at the first two stages of the mill. This anomaly was overcome by the last stage and the section leaving the last stage was reasonably symmetrical. An alignment error will effect the strain that occurs, so it cannot be ignored even if it only exists at the first and second stages. If alignment errors do occur, it is essential that the necessary information is supplied to the theoretical model to allow the condition to be considered in the mathematical analysis.

11.13 Sheet Alignment Errors : Future Work.

Alignment errors may be extremely common at the earlier stages of the mill if the mill setter has the sole objective of producing the correct section geometry downstream of the last stage. To simplify theoretical models, however, it is helpful if alignment problems are small enough to be ignored. Further inquires are necessary to establish if sheet alignment errors are a significant problem in industry and whether they cause inaccuracies in a theoretical model of the process.

11.14 Modelling the C.R.F. Process.

From the investigation using PAFEC it was found that shear forces were negligible compared to other forces acting on the sheet. By applying the displacement in increments, it was also established that geometric non-linearity is only significant in the bend regions of the section. Both of these assumptions helped to simplify the ROLFEA simulation of the C.R.F. process.

The theoretical model did not impose any constraints on the sheet between the stages, it was free to form any cross-section shape. Section geometry was only controlled at the stages, and the displacement was also applied at each stage. This accuracy of this has been verified because it was used by PAFEC and ROLFEA, and the general pattern of strain which they both produced correlated with experimental results.

11.15 Modelling the C.R.F. process : Future Work.

It was stated in section 11.14 that geometric non-linearity should only be considered in the bend region. Further investigations are necessary in order to confirm that this applies to all cold roll forming operations. If the material parameters or rolling conditions are altered substantially from that which existed during the investigation carried out in this research, different conclusions may be reached. Empirical studies have shown that the force with which the rolls grips the sheet is a highly important feature. The mill setter will frequently adjust the position of the top form-roll to mitigate production defects. The model used by ROLFEA requires further development in order to allow the common mill setting adjustments to be simulated in the mathematical analysis.

11.16 Accuracy of ROLFEA.

The strain calculated by ROLFEA are consistently greater than corresponding values recorded in the strain gauge experiments. Normally, a finite element analysis makes an over-estimation of the stiffness in the system and consequently, the calculated strains are less than the true values. The course mesh used by ROLFEA will reduce the degrees

of freedom in the system which has a net effect of further increasing the stiffness. Assuming the strain gauge data is correct, there must be an error in the ROLFEA simulation which results in strains that are approximately 25% greater than the true value.

11.17 Accuracy of ROLFEA : Future Work.

Verification of the results obtained from the strain gauges are required to confirm that ROLFEA is over-estimating the strains in the sheet. If the strain gauge results are correct, within acceptable experimental error, then a fault exists in the ROLFEA simulation. Finding errors in finite element software is a difficult and time-consuming task. There is a possibility, however, that using a flat plate element combined with a complicated elastic-plastic analysis may have caused inaccuracies. Replacing the flat plate element with the more sophisticated shell element may be worthwhile.

11.18 Computer processing time.

A major disadvantage of the finite element method is that there are usually a large number of unknowns which must be solved. If the method is used to model the cold roll forming process there is a likely possibility of large computer processing times. During the design of the ROLFEA software many decisions were taken with the objective of reducing processing time, but the effort was not rewarded. Although very simple sheet geometry was involved, the computer processing time was extremely large. If complicated section geometry is studied, such as wide profiles which often involve 5 or 6 simple channel shapes, the processing time will be much greater. There is a possibility that large processing times may make it impractical to install a software design aid such as ROLFEA in an industrial environment. Using the finite element method to model the cold roll forming process may not be a feasible approach solely because of the large computer processing time. A different mathematical analysis may be required which reduces processing time to an acceptable level.

The strain in the sheet was investigated to create a basis from which the residual strains could be evaluated.

Having obtained the residual strains, then further research is required in order to be able to predict the resultant forces or geometry of the section, and to use this information to verify whether a roll schedule design is satisfactory before the rolls have been manufactured. Obviously, a quick and accurate evaluation of the residual strains is difficult to achieve. Thus, the conclusion from this research suggests that the feasibility of using the finite element method to calculate the strain in the sheet, in a reasonable processing time, must be questioned.

References.

(1) Ng, K. H., "Computer aided geometric design of form rolls for N.C. manufacture",Ph.D thesis, Aston University, 1981.

(2) Wong, T.N., "Computer aided design and manufacture of form rolls", Ph.D. thesis, Aston University, 1983.

(3) Kalvzhskii, V. B., "Developing a technology for shaping and joining rolls for cold-bent shapes", Metallurgist (U.S.S.R), **27**, 371-374, 1983

(4) Angel, R. T., "Designing tools for cold roll forming", The Iron Age, **16**, 83-88, 1949.

(5) Sarantidis, T. M., "Cold roll forming", M.Sc. dissertation, University of Manchester Institution of Science and Technology, 1977.

(6) Cadney, S., "Cold roll forming. The art that could do with some science",Production Engineer, **60**, 19-21, 1981

(7) Vanderploeg, E, J., "Roll forming-simple method for designing rolls", Tool Engineer, **54**, 59-65, 1953.

(8) Rhodes, A., "Computer aided design and manufacture of rolls for cold roll forming machinery", Proc. 1st Int. Conf. on Rotary Metalworking Processes, London, 1979.

(9) Kato, K., "A basic study on cold roll forming technique", Nippon Kokan Kubushi Kaisha Technical Report Overseas, 44-54, 1963.

(10) Gardiner. J. F., "The springback of metals", Transactions of the American Society of Mechanical Engineers, **71**, 1-9, 1957.

(11) Panton, S. M., "Computer aided form roll design", Ph.D. thesis, Aston University, 1987.

(12) Rhodes, A., "Computer aided design and manufacture of rolls for cold roll forming", Sheet Metal Industries, **59**, 643-651, 1982.

(13) Research Division Industrie Secco, Italy., "Computer aiding design program developed to assist in the design of the forming sequence of cold roll forming profiles", Proc. 3rd. Int. Conf. on Rotary Metalworking Processes, Tokyo, 1984.

(14) Riedlinger, T., "Roll form die design time slashed from days to hours", Modern Metals, **36**, 38-40, 1980.

(15) Halmos, G.T., "Computer program aids roll forming designers", Modern Metals, **41**,22-26, 1985.

(16) Yuen, W. Y., "New developments in CAD for roll forming", Advanced Technology of Plasticity, **1**, 514-519, 1984.

(17) Ona, H., Jimma, T., Kozono, H., "A computer aided design system for cold roll forming ", Advanced Technology in Plasticity, **1**, 508-519, 1984.

(18) "Programming in VAX FORTRAN", Digital Equipment Corporation, Sept. 1984.

(19) "Gino-F User Manual", Computer Aided Design Centre, Cambridge, 1976.

(20) American Society, "A.S.M.E. Handbook-Metals Engineering Process (cold roll forming)", McGraw- Hill, 1958.

(21) British Standards, "BS 2994 : Specifications for cold rolled steel sections", 1976.

(22) Vasiliou, V. C., "Computer integrated manufacture of form rolls", Ph.D. thesis, Aston University, 1985.

(23) Feigenbaum, E., McCorduck, P., "The fifth generation", Addison-Wesley, March 1983.

(24) Lederberg, J., Buchanan, B., "Generality and problem solving : A case study using the DENDRAL program", Machine Intelligence, ed. Meltzer, B. and Michie, D., Elsevier Publishing, New York, 1971.

(25) Shortcliffe E. H., "Computer-based medical consultations: MYSIN", Elsevier Publishing, New York, 1979.

(26) Ona, H., Jimma, T., "Prevention of shape defects in the cold roll forming process of wide profiles", Bulletin Research Laboratory of Precision Machinery and Electronics, **53**, 1-13, 1984.

(27) Ona, H., Jimma, T., Fukaya, N., "Experiments into the cold roll forming of straight Asymmetrical Channels", Journal of Mechanical Working Technology, **8**, 273-291, 1983.

(28) Kiuchi, M., Suzuki, H., Nakajima, S., "Experimental investigation on cold roll forming process", Report of the institute of industrial Science, University of Tokyo, **22**, 2, Sept. 1972.

(29) Bhattacharyya, D., Smith, P. D., "The development of longitudinal strain in cold roll forming and its influence on product straightness", Advanced Tech. of Plasticity, **1**, 422-477, 1984.

(30) Nobel, C. F., Sarantidis T. M., "A study of cold roll forming", Proc. 1st. Conf. Rotary Metalworking Processes, London, 1979.

(31) Starchenko, D. I., Chelovan, M. I., "Effects of lubricants on roll forming force", Stal in English, **12**, 139-140, 1968.

(32) Jimma, T., Ona H., "Optimum roll pass schedules of the cold roll process of symmetrical channels", Proc. 21st. Int. Conf. Machine Tool Design and Research, ed. J. M. Alexander, MacMillan, 1980.

(33) Griffin, E., "Cold roll forming of strip and sheet metals", Proc. 2nd. Int. Conf. Rotary Metalworking Processes, Stratford-upon-Avon, 1982.

(34) Kato, K., Saito, Y., Shinto, H., "Effects of metal properties on shape of roll formed product -circular arc section", Technology Reports of the Osaka University, **30**, 1561, 405-410, 1980.

(35) Ford, H., Alexander, J. M., "Advanced mechanics of materials", Longmans, 1963.

(36) Spiegel, M. R., "Schaum's outline of theory and problems of vector analysis : and an introduction to tensor analysis.", McGraw-Hill, 1974.

(37) Avitzur, B., "Metal forming, the application of limit analysis", New York Dekker, 1980.

(38) Hearn, E. J., "Mechanics of materials.", Pergamon Press, 1982.

(39) Hill, R., "The mathematical theory of plasticity", Oxford Clarendon Press, 1950.

(40) Masuda, M., Murota, T., Jimma, T., "Fundamental research on the cold roll forming of metals", Bulletin of the Japanese Society of Mechanical Engineers, **28**, 827-833, 1964.

(41) Invarsson, L., "Cold forming residual stresses", Proc. 3rd. Int. Conf. on cold formed steel structures, St. Louis, 1975.

(42) Bhattacharyya, D., Smith, P. D., Yee, C. H., "The prediction of deformation length in cold roll forming", Journal of Mechanical Working Technology, **9**, 181-191, 1984.

(43) Richards T. H. E., "Energy methods in stress analysis", Ellis Horwood, 1977.

(44) Kiuchi, M., Koudabashi, T., Sato, T., "Automated design system of optimal roll profiles for roll forming of welded pipe and tube", Proc. 3rd. Int. Conf. on Steel Rolling, Tokyo, 1985.

(45) Yamada, Y., Yoshimura, N., Sakurai, T., "Plastic stress-strain matrix and its application for the solution of elastic-plastic problems by the finite element method", Int. J. Mech. Sci., **10**, 343-354, 1968.

(46) Nelder, J. A., Mead, R., "A simplex method for function minimisation", Computer Journal, **7**, 308-318, 1985.

(47) Wood, R. D., "The finite element method and sheet-metal forming", Metal Forming Technology, Sheet Metal Industries, 561-567, August 1981.

(48) "PAFEC finite element data preparation user manual level 6.1", PAFEC Ltd., 1984.

(49) Zienkiewicz, O. C., "The finite element method in engineering science", 2nd edn., McGraw-Hill, 1971.

(50) "PAFEC finite element system theory manual", PAFEC Ltd., 1984.

(51) Jeffery, A., "Mathematics for engineers and scientists", 4th edn., Van Nostrand Reinhold, 1989.

(52) Irons, B. M., Ahmad, S., "Techniques of finite elements", Ellis Horwood, Chichester, 1977.

(53) Banerjee, P. K., Butterfield, R., "Boundary element methods in engineering science", McGraw-Hill, 1981.

(54) Irons, B. M., "A frontal solution program for finite element analysis", Int. J. Num. Eng. **2**, 1, 5-32, 1970.

(55) Hinton, E., Owen, D. R. J., "Programming in finite elements", Pineridge Press, 1977.

(56) Marcal, P. V., King, I. P., "Elastic-plastic analysis of two dimensional stress systems by the finite element method", Int. J. Mech. Sci., **9**, 143-155, 1967.

(57) Argyris, J. H., "Elasto-plastic matrix displacement analysis of three dimensional continua", J. Roy. Aero. Soc., **69**, 633-635, 1965.

(58) Mendelson, A., "Plasticity : theory and applications", MacMillan, 1968.

(59) Hinton, H., Owen, D. J. R., "Finite elements in plasticity : theory and practice", Pineridge Press, 1977.

(60) Zienkiewicz, O. C., Valliappan, S., King, I. P., "Elasto-plastic solutions of engineering problems. Initial stress, finite element approach", Int. J. Num. Meth. in Eng., **1**, 75-100, 1969.

(61) Ahmad, S., "Curved finite elements in the analysis of solid shell and plate structures", Ph.D. thesis, University of Wales, Swansea, 1969.

(62) Rockey, K. C., Evans, H. R., "A finite element solution for folded plate structures", in Space Structure, Blackwell Scientific Publications, 165-188, 1967.

(63) Rockey, K. C., Evans, H. R., Nethercot, D. A., "The finite element method", Granada Publishing Ltd., 1975.

(64) Evans, H. R., "The analysis of folded plate structures", Ph.D. thesis, University of Wales, Swansea, 1967.

(65) Zienkiewicz, O. C., Parekh, C. J., King, I. P., "Arch dams analysed by a linear finite element shell solution program", Proc. Symp. Arch Dams., Inst. Civ. Eng., London, 1968.

(66) Timoshenko, S., Woinowsky-Keiger, S., "Theory of plates and shells", McGraw-Hill, 1959.

(67) Bäcklund, J., "Finite element analysis of elasto-plastic shells", Int. J. Num. Meth. Eng., **8**, 415-424, 1974.

(68) Kikuchi N., "Finite element methods in mechanics", Cambridge University Press, 1986.

(69) Hinton, E., Owen, D. R. J., "Finite element software for plates and shells", Pineridge Press, 1983.

(70) Fewtrell J., "An experimental analysis of operating conditions in cold roll forming", Ph.D. thesis, Aston University, 1990.

Appendix 1.

ROLFOM SESSION.

```
ROLFORM  METAL DIRECTORY
-------------------------

        METAL                                   KEYWORD
        -----                                   -------

(1)     STEEL                                   STEEL
(2)     HIGH STRENGTH STEELS                    HIGH
(3)     STAINLESS STEEL'S                       STAINLESS
(4)     NON FERROUS METAL'S                     NONFE

     PLEASE TYPE KEYWORD
                 =======

METAL : STEEL

     ROLFORM CAD/CAM SYSTEM
     ======================

           PROGRAM                              KEYWORD
           =======                              =======

 (1)     INPUT SECTION DATA                     SECTION
 (2)     RERUN SECTION ON SCREEN                NSECTION
 (3)     INPUT FLOWER PATTERN DATA              FLOWER
 (4)     RERUN FLOWER PATTERN ON SCREEN         NFLOWER
 (5)     RERUN FLOWER PATTERN SEPERATELY        SFLOWER
 (6)     RUN TEMPLATE PROGRAM                   TEMPLATE
 (7)     INPUT ROLL DESIGN DATA                 DESIGN
 (8)     INPUT ROLL D-DATA IN SINGLE STAGE      SDESIGN
 (9)     RERUN ROLL DESIGN ON SCREEN            NDESIGN
(10)     RUN WIRE FRAME ON SCREEN               WIRE
(11)     RUN PLAN/SIDE ON SCREEN                VIEW
(12)     EDIT ROLL DESIGN                       AEDITOR
(13)     UPDATED ROLL EDITOR                    EDITOR
(14)     FINITE ELEMENTS ANALYSIS               ROLFEA
(15)     EXPERT SYSTEM MACHINING                ROLCUT
(16)     DELETION OF D FILES                    DELETE
(17)     CONVERT ROLCUT CUTTING COMMANDS        CONVERT
(18)     INPUT CUTTING COMMANDS                 CUTPLOT
(19)     RUN POST PROCESSOR                     MFPOST
(20)     CHECK NC TAPE ON SCREEN                CHK

    TYPE 99 TO EXIT                          (KEYWORD)

  PLEASE TYPE KEYWORD TO SELECT A PROGRAM
              =======

CHOICE : SECTION


NSECTION        VERSION 1.1


          *** ROLFOM ***
              ******
```

```
   ** FINISHED SECTION PROGRAM **

*** PLEASE INPUT THE SECTION NO. ***
section no. = 1270

 ****************************************
 **                                    **
 **        TERMINAL DEFINITION         **
 **        PLEASE INPUT  1,2,3,4       **
 **        (1) FOR T4010               **
 **        (2) FOR T4107               **
 **        (3) FOR T4113               **
 **        (4) FOR T4014               **
 **                                    **
 ****************************************
  GINO-F   2.7C 01-NOV-1986 - ISSUE 1

    * PLOTTING PROGRAM NO. 1 FOR ROLLED-SECTION *

                FINISHED SECTION
                ----------------

PLEASE SUPPLY THE FOLLOWING DATA ACCORDING TO THE GIVEN FORMAT:-

  INPUT UNIT      OUTPUT UNIT      THICKNESS      ORIGIN
  ----------      -----------      ---------      ------

  (INTEGER)        (INTEGER)         (REAL)      (INTEGER)

   WHERE,

   INPUT UNIT IS IN INCH(1) OR MM(2),
   OUTPUT UNIT IS ALSO IN INCH(1) OR MM(2),
   THICKNESS IS THICKNESS OF STRIP,
   ORIGIN IS THE STARTING POINT FOR ELEMENT DEFINITION
   SEQUENCE LATER ON.

   ORIGIN=1 IF FROM LEFT TOWARDS RIGHT (ONE-SIDED).
   ORIGIN=2 IF FROM RIGHT TOWARDS LEFT (ONE-SIDED).
   ORIGIN=3 IF FROM CENTRE TOWARDS RIGHT AND THEN FROM
            CENTRE TOWARDS LEFT.
   ORIGIN=4 IF FROM CENTRE TOWARDS LEFT AND THEN FROM
            CENTRE TOWARDS RIGHT.
   ORIGIN=5 IF FROM CENTRE TOWARDS RIGHT (SYMMETRICAL SECTION).


   ** PLEASE INPUT IUNIT,OUNIT,THICK,ORIGIN **

       1 1 3 5

   PLEASE ENTER THE DATA FOR ELEMENT DEFINITION SEQUENCE
   ACCORDING TO THE GIVEN FORMAT, ONE DEFINITION STATEMENT
   FOR EVERY ELEMENT ENTERED :-
```

SEQUENCE NUMBER	ELEMENT TYPE	LENGTH OR RADIUS	ANGLE OF BENDING
(INTEGER)	(INTEGER)	(REAL)	(REAL)
START FROM 1, INCREMENT BY 1 UP TO 50, TO TERMINATE ENTER 0.	1 = LINEAR, 2 = CIRCULAR, THE REST ARE ILLEGAL.	POSITIVE LENGTH FOR TYPE 1, INSIDE RADIUS FOR TYPE 2 (MAY BE 0).	FOR TYPE 2 ELEMENTS ONLY, ZERO FOR TYPE 1*

*THE EXCEPTION BEING, WHEN N=1 AND TYPE=1 (AND ORIGIN NOT 5!), ANGLE OF BENDING IS TAKEN AS THE ANGLE OF INCLINATION BETWEEN THE HORIZONTAL-AXIS AND THE FIRST LINEAR ELEMENT, PERMISSIBLE RANGE IS FROM -90 TO +90 DEGREES.

NOTE THAT WHEN ORIGIN IS 3 OR 4 (DOUBLE SIDED DEFINITION), 2 SETS OF DEFINITION SEQUENCE ARE REQUIRED, ONLY 1 SET IS REQUIRED WHEN ORIGIN IS 1,2 OR 5.
FIRST ELEMENT AND LAST ELEMENT OF THE SEQUENCE MUST BE LINEAR.
MAXIMUM NO. OF ELEMENTS IN EACH SEQUENCE MUST BE LESS THAN 50.

1	1	25.00 MM.	0.00
2	2	5.00 MM.	120.00
3	1	30.00 MM.	0.00
4	2	5.00 MM.	-120.00
5	1	10.00 MM.	0.00
0	0	0.00 MM.	0.00

MEANLENGTH INFORMATION FOR INDIVIDUAL ELEMENTS:-

ELEMENT NO.	MEANLENGTH (MM.)
1	25.000
2	13.614
3	30.000
4	13.614
5	10.000
6	25.000
7	13.614
8	30.000
9	13.614
10	10.000

TOTAL MEANLENGTH= 184.454 MM.

```
 PLEASE SELECT THE PAPERSIZE AND THE SCALE
 ACCORDING TO THE GIVEN FORMAT :-

      PAPERSIZE              SCALE
      ---------              -----

      (INTEGER)              (REAL)

PAPERSIZE = 0,1,2,3,4 FOR A0,A1,A2,A3,A4 SIZES RESPECTIVELY.
SCALE= ANY POSITIVE VALUE LESS OR EQUAL TO THE FOLLOWING
 LIMITS BASED ON THE SELECTED PAPERSIZE.


FOR PAPERSIZE A0, MAXIMUM PERMISSIBLE SCALE = 15.26
FOR PAPERSIZE A1, MAXIMUM PERMISSIBLE SCALE = 10.31
FOR PAPERSIZE A2, MAXIMUM PERMISSIBLE SCALE =  6.60
FOR PAPERSIZE A3, MAXIMUM PERMISSIBLE SCALE =  4.09
FOR PAPERSIZE A4, MAXIMUM PERMISSIBLE SCALE =  2.27
  *** PLEASE INPUT THE PSIZE AND PSCALE ***

   4 2.0
  PAPERSIZE A4     SCALE  2.0 : 1.0


DO YOU WANT ANY DIMENSIONING?

ENTER 1 IF YES, OR 0 IF NO.
    1


DO YOU WISH TO SUPPLY ANY TITLE-BLOCK INFORMATION ?

ENTER 1 IF YES, OR 0 IF NO.

    0
                      ******
```

```
                FLOWER PATTERN PROGRAM


   * PLOTTING PROGRAM NO. 2 FOR ROLLED-SECTION *


                --- FLOWER PATTERNS ---


      ** PLEASE INPUT THE SECTION NO. **
   section no. = 1270

  ****************************************
  **                                    **
  **         TERMINAL DEFINITION        **
  **         PLEASE INPUT  1,2,3,4      **
  **         (1) FOR T4014              **
  **         (2) FOR T4107              **
  **         (3) FOR T4113              **
  **         (4) FOR T4105              **
  **                                    **
  ****************************************
GINO-F   2.7C 01-NOV-1986 - ISSUE 1

** INPUT JRUN = 1 IF FLOWER PATTERN ONLY,OR
               2 IF ROLLER-PLOTTINGS ONLY,OR
               3 IF BOTH OF THE ABOVE
JRUN = 3

** INPUT NSTAGE (NSTAGE = TOTAL NO. OF PASS,MAXIMUM 50
NSTAGE = 9

** INPUT JBEND (SELECTION OF CIRCULAR-ELEMENT BENDING OPTION,
(TYPE 0 IF SIMPLE ELEMENT DEFINITION, OR
      1 IF COMPOSITE PERCENTAGE ELEMENT DEFINITION)
JBEND = 0

** THE SECTION IS A SYMMETRICAL SECTION **
-----THUS INPUT THE FOLLOWING :
PASS      ELEMENT TO        ANGLE OF
 NO.     BE BENT(RIGHT)       BEND
   (terminate input by typing
     0        0                  0.0)
     1        2                 30.0
     2        2                 55.0
     2        4                -25.0
     3        2                 75.0
     3        4                -45.0
     4        2                 90.0
     4        4                -75.0
     5        2                 90.0
     5        4                -91.0
     6        2                100.0
     6        4                -95.0
     7        2                108.0
     7        4               -100.0
```

```
     8        2            116.0
     8        4           -110.0
     9        2            120.0
     9        4           -120.0
     0        0              0.0


** DO YOU WANT THE OPTION FOR SHARPENING OF INSIDE RADII ?
-- input JSHARP = 0 if radii-sharpening is not required
      1 if stage no. are to be entered individually, or
     -1 if all stages except last stage require sharpening
**** JSHARP =-1

** DO YOU WANT THE FIXED PERCENTAGE OPTION ?
INPUT THE FOLLOWING :-
LINE     RHS ELEMENT     STAGE NO     STAGE NO
NO.      NO.             START        FINISH
(skip or terminate the input for this option by typing :
        0        0                0           0)
     0        0        0       0
```

```
                ROLL DESIGN PROGRAM.

     --- ROLL NDESIGN PROGRAM VERSION 1.1 ---


                  *** ROLFOM ***
                      ******


            CHOOSE TERMINAL TYPE

                  1-VT125
                  2-T4107
                  3-T4105
                  4-T4010
        GINO-F MARK 2.7A 31/10/83

** INPUT THE SECTION NO.,PLEASE! **
    section no. = 1270


 * PLOTTING PROGRAM NO.4 FOR ROLLED-SECTION *


           --- ROLLER PROFILES ---


DO YOU WANT CONSISTENT PASS-HEIGHTS & C-C DISTANCE?
 INPUT IPASHT =  1 IF YES,OR
                -1 IF YOU WANT INCONSISTENT PASS HEIGHTS
                   AND C-C DISTANCE
 IPASHT = -1
PLEASE INPUT THE PASS HEIGHT (PASHT) AND C-C DISTANCE (CTOC)
  INPUT PASHT & CTOC FOR STAGE 1 PLEASE
     53.5      113.180
  INPUT PASHT & CTOC FOR STAGE 2 PLEASE
     53.5      120.800
  INPUT PASHT & CTOC FOR STAGE 3 PLEASE
     53.5      147.800
  INPUT PASHT & CTOC FOR STAGE 4 PLEASE
     53.5      152.600
  INPUT PASHT & CTOC FOR STAGE 5 PLEASE
     53.5      147.800
  INPUT PASHT & CTOC FOR STAGE 6 PLEASE
     53.5      147.800
  INPUT PASHT & CTOC FOR STAGE 7 PLEASE
     53.9      147.800
  INPUT PASHT & CTOC FOR STAGE 8 PLEASE
     54.6      149.100
  INPUT PASHT & CTOC FOR STAGE 9 PLEASE
     53.9      147.800

  PLEASE SPECIFY IF
      1- ONE SET OF TOLERANCES IS USED FOR ALL STAGES
   or -1- DIFFERENT TOLERANCES FOR EACH STAGE IS REQUIRED
  ITOC=1
```

```
    NOW INPUT THE TOLERANCES, WHERE
 TOLLH = LH TOLERANCE BETWEEN ROLLER & LAST ELEMENT,
 TOLRH = RH TOLERANCE BETWEEN ROLLER & LAST ELEMENT.
 INPUT TOLLH & TOLRH PLEASE
     0.1    0.1

INPUT JTEMP = 1 IF YOU WANT COMPONENT DRAWING IN HIDDEN LINE,
                  OTHERWISE 0
     RSCALE = DESIRED SCALE FOR THE ROLLER DRAWINGS
       RGAP = THE GAP DIMENSION BETWEEN TOP AND BOTTOM ROLL
NOW INPUT JTEMP,RSCALE & RGAP PLEASE
            0  1.0  10.0

INPUT JSTAGE(1) =-1 IF ALL STAGES REQ'D FOR ROLLERS,OR
      JSTAGE(1) = 1 IF NO STAGES REQ'D ,OR
      JSTAGE(1) = ANY POSITIVE INTEGER LESS THAN NSTAGE
                  IF SELECTED STAGES REQ'D FOR ROLLERS
JSTAGE(1)=-1

DO YOU WANT THE PINCH DEIFFERENCE OPTION?
INPUT JPINCH = 0 IF NO EXTERNAL PINCH DIFFERENCE DIMENSION
                 DEFINITION IS SUPPLIED, OR
   1 IF ONLY ONE PINCH DIFFERENCE DIMENSION DEFINITION
     IS SUPPLIED FOR ALL BENDING STAGES, OR
  -1 IF PINCH DIFFERENCE DIMENSION DEFINITION IS SUPPLIED
     INDIVIDUALLY FOR EACH BENDING STAGE, OR
   2 IF SINGLE THICKNESS OPTION WITH ONE COMMON CLEARANCE
     VALUE FOR ALL STAGES SELECTED, OR
  -2 IF SINGLE THICKNESS OPTION WITH INDIVIDUAL CLEARANCE
     VALUE FOR EACH STAGE SELECTED.
JPINCH=-1

INPUT THE PINCH DEFFERENCE DIMENSIONS,WHERE
  PDIM1 = THICKNESS BETWEEN THE DRIVE SURFACES
  PDIM2 = THICKNESS BETWEEN THE CLEARANCE SURFACES
 INPUT PDIM1 & PDIM2 FOR STAGE 1 PLEASE
     0.787  0.865
 INPUT PDIM1 & PDIM2 FOR STAGE 2 PLEASE
     0.787  0.914
 INPUT PDIM1 & PDIM2 FOR STAGE 3 PLEASE
     0.823  0.914
 INPUT PDIM1 & PDIM2 FOR STAGE 4 PLEASE
     0.838  0.914
 INPUT PDIM1 & PDIM2 FOR STAGE 5 PLEASE
     0.838  0.914
 INPUT PDIM1 & PDIM2 FOR STAGE 6 PLEASE
     0.838  0.914
 INPUT PDIM1 & PDIM2 FOR STAGE 7 PLEASE
     0.838  0.914
 INPUT PDIM1 & PDIM2 FOR STAGE 8 PLEASE
     0.838  0.914
 INPUT PDIM1 & PDIM2 FOR STAGE 9 PLEASE
     0.838  0.914

 NOW INPUT ELEMENT NO. WHICH DEFINES DRIVE SURFACE
  2 DEFINITION STATEMENTS PER STAGE REAUIRED,WHERE
    ISQP=CURRENT BENDING STAGE SEQUENCE NO.
 IEPL = L.H.S. ELEMENT DEFINING THE DRIVE SURFACE CONTOUR
 IEPR = R.H.S. ELEMENT DEFINING THE DRIVE SURFACE CONTOUR
   (TERMINATE INPUT BY TYPING  0  0  0)
```

```
      ISQP  IEPL  IEPR
       1     1     1
       1     1     1
       2     1     1
       2     1     1
       3     1     1
       3     1     1
       4     1     1
       4     1     1
       5     1     1
       5     1     1
       6     1     1
       6     1     1
       7     1     1
       7     1     1
       8     1     1
       8     1     1
       9     1     1
       9     1     1
       0     0     0

     **THE NEW PINCH OPTION**
PLEASE INDICATE WHERE THE CLEARANCE TO BE ADDED
     ENTER 1 FOR OUTSIDE FACES
           2 FOR INSIDE FACES
       OR  3 IF EQUALLY DISTRIBUTED ON BOTH FACES
(1/2/3) 3

ARE YOU GOING TO CHOOSE THE SIDE ROLL OPTION?
 ENTER ISROL = 1 IF YES,OR
             = 0 IF NO
ISROL = 1

ENTER IOTOS = 1 IF CONSISTENT ORIGIN TO SIDE-ROLL AXES
 -1 IF INCONSISTENT ORIGIN TO SIDE-ROLL AXES DISTANCES
IOTOS = -1

 INPUT ORIGIN TO SIDE-ROLL AXES DISTANCE,WHERE
  OTOSL = DISTANCE BETWEEN ORIGIN AND LEFT SIDE-ROLL CENTRE
  OTOSR = DISTANCE BETWEEN ORIGIN AND RIGHT SIDE-ROLL CENTRE.
 INPUT OTOSL & OTOSR FOR STAGE 1 PLEASE
       100.0   100.0
 INPUT OTOSL & OTOSR FOR STAGE 2 PLEASE
       100.0   100.0
 INPUT OTOSL & OTOSR FOR STAGE 3 PLEASE
       106.0   106.0
 INPUT OTOSL & OTOSR FOR STAGE 4 PLEASE
       98.5    98.5
 INPUT OTOSL & OTOSR FOR STAGE 5 PLEASE
       90.5    90.5
 INPUT OTOSL & OTOSR FOR STAGE 6 PLEASE
       96.5    96.5
 INPUT OTOSL & OTOSR FOR STAGE 7 PLEASE
       100.0   100.0
 INPUT OTOSL & OTOSR FOR STAGE 8 PLEASE
       90.5     90.5
 INPUT OTOSL & OTOSR FOR STAGE 9 PLEASE
       90.5     90.5
```

```
INPUT THE SIDE-ROLL CONTOUR DEFINITION, WHERE
ISQS  = CURRENT BENDING STAGE SEQUENCE NO.,
IESL1 = L.H.S. ELEMENT CONSTITUTING L.H.S. SIDE-ROLL CONTOUR,
IESL2 = WHICH FACE OF THE L.H.S. ELEMENT IS DESIRED,
IESR1 = R.H.S. ELEMENT CONSTITUTING R.H.S. SIDE-ROLL CONTOUR,
IESR2 = WHICH FACE OF THE R.H.S. ELEMENT IS DESIRED.
 INPUT ISQS,IESL1,IESL2,IESR1 & IESR2 PLEASE
       (TERMINATE INPUT BY TYPING
            0  0  0  0  0 )
    3  2  1  2  1
    3  5  4  5  4
    4  2  1  2  1
    4  5  4  5  4
    5  2  1  2  1
    5  5  4  5  4
    6  2  1  2  1
    6  5  4  5  4
    7  2  1  2  1
    7  5  4  5  4
    8  2  1  2  1
    8  5  1  5  1
    9  2  1  2  1
    9  5  1  5  1
    0  0  0  0  0

INPUT SELECTION FOR EXTENSION-CONTOUR OPTION,ENTER
 IEXTN = 1 IF EXTENSION CONTOUR OPTION WILL BE USED
       = 0 IF EXTENSION CONTOUR OPTION WILL NOT BE USED
IEXTN = 1

INPUT TYPE AND DIMENSION FOR EACH DESIGNATED SIDE-CONTOUR
      EXTENSION, WHERE
  ISC1 = SIDE-CONTOUR NO.
  ISC2 = SIDE-CONTOUR TYPE
  SCDIM1 = DIMENSION DEFINITION FOR SIDE-CONTOUR PART 1
  SCDIM2 = DIMENSION DEFINITION FOR SIDE-CONTOUR PART 2
  SCDIM3 = DIMENSION DEFINITION FOR SIDE-CONTOUR PART 3
  SCDIM4 = DIMENSION DEFINITION FOR SIDE-CONTOUR PART 4
      (TERMINATE INPUT BY TYPING
         0  0  0.0  0.0  0.0  0.0 ),NOW INPUT
   ISC1  ISC2  SCDIM1  SCDIM2  SCDIM3  SCDIM4
    1     3     9.5     9.5     8.0     13.0
    2     3     9.0    12.7     8.0     19.0
    3     1     0.0     9.5    35.0      0.0
    4     1     0.0     4.5    21.0      9.5
    5     1     0.0     9.5    31.0      0.0
    6     1     8.0    11.5    12.5      0.0
    7     1     0.0     9.5    20.5      0.0
    8     1     0.0     0.0    10.0      9.5
    9     1     0.0     9.5    28.0      0.0
   10     1     6.5     8.5    12.0      0.0
   11     1     0.0     9.5    19.5      0.0
   12     1     0.0     0.0     8.0      9.5
    0     0     0.0     0.0     0.0      0.0


INPUT SIDE-CONTOUR SELECTION FOR EACH BENDING STAGE WHERE
ISQD  = BENDING STAGE NO. FOR WHICH SIDE-CONTOUR DEFINITION
        IS INTENDED
```

```
IELD1 = TYPE OF SIDE-CONTOUR ON L.H.S.
IELD2 = SIDE-CONTOUR NO. WHICH HAS BEEN DEFINED PREVIOUSLY
        AND IS TO BE SELECTED FOR THIS STAGE NO. ON L.H.S.
IERD1 = TYPE OF SIDE-CONTOUR ON R.H.S.
IERD2 = SIDE-CONTOUR NO. WHICH HAS BEEN DEFINED PREVIOUSLY
        AND IS TO BE SELECTED FOR THIS STAGE NO. ON R.H.S.
     (TERMINATE INPUT BY TYPING
           0  0  0  0  0 ),NOW ENTER
    ISQD  IELD1  IELD2  IERD1  IERD2
     1      3      1      3      1
     2      3      2      3      2
     3      1      4      1      4
     3      1      3      1      3
     4      1      6      1      6
     4      1      5      1      5
     5      1      8      1      8
     5      1      7      1      7
     6      1     10      1     10
     6      1      9      1      9
     7      1     10      1     10
     7      1      9      1      9
     8      1     12      1     12
     8      1     11      1     11
     9      1     12      1     12
     9      1     11      1     11
     0      0      0      0      0

        ** INPUT FILE ENDS **
```

The output data files generated by ROLFOM.

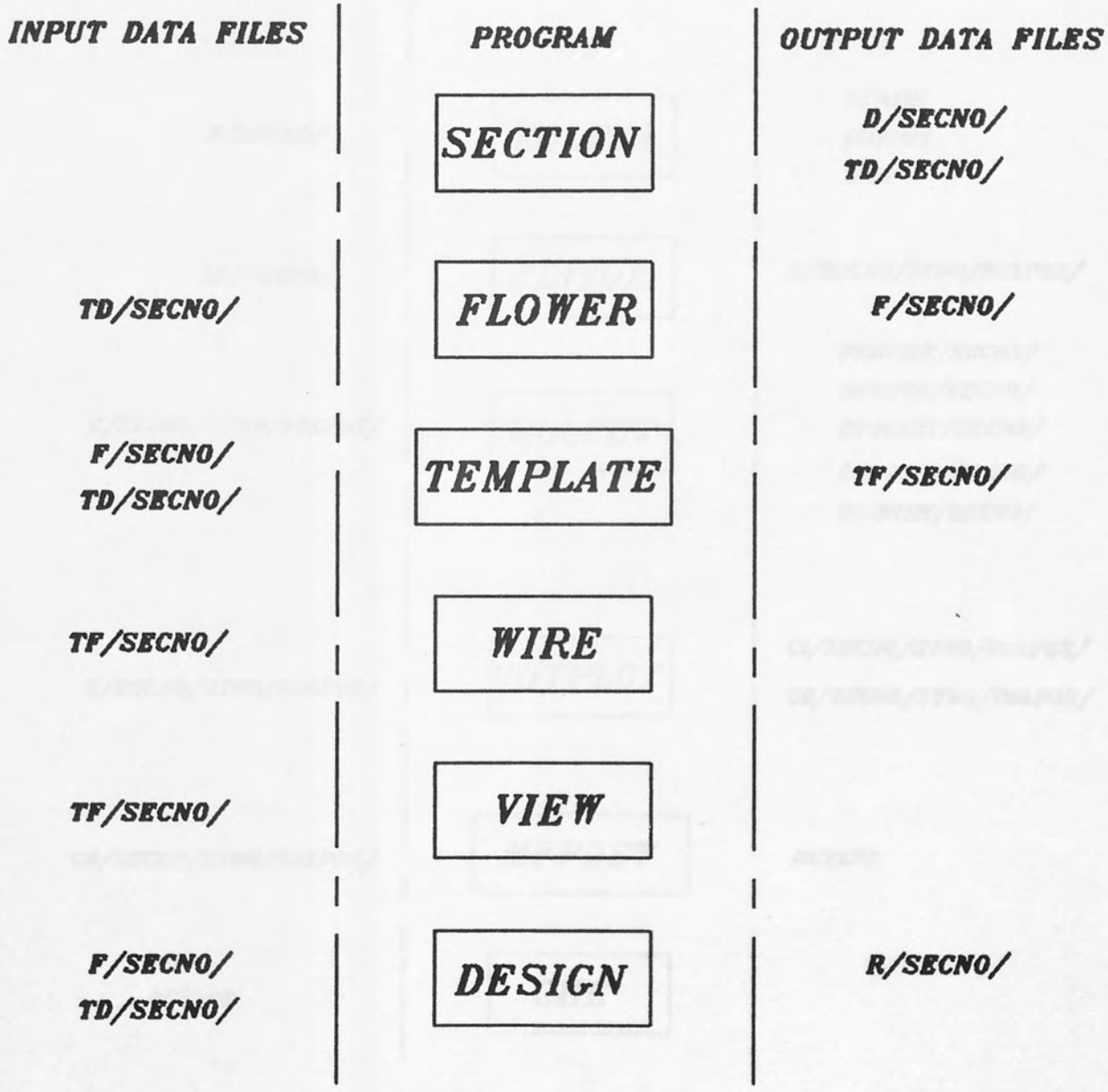

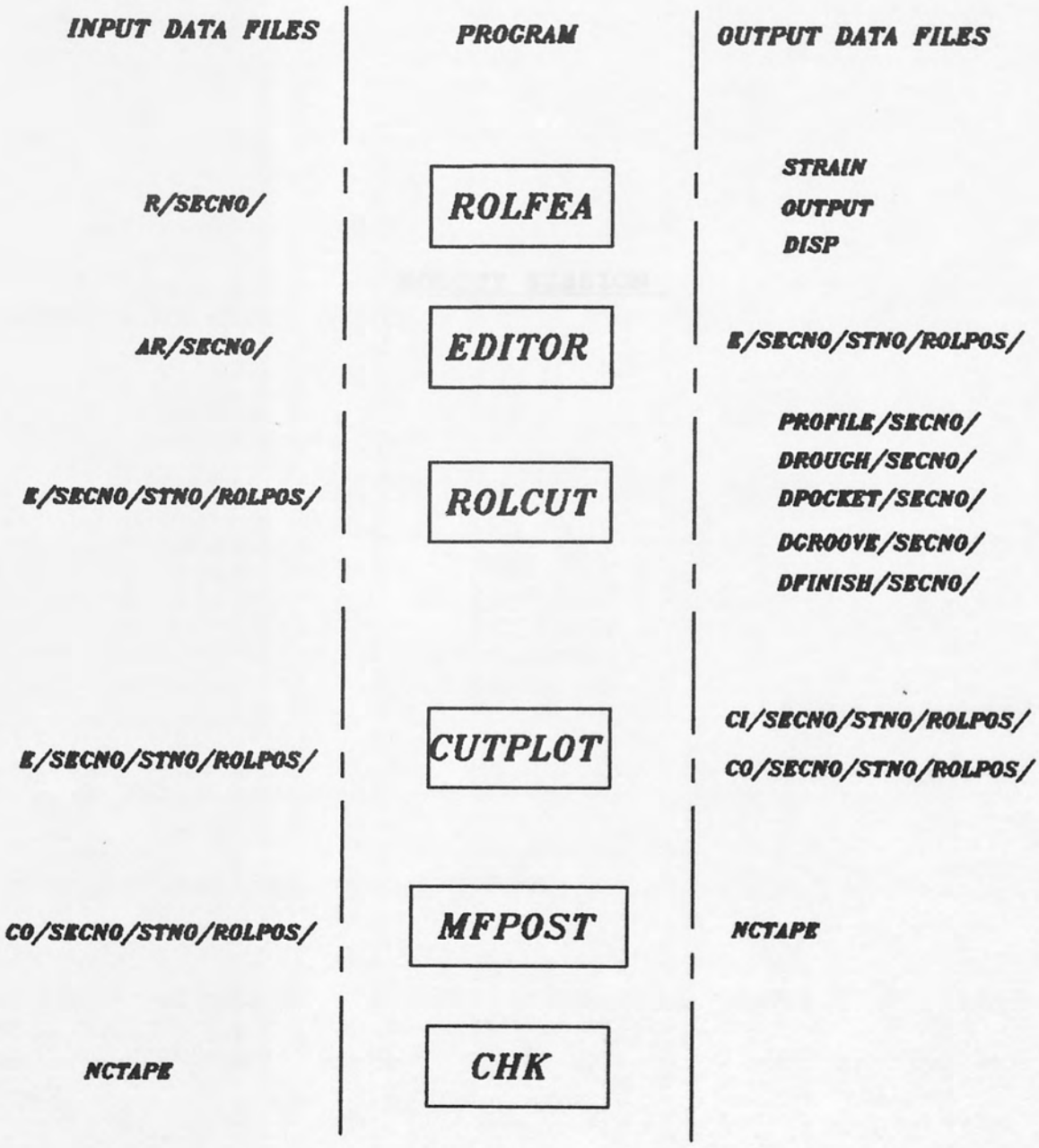
INPUT DATA FILES
PROGRAM
OUTPUT DATA FILES
R/SECNO/
ROLFEA
STRAIN
OUTPUT
DISP
AR/SECNO/
EDITOR
E/SECNO/STNO/ROLPOS/
E/SECNO/STNO/ROLPOS/
ROLCUT
PROFILE/SECNO/
DROUGH/SECNO/
DPOCKET/SECNO/
DGROOVE/SECNO/
DFINISH/SECNO/
E/SECNO/STNO/ROLPOS/
CUTPLOT
CI/SECNO/STNO/ROLPOS/
CO/SECNO/STNO/ROLPOS/
CO/SECNO/STNO/ROLPOS/
MFPOST
NCTAPE
NCTAPE
CHK

Appendix 2.

ROLCUT SESSION.

```
PLEASE INPUT THE SECTION NUMBER TO BE USED

708

The amount for the final finish cut is given a default
value of 0.5mm if this is acceptable please input -1
otherwise input the finish cut value

  -1

    ******************************************
    **                                      **
    **         TERMINAL DEFINITION          **
    **              1)   T4010              **
    **              2)   T4107              **
    **              3)   T4113              **
    **              4)   T4014              **
    **              5)   T4105              **
    **                                      **
    ******************************************


**PLEASE INPUT THE TERMINAL TYPE (either 1,2,3,4 OR 5)**

        2


    ***********************************************
    **                                           **
    **    Please enter either -:                 **
    **    0  for TLIB0  - TOOL LIBRARY 0         **
    **    1  for TLIB1  - TOOL LIBRARY 1         **
    **    2  for TLIB2  - TOOL LIBRARY 2         **
    **    3  for TLIB3  - TOOL LIBRARY 3         **
    **    4  for TLIB4  - TOOL LIBRARY 4         **
    **    5  for TLIB5  - TOOL LIBRARY 5         **
    **    6  for TLIB6  - TOOL LIBRARY 6         **
    **                                           **
    ***********************************************


THE TOOL LIBRARY REQUIRED IS NUMBER

    1

 CONTOUR     CONTOUR       LENGTH     ANGULAR   CENTRE COORDINATES
  NUMBER       TYPE     OR RADIUS       DISP.        Z            X
(INTEGER)  (INTEGER)     (REAL)        (REAL)    (REAL)       (REAL)
    1          1           80            90         0            0
    2          2           5             90         5            80
    3          1           20             0         0            0
    4          2           5             90        25            80
    5          1           30           270         0            0
    6          2           5            -90        35            50
    7          1           50             0         0            0
    8          2           5             90        85            40
    0          0           0              0         0            0
```

DATA GENERATION STARTED

***** GEOMETRICAL WARNING! *****

YOU HAVE NOT DEFINED THE LAST CONTOUR CORRECTLY EITHER
THE ANGLE OF THE LAST CONTOUR IS NOT 270 DEG. OR THE LENGTH
OF THE CONTOUR DOES NOT COINSIDE WITH THE CENTRE-AXIS.
THESE ERRORS WILL BE CORRECTED AUTOMATICALLY.

PLEASE INPUT THE OUTSIDE DIAMETER OF THE BLANK IN MM

100.0

DATA GENERATION COMPLETED

(PROFILE708.DAT CREATED)

DO YOU WISH TO DRAW THE PROFILE;   ANSWER Y OR N *

N

**PLEASE INPUT Y TO PROCEDE WITH THE ROUGHING CYCLE; OR
INPUT N TO QUIT***

N

```
@@@@@@@@@@@@@@@@@@@@@@@@@@@@@@@@@@@@@@@@@@@@@@@@@@@@@
@@                                                 @@
@@                                                 @@
@@     INPUT                OPTIONS                @@
@@                                                 @@
@@       0       for      PROFILE ONLY             @@
@@       1       for      ROUGHING CYCLE           @@
@@       2       for      POCKETING CYCLE          @@
@@       3       for      GROOVING CYCLE           @@
@@       4       for      FINISHING CYCLE          @@
@@       5       for      ALL CYCLES COMBINED      @@
@@       6       to       CHANGE SECTION NO.       @@
@@       7       to       SELECT NEW TOOL LIBRARY  @@
@@       8       to       ALTER FINAL FINISH CUT   @@
@@      99       to       EXIT                     @@
@@                                                 @@
@@                                                 @@
@@@@@@@@@@@@@@@@@@@@@@@@@@@@@@@@@@@@@@@@@@@@@@@@@@@@@
```

Please input your option 99

OFFSET RULES

These rules are derived from straight line and circular arc formulas in Cartesian Coordinates.

(1) Intersection of Two Straight Lines.

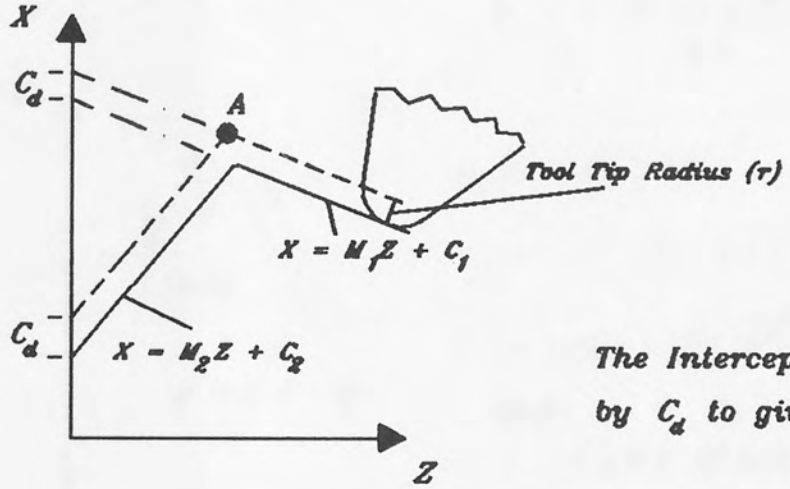

The Intercept values are altered by C_d to give :-

$$Z_A = \frac{(C_2 - C_1) + r\sqrt{(M_1^2 + 1)} + r\sqrt{(M_2^2 + 1)}}{(M_1 - M_2)}$$

and

$$X_A = M_1 Z_A + C_1$$

(2) Intersection of a Straight Line and a Circular Arc.

Firstly a test is carried out to establish whether the Straight Line is vertical. This automatically sets the value of Z

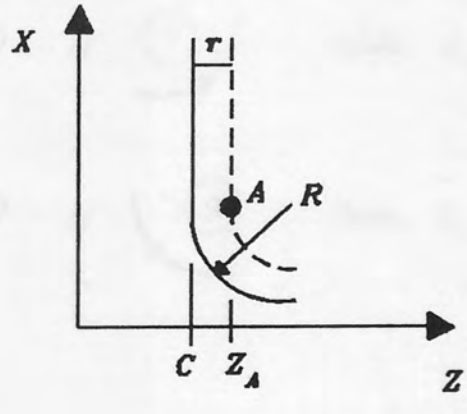

If Contour Code = 2 Then

$$Z_A = C - r$$

Else

If Contour Code = 6 Then

$$Z_A = C + r$$

If the Straight Line is not Vertical then solution of the following quadratic equation is required.

$$Z_A = \frac{-B \mp \sqrt{B^2 + 4.A.D}}{2.A}$$

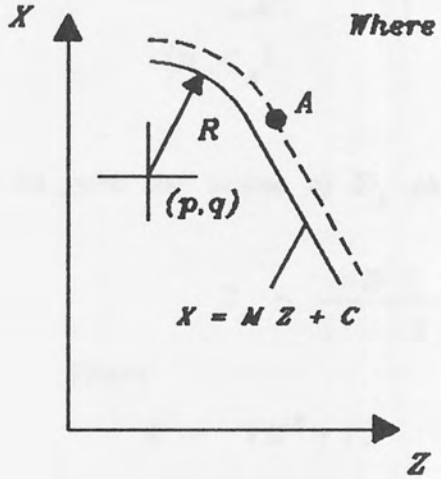

Where

$$A = (M^2 + 1)$$

$$B = 2M\,(C + r\sqrt{(M^2 + 1)} - q) - 2p$$

$$D = (C + r\sqrt{(M^2 + 1)} - q)^2 - E + p^2$$

and

$E = (R + r)$ *if arc contour code = 3 or 8*

Else

$$E = (R - r)$$

Knowing Z_A *the* X_A *value is calculated according to the Arc Contour Code.*

2) *If* (3) *Then* $X_A = \sqrt{(C + r)^2 - (Z_A - p)} + q$

3) *If* (8) *Then* $X_A = \sqrt{(C + r)^2 - (p - Z_A)} + q$

4) *If* (9) *Then* $X_A = q + \sqrt{(C - r)^2 - (Z_A - p)}$

5) *If* (4) *Then* $X_A = q + \sqrt{(C - r)^2 - (p - Z_A)}$

(3) Intersection of Two Circular Arcs.

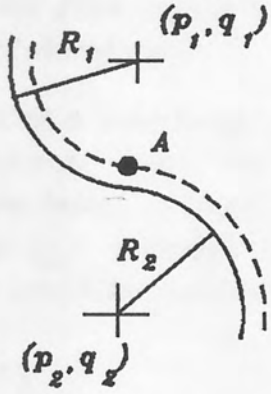

Thr Subscripts $_1$ and $_2$ are used to indicate the different arcs

To find the value of Z_A the quadratic equation is solved.

$$Z_A = \frac{-B \mp \sqrt{B^2 + 4.A.D}}{2.A}$$

Where

$$A = (M^2 + 1)$$

$$B = 2(M\,C - M\,q_1 - p_1)$$

$$D = p_1^2 + (q_1 - C)^2 - E_1^2$$

and

$$M = \frac{p_1 - p_2}{q_2 - q_1}$$

$$C = \frac{E_1^2 - E_2^2 - p_1^2 - q_1^2 + q_2^2 + p_2^2}{2(q_2 - q_1)}$$

The value of E_1 and E_2 will depend on the contour code of the arcs

If Contour Code = 3 or 8 Then $E = (R + r)$

Else

$$E = (R - r)$$

The value of X_A is dependent on the contour code of the second arc and is found by implimenting rules 2 to 5 described in the previous section.

The Pocket Rules.

The following rules are applied by the "Pocket" Program to enable recess regions with complicated geometry to be machined.

(1) The recess regions of the profile are analysed from right to left, (i.e. the first region to be studied is the one at the extreme right hand side)

(2) To test if a protrusion occurs within the recess region the X coordinate values are examined, (i.e. Referring to the diagram below, a study of the X coordinates will establish that contour (7) protrudes above contours (5) . (6) and (8) . (9) If this condition occurs then apply Rule (2a) Else Goto Rule (3)

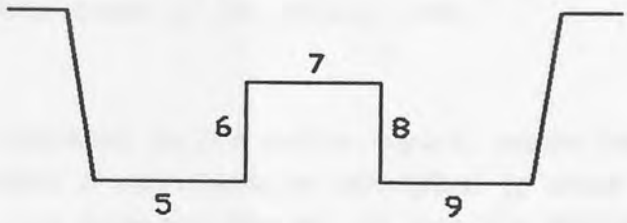

(2a) To test if a protrusion involves a "Shoulder Stop" a study of the geometry is carried out to identify the occurrance of a contour with a length similar to that shown below.

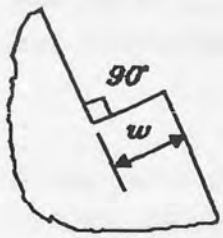

If w is less than the sheet thickness + 2 mm then the "Shoulder" rules are invoked.

(3) To control the positioning of the dig_in line the point H shown in diagram (a) below is calculated.

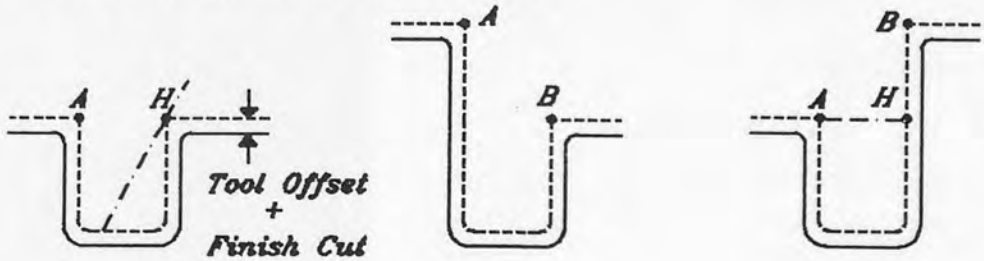

(a) *(b)* *(c)*

If the X coordinate of point A is equal to or greater than that of point B {as shown in diagrams (a) and (b)} then H = B
If it is less than point B then H must be repositioned as shown in diagram (c), with its X coordinate equal to that of point A.

(4) The dig_in line is positioned by the stipulation that it passes through point H and its angle is 2 degrees greater than the trailing angle of the cutting tool.

(5) The contour, in the recess region, whose starting point has the smallest X coordinate is identified. If other contours apart from this one intersect the dig_in line the POCKET_CRASH rules are invoked to check if the dig_in line location needs adjustment.

(6) The POCKET_CRASH Rules are invoked to investigate any general tool obstructions. This is done for every pocket machining cycle.

(7) If the possibility of a tool obstruction is not detected by the POCKET_CRASH Rules, the pocket machining cycle is applied to the recess region in the normal manner.

Pocket_Crash Rules.

The following rules investigate the possibility of tool obstruction during the pocket machining cycle. Information regarding the tool geometry is obtained by reference to the TOOLIB program.

(1) An investigation is carried out to establish if the dig_in line needs to be relocated further to the left of the recess region The diagram below shows a situation where the point H, which the dig_in line passed through, is moved towards the right to avoid tool obstruction

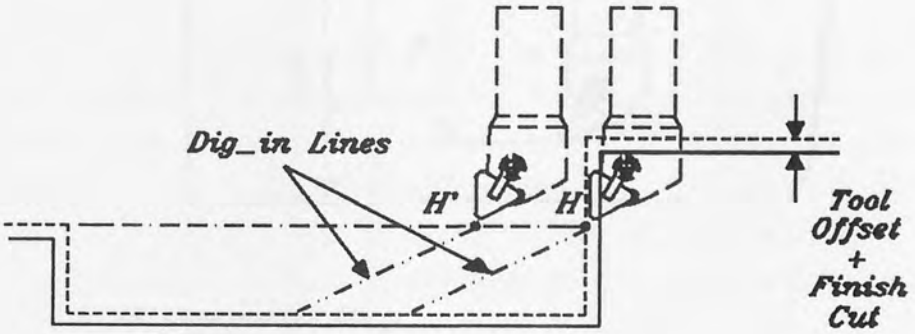

(2) The contour which the dig_in line intersects is compared to the contour with the smallest X coordinate. If the contour number of the latter is greater than the former then a situation similar to the one shown below is found. The dig_in line is moved towards the left so that the pocket cycle can remove more material from the recess region.

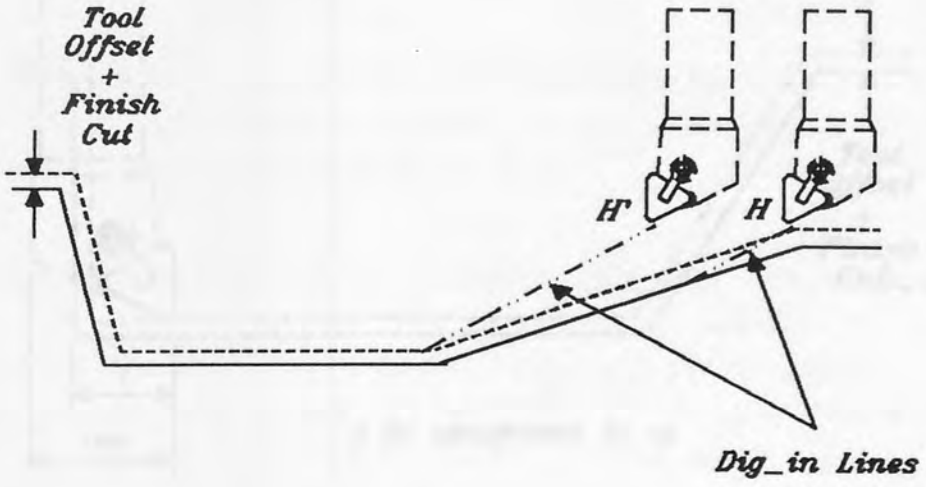

(3) The distance the tool protrudes from the turret toolpost is an important characteristic. A recess region may be too deep to fully machine, as the diagram below indicates. The Pocket_ Crash Rules identifies this situation and the depth which the pocket machining cycle reaches is limited to avoid obstructions.

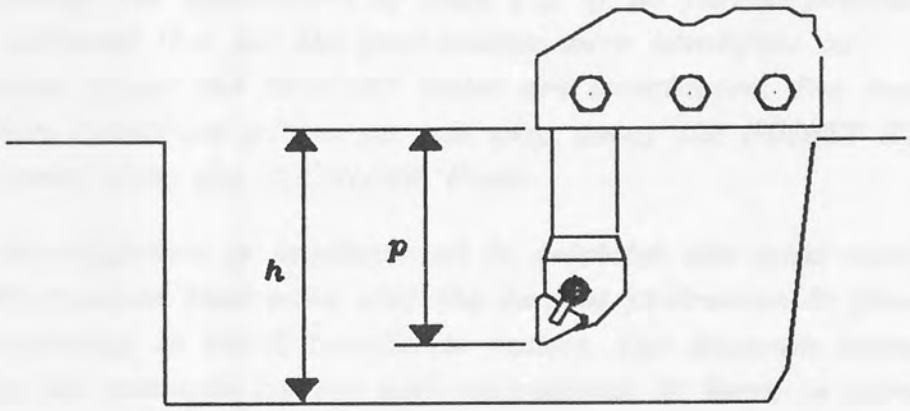

h is compared to p

(4) The possibility of tool obstruction caused by the R.H. pocket tool must also be investigated. As the following diagram shows the size of the tip toolholder can limit the width of recess that the pocket cycle can machine. If the situation shown in the following diagram occurs the recess is machined by the Groove cycle.

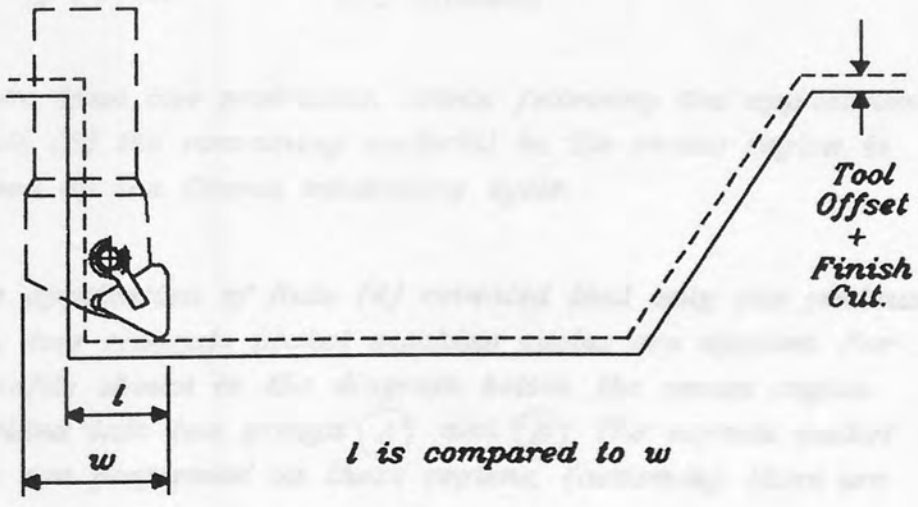

l is compared to w

XPOCKET RULES.

The following rules enable recess regions involving shoulder stops or complicated profiles to be machinined.

(1) The possibility that a protrusion within the recess region is a "shoulder stop" (or has very similar geometric features to a shoulder stop) is investigated. If this is the case the "SHOULDER" Rules will be invoked.

(2) Following the application of Rule (1), if no further protrusions are detected (i.e. all the protrusions were identified as shoulder stops) the XPOCKET Rules are terminated. The recess is then machined in the normal way using the POCKET Rules combined with the SHOULDER Rules

(3) An investigation is implimented to establish the total number of protrusions that exist and the largest protrusion is found by referring to the X coordinate values. The diagram below shows an example having two protrusions. If there is more than one protrusion the "POCKET" Rules are invoked which will machine to a depth according to the largest protrusion (as shown below)

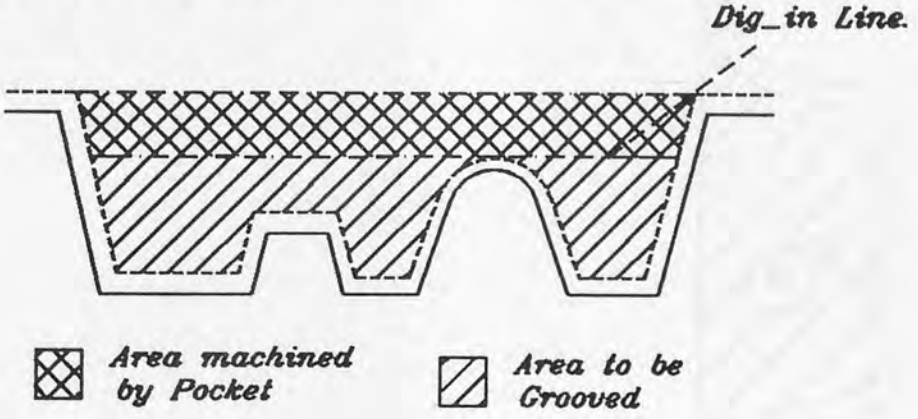

(4) If more than one protrusion exists, following the application of Rule (3) the remaining material in the recess region is removed by the Groove machining cycle.

(5) If the application of Rule (4) revealed that only one protrusion exists, two separate pocket machine cycles are applied. For the profile shown in the diagram below, the recess region is divided into two groups (A) and (B). The normal pocket cycles are performed on these regions, (assuming there are no tool obstructions).

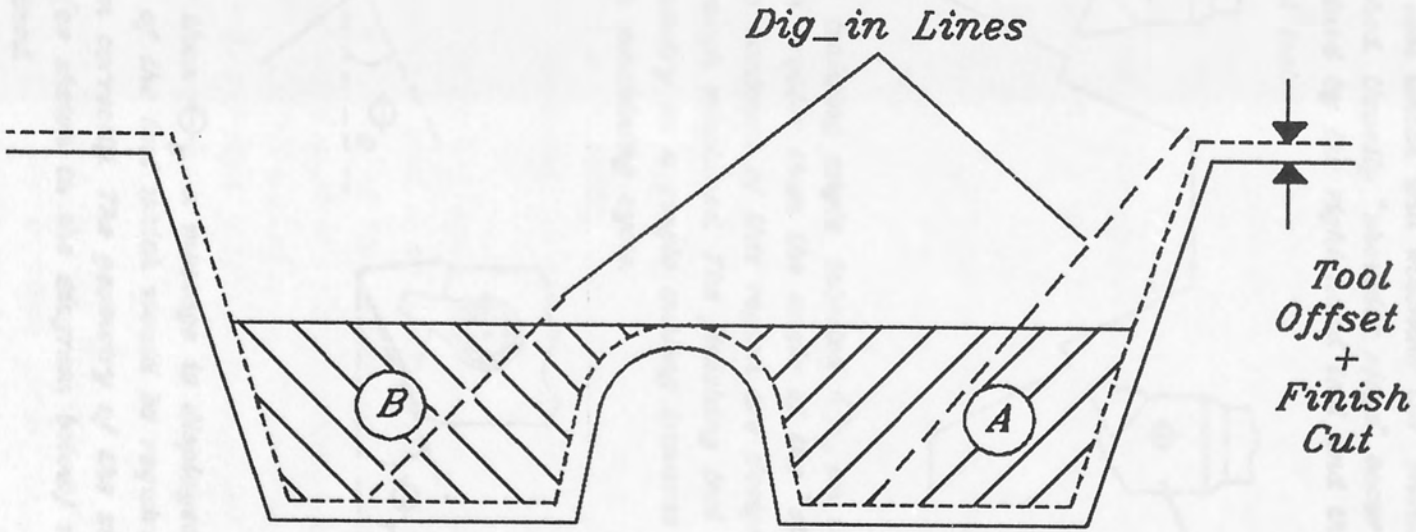
Dig_in Lines
B
A
Tool
Offset
+
Finish
Cut

Shoulder Rules.

The following rules allow small geometric irregularities in the profile to be efficiently machined.

(1) The hand of the tool which will machine the "shoulder stop" region is established. Usually "shoulder stops" occur in pairs and one is machined by the right hand tool and the other using a left hand tool.

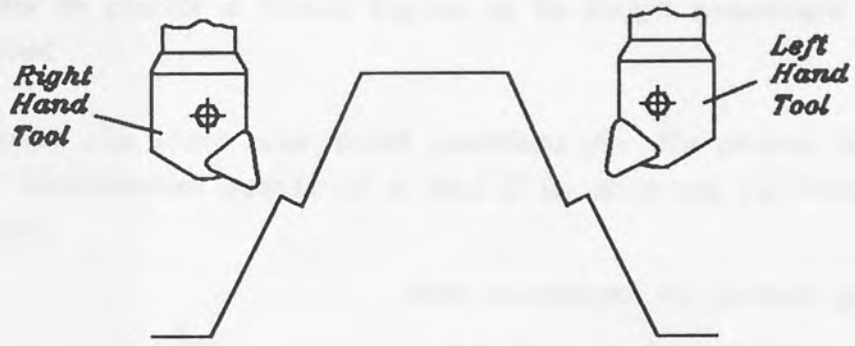

(2) If the finish tool trailling angle, labelled Θ_T on the diagram below, is greater than the angle of the "step" contour, Θ_C, the contours of this region are designated as having been rough machined. The finishing tool will generate this geometry in a single cutting traverse using the normal finish machining cycle.

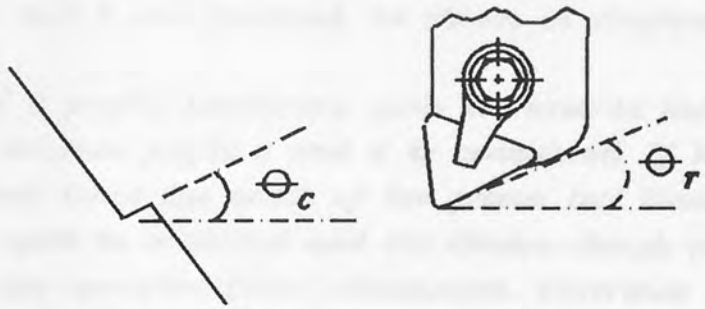

(3) If Θ_T is smaller than Θ_C a message is displayed stating the trailing angle of the tool which would be required to machine the region correctly. The geometry of the step would then be modified (as shown in the diagram below) so that the step can be machined.

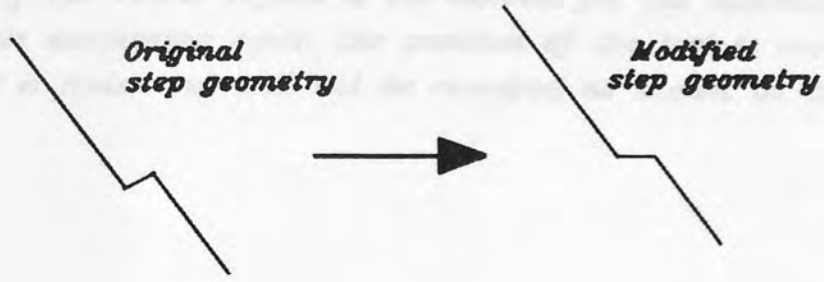

Groove Program.

The groove machining cycle can be divided into two fundamentally different machining processes. The groove tool first rough machines the recess and then produces the specified final dimensions by applying a single profile machining cycle.

The following rules are applied by the GROOVE-ROUGH subroutine to enable a recess region to be rough machined by the groove tool.

(1) To define the start and finish positions for the groove tool the offset intersection points at A and B in diagram (a) below are obtained.

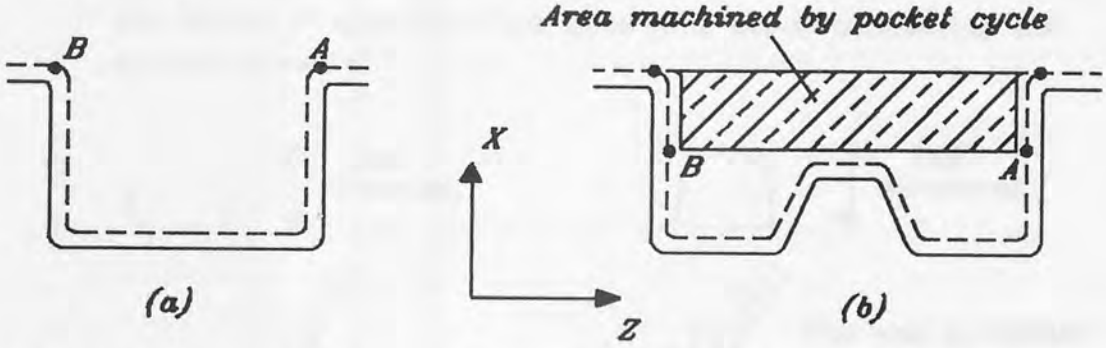

If the recess region has been partly machined by a pocket cycle the points A and B are relocated, as shown in diagram (b).

(2) To test if a profile machining cycle is required the horizontal distance between points A and B is considered. If this distance is less than twice the width of the groove tool blade, a profile machine cycle is ommitted and the Groove-Rough routine directly produces the specified finish dimensions. Otherwise material is left on by the Groove-rough program to provide a finish cut for the Groove profile program.

(3) Prior to commencement of the cutting traverse the groove tool is moved at rapid speed to the location shown in the diagrams below. If the recess region is too narrow for the application of a profile machining cycle, the position of the tool is modified so that a finish cut will not be required as shown in diagram (b)

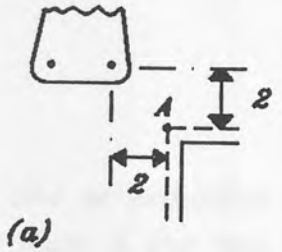

(a)

All dimensions in mm

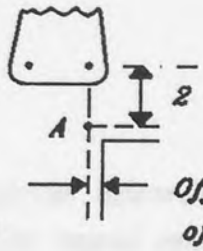

(b)

Offset path of groove tool

(4) To control the depth of the cutting traverse the points E and F shown in diagram (a) below are calculated. If both points coincide with the offset path of the same contour, the one with the largest X–coordinate will determine the termination of the cutting traverse.

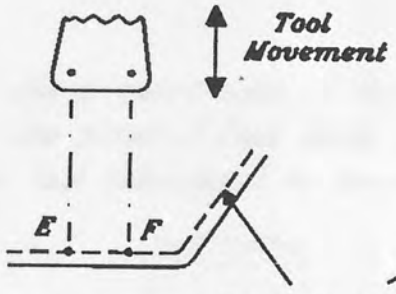

Tool Offset path plus finish cut (if applicable)

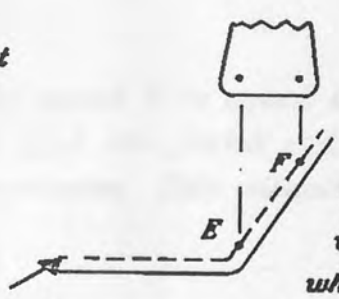

Tool will terminate its cutting traverse when it reaches the X coordinate of point F

(5) If points E and F intersect the offset path of different elements, as shown below, the X coordinate of all the offset path elements that intersect between points E and F are calculated. The largest X coordinate of the points E, F and C in the example below will determine the termination of the cutting traverse

Tool Offset path plus finish cut (if applicable)

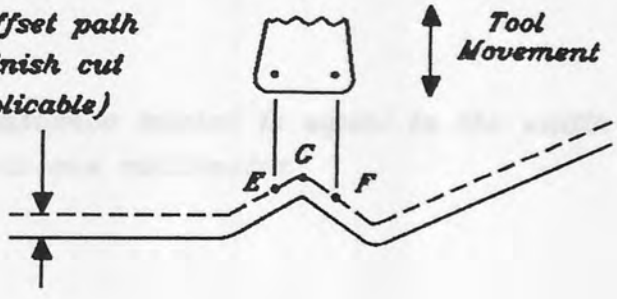

(6) Following the termination of the cutting traverse according to Rule 4 or Rule 5 the tool is traversed back at rapid speed to its position before the cutting traverse commenced.

(7) When Rule 6 has been completed the tool is moved horizontally towards the left to position it for the next cutting traverse. The horizontal movement is terminated when either of the following two conditions are applicable.

a) If the Z coordinate of the point C is equal to the Z coordinate of the point B (see Rule 1) + the finish cut, if applicable, then the tool movement is terminated. This situation is shown below.

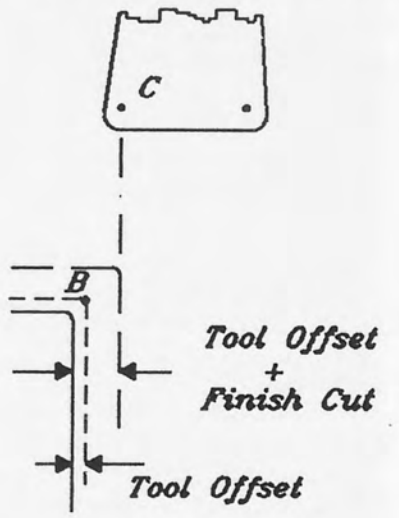

b) The total distance moved is equal to the width of the cutting blade, minus one millimetre.

Appendix 3.

ROLFE A SESSION.

```
The following data is required :-

      The SECTION NUMBER

      The STAGE NUMBER

      The TERMINAL TYPE

The TERMINAL TYPE is categorised into four main groups

   ****************************************
   **                                    **
   **      GROUP          TYPE           **
   **                                    **
   **        1     for    T4014          **
   **        2     for    T4107          **
   **        3     for    T4113          **
   **        4     for    T4105          **
   **                                    **
   ****************************************


Please input the SECTION NUMBER : 1100


Please input the STAGE NUMBER : 2


Please input the TERMINAL TYPE : 2


Please indicate whether this SECTION and STAGE number
         has already been processed.

Please input
               Y for YES
      or
               N for NO

CHOICE : N


This program will only work if the SFLOWER program
has been run during this session for the required section
number.
  The SFLOWER program will be run automatically if the
answer to the following question is NO

   Has the SFLOWER been run-:
               Y for YES
    or         N for NO


CHOICE : Y

PLEASE INPUT THE INTERPASS DISTANCE IN METRES
  0.24
```

```
This program can create either :-
  A) A complete PAFEC data file to run an elastic model OR
  B) A data input file to be run on the tailored finite
     element package using an elasto-plastic model.

Please indicate which analysis is required. A) OR B)

B

Please input the number of nodes in each element.
  Either a 4 or 8 noded element can be used.
(Note: an 8 noded element will be more accurate but
  will take longer to process)

8

Is the AUTOMATIC system of defining the number of elements
along the longitudinal X axis
(Users who are unfamiliar with the package should input
 Y for YES)

Y

PLEASE INPUT THE CONTOURS WHICH ARE TO BE DRIVEN ON STAGE
NUMBER 2
   Input ZERO when finished.
(To obtain the default values taken from the ROLFOM system.
 PLEASE INPUT -1)

 -1

The materials available are -:
MATERIAL  MATERIAL  YOUNG'S   POISSON'S  UNIAXIAL    STRAIN
  NAME     NUMBER   MODULUS     RATIO     YIELD     HARDENING
                  (IN N/M*M)              STRESS      RATE
STEEL        1      0.21E+12    0.30     0.80E+06  0.000E+00
 CR3         2      0.209E+12   0.25     0.28E+09  0.100E+15
 CR4         3      0.209E+12   0.50     0.23E+09  0.100E+15
 CR5         4      0.209E+12   0.34     0.23E+09  0.120E+15
 CR6         5      0.456E+13   0.46     0.37E+11  0.128E+18
COPPER       6      0.209E+12   0.67     0.45E+10  0.120E+15

You can choose either a material number as shown, OR by
      7 is used a new material can be defined.

 3

Please input the title of the job
     ( a maximum of 40 characters can be used)

  SECTION 1100 STAGE 2

Automatic default values can be used for the following
data.
    Tolerance= 3
    Maximum number of iterations= 45
    Output code at beginning of each load increment= 3
    Output code at end of program= 3
PLEASE INPUT 0 TO ACCEPT THE DEFAULT VALUES.
  For more information on the above parameters or to
  alter their default values.
```

```
PLEASE INPUT 1

 1

 PLEASE INPUT VALUES FOR THE FOLLOWING PARAMETERS
  TOLERANCE -:This value will control the accuracy of the
  final answer. For example suppose a tolerance value of 2
  is chosen, if the answer providedby the current iteration
  process is within 2% of the answer provided by the last
  iteration carried out, the criteria for convergence is
  satisfied.
  (Note: anything less than 1% will result in a long process
  time and anything greater than 10% is likely to result in
  unacceptable inaccuracies)

 TOLERANCE= 6


 MAXIMUM NUMBER OF ITERATIONS -:This acts as a safety
  measure so that if anything goes wrong the iteration
  process will not continue indefinitely.
    (A value between 10 to 60 is suggested)

 MAXIMUM NUMBER OF ITERATIONS= 60


 OUTPUT CODES -:In order to keep a check on the
  convergency of the iterative process the output can be
  displayed at the beginning and end of each load increment.
  The output format is described by the following codes -:
       0- for no output
       1- for displacements only
       2- for displacements and reactions
       3- for displacements, reactions and strains
   (Note: all the displacements and strains are
  automatically written to data files at the end of the
  analysis, so this data is never lost)

 OUTPUT CODE AT BEGINNING OF EACH LOAD INCREMENT= 1

 OUTPUT CODE AT END OF EACH LOAD INCREMENT= 1

 To analyse material non-linearity, the loading is applied
   in small increments.
    INPUT Y if the automatic default values are required
  for the load increment
 For more information on the load increment values, or
 to alter their default values, PLEASE INPUT N

 N

  By default the number of load increments is 20. Each
  load increment has the same value of 0.05. This means
  that for the first load increment a load which is 5% of
  the total load is applied. For the second increment a
  further 5% is added. Thus after the second load increment
  10% of the total load is applied to the structure. This
  procedure is continue until all the load increments have
  been applied. Thus it is clear that to apply the total
  load then all the load increments must add up to ONE.
```

```
  In order to save time if the default values are still
 required then INPUT -1 for the number of load increments

Please input the number of load increments= 2

  Please input the  1 load increment= 0.5
  Please input the  2 load increment= 0.5

The data file has now been completed and is ready for
analysis.
      Do you wish to continue with the analysis?


Input : Y

   Which type of analysis is required

    A) for the PAFEC package

    B) for the tailor-made Finite Element package.


Input either A or B


Input : B


    You have chosen the tailor-made Finite Elements
  package as an initial check of the data it is possible
  to draw a wire-frame model of the structure in it's
  original position. By carrying out this check of the
  input data a great deal of time can be saved when things
  go wrong.


Please indicate Y[es] or N[o] whether this plot is
required.

Input : Y

Has the DISPLACEMENTS been found yet Y or N

N


     ****************************************
     **                                    **
     **       TERMINAL DEFINITION          **
     **      PLEASE INPUT  1,2,3,4         **
     **        (1) FOR T4014               **
     **        (2) FOR T4107               **
     **        (3) FOR T4113               **
     **        (4) FOR T4105               **
     **                                    **
     ****************************************
GINO-F Version 3.0  (c) Copyright Bradly Associates Ltd.
```

```
Do you wish to ROTATE the plot?

       ANSWER Y or N

N

Do you wish to check that the DISPlacements to be
     applied to the model are correct.
              PLEASE INPUT Y for YES

Y
GINO-F Version 3.0  (c) Copyright Bradly Associates Ltd.

Do you wish to return to the orginal drawing.

       N
GINO-F Version 3.0  (c) Copyright Bradly Associates Ltd.


Do you wish to run the finite element program : Y


             PLEASE ENTER
                          1 for Q1
                          2 for Q2
                          3 for Q3
                          4 for Q4

   Remember the higher the queue number the lower it's
   priority i.e. jobs on Q1,Q2 and Q3 are processed before
   jobs on Q4. However if a job has a greater processing
   time than the maximum processing time for that queue
   then the job will not be completed. It is suggested
   that Q3 should be used.

        Which queue is required.


Please input the QUE number : 2


   Job FILE (queue Q2, entry 486) started on SPOCK_Q1


         The data file has now been submitted onto the
   queue and is ready for processing. The computer will
   inform you when the processing is finished. Otherwise
   you can use SHOW QUE/ALL to verify that the job is
   still on the que.


     NO FURTHER PROCESSING OF THIS JOB IS POSSIBLE UNTIL
           THE JOB HAS BEEN SUCCESSFULLY COMPLETED.


You are now leaving the METDEF/FE suite of programs
```

```
      ROLFOM CAD/CAM SYSTEM
      =====================

            PROGRAM                                          KEYWORD
            =======                                          =======

(1)     INPUT SECTION DATA                                 SECTION
(2)     RERUN SECTION ON SCREEN                            NSECTION
(3)     INPUT FLOWER PATTERN DATA                          FLOWER
(4)     RERUN FLOWER PATTERN ON SCREEN                     NFLOWER
(5)     RERUN FLOWER PATTERN SEPERATELY                    SFLOWER
(6)     RUN TEMPLATE PROGRAM                               TEMPLATE
(7)     ANALYSIS OF STRAINS BY FINITE ELEMENTS             ROLFEA
(8)     INPUT ROLL DESIGN DATA                             DESIGN
(9)     INPUT ROLL D-DATA IN SINGLE STAGE                  SDESIGN
(10)    RERUN ROLL DESIGN ON SCREEN                        NDESIGN
(11)    RUN WIRE FRAME ON SCREEN                           WIRE
(12)    RUN PLAN/SIDE ON SCREEN                            VIEW
(13)    UPDATED ROLL EDITOR                                EDITOR
(15)    EXPERT SYSTEM MACHINING                            ROLCUT
(16)    DELETION OF D FILES                                DELETE
(17)    CONVERT ROLCUT CUTTING COMMANDS                    CONVERT
(18)    INPUT CUTTING COMMANDS                             CUTPLOT
(19)    RUN POST PROCESSOR                                 MFPOST
(20)    CHECK NC TAPE ON SCREEN                            CHK

      TYPE 99 TO EXIT                                      (KEYWORD)

    PLEASE TYPE KEYWORD TO SELECT A PROGRAM
               =======

CHOICE: ROLFEA


      The following data is required :-

            The SECTION NUMBER

            The STAGE NUMBER

            The TERMINAL TYPE

The TERMINAL TYPE is categorised into four main groups .

          ****************************************
          **                                    **
          **      GROUP          TYPE           **
          **                                    **
          **        1     for    T4014          **
          **        2     for    T4107          **
          **        3     for    T4113          **
          **        4     for    T4105          **
          **                                    **
          ****************************************
```

Please input the SECTION NUMBER: 1100

Please input the STAGE NUMBER: 2

Please input the TERMINAL TYPE: 2

Please indicate whether this SECTION and STAGE number has already been processed.

Please input

Y for YES

or

N for NO

Y

Which type of analysis is required

a) for the tailor-made Finite Element package.

or

b) for the PAFEC package

Input either a or b

A

Which of the following output displays are required -:

'W' for a wire-frame model of the structure.

or

'G' for a graphical display for which a number of possible variables can be chosen and plotted against each other.

Please input your choice: W

Has the DISPLACEMENTS been found yet Y or N

Y

```
   ****************************************
   **                                    **
   **       TERMINAL DEFINITION          **
   **      PLEASE INPUT  1,2,3,4         **
   **        (1) FOR T4014               **
   **        (2) FOR T4107               **
   **        (3) FOR T4113               **
   **        (4) FOR T4105               **
   **                                    **
   ****************************************
GINO-F Version 3.0  (c) Copyright Bradly Associates Ltd. 1990

   Do you wish to ROTATE the plot?

     ANSWER Y or N

Y


   Please input the rotation about each axis in the order.
Angle about X axis    Angle about Y axis    Angle about Z axis

 30 60 10


   Do you wish to ROTATE the plot?

     ANSWER Y or N

  N


Do you wish to superimpose the Displaced section on this plot.

  Y


  Please input the new line colour-:
0-black,1-white,2-red,3-orange,4-yellow,5-green
6-cyan,7-blue,8-violet,9-brown,10-white

   2

 Please indicate if a multiplying factor is required
  The maximum values in X & Y ARE  0.41859E-02   0.17226E-02
  Input the X factor followed by the Y factor ZERO in each
     factor will avoid any alterations being made.

   0 0
```

Do you wish to ROTATE the plot?

ANSWER Y or N

N

Do you wish to superimpose the Displaced section on this plot.

N

Do you wish to check that the Displacements to be applied to the model are correct. PLEASE INPUT Y for YES

N

Do you wish to return to the orginal drawing.

N

GINO-F Version 3.0 (c) Copyright Bradly Associates Ltd. 1990

Do you require anymore graphical output.
Input Y[es] or N[o]

Y

Which of the following output displays are required -:

'W' for a wire-frame model of the structure.

or

'G' for a graphical display for which a number of possible variables can be chosen and plotted against each other.

Please indicate your choice: G

Any of the following variables can be plotted against each other:-

Coordinates

1 for the absolute value of the X coordinates
2 for the absolute value of the Y coordinates
3 for the absolute value of the Z coordinates
4 for the displacements in the X direction
5 for the displacements in the Y direction
6 for the displacements in the Z direction

Strains

7 for the longitudinal strain in the X direction.

It is recommended to use '6' vs '1' (side view), '3' vs '2' (end view) and '7' vs '1' for strains longitudinally along the section (i.e. position along the section is asked for later in the program.)

To find the position on the section a line of constant X or Y values is required.

Once the variables & 'constant line' has been inputted then the nodal coordinates are printed. Just choose one nodal point. The variables will be plotted for all values which have the same X or Y value (depending on the 'constant line') as the nodal point.

```
Please input the variables required (i.e 1 to 16)
  7 1

Please input the line of constant values X,Y or Z
  Y

PLEASE INPUT THE TITLE (N.B Upto 30 characters can be used)
  EDGE STRAIN
```

1	0.007890	0.002254	0.000000
2	0.007890	0.010000	0.000000
3	0.007890	0.017746	0.000000
4	0.035000	0.002254	0.000000
5	0.035000	0.010000	0.000000
6	0.035000	0.017746	0.000000
7	0.062110	0.002254	0.000000
8	0.062110	0.010000	0.000000
9	0.062110	0.017746	0.000000
10	0.007890	0.020787	0.000203
11	0.007890	0.023375	0.000904
12	0.007890	0.025989	0.001605
13	0.035000	0.020787	0.000203
14	0.035000	0.023375	0.000904
15	0.035000	0.025989	0.001605
16	0.062110	0.020787	0.000203
17	0.062110	0.023375	0.000904
18	0.062110	0.025989	0.001605
19	0.007890	0.028525	0.002846
20	0.007890	0.034630	0.006410
21	0.007890	0.040734	0.009975
22	0.035000	0.028525	0.002846
23	0.035000	0.034630	0.006410
24	0.035000	0.040734	0.009975
25	0.062110	0.028525	0.002846
26	0.062110	0.034630	0.006410
27	0.062110	0.040734	0.009975
28	0.007890	0.028525	0.002846
29	0.007890	0.055680	0.018618

30	0.007890	0.024510	0.065893
31	0.035000	0.047780	0.014053
32	0.035000	0.055680	0.018618
33	0.035000	0.024510	0.065893
34	0.062110	0.047780	0.014053
35	0.062110	0.055680	0.018618
36	0.062110	0.024510	0.065893
37	0.077890	0.002254	0.000000
38	0.077890	0.010000	0.000000
39	0.077890	0.017746	0.000000
40	0.105000	0.002254	0.000000
41	0.105000	0.010000	0.000000
42	0.105000	0.017746	0.000000
43	0.132110	0.002254	0.000000
44	0.132110	0.010000	0.000000
45	0.132110	0.017746	0.000000
46	0.077890	0.020787	0.000203
47	0.077890	0.023375	0.000904
48	0.077890	0.025989	0.001605
49	0.105000	0.020787	0.000203
50	0.105000	0.023375	0.000904
51	0.105000	0.025989	0.001605
52	0.132110	0.020787	0.000203
53	0.132110	0.023375	0.000904
54	0.132110	0.025989	0.001605
55	0.077890	0.028525	0.002846
56	0.077890	0.034630	0.006410
57	0.077890	0.040734	0.009975
58	0.105000	0.028525	0.002846
59	0.105000	0.034630	0.006410
60	0.105000	0.040734	0.009975
61	0.132110	0.028525	0.002846
62	0.132110	0.034630	0.006410
63	0.132110	0.040734	0.009975
64	0.077890	0.028525	0.002846
65	0.077890	0.055680	0.018618
66	0.077890	0.024510	0.065893
67	0.105000	0.047780	0.014053
68	0.105000	0.055680	0.018618
69	0.105000	0.024510	0.065893
70	0.132110	0.047780	0.014053
71	0.132110	0.055680	0.018618
72	0.132110	0.024510	0.065893
73	0.147870	0.002254	0.000000
74	0.147870	0.010000	0.000000
75	0.147870	0.017746	0.000000
76	0.175000	0.002254	0.000000
77	0.175000	0.010000	0.000000
78	0.175000	0.017746	0.000000
79	0.202110	0.002254	0.000000
80	0.202110	0.010000	0.000000
81	0.202110	0.017746	0.000000
82	0.147870	0.020787	0.000203
83	0.147870	0.023375	0.000904
84	0.147870	0.025989	0.001605

85	0.175000	0.020787	0.000203
86	0.175000	0.023375	0.000904
87	0.175000	0.025989	0.001605
88	0.202110	0.020787	0.000203
89	0.202110	0.023375	0.000904
90	0.202110	0.025989	0.001605
91	0.147870	0.028525	0.002846
92	0.147870	0.034630	0.006410
93	0.147870	0.040734	0.009975
94	0.175000	0.028525	0.002846
95	0.175000	0.034630	0.006410
96	0.175000	0.040734	0.009975
97	0.202110	0.028525	0.002846
98	0.202110	0.034630	0.006410
99	0.202110	0.040734	0.009975
100	0.147870	0.028525	0.002846
101	0.147870	0.055680	0.018618
102	0.147870	0.024510	0.065893
103	0.175000	0.047780	0.014053
104	0.175000	0.055680	0.018618
105	0.175000	0.024510	0.065893
106	0.202110	0.047780	0.014053
107	0.202110	0.055680	0.018618
108	0.202110	0.024510	0.065893
109	0.213380	0.002254	0.000000
110	0.213380	0.010000	0.000000
111	0.213380	0.017746	0.000000
112	0.225000	0.002254	0.000000
113	0.225000	0.010000	0.000000
114	0.225000	0.017746	0.000000
115	0.236620	0.002254	0.000000
116	0.236620	0.010000	0.000000
117	0.236620	0.017746	0.000000
118	0.213380	0.020787	0.000203
119	0.213380	0.023375	0.000904
120	0.213380	0.025989	0.001605
121	0.225000	0.020787	0.000203
122	0.225000	0.023375	0.000904
123	0.225000	0.025989	0.001605
124	0.236620	0.020787	0.000203
125	0.236620	0.023375	0.000904
126	0.236620	0.025989	0.001605
127	0.213380	0.028525	0.002846
128	0.213380	0.034630	0.006410
129	0.213380	0.040734	0.009975
130	0.225000	0.028525	0.002846
131	0.225000	0.034630	0.006410
132	0.225000	0.040734	0.009975
133	0.236620	0.028525	0.002846
134	0.236620	0.034630	0.006410
135	0.236620	0.040734	0.009975
136	0.213380	0.028525	0.002846
137	0.213380	0.055680	0.018618
138	0.213380	0.024510	0.065893
139	0.225000	0.047780	0.014053

```
 Please input the node number
      30

    ****************************************
    **                                    **
    **        TERMINAL DEFINITION         **
    **       PLEASE INPUT  1,2,3,4        **
    **         (1) FOR T4014              **
    **         (2) FOR T4107              **
    **         (3) FOR T4113              **
    **         (4) FOR T4105              **
    **                                    **
    ****************************************
 GINO-F   2.7C 01-NOV-1986 - ISSUE 1

 IS ZERO OF X-AXIS REQUIRED_1 FOR YES
 1

 THE LIMITS IN THE X-DIRECTION ARE BETWEEN  0.000000E+00 AND
 0.332110E+00

 PLEASE INPUT THE ABSOLUTE INCREMENTAL VALUE AND THE INTEGER
 POWER VALUE

 0.04 -3

 THE LIMITS IN THE Y-DIRECTION ARE BETWEEN  -0.283382E-02 AND
  0.179625E-01

 PLEASE INPUT THE ABSOLUTE INCREMENTAL VALUE AND THE INTEGER
 POWER VALUE

 0.002 -2

 DO YOU WISH TO JOIN INDIVIDUAL POINTS
     N

 PLEASE INPUT THE NODE NUMBERS TO BE DRAWN TOGETHER
    1 18

 If this is incorrect then PRESS Y for another go
     PRESS the ENTER key to QUIT

 GINO-F   2.7C 01-NOV-1986 - ISSUE 1


          Do you require anymore graphical output.
                  Input Y[es] or N[o]

 N

       You are now leaving the METDEF/FE suite of programs.
```